ROLE OF FtsA IN CELL DIVISION IN *Neisseria gonorrhoeae*

A Thesis Submitted to the
College of Graduate Studies and Research
In Partial Fulfillment of the Requirements
For the Degree of Doctor of Philosophy
In the Department of Biology
University of Saskatchewan
Saskatoon

By
YAN LI

PERMISSION TO USE

In presenting this thesis in partial fulfillment of the requirements for a Postgraduate degree from the University of Saskatchewan, I agree that the Libraries of this University may make it freely available for inspection. I further agree that permission for copying of this thesis in any manner, in whole or in part, for scholarly purposes may be granted by the professor or professors who supervised my thesis work or, in their absence, by the Head of the Department or the Dean of the College in which my thesis work was done. It is understood that any copying or publication or use of this thesis or parts thereof for financial gain shall not be allowed without my written permission. It is also understood that due recognition shall be given to me and to the University of Saskatchewan in any scholarly use which may be made of any material in my thesis.

Requests for permission to copy or to make other use of material in this thesis in whole or part should be addressed to:

Head of the Department of Biology
University of Saskatchewan
112 Science Place
Saskatoon, Saskatchewan,
Canada S7N 5E2

Abstract:

Bacterial cell division is an essential process, which is initiated by forming the Z-ring as a cytoskeletal scaffold at the midcell site, followed by the recruitment of a series of divisome proteins. In *Escherichia coli* (Ec), at least 15 divisome proteins (FtsZ, FtsA, ZipA, FtsK, FtsQ, FtsB, FtsL, FtsI, FtsW, FtsN, FtsE, FtsX, ZapA, AmiC, EnvC) have been implicated in this process. The components of the cell division machinery proteins in *Neisseria gonorrhoeae* (Ng) differs from *E. coli*. *N. gonorrhoeae* possesses FtsA, but lacks FtsB. ZipA and FtsL in *N. gonorrhoeae* have low identity to ZipA and FtsL from *E. coli*. Our laboratory has studied the central division protein FtsZ in *N. gonorrhoeae*. Thus, my research investigated the role of *N. gonorrhoeae* FtsA in cell division and investigated the interactions between divisome proteins from *N. gonorrhoeae* to understand divisome assembly.

This study determined the association of $FtsA_{Ng}$ with $FtsZ_{Ng}$ and other divisome proteins in *N. gonorrhoeae* and identified the functional domains of $FtsA_{Ng}$ involved in these interactions using a bacterial two-hybrid (B2H) assay. $FtsA_{Ng}$ interacted with $FtsZ_{Ng}$, $FtsK_{Ng}$, $FtsW_{Ng}$, $FtsQ_{Ng}$, and $FtsN_{Ng}$. Self-interactions of $FtsA_{Ng}$ and $FtsZ_{Ng}$ were also detected. $FtsI_{Ng}$, $FtsE_{Ng}$ and $FtsX_{Ng}$ did not interact with $FtsA_{Ng}$. The $2A_1$, $2A_2$ and 2B domains of $FtsA_{Ng}$ were sufficient to interact with $FtsZ_{Ng}$ independently. Domain $2A_1$ interacted with $FtsK_{Ng}$ and $FtsN_{Ng}$. Domain 2B of $FtsA_{Ng}$ interacted with $FtsK_{Ng}$, $FtsQ_{Ng}$, and $FtsN_{Ng}$. Domain $2A_2$ of $FtsA_{Ng}$ interacted with $FtsQ_{Ng}$, $FtsW_{Ng}$, and $FtsN_{Ng}$. These data suggest that FtsA in *N. gonorrhoeae* plays a key role in interactions with FtsZ and other divisome proteins.

The potential interactions between divisome proteins in *N. gonorrhoeae* were examined using B2H assays. The comparisons between the *N. gonorrhoeae* divisome protein interaction network and those of *E. coli* and *S. pneumoniae* indicates that the divisome protein interactome of *N. gonorrhoeae* is more similar to that of *S. pneumoniae* and differs from that of *E. coli*. The comparisons revealed that compared to the interactions in *E. coli* and *S. pneumoniae*, more interactions between divisome proteins upstream of $FtsA_{Ng}$ (including $FtsA_{Ng}$) and downstream of $FtsA_{Ng}$ were observed in *N. gonorrhoeae* while fewer interactions between divisome proteins downstream of $FtsA_{Ng}$ were observed in *N. gonorrhoeae*. Possible reasons for this include the inability of $ZipA_{Ng}$ to interact with other divisome proteins and the absence of FtsL and FtsB in *N. gonorrhoeae*, resulting in the lack of an FtsQ-FtsB-FtsL complex in *N. gonorrhoeae*. These results indicate a possibly different divisome assembly in *N. gonorrhoeae* from that proposed models for *E. coli*.

A model for $FtsA_{Ng}$ structure was predicted based on structural homology modeling with the resolved crystal structure of *Thermotoga maritima* FtsA. Four domains on the molecule were identified, designated 1A, 1C, 2B and 2A (including $2A_1$ and $2A_2$). Domains 2A and 2B of FtsA were highly conserved based on multi-sequence alignments of FtsAs from 30 bacteria. $FtsA_{Ng}$ located to the division site in *N. gonorrhoeae* cells and the ratio of FtsA to FtsZ ranged from 1:24 to 1: 33 in three *N. gonorrhoeae* strains, which gave a lower cellular concentration of FtsA compared to other organisms.

I also determined that overexpression of $FtsA_{Ng}$ in *E. coli* led to cell filamentous in rod-shaped *E. coli* and cell enlargement and aggregation in mutant, round *E. coli*. $FtsA_{Ng}$ failed to complement an $ftsA_{Ec}$-deletion *E. coli* strain although the overexperssion of $FtsA_{Ng}$ disrupted *E. coli* cell division. In addition, overexpression of $FtsA_{Ng}$ only affected cell division in some cells and its localization in *E. coli* was independent of interaction with *E. coli* FtsA or FtsZ. These results indicate that $FtsA_{Ng}$ exhibits a species-specific functionality and *E. coli* is not a suitable model for studying $FtsA_{Ng}$ functionality.

This is the first study to characterize FtsA from *N. gonorrhoeae* in cell division. I identified novel functional domains of $FtsA_{Ng}$ involved in interactions with other divisome proteins. The *N. gonorrhoeae* divisome protein interaction network determined by B2H assays provides insight into divisome assembly in *N. gonorrhoeae*.

ACKNOWLEDGEMENTS

First and foremost, I would like to thank Dr Jo-Anne Dillon, for giving me the opportunity to work in her laboratory at the University of Saskatchewan on this project. Throughout my studies she provided me with much appreciated freedom to explore my own ideas. I would also like to thank her for always making time for me, despite her feverishly busy schedule.

I also thank my advisory committee members, Dr Chris Todd, Dr Peter Howard, and Dr Hong Wang, for all their useful comments and advice regarding this project. I would also like to thank Dr. Sebastien Pichoff, University of Kansas Medical Center, for providing *E. coli* strain P163 and plasmid pSEB306-*ftsA*$_{Ec}$D242E which were important in completing my research. I thank Dr Ming Chen, Department of Pharmacy Center, University of Alberta, for taking the immuno-EM images. I am very grateful to the Saskatchewan Health Research Foundation (grant to JRD) and the University of Saskatchewan for financially supporting the research of my program.

A big thank to the past and present lab crew in Saskatoon. Thanks to Mingmin for all his helpful advice, both scientific and life-related! Your kindness and generosity will never be forgotten. To the summer student Swati, you allowed me to exercise my supervisory skills. Thanks for your contributions in gene cloning and B2H assays. I hope you learned as much from me as I did from each of you. Thanks Sarah for working on divisome protein purification and antibody production. Your great work will help for further investigation in divisome assembly. To Monica, Monique and Cherise, Debu, Sarah, Sidharath, Sinisa, Rajinder, Guanqun, thanks for being great lab members. In addition, many other former members of the Dillon lab, as well as other graduate students and staff in the Department of Biology and VIDO should be acknowledged for making this an unforgettable experience, including Fei, Chao, Enqi, Yang, Jin, Shawn, Tao, Gillian, Bonita, Joan, Vasu, Guosheng, Deidre, and Joel, thank you.

Finally, thank you to my family. My Mom, Dad and brother, they are the emotional anchors in my life, even though they never quite understood exactly what I was up to. To my husband, Peter, I thank you for always being there. As well, to all my friends and relatives, I thank you all.

Cheers,

Yan

TABLE OF CONTENTS

LIST OF TABLES

LIST OF FIGURES

Chapter 1

Chapter 2

Chapter 3

Appendix

LIST OF COMMONLY USED ABBREVIATIONS

aa	amino acids
AD	activating domain
Amp	ampicillin
ATP	adenosine 5’ triphosphate
BD	binding domain
B2H	Bacterial Two-Hybrid
Bs	*Bacillus subtilis*
BSA	bovine serum albumin
CDC	Centers for Disease Control and Prevention
CIAP	Calf Intestinal Alkaline Phosphatase
Co-IP	Co-immunoprecipitation
Cm	chloramphenicol
DAPI	4',6-diamidino-2-phenylindole
dcw	division cell wall cluster
dca	division cluster associated
DIC	differential interference contrast
DNA	deoxyribonucleic acid
dNTP	deoxynucleoside triphosphate
Ec	*Escherichia coli*
EGFP	enhanced green fluorescent protein
FRET	fluorescence resonance energy transfer
Fts	filamentous temperature sensitive
GFP	green fluorescent protein
HIV	human immunodeficiency virus
hr	hour
interactome	interaction network
IPTG	isopropyl-β-D-thiogalactopyranoside
Kan	kanamycin
kb	kilobase
kDa	kilodalton
LOS	lipooligosaccharide
min	minute
min	minicell

Ng	*Neisseria gonorrhoeae*
OD	optical density
O/N	overnight
ONPG	o-nitro-phenyl-D-galactopyranoside
Opa	opacity
PBP	penicillin binding protein
PBS	phosphate buffered saline
PCR	polymerase chain reaction
PG	peptidoglycan
PID	pelvic inflammatory disease
PHAC	Public Health Agency of Canada
Rmp	reduction-modifiable protein
rpm	rotations per minute
s	second
SEDS	shape, elongation, division and sporulation
SDS-PAGE	sodium dodecyl sulphate polyacrylamide gel electrophoresis
Sp	*Streptococccus pneumoniae*
STD	sexually transmitted disease
Tm	*Thermotoga maritima*
WHO	World Health Organization
X-gal	5-bromo-4-chloro-3-indolyl-β-D-galactopyranoside
Y2H	Yeast Two-Hybrid

CHAPTER 1 INTRODUCTION

1. Cell division in bacteria

Cell division, or cytokinesis, is an essential process that permits proper growth, development and reproduction of all living organisms. It involves a variety of proteins with unique and specific functions that work together towards complete cytokinesis. In bacteria, cell division occurs by the formation of a division septum and generally results in the formation of equivalent viable daughter cells, each that possesses a full genetic complement. In order to achieve this result, bacteria must coordinate events spatially and temporally. After DNA replication has begun, but before the chromosomes are completely partitioned, the divisome will assemble at midcell, assist in the final separation of deoxyribonucleic acid (DNA), synthesize peptidoglycan (PG) *de novo*, constrict, and finally digest the layer of PG separating daughter cells, releasing two new cells (Donachie, 1993).

Since the discovery that the crucial bacterial cell division protein, FtsZ, formed a ring-like structure at midcell in *Escherichia coli* (Ec, Bi and Lutkenhaus, 1991), the knowledge concerning bacterial cell division has increased greatly. Molecular studies have substantially advanced the identification of many of the components required for successful bacterial cytokinesis. Most of the studies of this event focused on rod-shaped bacteria, such as *E. coli* and *Bacillus subtilis* (Bs), which, under normal conditions, will divide in parallel planes at the middle of the cell to form two equally sized daughter cells.

Bacterial cell division is initiated by FtsZ polymerizing into the Z-ring at the poteintial division site (Bi and Lutkenhaus, 1991), followed by the recruitment of other proteins to form the divisome. In *E. coli*, at least 15 divisome proteins have been identified to assemble at the midcell site through a series of protein-protein interactions. The composition of different bacterial genomes has shown that although cell division genes are highly conserved among bacteria, none of the genes is present in all the phylogenetic groups (Lutkenhaus and Addinall, 1997; Mingorance *et al*., 2004). The implications for cell division of the absence of

some proteins or the presence of others, in different bacteria, are largely uninvestigated. In coccal bacteria, the midcell site is not intrinsically obvious. Some coccal bacteria, such as *Neisseria gonorrhoeae*, divide in alternating perpendicular planes (Westling-Häggström *et al.*, 1977; Woldringh *et al.*, 1990) while rod-shaped *E. coli* cells separate in parallel planes, indicating that the modality for septum formation in *N. gonorrhoeae* should be intrinsically more complicated than organisms such as *E. coli*. The present research characterizes the early cell division protein FtsA from *N. gonorrhoeae* and its interaction with other divisome proteins identified in *N. gonorrhoeae*.

In the first section of the Introduction, an overview of bacterial cell division in *E. coli*, including the *d*ivision *c*ell *w*all (*dcw*) cluster, the placement and formation of the Z-ring, and divisome assembly will be discussed. Bacterial cell division in *B. subtilis*, *Caulobacter crescentus* and *N. gonorrhoeae* will be described in the second, third and forth sections, respectively. The key components of cell division machinery in each organism will be described. In particular, the cell division components of *E. coli* will be reviewed more extensively, as it is a Gram-negative organism like *N. gonorrhoeae*. The final section of the Introduction will describe the functions of FtsA from various bacteria.

1.1. Cell division in Gram-negative rod *Escherichia coli*

1.1.1. The *d*ivision *c*ell *w*all (*dcw*) cluster

Most of our current knowledge of bacterial cell division has been derived from studies of the Gram-negative rod *E. coli*. Proteins involved in cell division were first described in *E. coli* as having a *f*ilamentous *t*emperature *s*ensitive (*fts*) phenotype when mutated (Bi and Lutkenhaus, 1991). Mutations in these Fts proteins caused the *E. coli* cells to become filamentous at the non-permissive temperature (Bi and Lutkenhaus, 1991). In *E. coli*, a group of 16 essential genes that encode cell division proteins and proteins for cell wall synthesis has been identified: *mraZ, mraW, ftsL, ftsI* (*pbp3*), *murE, murF, mraY, murD, ftsW, murG, murC, ddlB, ftsQ, ftsA, ftsZ,* and *envA* (Fig. 1.1) (Ayala *et al.*, 1994). This group of highly conserved genes is known as the *dcw* cluster. Within the *dcw* cluster of *E. coli*, all of the genes are organized as an operon with transcription in the same direction. Several promotors have been identified within the *E. coli dcw* cluster; however the main promoter seems to be *mraZ1p,* located upstream of *mraZ* (Mengin-Lecreulx *et al.*, 1998), which drives co-transcription of all *dcw* genes, ending at the single transcriptional terminator identified downstream of *envA* (Vicente *et al.*, 1998). While there are no internal terminators within the *dcw* cluster of *E. coli*, there are many other internal promoters, suggesting the presence of partial transcripts (Mengin-Lecreulx *et al.*, 1998). The remaining promoters are likely involved in regularing different expression levels of individual genes (Lutkenhaus and Addinall, 1997; Vicente *et al.*, 1998). Indeed, DNA microarrays have shown that there are three regions of differing mRNA levels (Selinger *et al.*, 2003).

The *dcw* cluster has been identified in most other bacteria as well, including *N. gonorrhoeae* (Francis *et al.*, 2000), *B. subtilis* (Real and Henriques, 2006), *Staphylococcus aureus* (Pucci *et al.*, 1997), *Streptococccus pneumoniae*(Sp) (Massidda *et al.*, 1998), *Haemophilus influenzae* (Fleischmann *et al.*, 1995), and *Enterococcus faecalis* (Ramirez-

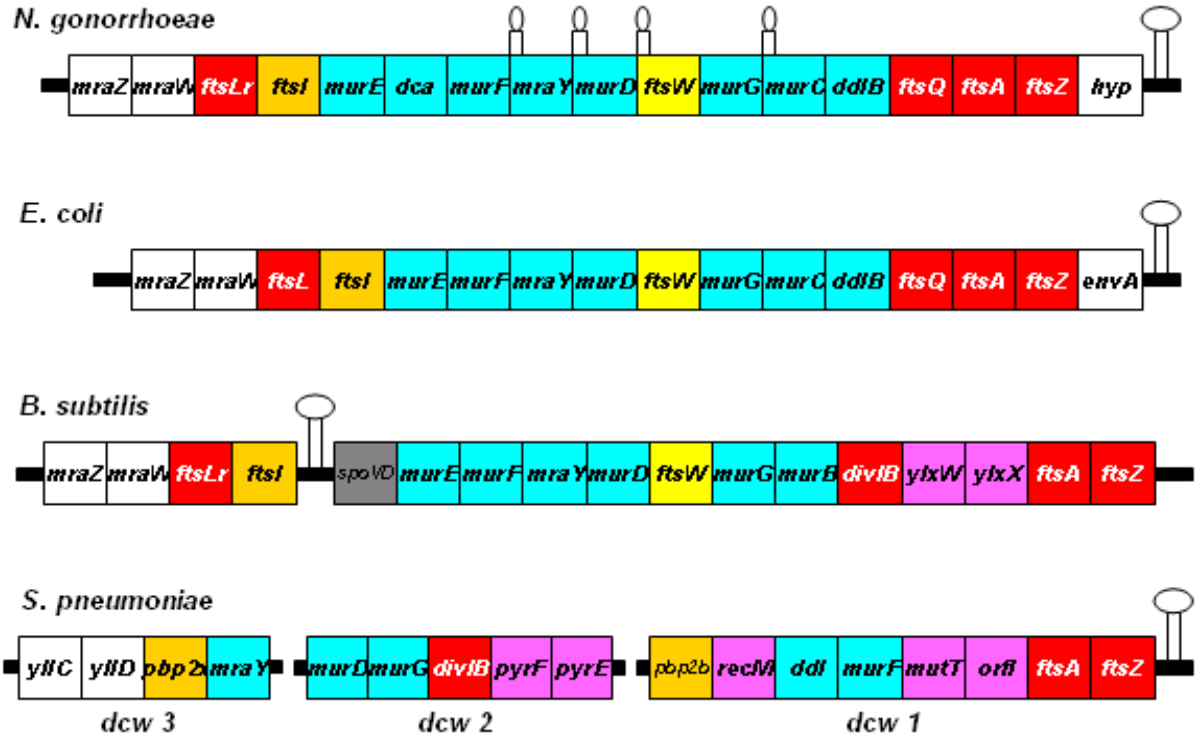

Fig. 1.1. Schematic representation of the *dcw* clusters from *E. coli* (Ayala *et al*., 1994; Mingorance *et al*., 2004), *N. gonorrhoeae* (Francis *et al*., 2000; Snyder *et al*., 2001), *B. subtilis* (Real and Henriques, 2006; Mingorance *et al*., 2004) and *S. pneumoniae* (Massidda *et al*., 1998). The *dcw* genes of *S. pneumoniae* were found distributed in three genetically separate regions of the *S. pneumoniae* chromosome, which were aligned with the corresponding regions in the other species, as the organization of the chromosome is not yet known (Massidda *et al*., 1998). Transcription terminators are indicated on the top of each column.

Arcos *et al.*, 2005). Fig. 1.1 shows the *dcw* clusters of *E. coli*, *N. gonorrhoeae*, *B. subtilis*, and *S. pneumoniae*. Genes within the *dcw* cluster, such as *ftsZ* and *ftsA,* are highly conserved between Gram-negative and Gram-positive bacteria, but there are some significant differences between them, particularly the organization of the gene homologues within the *dcw* cluster. While the *dcw'*s genes themselves are highly conserved, it has been proposed that the gene order might be a factor in determining cell shape based on phylogenetic tree comparisons between the *dcw* genes and FtsZ (Mingorance *et al.*, 2004; Tamames *et al.*, 2001). As such, the term "genomic channelling" is used to describe how the order of the *dcw* cluster may be linked to grouped protein assembly that can affect how a cell elongates and septates (Mingorance *et al.*, 2004). The "genomic channelling" model suggests that a specific gene order is needed to coordinate elongation and septation. Although the order of gene arrangement is generally conserved (Vicente *et al.*, 1998), the *dcw* arrangement in round bacteria is predicted to be less conserved relative to rod-shaped bacteria, since elongation is not necessary (Mingorance *et al.*, 2004). In this model, the selective pressure to maintian the cluster arises from the need to efficitntly coordinate the processes of elongation and septation in rod-shapbed bacteria (Mingorance *et al*., 2004). However, there are examples that disagree with this idea, for example, the bacillus *E. coli* and the coccus *N. gonorrhoeae* have very similar *dcw* cluster arrangements (Fig. 1.1, Mingorance *et al.*, 2004).

Many of the proteins involved in the cell division machinery are encoded in the *dcw* cluster, such as FtsZ, FtsA, FtsQ, FtsW, FtsI and FtsL (Fig. 1.1). Knowing the function of key divisome proteins is crucial for understanding bacterial cell division. Studying the genes and corresponding proteins involved with the *dcw* clusters will give researchers an understanding of bacterial cell division initiation and regulation.

1.1.2. Cell division site selection

There are two negative regulatory systems that ensure FtsZ assembly in the nucleoid-free region at midcell in *E. coli*; nucleoid occlusion and the Min system (Woldringh *et al.*, 1990; de Boer and Crossley, 1989, Fig. 1.2).

Nucleoid occlusion

The nucleoid occlusion model states that the nucleoid inhibits division wherever it occupies space in the cell, preventing the Z-ring formation over the chromosome (Woldringh *et al.*, 1990). It was supported by FtsZ localization studies showing that Z-rings usually do not form over nucleoids (Yu and Margolin, 1999; Sun and Margolin, 2001). *E. coli* SlmA protein, the actual effector, was identified recently as a nucleoid-associated division inhibitor capable of mediating nucleoid occlusion (Bernhardt and de Boer, 2005). SlmA is able to bind FtsZ directly *in vitro*, which may recruit FtsZ away from the cell membrane and competes with other FtsZ binding proteins, such as ZapA (Bernhardt and de Boer, 2005). Hence, SlmA reduces the ability of FtsZ polymers to develop into a functional cytokinetic ring near the nucleoid.

Min system

The *min* genes were first identified, as FtsZ assembly regulators, by characterizing *E. coli* cells that displayed a *min*icell (*min*) phenotype due to mutations (Davie *et al*., 1984; de Boer *et al*., 1988, 1989). *E. coli* encodes three Min proteins that work together, MinC, MinD and MinE (de Boer *et al*., 1988, 1989). MinC is the inhibitor of division and a direct effect of MinC action preventing FtsZ assembly has been shown for *E. coli* (Johnson *et al.*, 2002; Hu *et al.*, 2003). Recent studies have shown that *E. coli* MinC antagonizes the scaffolding function of FtsZ by inhibiting lateral interactions of FtsZ (Dajkovic *et al.*, 2008). Overexpressed MinC binding to the C-terminal domain of FtsZ displaced FtsA (and/or even ZipA), which would prevent the recruitment of late division proteins, thus in turn

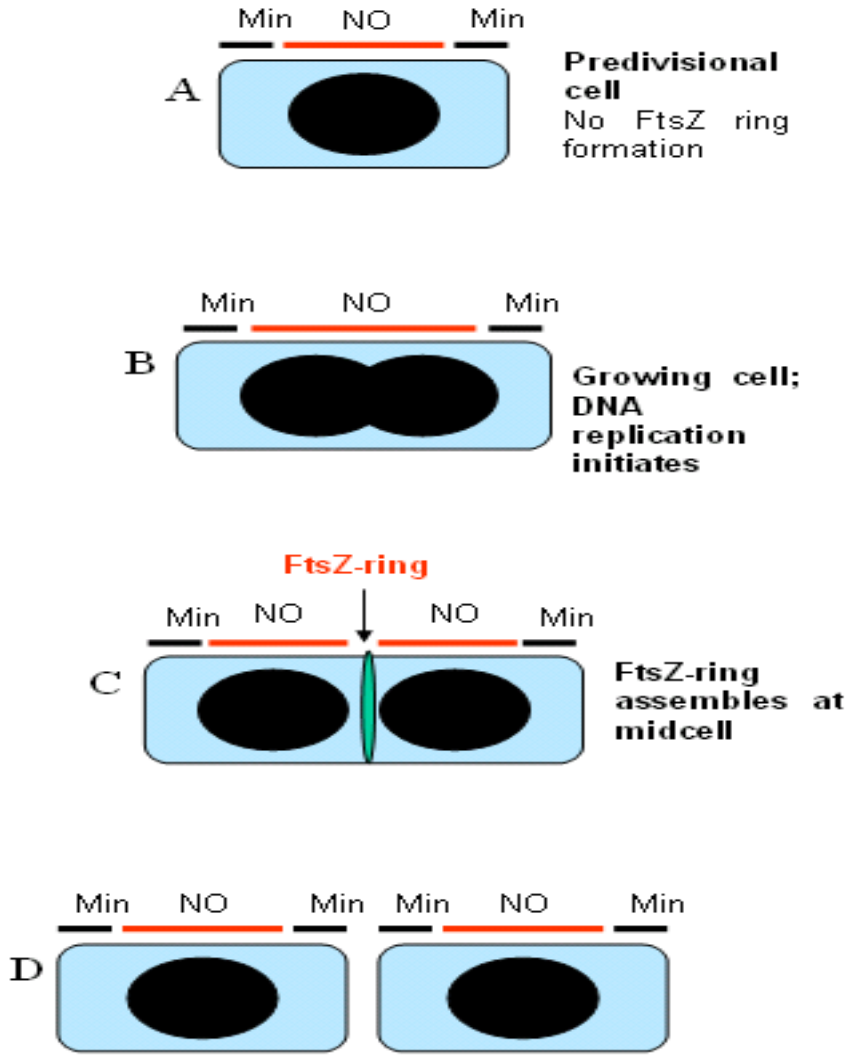

Fig. 1.2. Nucleoid occlusion (NO) and the Min protein system act to toporegulate cell division in *E. coli*. (A-B) In the predivisional cell, the nucleoid mass (black oval) prevents FtsZ ring formation throughout the central region of the cell (red bar). The Min system acts to prevent FtsZ ring formation at cell pole regions (black bars). (C) As DNA replication terminates, a nucleoid-free zone between each daughter chromosome is formed. The lack of nucleoid occlusion in this central region allows FtsZ polymerization to proceed (green circle). The Min system continues to inhibit cell division at cell pole regions. (D) Cell division is completed and nucleoid occlusion and the Min system are re-established in each daughter cell (Adapted from Szeto Ph.D. Thesis, 2004).

destabilizing the Z-ring assembly (Shiomi and Margolin, 2007a； Shen and Lutkenhaus, 2009). MinD is ATPase (Cordell and Lowe, 2001) and associates with the cell membrane (Hu and Lutkenhaus, 2003). Studies have shown that dimerized MinD binds to the cell membrane in an adenosine 5' triphosphate (ATP) dependent manner (Hu and Lutkenhaus, 2001) and subsequently recruites MinC in bulk to the membrane, apparently increasing the local concentration of MinC, which is critical for its function (Hu and Lutkenhaus, 2003). Membrane association of the MinCD complex is essential for proper FtsZ inhibition, since MinD overexpression does not cause filamentatious phenotype in cells devoid of MinC. In the absence of MinD, MinC remains in the cytoplasm and is unable to inhibit Z-ring formation (Johnson *et al.*, 2004). MinE is a topological factor and forms as a ring-structure adjacent to the midcell (Shih *et al.*, 2003), which drives the remarkable oscillation of MinCDE between the poles of *E. coli* cells (Lackner *et al.*, 2003). In the absence of MinE, MinCD remains statically colocalized to the membrane and prevents the Z-ring formation throughout the cell (Raskin and de Boer, 1999; Rowland *et al.*, 2000). By interacting with MinD, MinE effectively displaces MinC from the complex by competing with MinC for MinD binding (Hu and lutkenhaus, 2003) and stimulates ATP hydrolysis of MinD. MinD ultimately is released from the membrane into the cytoplasm (Ma *et al.*, 2004; Lackner *et al.*, 2003). The cytolosic MinD binds to ATP and reassembles on the membrane at the opposite pole. MinC is then recruited to the opposite pole with the MinD reassembly. MinE ring subsequently reforms and acts on the nascent MinD (and hence MinC), thus inducing the oscillation patterns observed (Lackner *et al.*, 2003). As a result of this oscillation of MinCDE, time-averaged concentration of the division inhibitor MinC is maintained highest at the cell poles and lowest at the midcell, thereby preventing FtsZ polymerization at the cell poles but not at the midcell site (Raskin and de Boer, 1999).

1.1.3. Divisome assembly models

Once the specific division site has been determined, FtsZ initiates cell division by polymerizing into the Z-ring at the midcell, which provides a scaffold for the recruitment of subsequent proteins to form a division complex or divisome at the midcell. Two models of divisome assembly in *E. coli* have been proposed: the linear model and the concerted model.

The linear model

Studies on the localization of cell division proteins in conditional lethal mutants revealed that they localize according to a defined and linear hierarchy of dependence (Buddelmeijer and Beckwith, 2002; Errington *et al.*, 2003). In this hierarchy, a given protein requires the presence of all upstream proteins to localize to midcell and is in turn required for the localization of all downstream proteins (Buddelmeijer and Beckwith, 2002). For example, FtsK localization is dependent on FtsA and ZipA (Pichoff and Lutkenhaus, 2002; Yu *et al.*, 1998), and FtsQ, FtsL and FtsI appearance at midcell requires the presence of FtsK (Chen *et al*., 1999; Chen and Beckwith, 2001). Thus, a linear model has been proposed for how the divisome assembles based on these localization studies (Fig. 1.3).

In this model, the process starts with polymerization of FtsZ into a Z-ring at the midcell (Addinall *et al.*, 1996). FtsA and ZipA bind directly to FtsZ and localize next, presumably, as the Z-ring is assembling (Fig.1.3). Once both FtsA and ZipA are in place, the remaining proteins are recruited in the following order: [FtsE-FtsX]-FtsK-FtsQ-[FtsL+FtsB]- FtsW-FtsI-FtsN-AmiC-EnvC. The proteins within brackets are independent of each other but dependent on FtsZ and the upstream proteins. There are two possible mechanisms by which cell division proteins localize to midcell in a sequential dependency. First, each protein, recruited to the midcell via protein-protein interactions, alters in its own structure or alters the structure of a protein complex so as to provide a template for the next protein to bind to. Second, each protein, once it localizes to the division site, modifies some component of the

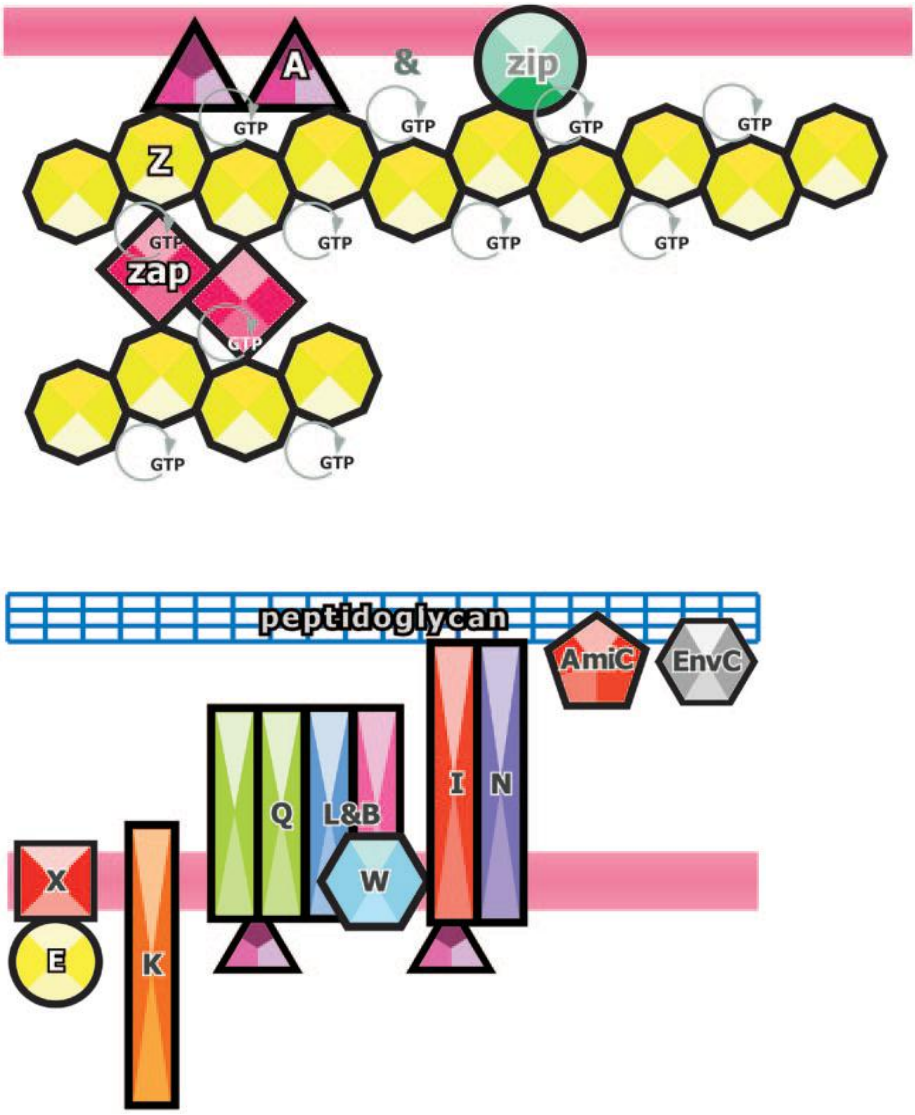

Fig. 1.3. A linear model for divisome assembly in *E. coli*. Top, proteins of the early assembly step of the division ring. FtsZ (Z) initiates polymerization at the division site to form the Z-ring and interacts with FtsA (A) and ZipA, which bind FtsZ to the inner cell membrane (magenta stripe). ZapA, which presents in *E. coli* but is not essential for cell division, promotes the bundling of FtsZ protofilaments. **Bottom**, proteins of the late assembly step of the division ring. Schematic view of the assembly of the late cell division proteins showing their relation to the cell membrane (magenta stripe) and PG (blue grid). The protein icons are ordered from left to right according to the linear assembly sequence of proteins: FtsX (X), FtsE (E), FtsK (K), FtsQ (Q), FtsL (L), FtsB (B), FtsW (W), FtsI (I), FtsN (N), AmiC and EnvC. An ampersand indicates that both proteins assemble simultaneously (Vicente *et al.*, 2006).

septum via either a biochemical (e.g. enzymatic reasctions) or structural alteration. This alternation provides a structure now recognized by the next protein in the pathway (Goehring *et al*., 2005).

The concerted model

It is important to note that the recruitment hierarchy reflects dependent relationships but does not necessarily reflect a temporal order. There is some evidence for a time lag between Z-ring formation (FtsZ, FtsA and ZipA) and localization of the downstream proteins (FtsQ, FtsW, FtsI and FtsN), indicating a two-step assembly of divisome proteins in *E. coli* (Aarsman *et al*., 2005; Alexeeva *et al.*, 2010). While FtsZ, FtsA and ZipA are assembled early to the division site simultaneously (so called early divisome proteins), the downstream proteins localize into the Z-ring nearly at the same time and 14 to 21 minutes later after FtsZ, FtsA, and ZipA (so called late divisome proteins) (Aarsman *et al*., 2005). (In this thesis, the term "early divisome proteins" is used to describe the first set of proteins in *E. coli* and *B. subtilis* that are recruited to the division ring, including FtsZ, FtsA and ZipA. The term -"late divisome proteins" is used to describe the second set of proteins in *E. coli* and *B. subtilis* that are recruited to the division ring, including FtsK, FtsQ, FtsB, FtsL, FtsW, FtsI, and FtsN. It is still not clear how divisome assembles in other organisms. Thus, in other organisms, FtsZ, FtsA and ZipA are decribed as "upstream" divisome proteins, corresponding to the "early" divisome proteins in *E. coli*. The rest of divisome proteins, including FtsK, FtsQ, FtsI, FtsW, FtsN, FtsE and FtsX are described as "downstream" divisome proteins, corresponding to the "late" divisiome proteins in *E. coli*.)

At the same time, several groups demonstrated a remarkably high number of potential interactions amongst divisome proteins using various interaction assays, such as co-immunoprecipitation experiments, two-hybrid systems and fluorescence resonance energy transfer (FRET) (Karimova *et al.*, 2005; Di Lallo *et al.*, 2003; Alexeeva *et al.*, 2010). Many

proteins exhibited interactions with multiple partners and each protein binds to a slightly different subset of a protein group, suggesting a surprising degree of interconnectivity within the divisome. Moreover, the hierarchy theoretically allows for a subcomplex of proteins and the linear model also reflects the existence of multiprotein complex, which can be formed independently. For example, the formation of the FtsQ-FtsL-FtsB complex did not require FtsK, a protein required for the localization of all three members of the complex (Buddelmeijer and Beckwith, 2004). Goehring *et al*. (2005, 2006) showed that not only FtsL and FtsQ, but also FtsW and FtsI can be recruited to the midcell, in the absence of the FtsA and FtsK. Interestingly, the expression of the ZapA-FtsQ fusion can effectively back-recruit FtsK to the septum even in the absence of the upstream protein FtsA (Goehring *et al.*, 2005, 2006).

Taken together, these data suggest that the cell division proteins may not follow a strictly linear assembly hierarchy as first expected but follow a complex cooperative or concerted recruitment. Using the premature targeting approach, Goehring *et al.* (2005, 2006) provides evidence for a concerted model in *E. coli*, in which divisome formation occurs in early and late/FtsA-independent assembly stages (Fig. 1.4). First, FtsZ polymerizes into the Z-ring at the division site (Lutkenhaus and Addinall, 1997), which recruits two essential proteins FtsA and ZipA to form the Z-ring complex at the same time. Meanwhile, the late divisome proteins are assembled into pre-formed complexes independent of FtsA: a periplasmic connector protein complex, consisting of FtsQ, FtsB and FtsL forms and a murein synthesis complex of FtsW-FtsI is formed simultaneously. Once the Z-ring complex is established, FtsK connecting the connector complex and the synthesis complex can be recruited to midcell. FtsN is then recruited to the divisome to regulate the initiation of Z-ring constriction and stability (Goehring *et al.*, 2006; Gerding *et al.*, 2009; Rico *et al.*, 2010).

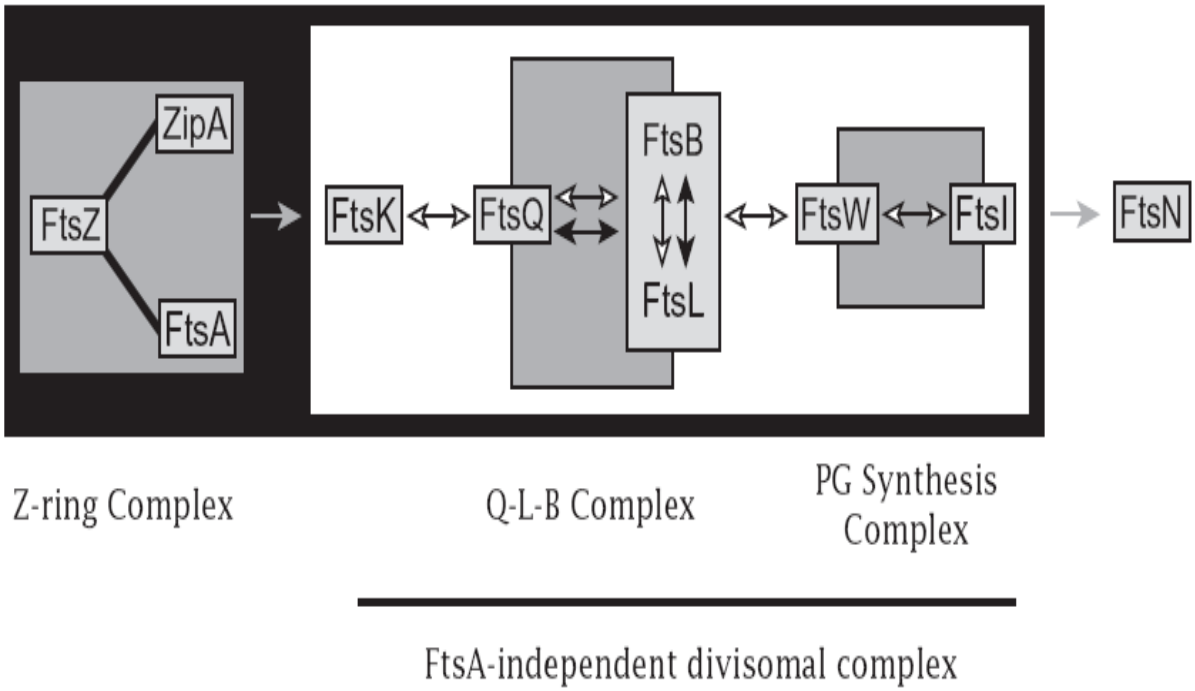

Fig. 1.4. A concerted model for divisome assembly in *E. coli*. Recent evidence in *E. coli* indicates that proteins do not assemble in a linear manner but in pre-formed complexes. First, the stability of the Z-ring complex requires ZipA and FtsA. The remaining divisome proteins can form complexes independently of FtsA. A periplasmic connector consisting FtsQ, FtsB, and FtsL form together, while a murein synthesis complex of FtsW and FtsI is formed simultaneously. It is believed that FtsK interconnects the Z-ring with the connector and the synthesis complex. Once assembled, FtsN is then recruited to the divisome to possibly regulate the initiation of Z-ring constriction. [Reprinted with permission from Wiley-Blackwell (Goehring *et al*., 2006)].

1.1.4. Proteins involved in divisome formation

Most of the genes that code for the divisome proteins have been identified in *E. coli* in screening for conditional lethal mutants unable to divide under nonpermissive conditions, usually high temperatures (e.g. 42ºC). These mutants are normal at the permissive termerature but grow as multinucleated filaments at the nonpermissive termperature, so they were named *fts* for *f*ilamentous *t*emperature *s*ensitive. At least 15 Fts proteins are known to be involved in *E. coli* cell division (Table 1.1). These proteins can fall into several functional classes (Table 1.1): i) assembly of the Z-ring at a specified division site (FtsZ); ii) regulating the assembly state of FtsZ (ZapA); iii) anchoring the Z-ring to the membrane (FtsA and ZipA); iv) coordinating septation with chromosome segregation (FtsK); v) synthesis of PG cell wall (FtsI-FtsW) and synthesis of cell envelope material (FtsQ-FtsL-FtsB periplasmic connector); vi) regulating the initiation of Z-ring constriction (FtsN); vii) hydrolysis of PG to separate daughter cell (Amic and EnvC, FtsE, FtsX). Within these proteins, the first six classes are essential and involved in divisome formation.

Cell division initiation: FtsZ polymerizaiton and the nature of the Z-ring

FtsZ is the most important and most highly conserved bacterial cell division protein. It is present in most bacteria and archaea, as well as in chloroplasts and mitochondria of some algae and amoeba but not in those of higher plants or animals (Margolin, 2005; Addinall and Holland, 2002). FtsZ is a cytoplasmic protein and shows remarkable structural resemblance to that of tubulin despite the low level of sequence identity (~10%) (Löwe and Amos, 1998).

E. coli FtsZ appears to comprise four domains (Vaughan *et al.*, 2004). There is a short and poorly conserved N-terminal leader (~15 residues), a highly conserved domain (~300 - residues) that is structurally and functionally similar to tubulin, a variable linker (~50 residues) and well-conserved C-treminal tail (~15 residues). The C-terminus of FtsZ has been shown to interact with other proteins, such as ZipA, FtsA and FtsK as determined by bacterial

TABLE 1.1. Essential divisome proteins encoded in different bacterial genomes

Divisome protein[α]	Function	Homologue[β] in		
		E. coli	*B. subtilis*	*N. gonorrhoeae*
FtsA	Positive regulator of FtsZ assembly, membrane associated, actin like	+	+	+
FtsB	Bridge cytoplasmic with periplasmic, transmembrane, forms tripartite complex with FtsL and FtsQ	+	DivIC	_
FtsI	Synthesize septal PG, transpeptidase (PBP 3)	+	+	+
FtsK	DNA partitioning, large multifunctional membrane protein	+	SpoIIIE	+
FtsL	Bridge cytoplasmic with periplasmic, transmembrane, forms tripartite complex with FtsB and FtsQ	+	+	?
FtsN	Regulate the assembly and stability of the Z-ring, weak homology to amidase, binds PG	+	_	+
FtsQ	Bridge cytoplasmic with periplasmic, many protein-protein interactions, transmembrane	+	DivIB	+
FtsW	Predicted transporter of PG precursors, multitransmembrane protein	+	+	+
FtsZ	Initiates Z ring, helps constrict ring, tubulin like, GTPase	+	+	+
ZipA	Positive regulator of FtsZ assembly, membrane associated	+	ZapA	?

[α] FtsH, FtsJ, and FtsY are not involved in cell division.

[β] +, present in genome; -, not found in genome; ?, other homologues may exist.

two-hybrid (B2H) assays and other methods (Di Lallo *et al*., 2003; Datta *et al.*, 2006; Hale and de Boer, 1997; RayChaudhuri, 1999). The core of FtsZ (a highly conserved domain), between the N-terminus and the variable linker is required for binding and hydrolyzing GTP as well as assembling the protofilament (de Boer *et al.*, 1992). FtsZ fused to green fluorescent protein (GFP), as well as immunostaining with FtsZ antibody, has shown that the protein localizes as a distinct ring-like structure (Z-ring) to the division site in *E. coli* (Fig.1.5A) (Bi and Lutkenhaus, 1991; Ma *et al*., 1996; Addinall and Holland, 2002). Like tubulin, FtsZ is able to polymerize in a GTP-dependent manner; FtsZ bound to GTP assembles head to tail in a linear manner (Mukherjee and Lutkenhaus, 1994; Weiss, 2004). *In vitro* studies have shown that FtsZ-GTP is able to assemble into several structures, including protofilaments and sheets (Löwe and Amos, 1999). The initial assembly of single-stranded protofilaments occurs under low concentration (around 0.5~1 μM) and these protofilaments interact with each other and form long but narrow sheets when FtsZ concentration is high (~3 μM) (Wang and Lutkenhaus, 1993; Mukherjee and Lutkenhaus, 1998; Chen and Erickson, 2005; Dajkovic *et al.*, 2008).

Fluorescence recovery after photobleaching (FRAP), as well as other studies, has revealed that the Z-ring is not a static structure; it undergoes constant remodelling throughout its existence, with rapid turnover dynamics that depend on the intrinsic GTPase activity of the FtsZ polymer (Rueda *et al.*, 2003; Stricker *et al.*, 2002; Anderson *et al.*, 2004). FtsZ polymerization depends on GTP binding (Mukherjee and Lutkenhaus, 1994), but the high GTP hydrolysis rate, as an important feature of FtsZ assembly *in vitro*, is always coupled to FtsZ assembly (Chen and Erickson, 2005). Indeed, GTP hydrolysis promotes the disassembly of the protofilament and drives the highly dynamic nature of the FtsZ polymers that are observed both in the cell and *in vitro,* as well as limiting the length of individual protofilaments (Mukherjee *et al.*, 1998, 2001; Chen and Erickson, 2005; Stricker *et al.*, 2002;

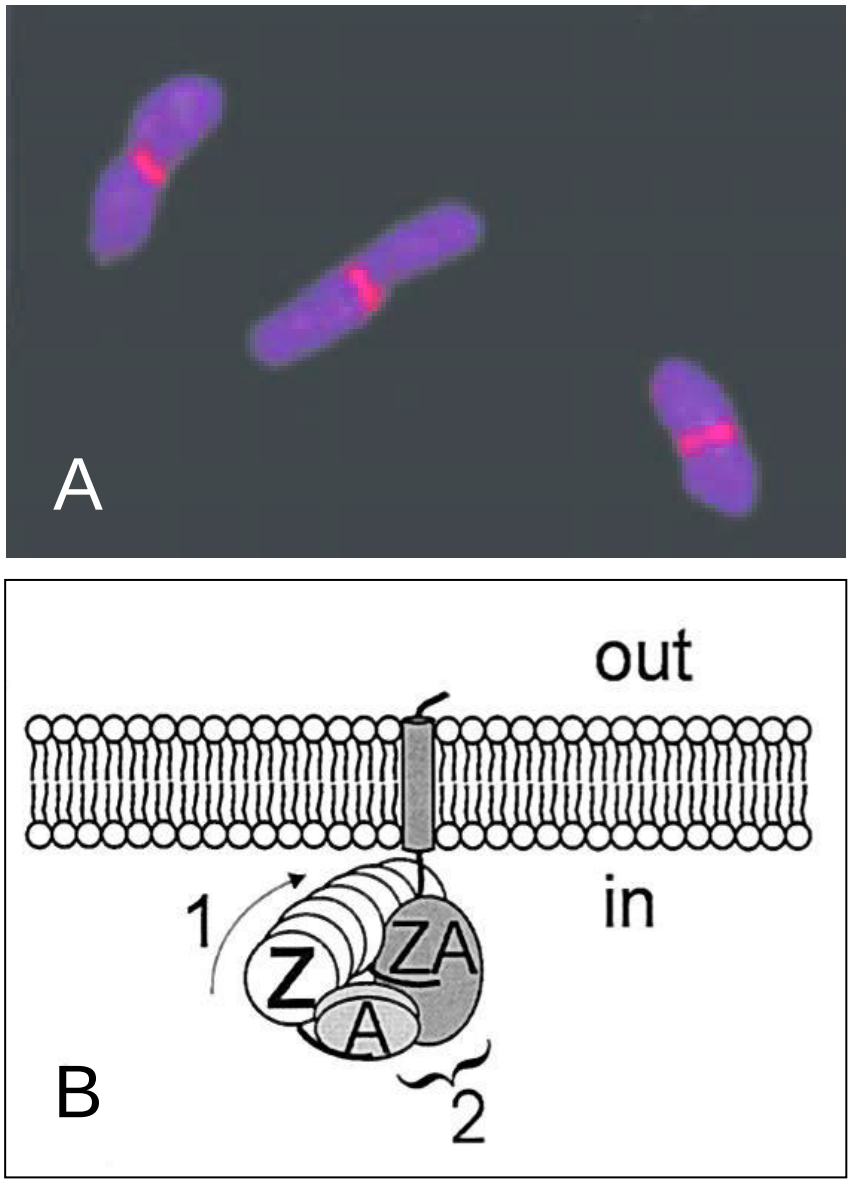

Fig. 1.5. (A) FtsZ localization in *E. coli.* *E. coli* stained with anti-FtsZ antisera shows FtsZ localization at the middle of each cell (Reprinted with permission from Elsevier (Addinall and Holland, 2002). **(B). Formation of the Z-ring and anchoring of the Z-ring to the membrane.** FtsZ (Z) initiates polymerization to form a Z-ring at the division site and may be anchored to cell membrane by interacting with FtsA (A) and ZipA (ZA) (reprinted with permission from the American Society for Microbiology (Errington *et al*., 2003)].

Anderson *et al.*, 2004).

FtsZ filament curvature and lateral interactions between FtsZ filaments appear to be two potential elements that generate the force needed for membrane constriction (Mingorance *et al.*, 2010). Both straight and curved protofilaments were observed in some specific conditions, suggesting that the conformational change from a straight GTP-bound FtsZ polymer to a curved GDP-bound FtsZ polymer might transmit mechanical work to the membrane (Li *et al.*, 2007; Lu *et al.*, 2000). A recent study demonstrated that Z-rings can impart a force on a tubular membrane *in vitro* (Osawa *et al.*, 2008), reinforcing the possibility of force generation by the Z-ring. A mathematical model of how the Z-ring coalesces into a condensed, functional cytokinetic ring was reported (Dajkovic *et al.*, 2008), which showed that force generation could be achieved independently of FtsZ GTPase activity (Dajkovic *et al.*, 2008; Lan *et al.*, 2008, 2009). In addition, as an *in silico* alternative, lattice models have been used for the modeling of FtsZ polymerization and all point to a central role for the lateral interactions between filaments in force generation (Mingorance *et al.*, 2010). This role is supported by experimental evidence obtained *in vivo* (Mingorance *et al.*, 2010).

Aside from its proposed 'contractile' role during septation, the *E. coli* Z-ring is also believed to serve as a scaffold for the assembly of at least 10 additional proteins into the midcell (Goehring *et al.*, 2006).

Z-ring dynamic regulator: ZapA

The assembly, stability and function of the Z-ring must be regulated both spatially and temporally during the normal divison cycle. In most cases, regulation is accomplished by the use of positive and negative factors. A number of proteins have been identified and can be divided into two groups: stabilizing proteins such as ZapA, ZipA and FtsA as well as destabilizing proteins, such as MinC and MinD. The function of MinC and MinD in disassembly of FtsZ has been discussed above. The positive regulators are discussed below.

ZapA is a widely conserved FtsZ binding protein. *E. coli* cells lacking ZapA exhibit no phenotype change, indicating that ZapA is not essential for cell division (Gueiros-Filho and Losick, 2002). However, ZapA interacts with FtsZ and is recruited to the division site early (Di Lallo *et al.*, 2003). It was found to promote the bundling of FtsZ protofilaments (Gueiros-Filho and Losick, 2002; Low *et al.*, 2004; Small *et al.*, 2007) and to antagonize the inhibitory activity of MinC *in vitro* (Dajkovic *et al*., 2008; Scheffers, 2008), indicating a role in enhancing the stability of the Z-ring. A couple of models were proposed to explain the mechanisms of how ZapA stabilizes the FtsZ polymer (Small *et al.*, 2007; Low *et al.*, 2004; Dajkovic *et al*., 2010). *E. coli* ZapA promotes the polymerization of FtsZ by stabilizing longitudinal bonds between FtsZ molecules and cross-linking FtsZ polymers into coherent Z-rings (Dajkovic *et al*., 2010). The ability of ZapA to promote the formation of stable bundles of FtsZ has also been shown in other organisms, e.g. *B. subtilis* and *Pseudomonas aeruginosa* (Gueiros-Filho and Losick, 2002; Low *et al.*, 2004).

Tethering FtsZ to the membrane: FtsA and ZipA

A crucial element of the Z-ring assembly is the association between FtsZ and the cell membrane. The attachment of the Z-ring to the membrane assists both to maintain its structural integrity during septation and probably to transmit any constrictive force to the membrane (Errington *et al.*, 2003; Li *et al.*, 2007; Erickson, 2001). However, FtsZ does not possess any defined membrane spanning sequence, thus Z-ring formation requires the presence of proteins that can tether FtsZ filaments to the membrane. In *E.coli*, both FtsA and ZipA perform this function and collaborate in anchoring FtsZ to the membrane (Fig. 1.5B) (Pichoff and Lutkenhaus, 2002). They bind FtsZ to the membrane by interacting with a short conserved region near the extreme C-terminus of FtsZ (Ma and Margolin, 1999; Haney *et al.*, 2001) and possibly promote the Z-ring assembly and stability. The Z-ring could be formed in the presence of either one, but not if both are absent. In turn, assembly of FtsA and ZipA into

the ring is dependent solely on FtsZ and not on each other or on the other divisome proteins (Hale and de Boer, 1999; Pichoff and Lutkenhaus, 2002), indicating that FtsA or ZipA is sufficient to promote Z-ring assembly in *E. coli*.

ZipA is not a conserved protein and is absent in some bacteria. It is a bitopic protein that is composed of three domains: a transmembrane anchor at the N-terminal domain, a unstructured linker domain and a large C-terminal domain in the cytoplasm (Hale and de Boer, 1997; Mosyak *et al.*, 2000; Moy *et al.*, 2000). ZipA binds to the membrane through its N-terminal transmembrane anchor, which cannot be replaced by transmembrane segments of another membrane protein (Erickson, 2001; Hale and de Boer, 1997). The interaction between ZipA and FtsZ is mediated by the C-terminal domain of ZipA, which is necessary and sufficient for its recruitment to the Z-ring (Hale *et al.*, 2000). *In vitro*, the C-terminal domain of ZipA promotes the assembly of FtsZ into thick bundles and sheets of protofilaments that are aligned laterally (Mosyak *et al.*, 2000; Hale *et al.*, 2000; RayChaudhuri, 1999). The linker domain is likely to be pivotal in the tethering role, allowing the C-terminal domain to reach out from the membrane and bind to the C-terminus of FtsZ (Erickson, 2001; Ohashi *et al.*, 2002). Besides its role in promoting Z-ring assembly, ZipA is required for the recruitment of late divisome proteins, including FtsK, FtsQ, FtsL and FtsN to the septum in *E. coli* (Pichoff and Lutkenhaus, 2002; Hale and de Boer, 2002). However, ZipA is not involved in the interactions with these late divisome proteins in *E. coli* as determined by B2H (Di Lallo *et al.*, 2003).

Since my research mainly focuses on the role of FtsA from *N. gonorrhoeae*, FtsA will be reviewed in a separate section (1.5).

Completing the divisome: late divisome proteins

Once the Z-ring is established, the remaining essential proteins are recruited to form the divisome. FtsQ, FtsL, FtsB, FtsI and FtsN share similar bitopic membrane topologies; FtsK and FtsW are polytopic integral membrane proteins.

FtsK

FtsK is a multifunctional protein and plays two distinct roles in cell division (Draper *et al.*, 1998; Yu *et al.*, 1998) and chromosome segregation (Errington *et al.*, 2001). It is the first protein that localizes at midcell once the Z-ring complex is established, and its localization is required for the recruitment of the other divisome components (Wang and Lutkenhaus, 1998; Yu *et al*., 1998; Chen and Beckwith, 2001). FtsK consists of a smaller N-terminal domain, containing four transmembrane segments and a large C-terminal cytoplasmic domain connected by a linker region (Dorazi and Dewar, 2000).

FtsK interacts with several divisome proteins, including FtsZ, FtsQ, FtsL and FtsI and the functional domains of FtsK involved in these interactions were determined using B2H assays (Di Lallo *et al.*, 2003; D'Ulisse *et al.*, 2007; Grenga *et al.*, 2008). The N-terminal domain of FtsK is responsible for the interation with FtsQ and FtsL while the other interactions are localized outside the N-terminal domain. The linker is involved in interaction with FtsZ and FtsI and the C-terminal domains are also required to interact with FtsI (Grenga *et al.*, 2008). These results indicate that besides the N-terminal domain, other FtsK domains are also involved in the cell division process, which may play a role in divisome stabilization (Bigot *et al.*, 2004; Grenga *et al.*, 2008).

FtsK is a member of the SpoIII family of DNA translocases and its large soluble C-terminal domain contains an ATP-binding site that is required for chromosome segregation (Pease *et al.*, 2005; Bigot *et al.*, 2007). Upon deletion of this domain, *E. coli* exhibited defective chromosome segregation but cell division was not affected (Liu *et al.*, 1998). Since

FtsK is localized to the septum, the resolution of chromosome dimers is ensured prior to full septum closure (Draper and Gober, 2002). Thus, FtsK provides an intimate link between cell division and chromosome segregation.

FtsQ-FtsL-FtsB complex

Various approaches strongly indicate that *E. coli* FtsQ, FtsL, and FtsB proteins form a stable complex that is independent of other known divisome proteins and of the division status of the cell (Buddelmeijer and Beckwith, 2004). This complex can be targeted to the division site by the action of FtsQ. It appears to be the bridge between the predominantly cytoplasmic cell division protein FtsK and the predominantly periplasmic cell division proteins (e.g. FtsW and FtsI). The interactions between FtsQ, FtsL and FtsB were determined using B2H assays (Di Lallo *et al*., 2003) and three proteins share a similar bitopic topology: a short N-terminal cytoplasmic domain, one transmembrane segment and a larger C-terminal periplasmic domain. Evidence showed that the homologues of FtsB, FtsL, and FtsQ also assemble into complexes in *B. subtilis* and *S. pneumoniae* (Daniel *et al*., 2006; Noirclerc-Savoye *et al*., 2005; Robichon *et al*., 2008), indicating a central and conserved role of the FtsQ-FtlL-FtsB complex in organizing the divisome.

In *E. coli*, FtsQ assembles with FtsL and FtsB into a trimeric complex independent of FtsK, indicating that the complex could be formed in cells before movement to the midcell (Buddelmeijer and Beckwith, 2004). FtsQ localizes to the septum via its periplasmic domain in the absence of FtsL and FtsB, but is required for the localization and recruitment of both later proteins (Chen *et al.*, 1999; Weiss *et al.*, 1999). All three proteins are, in turn, required for the recruitment of FtsW and FtsI (Buddelmeijer and Beckwith, 2002; Mercer and Weiss, 2002; Weiss *et al.*, 1999).

FtsQ is the protein that establishes the highest number of interactions with the other components of the division ring. FtsQ interacted with almost all the divisome proteins,

including FtsA, FtsK, FtsL, FtsB, FtsW, FtsI, and FtsN as determined by B2H assays and other biochemical methods [such as co-Immunoprecipitation (Co-IP) assays] (Di Lallo *et al.*, 2003; Karimova *et al.*, 2005; D'Ulisse *et al.*, 2007; Buddelmeijer and Beckwith, 2004). FtsA and FtsK interacted with FtsQ via its cytoplasmic tail whereas all of other interactions were via its periplasmic domain and/or the transmembrane region (D'Ulisse *et al.*, 2007). The periplasmic domain is required for the localization of FtsB/FtsL and the transmembrane segment is required for FtsQ localization to the division site (van den Ent *et al.*, 2008; Chen *et al.*, 1999, Scheffers *et al.*, 2007). These entire domains act together to accomplish the role of FtsQ in linking upstream and downstream divisome proteins in the division process.

In *E. coli*, the FtsQ-FtsL-FtsB complex can be divided further into a subcomplex of FtsB-FtsL, which interact with each other and recruit FtsW and FtsI to the division site independent of FtsQ (Goehring *et al*, 2006). FtsB and FtsL are co-dependent for their stabilization and for localization; both require FtsQ for localization to midcell (Buddelmeijer *et al.*, 2002; Gonzalez and Beckwith, 2009). Using B2H assays, FtsB was determined to interact with ZapA, FtsI, FtsL and FtsQ; FtsL was determined to interact with FtsB, ZapA, FtsW and FtsQ (Di Lallo *et al.*, 2003). Both FtsB and FtsL contain predicted coiled-coil leucine zipper-like motifs in their periplasmic domains, which are important for the interaction between them (Buddelmeijer and Beckwith, 2004; Gonzalez and Beckwith, 2009; Guzman *et al.*, 1992). The C-terminal periplasmic domains of FtsB and FtsL are necessary for interaction with FtsQ while their N-terminal cytoplasmic domains are involved in the recruitment of FtsW and FtsI (Gonzalez *et al.*, 2010; Buddelmeijer and Beckwith, 2004). It is likely that the sole function of the subcomplex FtsB-FtsL is to act as a molecular scaffold to allow for proper divisome assembly (Gonzalez and Beckwith, 2009).

PG synthesis complex: FtsW-FtsI

FtsI (PBP3), a penicillin binding protein (PBP) clearly essential for cell division, is also involved in PG synthesis (Botta and Park, 1981). FtsI depletion inhibts cell division, resulting in cell filamentation (Pogliano *et al*., 1997). FtsI is a protein recruited late to the divisome (Weiss *et al*., 1997; Wang *et al.*, 1998) and its localization depends on the Z-ring, FtsA, FtsQ, FtsL and FtsW (Mercer and Weiss, 2002; Weiss *et al*., 1999). It interacted with FtsA and almost all the late divisome proteins in *E. coli*, including FtsQ, FtsB, FtsW, FtsK and FtsN as determined by two different B2H methods (Di Lallo *et al.*, 2003; Karimova *et al*., 2005). The transmembrane segment is the primary localization determinant in FtsI (Wissel and Weiss, 2004; Piette *et al*., 2004; Wissel *et al*., 2005) and its periplasmic domain is involved in interactions with other divisome proteins FtsA, FtsQ, FtsL and FtsW (Corbin *et al*., 2004; Wissel and Weiss, 2004). These interactions are important for the recruitment of FtsN and the regulation of the transpeptidase activity of FtsI (Nguyen-Disteche *et al*., 1998).

FtsW is a member of a large family of polytopic membrane proteins present in all bacteria that have a PG cell wall (Ikeda *et al*., 1989; Henriques *et al*., 1998). This family has been named SEDS for shape, elongation, division and sporulation (Henriques *et al.*, 1998). Each SEDS protein usually works in conjunction with a specific single PBP (Matsuhashi *et al*., 1990). Hence, FtsW was proposed to act in connection with FtsI in cell division (Ikeda *et al*., 1989) and is encoded in the same operon. The primary function of FtsW has been suggested to facilitate PG synthesis by recruiting FtsI to the division site (Mercer and Weiss, 2002). Depletion of FtsW severely destabilized the Z-ring, indicating a role in stabilization of Z-ring (Boyle *et al*., 1997), although no evidence for a direct FtsZ-FtsW interaction has been reported in *E. coli*. However, FtsZ-FtsW interaction has been reported in *S. pneumoniae* as determined by B2H assays (Maggi *et al*., 2008).

FtsN

FtsN is the last known essential protein to be recruited to the divisome (Chen and Beckwith, 2001; Addinall *et al*., 1997). It interacts with many other components of the division machinery, including FtsA, ZapA, FtsQ, FtsI, and FtsW as determined by B2H and other methods (Di Lallo *et al*., 2003; Karimova *et al*., 2005; Alexeeva *et al*., 2010). These interactions are important for the localization of FtsN and its C-terminal domain is required to localize to the septum (Ursinus *et al.*, 2004; Addinall *et al*., 1997; Yang *et al*., 2004). In addition, FtsN was shown to suppress a number of temperature-sentitive mutations in *ftsA, ftsK, ftsQ* and *ftsI* (Dai *et al*., 1993). Overexperssion of FtsN can compensate for a complete lack of FtsK and both the cytoplasmic and transmembrane domains are critical for the suppression (Goehring *et al.*, 2007). Recently, FtsN has been assigned a role in triggering constriction of the Z-ring as well as the assembly and stabilization of the division ring (Gerding *et al*., 2009; Arends *et al*., 2010; Rico *et al*., 2010; Alexeeva *et al*., 2010).

1.2. Cell division in Gram-positive rod *B. subtilis*

Division site selection in *B. subtilis*

The Gram-positive rod-shaped bacillus, *B subtilis*, is another organism which has been extensively studied for its cell division mechanisms. It differs from *E. coli*, especially with regard to the positioning of the Z-ring. In *B. subtilis*, nucleoid occlusion prevents the Z-ring formation over the nucleoid (Wu and Errington, 2004). Noc of *B. subtilis* has been characterized as an inhibitor of division, which is a nonspecific DNA binding protein (Wu *et al*., 2009). In *noc* mutant cells, the Z-ring can form directly over the central DNA mass, resulting in a division event that cuts the chromosome. In contrast, overproduction of Noc in *B. subtilis* inhibited cell division, leading to a filamentous phenotype (Wu and Errington, 2004).

B. subtilis also has the Min system to determine the placement of the Z-ring as in *E. coli*. One major difference between them is that *B. subtilis* contains MinC and MinD but lacks a MinE homologue (Cha and Stewart, 1997; Edwards and Errington, 1997). *B. subtilis* MinC and MinD function similarly to their *E. coli* equivalents to form the inhibitory complex MinCD. The topological specificity activity of MinE is replaced by DivIVA, a protein unrelated to MinE (Cha and Stewart, 1997; Edwards and Errington, 1997). GFP-tagged DivIVA localizes at the cell poles and at nascent division sites just before division completion (Edwards and Erington, 1997). In contrast to the oscillatory behavior of the Min system in *E. coli*, DivIVA was thought to control cell division by sequestering MinCD at the cell poles in *B. subtilis* (Edwards and Errington, 1997). Recent evidence indicates that MinC (and hence MinD) is not absolutely static in *B. subtilis*, but rather dynamically relocalized from the old poles to the site of septation during cell division (Gregory *et al.*, 2008).

In addition, a novel component of division site selection, MinJ, has been identified in *B. subtilis* and has been shown to act as an adaptor protein, linking the topological factor

DivIVA to the inhibitory complex MinCD (Bramkamp *et al.*, 2008; Partick and Kearns, 2008). MinJ is necessary for correct localization of MinD (and hence MinC) (Bramkamp *et al.*, 2008) while its localization at the cell poles and the division site depends on DivIVA (Partick and Kearns, 2008). Interestingly, MinJ was found to interact with several divisome proteins and facilitates the localization of membrane-integral divisome proteins like FtsK or Pbp2B, indicating that MinJ connects the membrane-integral part of the divisome with the Min system (van Baarle and Bramkamp, 2010). Recent studies showed that the MinCDJ system in *B. subtilis* prevent minicell formation adjacent to recently completed division sites by promoting divisome disassembly, thereby ensuring that cell division occurs only once per cell cycle (van Baarle and Bramkamp, 2010).

Divisome assembly in *B. subtilis*

In *B. subtilis*, divisome assembly follows a concerted or cooperative mode, because most divisome proteins are interdependent for septal localization (Fig. 1.6) (Errington *et al.*, 2003). A two-step dynamic assembly of the divisome in *B. subtilis* was determined using time series and time-lapse microscopy (Gamba *et al.*, 2009). There is a considerable delay (at least 20% of the cell cycle) between the assembly of early and late cell division proteins. The Z-ring assembles early and concomitantly with FtsA, ZapA and EzrA, and after a delay time, a second set of division proteins, including GpsB, FtsL, DivIB, FtsW, Pbp2B and DivIVA are recruited to the midcell (Gamba *et al.*, 2009).

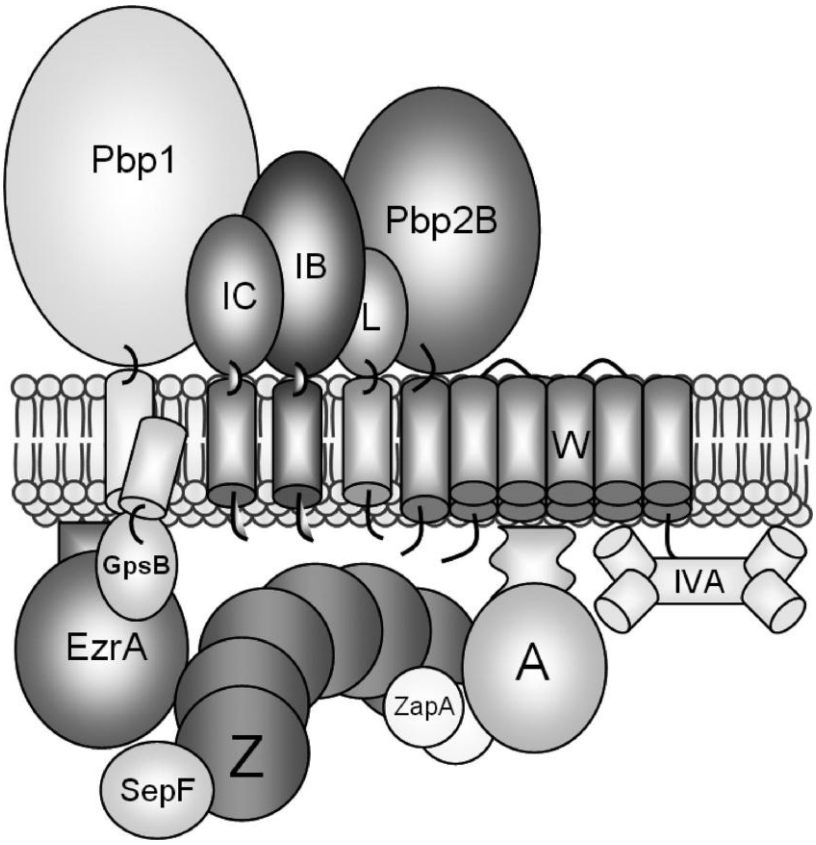

Fig. 1.6. Schematic representation of the *B. subtilis* divisome. The classical view of the *B. subtilis* divisome is represented; protein names have been abbreviated by excluding Fts and Div (Z, FtsZ; A, FtsA; L, FtsL; W, FtsW; IB, DivIB; IC, DivIC; IVA, DivIVA) (Gamba *et al*., 2009).

Divisome proteins in *B. subtilis*

B. subtilis FtsZ plays a key role in the initiation of cell divison and polymerizes in a GTP-dependent manner to form the Z-ring on the inside of the cytoplasmic membrane (Lutkenhaus and Addinall, 1997). In the absence of ZipA in *B. subtilis*, FtsA tethers FtsZ to the membrane and interacts with FtsZ prior to Z-ring formation, indicating its critical role in the efficient formation of functional Z-rings (Jensen *et al.*, 2005). FtsA has been shown to bind and hydrolyze ATP and to localize in FtsZ-dependent manner to the division site in *B. subtilis* (Feucht *et al.*, 2001). Two proteins, ZapA and EzrA, are involved in maintaining Z-ring integrity in *B. subtilis*. *In vitro,* ZapA can also bind FtsZ and promote FtsZ-GTP protofilament bundling into branched networks; therefore, ZapA might positively modulate Z-ring assembly (Gueiros-Filho and Losick, 2002). The EzrA protein has a similar topology to ZipA, which is a negative regulator, and acts to promote Z-ring depolymerization since deletion of *erzA* lowers the critical concentration of FtsZ needed to form the Z-rings (Haeusser *et al*., 2004; Levin *et al*., 1999).

The *B. subtilis* FtsK homologue SpoIIIE is not required for septation, but displays DNA translocation activity, which ensures proper chromosome translocation into the prespore compartment of sporulating cells (Bath *et al.*, 2000). FtsQ, FtsL and FtsB homologues ($DivIB_{Bs}$, FtsL and $DivIC_{Bs}$) have also been identified in *B. subtilis* and exhibited a similar complex as in *E. coli* (Daniel *et al*., 2006). FtsL requires DivIB for its own stability, which is, in turn, required for the stability of the DivIC (Daniel *et al*., 2000; Katis *et al.*, 2000; Daniel *et al.*, 1998). *B. subtilis* FtsI homologue PBP-2B and FtsW are required for septation and may also be involved in PG synthesis (Errington *et al.*, 2003; Daniel *et al.*, 2000; Yanorui *et al*., 1993). There is no apparent homologue of FtsN identified in *B. subtilis*.

1.3. Cell division in *Caulobacter crescentus*

I chose to describe *C. crescentus* because it exists as morphologically and functionally distinct cell types, and cellular differentiation is an integral part of its cell cycle (Jensen *et al.*, 2002; Ryan and Shaprio, 2003; Skerker and Larub, 2004). *C. crescentus* cells have a stalk at one pole for surface attachment and a flagellum at the other pole for motility; cells always divide slightly closer to the flagellated pole than the stalked pole, resulting in an asymmetric division (Brun *et al.*, 1994; Marczynski, 1999). Its DNA replication process is also asymmetric (Jensen *et al.*, 2002).

C. crescentus lacks both a nucleoid occlusion system and Min proteins (Jensen, 2006), thus different strategies for proper localization of the Z-ring and cell division are required. A new protein, MipZ, with a new mechanism, was identified, whose function combines the roles involved with both nucleoid occlusion and Min systems (Thanbichler and Shapiro, 2006). *C. crescentus* ParB is a chromosome partitioning protein, which facilitates replicated DNA being held at each pole to prevent spontaneous drifting to midcell (Figge *et al*., 2003). MipZ binds to ParB, which in turn, binds to a DNA sequence near *oriC* (Figge *et al*., 2003). Once one of the duplicated *oriC* rapidly moves from the stalked pole to the flagellated pole, the bound MipZ stimulates the GTPase activity of FtsZ there, causing FtsZ protofilaments to shorten and curve, thereby destabilizing the Z-ring. Therefore, the FtsZ only can be formed into the Z-ring at midcell where division eventually takes place.

Asymmetrical cell division results in two different progeny cells, a replicative stalked cell and a nonreplicative swarmer cell with a flagellum. After an obligate, non-replicative delay, the swarmer cell sheds its flagellum and differentiates into a stalked cell that undergoes one round of DNA replication per cell division cycle (Marczynski, 1999). Because of the asymmetrical cell division and cellular differentiation, the concentrations of FtsZ and other essential proteins involved in *C. crescentus* cell division are highly dynamic through the

cell cycle, which is in contrast to the static levels of proteins in *E. coli* (Rueda *et al*., 2003). FtsZ is degraded as the Z-ring constricts, thus newly divided swarmer and stalked cells are devoid of FtsZ (Kelly *et al*., 1998; Quardokus *et al*., 2001). *C. crescentus* FtsZ is not present in swarmer cells and accumulates only in the stalked and early pre-divisional cells that are actively building a Z-ring (Quardokus *et al*., 1996, 2001; Kelly *et al*., 1998). During swarmer cell differentiation, FtsZ is synthesized and first localizes at the developing stalked pole until later in the cell cycle when FtsZ becomes more abundant and is destabilized by MipZ to localize at the midcell (Quardokus *et al*., 2001). In *C. crescentus*, FtsZ plays an additional role in cell wall synthesis in non-dividing cells through the incorporation of cell wall material at the midcell (Aaron *et al.*, 2007).

Direct interaction between FtsA and FtsZ has been demonstrated in *C. crescentus* (Din *et al.*, 1998) and constitutive expression of FtsA causes cell division defects, indicating that FtsA is required for the progression of cell division (Ohta *et al*., 1997). Actually, *ftsQ* and *ftsA* are cotranscribed in a cell cycle-dependent manner in *C. crescentus* (Sackett *et al*., 1998). FtsA and/or FtsQ is limiting for cell division in nascent cells to coordinate the cell division with progression of the DNA replication cycle. *ftsQA* is transcribed at a later stage of the cell cycle than *ftsZ* and recruited to the midcell during a short period in late pre-divisional cells, consistent with the demonstrated requirement of FtsA and FtsQ for late stages of cell division (Martin *et al.*, 2004). As for FtsZ, the concentration of FtsA and FtsQ varies during the cell cycle, which is low in swarmer and stalked cells, peaks in pre-divisional cells, and then dramatically decreases after cell division (Martin *et al.*, 2004). Similarily, the localization of FtsA and FtsQ is also cell type-specific. In addition, *Caulobacte*r FtsK protein, which localizes to the division plane, mediates, in part, the interdependence between chromosome segregation and cell division (Wang *et al.*, 2006). The *C. crescentus* FtsI homologue PBP3 accumulates at the new pole at the beginning of the cell cycle and is

recuited to the Z-ring shortly after the Z-ring formation and well before cell constriction starts (Costa *et al.*, 2008). By the time cell constriction is initiated, all PBP3 polar accumulation has disappeared in favour of FtsZ-dependent localization near midcell, consistent with PBP3 function in cell division. Accumulation of PBP3 near the midcell is also highly dynamic with a rapid exchange of PBP3 molecules between midcell and cellular poles during the cell cycle (Costa *et al.*, 2008).

1.4. Cell division in Gram-negative coccus *Neisseria gonorrhoeae*

1.4.1. Morphological analyses of dividing *N. gonorrhoeae*

Unlike rod-shaped *E. coli* cells which divide along a single plane, resulting in two daughter cells (Nanninga, 1998), *N. gonorrhoeae* divides in two planes that are perpendicular to each other (Westling-Haggstrom *et al*., 1977). The first round of division results in diplococci, followed by a second divisional event, in which the division plane is perpendicular to the septum, giving rise to tetrad formation in two-by-two arrangement (Ramirez-Arcos *et al*., 2001a; Westling-Haggstrom *et al.*, 1977). *N. gonorrhoeae* cells usually are seen as a single, pair or a tetrad of cells. Clinically, they often appear as diplococci. The perpendicular planes of cell division pattern in *N. gonorrhoeae* were observed using scanning electron microscopy and transmission election microscopy (Westling-Haggstrom *et al*., 1977).

Using transmission electron microscopy, the earliest visible event of gonococcal cell division appeared to be a slight invagination on one side of the coccus (Fitz-James, 1964). As division proceeded, the growing constrictions did not appear to have any close association with chromosomal material (Fitz-James, 1964); hence, the initial constriction serves as a marker for cell division. Tetrads need to physically separate in order to divide again, since single and diplococcal morphologies are often seen. The physical separation of gonococcal cells from each other may be partly mediated by the product of the *tpc* (tetrapac) gene (Fussenegger *et al*., 1996). Disruption of *tpc* results in over 95% of cells exhibiting a tetrad arrangement that were connected by two layers of PG. Hence, *tpc* may encode a murein hydrolase that would seprate the nascent cell wall PG between divided gonococcal cells (Fussenegger *et al*., 1996).

1.4.2. Microbial and medical importance of *N. gonorrhoeae*

Neisseria gonorrhoeae (Ng) is a Gram-negative coccus that is the etiologic agent of the sexually transmitted disease (STD) gonorrhea. The World Health Organization (WHO, 1995) reported that there are approximately 62 million reported cases of gonorrhea annually worldwide. Globally, the reported rate of infection declined in the late 1980s and early 1990s and rose in late 1990s (WHO, 2009). Canada reported infection rates of 14.9 per 100,000 in 1997 rising to 36.1 in 2007. In 2009, a total of 10,133 cases of gonorrhoea were reported across Canada with a rate of 31 per 100,000 (Public Health Agency of Canada - PHAC). Nevertheless, the actual number of infections is likely much higher due to asymptomatic infections, especially in females.

N. gonorrhoeae is an obligate human pathogen that mainly infects the urogenital epithelia, although cases of infection of the conjuctiva, pharynx, and rectal mucosa are reported as well (Sparling, 1999). The primary site of infection in males is the urethra, characterized by a painful urethral discharge. Women typically experience endocervical infections; however, asymptomatic carriage of the disease is more common in females, making infection seem less obvious. Left untreated, this infection may cause severe complications such as pelvic inflammatory disease (PID) and involuntary infertility in women, or prostatitis and involuntary infertility in men (Howard, 1994, Sparling, 1999). As the microorganism infects mucosal epithelial cells, infections of the eye, throat and anus can also occur (Merz and So, 2000). Newborns can also acquire gonorrhea in their eyes as they pass through an infected birth canal. Rare cases of systemic infection have also been reported, leading to arthritis, endocarditis, and meningitis (Howard, 1994). Gonococcal infections are associated with the transmission of the Human Immunodeficiency Virus (HIV) infection (Chen *et al*., 2003; Cohen, 1998).

N. gonorrhoeae infects by adhering to and invading mucosal epithelial surfaces (Merz and So, 2000). The binding of gonococcal type IV pili and other adhesins can affect host cell signaling and stimulate bacterial ingestion. This is followed by transcytosis of bacteria to the basolateral surface, where they are released to the underlying tissue (Dehio *et al.*, 2000; Merz and So, 2000). A repertoire of virulence factors allows this diplococcus to adapt to many environmental condtions and to escape detection by the immune system. In addition, the surface antigens of *N. gonorrhoeae*, including pilin, opacity (Opa) outer memebrane proteins, and lipooligosaccharide (LOS) are extremely variable (Merz and So, 2000). While the highly variable porins are immunogenic and stable for a given gonococcal strain (Snapper *et al.*, 1997), they are often associated with the reduction-modifiable protein (Rmp) and with LOS. Blocking antibodies to Rmp and LOS impair an appropriate immune response against porin (Elkins *et al*., 1994). Thus both antigenic variation and lack of antigenic exposure ensure that the immune system cannot be effectively stimulated by *N. gonorrhoeae*.

In the absence of a vaccine, infections of *N. gonorrhoeae* are primarily controlled by clinical or laboratory diagnosis coupled with effective treatment with antimicrobial agents. The adequacy of currently recommended antibiotics is in question, as highly prevalent resistant isolates have precluded the use of antibiotics such as penicillins, tetracyclines, and fluoroquinolones (Centers for Disease Control and Prevention (CDC), 2008). Antimicrobial resistance to quinolones occurs in more than 90% of isolates in many areas (WHO, 2003; Yang *et al*., 2006), which has caused many countries to no longer recommend quinolones for the treatment of *N. gonorrhoeae* infections. Currently, the third generation cephalosporins are recommended for the treatment of gonococcal infections worldwide with spectinomycin often cited as an alternative drug (PHAC, 2006; CDC, 2005, 2006). Emerging resistance to third generation cephalosporins poses a significant challenge to maintaining an effective antimicrobial arsenal for the treatment of gonococcal infections (Tapsall, 2009; Dillon and

Pagotto, 1999). Therefore, to overcome resistance, there is an urgency to modify the existing antibiotics extensively to maintain activity against their targets and develop new antibiotics with novel mechanisms of action, new targets, and non-cross antibacterial resistance.

Cell division has been considered as an antibacterial target because it comprises a group of well conserved proteins that are all essential throughout the bacteria, and their activities are completely different from those of the proteins involved in the division of mammalian cells. A number of compounds that act on components of the cell division machinery have been described (Wang *et al.*, 2003; Paradis-Bleau *et al.*, 2007). So far, most of the effort has been directed at the FtsZ protein because it has several biochemical activities that can be assayed *in vitro*. Selective small-molecule inhibitors of FtsZ polymerization or GTPase activity have been screened and identified, which do not affect tubulin and could be new potential candidates for novel antibacterial agents (Paradis-Bleau *et al.*, 2007; Margalit *et al.*, 2004; Wang *et al.*, 2003; Lappchen *et al.*, 2005).

1.4.3. The *dcw* cluster and divisome proteins of *N. gonorrhoeae*

Using raw data from the *N. gonorrhoeae* strain FA1090 genome project (Roe *et al*., 2000), the *dcw* cluster of *N. gonorrhoeae* was identified and assembled (Francis *et al*., 2000). This gene cluster contained 17 genes in the following 5' to 3' order: *mraZ, mraW, ftsLr, ftsI (penA), murE, dca, murF, mraY, murD, ftsW, murG, murC, ddlB, ftsQ, ftsA, ftsZ,* and *hyp* as shown in Fig. 1.1 (Francis *et al*., 2000). The gene order of the gonococcal *dcw* genes was similar to that found in the *E. coli dcw* cluster. *N. gonorrhoeae dcw* cluster also contains genes that differ from *dcw* clusters in other microorganisms (Francis *et al*., 2000; Lutkenhaus and Addinall, 1997; Snyder *et al*., 2001). In *E. coli*, *ftsL* is located between *mraW* and *ftsI*; however, since the putative FtsL protein has only 22% amino acid (aa) similarity to *E. coli* FtsL, there are conflicting reports as to whether *ftsL* is (Snyder *et al*., 2001) or is not (Francis

et al., 2000) part of the *N. gonorrhoeae dcw* cluster. Compared to the *dcw* cluster in *E. coli*, *envA* is absent in the *N. gonorrhoeae dcw* cluster, replaced with a hypothetical protein of unknown (*hyp*) which is co-transcribed with *ftsZ*/*ftsA*/*ftsQ* (Francis *et al*., 2000). An additional gene, *dca* (division cluster associated), implicated in encoding an inner membrane protein that is essential for DNA uptake by *N. gonorrhoeae* competence, is downstream of *murE* (Snyder *et al.*, 2001) in *N. gonorrhoeae*.

Unlike the *E. coli dcw* cluster, which is transcribed as a single unit, the *N. gonorrhoeae dcw* cluster is transcribed as 5 units determined by 4 internal terminators (Francis *et al*., 2000). Three of these terminators consisted of inverted repeats of the gonococcal uptake sequence (5'-GCCGTCTGAA-3'), which were shown to be required for gonococcal DNA transformation and to act as transcriptional terminator sequences (Goodman and Scocca, 1988; Francis *et al*., 2000). These uptake sequence repeats were located at the junctions between *mraY-murD, murD-ftsW,* and *murG-murC* genes. A novel transciptional terminator consisting of a Correia element, a repetitive sequence commonly found in *Neisseria* species, was also found to act between *murF* and *mraY* (Francis *et al*., 2000). However, there is conflicting evidence for the role of this Correia element, as others studying the *dcw* clusters of *N. gonorrhoeae*, and the closely related *N. meningitidis*, have shown that the Correia element does not act to terminate transcription within the *dcw* cluster (Snyder *et al*., 2003). *N. gonorrhoeae* cell division genes *ftsL* and *ftsI* are in the first transcriptional unit, *ftsW* is in the fourth transcriptional unit and, *ftsZ, ftsA* and *ftsQ* are in the fifth transcription unit (Fig. 1.1) (Francis *et al.*, 2000).

Cell division site selection in *N. gonorrhoeae*

Interestingly, Min proteins (including MinC, MinD and MinE) were identified in Gram-negative coccus *N. gonorrhoeae*, which does not have an intrinsically obvious midcell (Ramirez-Arcos *et al.*, 2001b). *N. gonorrhoeae* Min proteins function similarly to their *E. coli*

equivalents to decide the placement of the Z-ring. *N. gonorrhoeae* MinC and MinD form the inhibitory complex MinCD and the topological specificity activity of MinE drives the oscillation of MinCD from the cell pole to pole, thereby allowing FtsZ polymerization at the midcell site (Ramirez-Arcos *et al.*, 2001b; Szeto *et al*., 2004, 2005; Eng *et al*., 2006).

***N. gonorrhoeae* FtsZ**

The gonococcal *ftsZ* gene was first identified using raw data from the *N. gonorrhoeae* FA1090 genome project (Salimnia *et al*., 2000). Gonococcal FtsZ ($FtsZ_{Ng}$) is 392 aa, 41.5 kDa protein that has high identity (95-98%) with FtsZ from *N. meningitidis.* The protein also has 67% and 65% identity with FtsZ from *E. coli* and *B. subtilis*, respectively. FtsZ was likely essential for gonococcal survival since all attempts to generate a *N. gonorrhoeae ftsZ* knockout were unsuccessful (Salimnia *et al*., 2000). $FtsZ_{Ng}$ localized at the division site as determined by immunogold fluorescence microscopy (Fig. 1.7). Overexpression of GFP-$FtsZ_{Ng}$ in *N. gonorrhoeae* from a shuttle vector resulted in the formation of aberrant cells that had multiple and atypically positioned division sites. However, most of the GFP fusion protein was insoluble and subcellular localization of FtsZ within the gonococcus was not possible (Salimnia *et al*., 2000). Furthermore, *E. coli* is an often used host organism to test the functionality of cell division proteins from other bacteria (Szeto *et al*., 2001, 2004; Ramirez-Arcos *et al.*, 2002, 2005). $FtsZ_{Ng}$ also exhibited cross-species functionality in *E. coli* and overexpression of $FtsZ_{Ng}$ could inhibit cell division in wild-type *E. coli* (Ramirez-Arcos *et al.*, 2002, 2005). A GFP-$FtsZ_{Ng}$ fusion could localize to the midcell in *E. coli*, similar to *E. coli* FtsZ (Salimnia *et al*., 2000).

$FtsZ_{Ng}$ expression can be regulated depending on environmental conditions. There are at least six promoters that control the expression of $ftsZ_{Ng}$ (Francis *et al*., 2000) and three of them are upstream of $ftsZ_{Ng}$ (Ramirez-Arcos *et al.*, 2001a). Under conditions of anaerobiosis, the $ftsZ_{Ng}$ promoter region had a significantly higher expression level than under aerobic

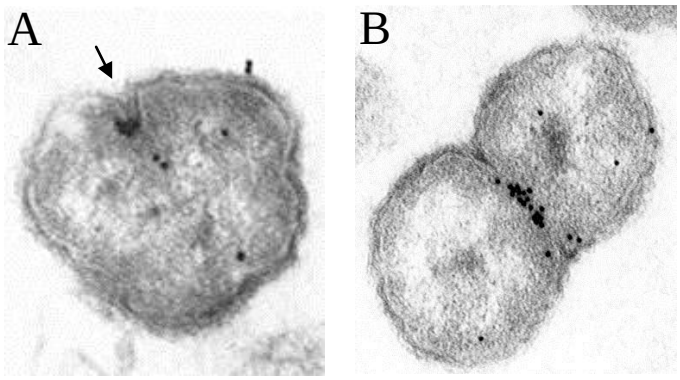

Fig. 1.7. Immunogold localization of *N. gonorrhoeae* FtsZ in dividing gonococcal cells. (A) In individual cocci, cell division is initiated at a single invagination point (arrows), where distinct accumulation of $FtsZ_{Ng}$ is observed (black dots). (B) As division proceeds, a single band of $FtsZ_{Ng}$ signal is observed between two daughter cells, prior to the formation of a diplococcus. (Adapted from Szeto Ph.D. thesis, 2004).

conditions. The promoter region directly upstream of *ftsZ*$_{Ng}$, particularly the most proximal promoter, is the most active under anaerobic conditions (Francis *et al*., 2000; Ramirez-Arcos *et al.*, 2001a). Interestingly, FtsZ$_{Ng}$ expression decreased in the presence of urea (Ramirez-Arcos *et al.*, 2001a). Since FtsZ$_{Ng}$ and other cell division proteins are partly regulated by environmental conditions, these findings provide a possible explanation that *N. gonorrhoeae* adapts to the environmental stress by mimicing the host genitourinary tract (Ramirez-Arcos *et al.*, 2001a).

Other cell division proteins in *N. gonorrhoeae*

ZipA is not conserved in bacteria and was thought not to be present in *N. gonorrhoeae*. However, a genetic screening approach and sequence analysis revealed that *N. gonorrhoeae* gene, SLO7ORF3 (called *zipA*$_{Ng}$), appears to be essential in *N. gonorrhoeae* since it was not possible to generate null mutations in the gene (Du and Arvidson, 2003). This gene shares some features with *zipA* of *E. coli* (Du and Arvidson, 2003). These features included similar chromosomal locations (with respect to linked genes) as well as similarities in the predicted protein domain structures. *E. coli* ZipA showed no significant similarities in its primary sequences to ZipA from *N. gonorrhoeae*. ZipA$_{Ng}$ is 428 residues, is larger than *E. coli* ZipA at 328 residues. However, both ZipA$_{Ec}$ and ZipA$_{Ng}$ have an unusually high number of proline and glutamine residues in the C-terminal region. Further amino acid sequence alignment showed that there is significant similiarity in this C-terminal region, supporting the idea of an ortholog of ZipA in *N. gonorrhoeae* (Du and Arvidson, 2003). These two proteins also share features of their predicted secondary protein structure (Du and Arvidson, 2003). In addition, ZipA$_{Ng}$ can complement the growth defect caused by ZipA$_{Ec}$ depletion in *E. coli*, but it only partially alleviates the defect in cell division (Du and Arvidson, 2003). These findings indicate that ZipA$_{Ng}$ is structurally and functionally related to the cell division protein ZipA of *E. coli*. Further studies are needed to examine if this protein is involved in Z-

ring stabilization and the recruitment of divisome proteins downstream of FtsA in *N. gonorrhoeae*.

As with *ftsZ*$_{Ng}$, the expression of FtsE$_{Ng}$ and FtsX$_{Ng}$ were also increased under anaerobiosis (Ramirez-Arcos *et al.*, 2001a). Sequence analysis of FtsE$_{Ng}$ and alignment with other FtsE indicated that it contained the conserved motif of ABC domains while the sequence alignment of FtsX$_{Ng}$ with other published FtsX sequences predicted that they all contain 4 transmembrane segmenents and a conserved motif which may prove to be important for FtsX function (Bernatchez *et al.*, 2000). Disrupting *ftsE*$_{Ng}$ and *ftsX*$_{Ng}$ by insertional mutagenesis did not alter the viability of mutant *N. gonorrhoeae* cells, suggesting that these genes were not essential to the gonococcus (Bernatchez *et al.*, 2000). However, transmission electron microscopy indicated that these mutants displayed aberrant gonococcal morphologies, indicating defective divisional patterns (Bernatchez *et al.*, 2000).

Since divisome components have been successfully targeted by antimicrobial compounds, understanding the mechanistic details of cell division in *N. gonorrhoeae* may therefore open unexplored possibilities of the development of new antibacterial agents for treating gonococcal infections. However, the mechanisms of cell division have been mostly investigated in rod-shaped model organisms, such as *E. coli* and *B. subtilis*. It is presently unknown how round bacteria, including *N. gonorrhoeae,* form a divisome at the midcell. Our laboratory has investigated the *dcw* cluster of genes in the gonococcus and various proteins (e.g. FtsZ, FtsA, FtsW, FtsI and FtsQ) implicated in divisome formation have been identified in *N. gonorrhoeae* (Francis *et al*., 2000). It is unknown whether these proteins actually interact and form protein complexes in *N. gonorrhoeae*. Since the role of FtsZ in cell division in *N. gonorrhoeae* has been previously studied (Salimnia *et al.*, 2000), this project focused on FtsA and initiated studies on divisome formation in *N. gonorrhoeae*.

1.5. Functionality of FtsA from various bacteria

1.5.1. FtsA Structure and ATPase Activity

FtsA, a conserved essential cell divsion protein, belongs to the actin/Hsp70/sugar kinase ATPase superfamily (Bork *et al.*, 1992). The crystal structure of FtsA from *Thermotoga maritima* (Tm, Fig. 1.8) shows that it is structurally similar to actin expecting for the presence of the 1C domain with a different spatial position within the molecule and the absence of 1B domain of actin (van den Ent and Löwe, 2000). The protein has the classical two-domain structure of actin family members, each of which can be further divided into two subdomians: two core subdomains (1A and 2A), forming the nucleotide-binding cleft, and two subdomains (1C and 2B) at opposite sides of the core (Fig. 1.8) (van den Ent and Löwe, 2000).

FtsA has been shown to bind ATP and FtsA T215 and G336 mutations reduce FtsA ATP binding activity (Sanchez *et al.*, 1994). The ATPase activity of FtsA has so far only been reported in *B. subtilis*, but not in other bacteria (Feucht *et al.*, 2001). Purified FtsA from *S. pneumoniae* is able to bind various nucleotides, the affinity being highest for ATP, and lower for other triphosphates and diphosphates (e.g. ATP is favoured over ADP, which is favoured over AMP) (Lara *et al.*, 2005). Furthermore, FtsA from *S. pneumoniae* has been reported to polymerize into corkscrew-like helices *in vitro* in a nucleotide-dependent manner. The polymers composed of 2+2 paired protofilaments are extremely stable in the presence of ATP and less stable in the present of ADP (Lara *et al.*, 2005). The report suggests a role for nucleotide hydrolysis in the regulation of FtsA polyerization.

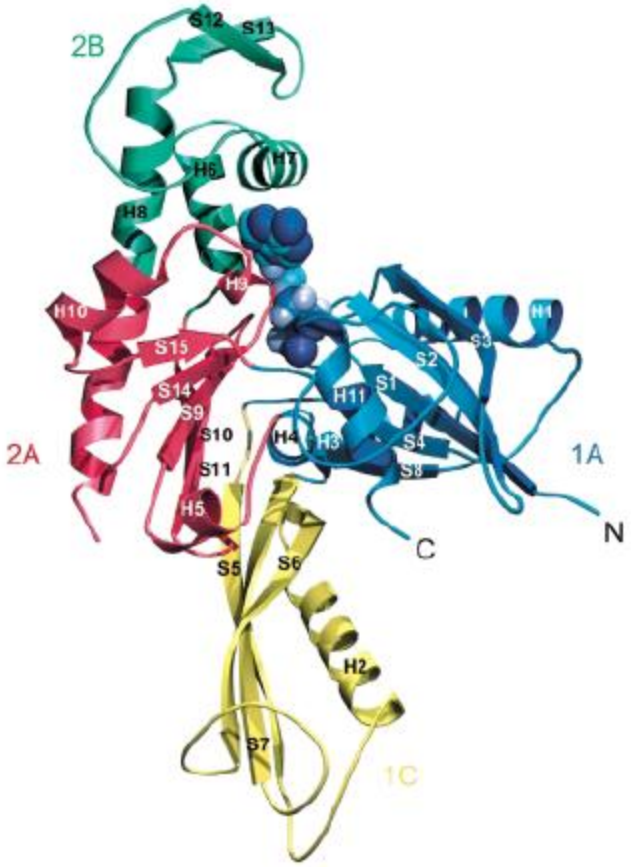

Fig. 1.8. Ribbon plot of the crystal structure of *T. maritima* FtsA. The structure is divided into four domains, in analogy to the action family of protein, which are designated 1A (blue), the FtsA-specific domain 1C (yellow), subdomain 2A (red) and subdomain 2B (green).(van den Ent *et al*., 2000).

1.5.2. The role of FtsA to tether the Z-ring to the membrane and stabilize the Z-ring

FtsA plays a role in anchoring the Z-ring to the cell membrane via its highly conserved membrane-targeting sequence (MTS) at its extreme C-terminus (Pichoff and Lutkenhaus, 2005). Deletion of the MTS renders FtsA non-functional and causes the protein to assemble into deleterious cytoplasmic rods (Pichoff and Lutkenhaus, 2005). Mutagenesis analysis indicated that amino acid W415 of FtsA localized in this region which is essential for Z-ring localization (Yim *et al*., 2000). In contrast to ZipA, the MTS of FtsA does not appear to be specific as it can be replaced by various unrelated MTSs (Pichoff and Lutkenhaus, 2005; Shiomi and Margolin, 2007a).

Aside from its role in Z-ring membrane binding, FtsA has been found to affect the integrity and stability of the Z-ring at various stages of divisome assembly (Pichoff and Lutkenhaus, 2007; Shiomi and Margolin, 2007b; Bernard *et al*., 2007). FtsA stabilizes the Z-ring by its direct interaction with FtsZ. The interaction between the two proteins has been shown *in vivo* and *in vitro* in different bacteria using various protein assays, such as two-hybrid assays, Co-IP assay and GST pull-down assay (Descoteaux and Drapeau, 1987; Vicente and Errington, 1996; Wang *et al*., 1997; Din *et al*., 1998; Ma and Margolin 1999; Yan *et al*., 2000). In addition, FtsA was shown to co-localize with FtsZ to the Z-ring in various bacteria (e.g. *E. coli, B. subtilis* and *S. pneumoniae*) using immuno-fluorescence microscopy studies (Addinall *et al*., 1996; Ma *et al*., 1996; Feucht *et al*., 2001; Lara *et al*., 2005). The 2B domain of FtsA is implicated in its interaction with FtsZ in *E. coli* (Pichoff and Lutkenhaus, 2007). Besides the interaction with FtsZ, domain 2B of FtsA is likely to have additional functions in cell division. The S12-S13 strands of domain 2B in FtsA affect the localization of the Z-ring as deletion of this region induces formation of misplaced rings (Rico *et al*., 2004). A couple of *E. coli* FtsA mutations, mapped to domain 2B and its adjacent region, were found to either reduce FtsA ATP binding ability (T215 or G336) (Sanchez *et al*.,

1994) or bypass the need for ZipA and FtsK in divisome formation (FtsAR286W, also called FtsA*, discussed below) (Geissler *et al*., 2003, 2007).

A recent study indicates that dimerization or oligomerization of FtsA enhances the integrity of the Z-ring (Shiomi and Margolin, 2007b). FtsA-FtsA interaction from *E. coli* has been demonstrated in both yeast two-hybrid (Y2H) and B2H system (Rico *et al*., 2004; Pichoff and Lutkenhaus, 2007; Di Lallo *et al*., 2003; Karimova *et al*., 2005). FtsA also formed in dimers in *B. subtilis* (Feucht *et al*., 2001) and purified FtsA polymerized *in vitro* in the presence of ATP and Mg^{2+} (Lara *et al*., 2005). Structural modeling suggests that FtsA dimerizes in a head-to-tail fashion, with the individual subunits rotated 180° to one another and predicted that specific portions of domains 1A, 1C, and 2B form a dimmer interface (Carettoni *et al*., 2003). Domain 1C and the C-terminus were subsequently shown to be required for FtsA self-interaction (Rico *et al*., 2004; Yim *et al*., 2000). Recently a mutagenesis study on FtsA mutation M71A shows that domain 1A is also specifically involved in FtsA self-interaction and this interaction is crucial for the integrity of the Z-ring (Shiomi and Margolin, 2007b).

An *E. coli* FtsA gain-of-function allele R286W, also call FtsA*, bypasses the requiement for ZipA and partially for FtsK (Geissler *et al*., 2003, 2007). Compared to wild-type FtsA, the presence of FtsA* accelerates the reassembly of Z-rings, and suppressed the cell-division block caused by excessively high levels of FtsZ, ZipA and MinC (Geissler *et al*., 2003, 2007). FtsA* interacts more strongly with FtsZ than does wild-type FtsA (Geissler *et al*., 2007). These results suggest that FtsA* has an altered interaction with FtsZ, which in turn enhances the stability of the Z-ring. In addtion, another gain-of-function mutation (FtsAE124G) in FtsA of *E. coli*, which shares some properties with the previously isolated FtsA*, can bypass the requirement for FtsN by increasing the integrity of the Z-ring (Bernard *et al*., 2007).

1.5.3. The ratio of FtsA to FtsZ is critical for cell division

In *E. coli*, overexpression of either FtsZ or FtsA inhibits the cell division process (Wang and Gayda, 1990), which can be suppressed by increasing the level of the other protein, re-establishing the proper ratio (Dai and Lutkenhaus, 1992; Dewar *et al*., 1992). This suggests that a certain ratio of FtsZ to FtsA is required for proper cell division to occur (Dai and Lutkenhaus, 1992; Dewar *et al*., 1992). A recent study in *E. coli* also demonstrated an FtsA:FtsZ ratio of 1:5 (Rueda *et al.*, 2003), although a previous study indicated that the ratio was 1:100 (Wang and Gayda, 1992). The ratio of FtsA to FtsZ was observed to be 1:1.5 in *S. pneumoniae* (Lara *et al.*, 2005) and 1:5 in *B. subtilis* (Feucht *et al*., 2001). The block to division appears to result from a disturbance in Z-ring structure. Once the level of any one of the proteins is increased, the Z-ring appaears to dissipate into spirals that are spread along the length of the cell, at least in *E. coli* (Ma *et al*., 1996; Pichoff and Lutkenhaus, 2005). In contrast, cell division is relatively insensitive to an increase in levels of late divisome proteins.

1.5.4. The role of FtsA in the recruitment of late divisome proteins

Several lines of evidence suggests that FtsA is required for recruitment of downstream division proteins (including FtsQ, FtsI and FtsN) in *E. coli* and that domain 1C is responsible for the recruiment (Corbin *et al*., 2004; Rico *et al*., 2004). Two different interaction networks (interactome) of divisome proteins have been established in *E. coli* and *S. pneumoniae* using B2H approaches, which provide evidence for interactions between FtsA and other essential divisome proteins (Di Lallo *et al*., 2003; Karimova *et al*., 2005; Maggi *et al*., 2008). FtsA interacts with FtsI, FtsQ and FtsN in *E. coli* while FtsA interacts with FtsI, FtsL and FtsK in *S. pneumoniae*. In contrast, *E. coli* ZipA interacts with FtsZ only as determined using B2H

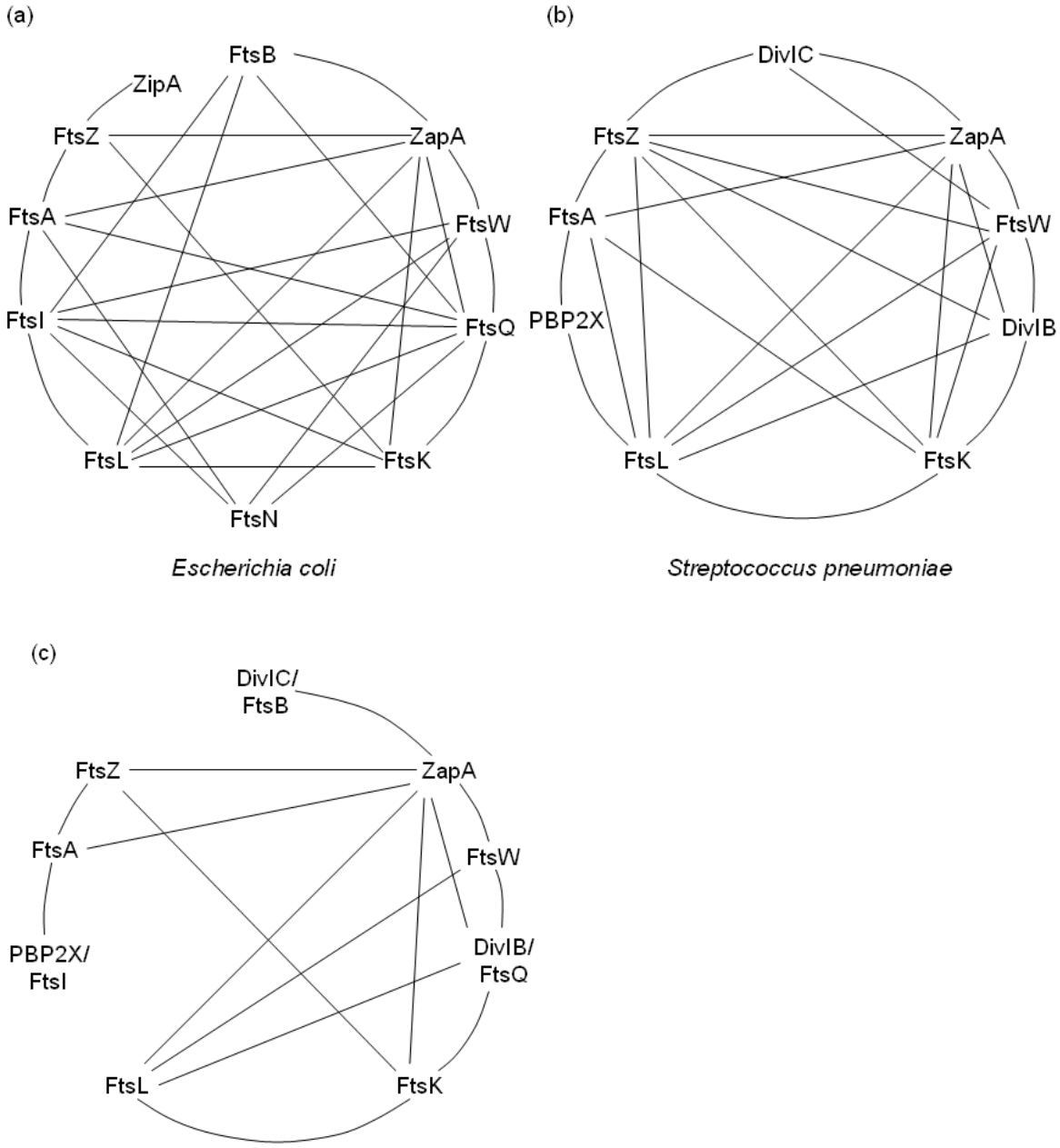

Fig. 1.9. Interaction networks of divisome proteins from *E. coli* and *S. pneumoniae* (a) Schematic drawing of the protein-protein interactions among the *E. coli* divisome proteins found in systematic functional B2H assays (Di Lallo *et al*., 2003; Karimova *et al*., 2006). (B) Schematic drawing of the protein-protein interactions among the *E. coli* divisome proteins found in systematic functional B2H assays (Maggi *et al*., 2008). (c). Schematic drawing of conserved protein interactions in both *E. coli* and *S. pneumoniae*.

assay (Di Lallo *et al*., 2003) and *S. pneumoniae* lacks a ZipA homologue (Fig. 1.9). Despite the interactions between FtsA and other divisome proteins have been identified, the FtsA domains involved in these interactions and the biological significance of these interactions in divisome formation have not been identified although the 1C domain was shown to recruit the late proteins in *E. coli*.

Although both FtsA and ZipA have overlapping functions in the stabilization of the Z-ring and the recruitment of late proteins, the role of FtsA is thought to be more important and direct. First, FtsA* bypasses the requirement of ZipA, indicating that ZipA may not be directly involved in the recruitment (Geissler *et al*., 2003). FtsA* is more resistant to the destabilizing effects of the inhibitor MinC. Second, FtsA not only interacts with FtsZ but also interacts with other proteins (FtsI, FtsQ, and FtsN) as determined by two-hybrid systems, while ZipA interact with FtsZ only rather than other divisome proteins in *E. coli* (Di Lallo *et al*., 2003; Karimova *et al*., 2005). In addition, FtsA is more widely conserved, while ZipA is less conserved and only found in bacteria closely related to *E. coli*, although some Gram-positive bacteria have a protein with a topologically similar role (Hale and de Boer, 1997; Levin *et al*., 1999), suggesting that the role of ZipA has either been replaced or become redundant (Hale and de Boer, 1997).

1.6. Hypothesis and Objectives

Hypothesis: Because the *dcw* cluster in *N. gonorrhoeae* is different from other known *dcw* clusters, *N. gonorrhoeae* FtsA might interact with different divisome proteins from this bacteria and novel functional domains of FtsA might be involved in these interactions.

Thus, the role of FtsA may provide insight to its unique properties in divisome protein interactions in *N. gonorrheae*.

Objectives:

1. To investigate the interactions amongst divisome proteins identified in *N. gonorrhoeae* using a bacterial two-hybrid assay. The interactome of *N. gonorrhoeae* will be compared with those of *E. coli* and *S. pneumoniae*, which have been established using the same protein interaction assays.
2. To identify the functional domains of $FtsA_{Ng}$ which are involved in interactions with $FtsZ_{Ng}$ and other division partners using gene truncations and protein interaction assays.
   a) Create FtsA truncations based on $FtsA_{Ng}$ homology structural modeling
   b) Examine the interactions of FtsA domains with FtsZ using both bacterial two-hybrid and GST pull-down assays;
   c) Examine the interactions of FtsA domains with other divisome proteins using bacterial two-hybrid assay.
3. To characterize the $FtsA_{Ng}$ function in its native organism, testing the ratio of FtsA to FtsZ and observating its localization in gonococcal cells using immuno-fluorescence microscopy.
4. To investigate the use of *E. coli* as an indicator system for studying $FtsA_{Ng}$ function. This will be achieved by heterologous expression studies of $FtsA_{Ng}$ in *E. coli* strains, coupled with examination of cell morphology, growth studies, and protein localization studies

using GFP-fusions. In addition, the ability of $FtsA_{Ng}$ to complement an *E. coli ftsA*-depletion strain and to interact with *E. coli* FtsA and FtsZ will be examined.

CHAPTER 2 MATERIALS AND METHODS

2.1. Strains and growth conditions

The bacterial strains and plasmids used in this study are presented in Table 1. *E. coli* DH5α and XL1-Blue were used as hosts for cloning. *E. coli* C41 (*DE3*) was used to overexpress proteins for purification of His-tagged Fts_{Ng} proteins. *E. coli* PB103 and KJB24 were used as heterologous backgrounds for the overexpression of $FtsA_{Ng}$ (Szeto *et al.*, 2001). *E. coli* P163 (Pichoff and Lutkenhaus, 2007) was used in complementation assays. *E. coli* R721 was used for B2H assays (Di Lello *et al*., 2001). *E. coli* DH5α, XL1-Blue, C41 and PB103 were grown at 37°C for 14-18 hours (hr) on Luria-Bertani (LB) medium (Difco, Becton, Dickinson Company, Sparks, MD, USA). *E. coli* R721 was incubated at 34°C and P163 was incubated at 30°C in LB medium. Any liquid cultures of the above were incubated with orbital shaking at 200 rotations per minute (rpm).

N. gonorrhoeae CH811 was used as template to amplify division genes by polymerase chain reaction (PCR) (Picard and Dillon, 1989). *N. gonorrhoeae* CH811, F62 and FA1090 were used to test the ratio of FtsA to FtsZ. All gonococcal strains were grown on GC medium base agar (GCMB, Oakville, ON) supplemented with Kellogg's defined supplement (GCMBK, 40 g D-glucose, 1 g glutamine, 10 ml of 0.5% ferric nitrate and 1 ml of 20% cocarboxylase per liter) at 35°C, in a humid, 5% CO_2 environment for 18 to 24 hrs (Kellogg *et al.*, 1963; Pagotto *et al.*, 2000). Cultures of *N. gonorrhoeae* were grown in liquid GCMBK supplemented with 0.04% $NaHCO_3$ with 5% CO_2 and shaking at 200 rpm at 35°C.

When required, antibiotics were added to LB medium in the following concentrations: 100 µg/ml ampicillin (Amp, Sigma, Oakville, ON), 50 µg /ml kanamycin (Kan, Sigma) for general bacterial selection. The B2H assays required the following concentrations: 34 µg /ml chloramphenicol (Cm, Sigma); 30 g/ml Kan and 50 g/ml Amp for the selection of double plasmid transformation.

Table 2.1. Bacterial strains used in the present study

Stain	Relevant characteristics	Source/reference
E. coli DH5□	*supE44* Δ*lacU169 (80lacZΔM15) hsdR17 endA1 gyrA96 thi-1 relA1*	Gibco
E. coli XL1-Blue	*recA1 endA1 gyrA96 thi-1 hsdR17 supE44 relA1 lac* [*F' proAB lacI*^{q} *ZΔM15]* Tn10	Stratagene
E. coli C41 (*DE3*)	F^{-} *ompT hsdS*$_{B}$ (r$^{-}_{B}$ m$^{-}_{B}$) *gal dcm Δ* (*srl-recA*) 306::Tn*10* (Tet^{r}) (*DE3*)	Miroux and Walker, 1996
E. coli PB103	*dadRI trpE61 trpA62 tna-5 purB*$^{+}$	de Boer *et al*., 1988
E. coli KJB24	W3110 [*rodA (Am)*]	Begg and Donachie，1998
E. coli P163	CH2 (*recA*::Tn*10 ftsA*^{0})/pDB280 (*repA*^{ts} *ftsA*$^{+}$)	Hale and de Boer, 1999
E. coli R721	*supE thy* D(*lac-proAB*) F' [*proAB*$^{+}$ *lacI*^{q} *lacZ*DM15] *glpT*::O-P$_{434/P22}$*lacZ*	Di Dello *et al*., 2001
N. gonorrhoeae CH811	Auxotype (A)/serotype (S)/plasmid content (P) class: nonrequiring/IB-2/plasmid-free, Str^{r}	Picard and Dillon, 1989
N.gonorrhoeae F62	A/ S/ P: proline/IB-7/2.6	West *et al.*, 1989
N. gonorrhoeae FA1090	A/ S/ P: proline/IB-2/2.6	West *et al*., 1989

E. coli and *N. gonorrhoeae* stock cultures were prepared in 2 ml polypropylene microtubes (Sarstedt, Montreal, QC) in brain heart infusion (BHI) broth (Difco) containing 20% glycerol and were stored at –80°C. Yeast cells to be frozen at –80°C were stored in YPAD with 20% glycerol as stated in the Clontech Yeast Manual.

2.2. Identification of *ftsA* in *N. gonorrhoeae*

2.2.1. *N. gonorrhoeae ftsA* gene sequence and protein sequence alignment of FtsA homilogues

The nucleotide and amino acid sequences of $FtsA_{Ng}$ were made available at the National Centre for Biotechnology Information (GenBank accession number YP_208577). To identify homologues of FtsA, $FtsA_{Ng}$ protein sequence from *N. gonorrhoeae* FA1090 was used for a BLAST search of the National Center for Biotechnology Information database (http://www.ncbi.nlm,nih,gov/). Protein sequences of FtsAs with ≥ 50% identity to $FtsA_{Ng}$ were used in multiple sequences alignments using Clustal W (http://searchlauncher.bcm.tmc.edu/multi-align/mutil-align.html). $FtsA_{Ec}$ was also included in the sequence alignment, it is 41% identical to $FtsA_{Ng}$. To obtain the percentages of identity and similarity, individual FtsA sequences were aligned with using the align tool on NCBI.

2.2.2. Structural homology modeling of *N. gonorrhoeae* FtsA

Homology modeling of $FtsA_{Ng}$ was generated by SWISS (Version 3.7) (http://swissmodel.expasy.org/) using the resolved crystal structure of *T. maritima* FtsA (PDB code, 1E4F, van den Ent and Lowe, 2000) as template.

2.3. Oligonucleotide primer design and PCR methods

Oligonucleotide primers (Table 2) were designed manually and synthesized by Invitrogen (Burlington, Ontario, Canada) for the PCR and DNA sequencing. Whole-cell

suspensions of *N. gonorrhoeae* CH811 or *E. coli* PB103 were used to provide chromosomal DNA templates for PCR reactions. The PCRs were performed in a GeneAmp® PCR system 9700 (Applied Biosystems, Foster City, CA, USA) as follows: 4 minutes (min) at 94°C; 30 cycles of denaturation for 1 min at 94°C, annealing for 45 seconds (s) at 55°C and extension for 1.5 mins at 72°C; 10 mins at 72°C; and held at 20°C.

PCR was performed in 100-µl (final volume) mixtures: 71.5 µl of double-distilled H_2O (ddH_2O), 10 µl of 10x PCR buffer containing 15 mM $MgCl_2$, 4 µl of 10 mM deoxynucleoside triphosphate (dNTP), 2 µl of each primer (0.2 µg/ml), 0.5 µl of Taq DNA polymerase (5 U/µl) (New England BioLabs, Ontario, Canada), and 10 µl of template cell suspension. For chromosomal DNA templates, *N. gonorrhoeae* CH811 and *E. coli* PB103 cell suspensions were prepared by resuspending cells from overnight (o/n) agar cultures in ddH_2O.

2.4. DNA purification, high-yield plasmid purification, and agarose gel electrophoresis methods

PCR amplicons and plasmid DNA that was biochemically modified (i.e. restriction endonuclease digestion, phosphorylation) were purified using the PCR Purification Kit (Qiagen, Mississauga, ON) in order to remove residual salts and nucleotides. Plasmids were isolated from *E. coli* using the Miniprep Kit (Qiagen) according to the manufacturer's instructions. DNA was separated on 1-2 % agarose gels using Tris-acetate EDTA (TAE) buffer (40 mM Tris-acetate, 1 mM EDTA) at various voltages and times, as required. The gels were stained in 1 mg/ml ethidium bromide solution and the DNA in agarose gels was visualized using an ultraviolet illuminator and photographed with the MultiImage Light Cabinet using Alpha Imager 1220 (Alpha Innotech, San Leandro, CA). Sizes of DNA fragments were approximated using 1 kilobase (Kb) plus DNA ladder and supercoiled DNA ladder (Invitrogen).

2.5. Gene cloning

2.5.1. Construction of plasmids for $FtsA_{Ng}$ overexpression studies

Gonococcal *ftsA* was PCR amplified from *N. gonorrhoeae* CH811 using primers P1 and P2 (Table 2). The amplicon was digested with EcoRI and BamHI and ligated into EcoRI/BamHI-digested pUC18 (Amersham Pharmacia Biotech, Montreal, Quebec, Canada), creating pUC18A (Table 3), which was transformed into *E. coli* strains to assess the effects of $FtsA_{Ng}$ expression in *E. coli* backgrounds, i.e. for the morphology of *E. coli* cells and localization of $FtsA_{Ng}$. The pUC18 vector was also transformed into *E. coli* strains as a negative control.

To construct an N-terminal EGFP (enhanced green fluorescent protein) fusion, *egfp* was amplified from plasmid pEGFP (Clontech, Mountain View, CA, USA) using primers P3/P4 (Table 2). pUC18A was digested with EcoRI and treated with Calf Intestinal Alkaline Phosphatase (CIAP) to remove 5′ or 3’ phosphates from nucleic acids. The *egfp* amplicon was digested with EcoRI and ligated into EcoRI-digested pUC18A (Table 3) to create pUC18EA in which *egfp* was fused to the N-terminus of $ftsA_{Ng}$. To construct an EGFP C-terminal fusion, $ftsA_{Ng}$ was PCR amplified from *N. gonorrhoeae* CH811 using primers P1/P5 (Table 2), and *egfp* was amplified from pEGFP with primers P6/P7 (Table 2). The SalI/HindIII-digested *egfp* amplicon was ligated to the C-terminus of EcoRI/SalI-digested $ftsA_{Ng}$ and then ligated into EcoRI/HindIII-digested pUC18, generating pUC18AE (Table 3). Both pUC18AE and pUC18EA were used to study the localization of $FtsA_{Ng}$ in *E. coli* cells.

2.5.2. Construction of plasmids for antibody production

Wild-type $ftsZ_{Ng}$ and $ftsA_{Ng}$ were PCR amplified from *N. gonorrhoeae* CH811 chromosomal DNA using the following primers: $ftsZ_{Ng}$- P42/P43; $ftsA_{Ng}$- P44/P45 (Table 2). The amplicons were digested with *EcoRI*/*BglII* and ligated into pre-digested pET30a to create pETZ and pETA, respectively (Table 3). The resultant plasmids were transformed

Table 2.2. Primer sequences used in present study

Primer name		Sequences (5'-3')
P1	ftsA-FwEcoRI-pUC18	ATTACGAATTCGATGGAACAGCAGAAAAGATACATC
P2	ftsA-reBamHI-Y2H	CCCGGGGATCCTCAGAGGTTGTTTTCAATCCACC
P3	FwEcoRI-EGFP	ATTACGAATTCGATGGTGAGCAAGGGCGAGGAG
P4	ReEcoRI-EGFP	ATTACGAATTCGCTTGTACAGCTCGTCCATGCC
P5	ftsA-ReSalI-pUC18	TGCAGGTCGACTGAGGTTGTTTTCAATCCACCG
P6	EGFP-FwSalI-pUC18	TGCAGGTCGACTTATGGTGAGCAAGGGCGAGGAG
P7	EGFP-ReHindIII-pUC18	TCTCTCAAGCTTGTTACTTGTACAGCTCGTCCAT
P8	EcFtsA-FwBamHI-pET30a	CGCGGGATCCATGATCAAGGCGACGGACAGAAAA
P9	EcFtsA-ReSalI-pET30a	GCGCGTCGACTTAAAACTCTTTTCGCAGCCAACT
P10	ftsA-fwEcoRI-Y2H	CGCCGGAATTCATGGAACAGCAGAAAAGATACATC
P11	FtsA-reBamHI	GCGCGGATCCTCAGAGGTTGTTTTCAATCC
P12	FtsA-FwSalI	GCGCGTCGACCATGGAACAGCAGAAAAGATAC
P13	ReftsAT1-BamHI	CGCGGGATCCTCATGCACCGGTAATGATGTGCACCCG
P14	ReftsAT2-BamHI	CGCGGGATCCTCACACCGCCTGCCCGCTTGCCAACGG
P15	ReftsAT3-BamHI	CGCGGGATCCTCAAATGACGGACGTATGGCGGATGGC
P16	FwftsAT4-SalI	GCGCGTCGACCCCGGCCGGTGGTAATCTGATTACC
P17	ReftsAT4-BamHI	CGCGGGATCCTCACTCCTGAATACGTGCGCTGATGAT
P18	ReftsAT5-BamHI	CGCGGGATCCTCAACCGGTGCGTACAGGCAAATCGAA
P19	FwftsAT7-SalI	GCGCGTCGACCATTTTTGGCGTAGTGCTGGGCGAACTGCAA
P20	FwftsAT8-SalI	GCGCGTCGACCGCGCCCCAAGAAATGGGCGGTTTGTCCGAC
P21	fwBglII-ZipA1	GCGCGAGATCTGATGATTTACATCGTACTGTTCCTC
P22	fwPstI-ZipA2	GCGCGCTGCAGAATGATTTACATCGTACTGTTCCTC
P23	reBamHI-ZipA	CGCGGGATCCTTATGAAAACAGGCGCAGGGC
P24	fwSalI-ftsK	GCGCGTCGACCATGTTTTGGATAGTTTTGATCGTTAT
P25	reBamHI-ftsK	CGCGGGATCCTCAAGCATTGTCCAAGGGGACGAG
P26	fwSalI-ftsI	GCGCGTCGACCATGTTGATTAAAAGCGAATATAAGCC
P27	reBamHI-ftsI	CGCGGGATCCTTAAGACGGTGTTTTGACGGCTGC
P28	fwSalI-ftsW	GCGCGTCGACCATGAAGATTTCGGAAGTATTGGTAAA

P29	reBamHI-ftsW	CGCGGGATCCTTACTCCACCCGGTAACCGCGCAT
P30	fwSalI-ftsQ	GCGCGTCGACCATGTGGGATAATGCCGAAGCGATG
P31	reBamHI-ftsQ	CGCGGGATCCCTATTCTTCGGATTCTTTTTCGGG
P32	fwSalI-ftsN	GCGCGTCGACCATGTTTATGAACAAATTTTCCCAATC
P33	reBamHI-ftsN	CGCGGGATCCTTATTTGCCTTCAATCGCACGGAT
P34	fwSalI-ftsE	GCGCGTCGACCATGATCCGTTTCGAACAAGTTTCC
P35	reBamHI-ftsE	CGCGGGATCCTCATGCGAGTCGTCCTTTCGAGAG
P36	fwSalI-ftsX	GCGCGTCGACCATGAGCATCATCCACTACTTCTCG
P37	reBamHI-ftsX	CGCGGGATCCTTATTTTTTGGCTTTGAAGCAGAG
P38	EcFtsZ-fwSalI-B2H	GCGCGTCGACCATGTTTGAACCAATGGAACTTACC
P39	EcFtsZ-reBamHI-B2H	CGCGGGATCCTTAATCAGCTTGCTTACGCAGGAA
P40	EcFtsA-FwSalI-B2H	GCGCGTCGACCATGATCAAGGCGACGGACAGAAAA
P41	EcFtsA-reBamHI-B2H	CGCGGGATCCTTAAAACTCTTTTCGCAGCCAACT
P42	FtsZ-fwBgl II-pET30a	AGCCCAGATCTGATGGAATTTGTTTACGACGTGGCA
P43	FtsZ-ReEcoRI-pET30a	AGCCCGAATTCTTATTTGTCTGAATTGTGTTGACG
P44	FtsA-reEcoRI-pET30a	ATATCGAATTCTCAGAGGTTGTTTTCAATCCACC
P45	FtsA-fwBglII-pET30a	AGCCCAGATCTGATGGAACAGCAGAAAAGATACATC
P46	ftsAT2-reEcoRI-pET30a	ATATCGAATTCTCACACCGCCTGCCCGCTTGCCAACGG
P47	ftsAT3-reEcoRl-pET30a	ATATCGAATTCTCAAATGACGGACGTATGGCGGATGGC
P48	ftsAT4-fwBgl ll-pET30a	AGCCCAGATCTGCCGGCCGGTGGTAATCTG ATTACC
P49	ftsAT4-reEcoRI-pET30a	ATATCGAATTCTCACTCCTGAATACGTGCGCTGATGAT
P50	ftsAT7-fwBgl ll-pET30a	AGCCCAGATCTGATTTTTGGCGTAGTGCTGGGCGAACTGCAA
P51	ftsAT8-fwBgl ll-pET30a	AGCCCAGATCTGGCGCCCCAAGAAATGGGCGGTTTGTCCGAC
P52	ftsZ-fwBamHI-pGEX-2T	CGCGGGATCCATGGAATTTGTTTACGACGTGGCA
P53	ftsZ-reEcoRI-pGET-2T	ATATCGAATTCTTATTTGTCTGAATTGTGTTGACGACG

independently into competent *E. coli* C41 cells for expression of 6xHis tagged $FtsZ_{Ng}$ and $FtsA_{Ng}$.

2.5.3. Construction of plasmids for complementation assays

ftsA$_{Ec}$ was PCR amplified from *E. coli* PB103 using primers P8 and P9 (Table 2). The amplicon was digested with BamHI and SalI and ligated into BamHI/SalI-digested pDSW209 (Weiss *et al.*, 1999) to create pDSW209-A_{Ec} (Table 3). *ftsA*$_{Ng}$ was PCR amplified from *N. gonorrhoeae* CH811 using primers P10 and P2 (Table 2). The amplicon was digested with EcoRI and BamHI and ligated into EcoRI/BamHI-digested pDSW209 to create pDSW209-A_{Ng} (Table 3).

2.5.4. Construction of plasmids for bacterial two-hybrid assays

B2H vectors pcIp$_{22}$-*cat* and pcI$_{434}$-*cat* containing SalI and BamHI sites for gene insertion were obtained from Di Lallo *et al.* (2001, Table 3). Wild-type *ftsA*$_{Ng}$ or its truncations (T1-T8) (Fig. 2.1) were PCR amplified from *N. gonorrhoeae* CH811 using the following primers: $FtsA_{Ng}$ -P12/P11; T1- P12/P13; T2- P12/P14; T3- P12/P15; T4- P16/P17; T5- P16/P18; T6- P16/P11; T7- P19/P11; T8- P20/P11 (Table 2). Other divisome proteins were PCR amplified from *N. gonorrhoeae* CH811 using the following primers: $FtsK_{Ng}$- P24/P25; $FtsI_{Ng}$- P26/P27; $FtsW_{Ng}$- P28/P29; $FtsQ_{Ng}$- P30/P31; $FtsN_{Ng}$- P32/P33; $FtsE_{Ng}$- P34/P35; $FtsX_{Ng}$- P36/P37. PCR products were digested with SalI and BamHI and ligated into pre-digested B2H vectors, yielding plasmids pcIp$_{22}$-A, pcIp$_{22}$-AT1, pcIp$_{22}$-AT2, pcIp$_{22}$-AT3, pcIp$_{22}$-AT4, pcIp$_{22}$-AT5, pcIp$_{22}$-AT6, pcIp$_{22}$-AT7, pcIp$_{22}$-AT8, pcIp$_{22}$-K, pcIp$_{22}$-I, pcIp$_{22}$-W, pcIp$_{22}$-Q, pcIp$_{22}$-N, pcIp$_{22}$-E, and pcIp$_{22}$-X; pcI$_{434}$-A, pcI$_{434}$-AT1, pcI$_{434}$-AT2, pcI$_{434}$-AT3, pcI$_{434}$-AT4, pcI$_{434}$-AT5, pcI$_{434}$-AT6, pcI$_{434}$-AT7, pcI$_{434}$-AT8, pcI$_{434}$-K, pcI$_{434}$-I, pcI$_{434}$-W, pcI$_{434}$-Q, pcI$_{434}$-N, pcI$_{434}$-E, and pcI$_{434}$-X (Table 3). *zipA*$_{Ng}$ was amplified from *N. gonorrhoeae* CH811 using the following primers: $ZipA_{Ng}$- P21/P23 and P22/P23. PCR products were digested with BglII and BamHI or PstI and BamHI, which were ligated into pre-digested modified B2H vectors,

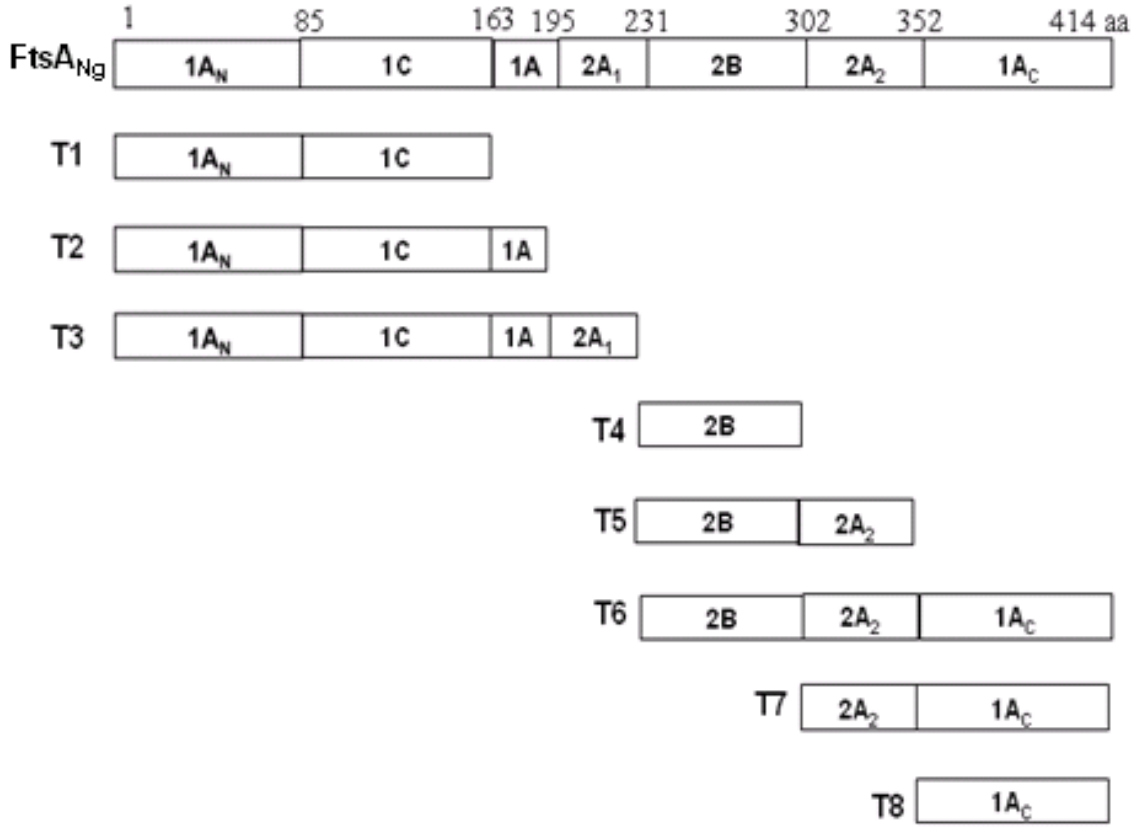

Fig. 2.1. Schematic representation of *N. gonorhoeae* FtsA and its truncations. T1 (162aa, Met1-Ala162) contained the N-terminal 1A and 1C domains of *ftsA*$_{Ng}$. T2 (194aa, Met1-Val194) included the N-terminal 1A, 1C and 1A domains of *ftsA*$_{Ng}$. T3 (230aa, Met1-Ile230) included the N-terminal 1A, 1C, 1A and 2A1 domains of *ftsA*$_{Ng}$. T4 (71aa, Pro231-Glu301) contained the 2B domain of *ftsA*$_{Ng}$. T5 (121aa, Pro231-Gly351) included the 2B and 2A2 domains of *ftsA*$_{Ng}$. T6 (185 aa, Pro231-Leu414) included the 2B, 2A2 and C-terminal 1A domains of *ftsA*$_{Ng}$. T7 (114aa, Ile301-Leu414) contained the 2A2 and 1A C-terminal domains of *ftsA*$_{Ng}$. T8 (64aa, Ala351-Leu414) contained the 1A C-terminal domain of *ftsA*$_{Ng}$.

pcIp22-linker and pcI434-linker (Appendix D), yielding plasmids $pcIp_{22}$-ZipA and pcI_{434}-ZipA. $pcIp_{22}$-Z and pcI_{434}-Z were previously constructed (Greco-Stewart *et al.*, 2007).

Wild-type $ftsZ_{Ec}$ and $ftsA_{Ec}$ were PCR amplified from *E. coli* PB103 using primers P38/P39 and P40/P40, respectively (Table 2). The PCR products were digested and ligated into B2H vectors as described above to create $pcIp_{22}$-Z_{Ec}, pcI_{434}-Z_{Ec}, $pcIp_{22}$-A_{Ec} and pcI_{434}-A_{Ec} (Table 3).

2.5.5. Construction of plasmids for GST pull-down assays

All FtsA truncations were tagged with 6xHis at the N-terminal for Western blot analysis using anti-6xHis antibody (BIO-RAD, Mississauga, Ontario, Canada). Wild-type $ftsZ_{Ng}$ or $ftsA_{Ng}$ and the $ftsA_{Ng}$ truncations (T2, T3, T4, T7 and T8) were amplified from *N. gonorrhoeae* CH811 using the following primers: $ftsZ_{Ng}$- P23/P24; $ftsA_{Ng}$- P25/P26; T2- P25/P27; T3- P25/P28; T4- P29/P30; T7- P31/P26; T8- P32/P26 (Table 2). PCR products were digested by BglII and EcoRI and ligated into pre-digested pET30a to form pETZ, pETA, pETAT2, pETAT3, pETAT4, pETAT7 and pETAT8, respectively (Table 3).

$ftsZ_{Ng}$ was amplified from *N. gonorrhoeae* CH811 using primers P33 and P34 (Table 2). The resulting amplicon was digested with BamHI and EcoRI and ligated into BamHI/EcoRI-digested pGEX2T to form pGEX-Z (Table 3).

2.6. Transformation of *E. coli* and verification of plasmid constructs by cracking and DNA sequencing

Plasmids were transformed into *E. coli* strains DH5α, XL1-Blue, R721, PB103, KJB24, P163 or C41 (DE3) according to standard $CaCl_2$ methods outlined in Sambrook *et al*. (1989). To verify if a DNA fragment was cloned into a vector, a cracking assay was performed. To lyse bacteria, about 25 µl of resuspended bacteria cells, that were matched to a 0.5 McFarland standard, was mixed with 25 µl of cell cracking assay buffer (50 mM EDTA, 100 mM NaOH,

Table 2.3. Plasmids created in the present study

Plasmid	Relevant genotype	Source/Reference
pUC18	Amp^R P_{lac}	Amersham
pUC18A	Amp^R $P_{lac::}$*ftsA*$_{Ng}$	This study
pEGFP	Amp^RCloning vector expressing GFP	Clontech
pUC18EA	Amp^R $P_{lac::}$ *egfp- ftsA*$_{Ng}$	This study
pUC18AE	Amp^R $P_{lac::}$*ftsA*$_{Ng}$-*egfp*	This study
pDSW209	Vector with low IPTG-inducible expression	Weiss *et al*., 1999
pDSW209-A_{Ec}	*ftsA*$_{Ec}$ in pDSW209	This study
pDSW209-A_{Ng}	*ftsA*$_{Ng}$ in pDSW209	This study
pSEB306-D242E	*ftsA*$_{Ec}$D242E in pSEB306	Pichoff and Lutkenhaus, 2007
$pcIp_{22}$	pC132 derivative carrying N-terminal end of P22 repressor	Di Dallo *et al*., 2001
pcI_{434}	pACYC177 derivative carrying N-terminal end of 434 repressor	Di Dallo *et al.*, 2001
$pcIp_{22}$-linker	$pcIp_{22}$ inserting a linker containing more restriction endonuclease sites	This study
pcI_{434}-linker	$pcIp_{434}$ inserting a linker containing more restriction endonuclease sites	This study
$pcIp_{22}$-A	$pcIp_{22}$ derivative carrying the *ftsA*$_{Ng}$ gene	This study
$pcIp_{22}$-AT1	$pcIp_{22}$ derivative carrying the *ftsA*$_{Ng}$ gene fragment encoding amino acids 1-162	This study
$pcIp_{22}$-AT2	$pcIp_{22}$ derivative carrying the *ftsA*$_{Ng}$ gene fragment encoding amino acids 1-194	This study
$pcIp_{22}$-AT3	$pcIp_{22}$ derivative carrying the *ftsA*$_{Ng}$ gene fragment encoding amino acids 1-230	This study
$pcIp_{22}$-AT4	$pcIp_{22}$ derivative carrying the *ftsA*$_{Ng}$ gene fragment encoding amino acids 231-301	This study
$pcIp_{22}$-AT5	$pcIp_{22}$ derivative carrying the *ftsA*$_{Ng}$ gene fragment encoding amino acids 231-351	This study
$pcIp_{22}$-AT6	$pcIp_{22}$ derivative carrying the *ftsA*$_{Ng}$ gene fragment encoding amino acids 231-414	This study

pcIp$_{22}$-AT7	pcIp$_{22}$ derivative carrying the *ftsA*$_{Ng}$ gene fragment encoding amino acids 302-414	This study
pcIp$_{22}$-AT8	pcIp$_{22}$ derivative carrying the *ftsA*$_{Ng}$ gene fragment encoding amino acids 351-414	This study
pcIp$_{22}$-ZipA	pcIp$_{22}$-linker derivative carrying the *zipA*$_{Ng}$ gene	This study
pcIp$_{22}$-K	pcIp$_{22}$ derivative carrying the *ftsK*$_{Ng}$ gene	This study
pcIp$_{22}$-I	pcIp$_{22}$ derivative carrying the *ftsI*$_{Ng}$ gene	This study
pcIp$_{22}$-W	pcIp$_{22}$ derivative carrying the *ftsW*$_{Ng}$ gene	This study
pcIp$_{22}$-Q	pcIp$_{22}$ derivative carrying the *ftsQ*$_{Ng}$ gene	This study
pcIp$_{22}$-N	pcIp$_{22}$ derivative carrying the *ftsN*$_{Ng}$ gene	This study
pcIp$_{22}$-E	pcIp$_{22}$ derivative carrying the *ftsE*$_{Ng}$ gene	This study
pcIp$_{22}$-X	pcIp$_{22}$ derivative carrying the *ftsX*$_{Ng}$ gene	This study
pcI$_{434}$-A	pcI434 derivative carrying the *ftsA*$_{Ng}$ gene	This study
pcI$_{434}$-AT1	pcI434 derivative carrying the *ftsA*$_{Ng}$ gene fragment encoding amino acids 1-162	This study
pcI$_{434}$-AT2	pcI434 derivative carrying the *ftsA*$_{Ng}$ gene fragment encoding amino acids 1-194	This study
pcI$_{434}$-AT3	pcI434 derivative carrying the *ftsA*$_{Ng}$ gene fragment encoding amino acids 1-230	This study
pcI$_{434}$-AT4	pcI434 derivative carrying the *ftsA*$_{Ng}$ gene fragment encoding amino acids 231-301	This study
pcI$_{434}$-AT5	pcI434 derivative carrying the *ftsA*$_{Ng}$ gene fragment encoding amino acids 231-351	This study
pcI$_{434}$-AT6	pcI434 derivative carrying the *ftsA*$_{Ng}$ gene fragment encoding amino acids 231-414	This study
pcI$_{434}$-AT7	pcI434 derivative carrying the *ftsA*$_{Ng}$ gene fragment encoding amino acids 302-414	This study
pcI$_{434}$-AT8	pcI434 derivative carrying the *ftsA*$_{Ng}$ gene fragment encoding amino acids 351-414	This study
pcI$_{434}$-ZipA	pcI434-linker derivative carrying the *zipA*$_{Ng}$ gene	This study
pcI$_{434}$-K	pcI434 derivative carrying the *ftsK*$_{Ng}$ gene	This study
pcI$_{434}$-I	pcI434 derivative carrying the *ftsI*$_{Ng}$ gene	This study
pcI$_{434}$-W	pcI434 derivative carrying the *ftsW*$_{Ng}$ gene	This study

pcI_{434}-Q	pcI434 derivative carrying the *ftsQ*$_{Ng}$ gene	This study
pcI_{434}-N	pcI434 derivative carrying the *ftsN*$_{Ng}$ gene	This study
pcI_{434}-E	pcI434 derivative carrying the *ftsE*$_{Ng}$ gene	This study
pcI_{434}-X	pcI434 derivative carrying the *ftsX*$_{Ng}$ gene	This study
$pcIp_{22}$-Z	$pcIp_{22}$ derivative carrying the *ftsZ*$_{Ng}$ gene	Greco-Stewart *et al*., 2007
pcI_{434}-Z	pcI434 derivative carrying the *ftsZ*$_{Ng}$ gene	Greco-Stewart *et al*., 2007
$pcIp_{22}$-Z_{Ec}	$pcIp_{22}$ derivative carrying the *ftsZ*$_{Ec}$ gene	This study
pcI_{434}-Z_{Ec}	pcI434 derivative carrying the *ftsZ*$_{Ec}$ gene	This study
$pcIp_{22}$-A_{Ec}	$pcIp_{22}$ derivative carrying the *ftsA*$_{Ec}$ gene	This study
pcI_{434}-A_{Ec}	pcI434 derivative carrying the *ftsA*$_{Ec}$ gene	This study
pET30a	Kan^R P_{T7}::6Xhis	Novagen
pETZ	Kan^R P_{T7}::*ftsZ*$_{Ng}$-6XHis	This study
pETA	Kan^R P_{T7}::*ftsA*$_{Ng}$-6XHis	This study
pETAT2	Kan^R P_{T7}::*ftsA*$_{Ng}$(T2)-6XHis	This study
pETAT3	Kan^R P_{T7}::*ftsA*$_{Ng}$(T3)-6XHis	This study
pETAT4	Kan^R P_{T7}::*ftsA*$_{Ng}$(T4)-6XHis	This study
pETAT7	Kan^R P_{T7}::*ftsA*$_{Ng}$(T7)-6XHis	This study
pETTA8	Kan^R P_{T7}::*ftsA*$_{Ng}$(T8)-6XHis	This study
pGEX2T	$Amp^R P_{tac}$::*gst*::*lacI*^{q}	Amersham
pGEX-Z	$Amp^R P_{tac}$::*gst-ftsZ*$_{Ng}$::*lacI*^{q}	This study

1% SDS, 0.05% bromophenol blue, 0.1% glycerol). After 15 mins, the cell lysates were centrifuged at 14,000 rpm, and 25 μl of supernatant was loaded and visualized on a 1% agarose gel. Gene integrity and reading frame for all constructs were verified by DNA sequence analysis (Plant Biotechnology Institute, National Research Council of Canada, Saskatoon, Saskatchewan).

2.7. Production of polyclonal antibodies

2.7.1. Purification of His-FtsZ$_{Ng}$ and His-FtsA$_{Ng}$ proteins

Single colonies of *E. coli* C41 with pETZ or pET30A in 5ml LB broth supplemented with Kan 50 μg/ml were incubated o/n at 37°C with shaking (200 rpm). 2 ml o/n culture was diluted into 300 ml of LB broth with Kan 50 μg/ml and incubated at 37°C with shaking (200 rpm) up to log phase (OD_{600}~0.35-0.5) (Szeto, Ph.D. Thesis, 2004). Exponential phase cultures were induced with a final concentration of 0.4 mM isopropyl-β-D-thiogalactopyranoside (IPTG) for 2-3 hrs with shaking (200 rpm) at 30°C. *E. coli* cells were pelleted by centrifugation at 6,000 rpm, 4°C for 10 mins and washed with 25 ml binding buffer (5mM Imidazole, 0.5M NaCl, 20mM Tris-HCl (pH 7.9)) twice. The pellet was stored at -20°C until use.

Pelleted cells were resuspended into 25 ml of binding buffer and sonicated 6 times for 45 s with one minute intervals on ice. Lysed cells were centrifuged at 25,000 rpm, 4°C for 30 mins. Supernatants were collected and checked by sodium dodecyl sulphate polyacrylamide gel electrophoresis (SDS-PAGE). However，either FtsA$_{Ng}$ or FtsZ$_{Ng}$ did not appear in the supernatant indicating the protein was insoluble. The following modified purification method under denaturing condition was applied and urea was used as a denaturant.

The pellets following the ultra centrifugation were sonicated briefly into 25 ml binding buffer with 1% Triton x-100 (Rico *et al.*, 2004) to resuspend thoroughly. The supernatant was

removed after the centrifugation and pellets were incubated with binding buffer containing 6 M of urea on ice for 1 hr with agitation as recommended by Novagen Company for inclusion body purification. The denatured His-tagged proteins recovered in the 6 M of urea supernatant were purified by metal affinity chromatography on a nickel column (Novagen) under denaturing condition (Novagen User protocol TB054 Rev. F0106, http://www.emdbiosciences.com/docs/docs/PROT/TB054.pdf). The His-tagged proteins were applied to a 3-ml His-Bind resin column (Novagen, Darmstadt, Germany) and purified under the denatured conditions that the wash and elution buffers contained 6 M urea (Novagen, Gibbstown, NJ, USA). The column was washed with 30 ml of binding buffer containing 5 mM imidazole and 21 ml of wash buffer containing 20 mM imidazole. Protein was eluted with elution buffer containing 250 mM imidazole. Eluted proteins were dialyzed o/n at 4°C against buffer B (0.05 M Tris, 0.02 M NaCl, 0.5 M EDTA, 0.3 mM imidazole). The purity of proteins were ascertained by SDS-PAGE with Coomassie brilliant blue staining (Sambrook *et al.*, 1989) and the concentrations were determined using the Bradford method (Bio-Rad, Mississauga, Ontario, Canada). Protein was stored in 1x phosphate buffered saline buffer (PBS) at -80°C.

2.7.2. Production of rabbit polyclonal antiserum

To produce rabbit polyclonal antisum, Freund's complete (Sigma), was used as adjuvant for the first injection and Freund's incomplete as adjuvant for the following boosters. 150 µl adjuvant was added to 150 µl purified 6x His-FtsA_{Ng} for injection of rabbits. The resultant mixtures (300 µl) were injected into female New Zealand White rabbits. The first booster was administered three weeks after the initial injection (300 µl Freund's incomplete for each rabbit). Blood was tested for the level of antibody 10 days after the first booster and a second booster was administered (Animal Care Unit, Western College of Veterinary Medicine, University of Saskatchewan). Serum was collected from rabbit blood 10 days after the last

booster using established procedures (Sambrook and Russell, 2001). Anti-$FtsZ_{Ng}$ antiserum was produced using a similar protocol.

2.7.3. Purification of polyclonal antibodies

Affinity purification of antisera was carried out using Protein G sepharose beads as previously described (Ramirez-Arcos *et al*., 2001b). Protein G sepharose beads (Amersham, Quebec, Canada) were packed in a column and equilibrated with PBS. A 1: 2 dilution of rabbit antiserum in PBS was added to the column and collected by gravity flow. The column was washed with PBS and IgG was eluted with 0.1 M glycine, pH 2.8, into tubes that contained 1.5 M Tris-HCl pH 8.8. Eluted antiserum was dialyzed in PBS o/n and collected and checked by 10% SDS-PAGE analysis for the presence of polyclonal anti-$FtsA_{Ng}$ antibody. Polyclonal anti-$FtsZ_{Ng}$ antibody was purified using a similar protocol.

2.8. Protein analysis and Western blots

Whole cell extracts were prepared by harvesting pellets of log phase *E. coli* or *N. gonorrhoeae* cells which were resuspended in 1x PBS, pH 7.4. 5x SDS sample buffer (50 mM Tris, pH 6.8, 2% SDS, 10% glycerol, 0.004% commassie brilliant blue, 5% β-mercaptoethanol) was added to cell extract or pure proteins. Lysed cells or pure proteins were boiled for 10 mins and centrifuged for 10 mins at 12,000 rpm (Sorvall MC 12V Microfuge), and the supernatant fraction was collected. Protein fractions were separated by 10-15% SDS-PAGE (5% stacking phase and 10-15% resolving phase) as described by Sambrook *et al*. (1989), using the Mini-PROTEAN II Electrophoresis Cell (Bio-Rad, ON, Canada). Coomassie blue staining for 1 hr, followed by the addition of a distaining solution (50% ddH_2O, 40% methanol, 10% acetic acid) was performed to visualize the purity of gonococcal proteins or to standardize the whole cell extracts for Western blotting. The intensities of protein bands in each whole cell extract were compared and standardized. From this analysis,

the amounts of whole cell extract to load for Western blotting was adjusted for equal loading on another resolved polyacrylamide gel.

Western blotting was performed with a few modifications (Ramirez-Arcos *et al*., 2001b; Szeto *et al.*, 2001). Resolved gels were incubated in transfer buffer (25 mM Tris, 192 mM glycine, 20% methanol, pH 8.3) to remove residual salts. The gel was then transferred to Immobilon-P^{SQ} membranes (Millipore Corporation, Bedford, MA, USA) that had previously been rinsed in pure methanol, ddH_2O, and transfer buffer as described by the manufacturer's instructions (Millipore), using the Mini Trans-Blot Electrophoretic Transfer Cell (BioRad) at 100 V for 1 hr. After transfer, membranes were blocked with 5% skim milk in TTBS (0.05% Tween-20 in Tris-buffered saline) for 2 hrs at room temperature, followed by 3x washes of TTBS (50 mM Tris, 1.25 M NaCl, 0.5% Tween-20, pH 7.5). Membranes were then probed o/n, at 4°C with a 1:500 dilution of anti-$FtsA_{Ng}$ or a 1:100 dilution of anti-$FtsZ_{Ng}$. On the second day, blots were then washed 3x10 mins in TTBS, followed by incubation of 1:3,000 dilution of goat anti-rabbit secondary antibody conjugated with alkaline phosphatase (Bio-Rad) for 1 hr at room temperature. After another 4xTTBS washing, the membranes were developed using AttoPhos Plus Kit (JBL Scientific Inc., San Luis Obispo, CA, USA) as the substrate for alkaline phosphatase and photographed using the Alpha imager 1220 software.

2.9. Quantitative Western blots for $FtsA_{Ng}$ and $FtsZ_{Ng}$

The concentration of FtsA and FtsZ in *N. gonorrhoeae* CH811, F62 and FA1090 was analyzed using quantitative immunoblot analysis. A cell extract (1 ml) from *N. gonorrhoeae* CH811 was resuspended in 400 µl solubilization buffer (Feucht *et al*., 2001) and boiled for 10 mins. Proteins were separated on 10% SDS-PAGE and Western blots were performed using anti-$FtsA_{Ng}$ and anti-$FtsZ_{Ng}$ antibodies, respectively. Each blot included a standard quantity of purified $FtsA_{Ng}$ or $FtsZ_{Ng}$ protein as controls to calculate the quantities of $FtsA_{Ng}$

and $FtsZ_{Ng}$ in cell extracts. A cell concentration of 6.2 x 10^9 per ml was obtained at an OD_{600} of 0.78 and this was determined by CFU as described below.

The concentration of FtsA and FtsZ in *N. gonorrhoeae* strains CH811, F62 and FA1090 was analyzed by quantitative immunoblot analysis as described by Feucht *et al.* (2001). The number of cells ml^{-1} was 6.2 x 10^9 as determined by c.f.u. when the culture was took at an OD_{600} of 0.78. *N. gonorrhoeae* CH811 cell extracts (1 ml) were resuspended in 400 µl solubilization buffer (Feucht *et al.*, 2001) and boiled for 10 mins. Different amounts of cell extract were loaded on SDS-PAGE and the density of both $FtsA_{Ng}$ and $FtsZ_{Ng}$ bands were detected by Western blotting analysis. Each blot included a standard quantity of purified $FtsA_{Ng}$ or $FtsZ_{Ng}$ protein used as controls to calculate the quantities of $FtsA_{Ng}$ and $FtsZ_{Ng}$ in cell extracts. The $FtsA_{Ng}$ or $FtsZ_{Ng}$ bands were compared with the density observed over a 2-10 ng or 40-100 ng concentration range of purified $FtsA_{Ng}$ and $FtsZ_{Ng}$ proteins respectively. The quantities of both FtsA and FtsZ were calculated by taking into account the dilution of the sample and the number of cells. Three independent experiments were conducted, and an average ratio was shown.

2.10. *E. coli* growth studies with overexpressed *N. gonorrhoeae* FtsA

The effect of $FtsA_{Ng}$ overexpression in *E.coli* PB103 and KJB24 was monitored by growth and viability studies. The method of colony-forming units (CFU) was used to measure viable cells at various time points. To determine the number of CFU/ml of *E. coli* transformed with either pUC18 or pUC18A (Table 3), each strain was diluted 30-fold from the o/n cultures into LB broth to obtain an initial standard inoculum at an optical density at 600 nm (OD_{600}) of ~ 0.03. Cultures were then incubated at 37°C with shaking (200 rpm). Viable cells of these strains were measured at 2-hr intervals for 20 hrs, and a total of 9 timepoints (0, 2, 4, 6, 8, 10, 12, 16, and 20-hr), was sampled. At each time point, 1 ml of *E.*

coli cells was removed; approximately 0.3 ml of each sample was further diluted 1:100 in 2.7 ml. Serial dilutions were then completed by serially diluting 100 µl of cells in 900 µl of LB broth (1:10 serial dilutions) up to a final dilution of 10^{-8}. Twenty microliters of samples from serial 10-fold dilutions, starting with the 10^{-1} dilution, was spotted in triplicate on LB agar supplemented with 100 µl/ml Amp. Plates were incubated for 14 to 18 hrs prior to counting colonies per spot. The average count was calculated per dilution. Two independent experiments in duplicate were performed.

2.11. Microscopy

2.11.1. Differential interference contrast light microscopy

To observe the morphology of *E. coli* PB103 harboring either pUC18 or pUC18A, or wild-type *N. gonorrhoeae* cells, log-phase cells were incubated as described above and were fixed with 0.2% glutaraldehyde (25% stock) and 6% formaldehyde (37% stock) for 15 mins at room temperature prior to adhesion to coverslips pre-coated with 0.01% polylysine. Coverslips with fixed cells were washed with PBS (pH 7.4) and air dried. Then each coverslip was placed onto a slide containing a drop of 50% glycerol and was sealed as previously described (Ramirez-Arcos *et al.*, 2001b).

Slides were examined using an Olympus BX61 microscope (Olympus Canada Inc. Markham, Ontario, Canada) with Differential Interference Contrast (DIC) and fluorescence microscopy capabilities, and equipped with a Photometrics CoolSmap ES camera, ImagePro Version 6 software (Media Cybenetics, Bethesda, MD) and InVitro 3 (Media Cybenetics) software. When required, raw images were enhanced using standard options available in the ImagePro software (revision 6.0).

2.11.2. Immuno-electron microscopy

Log-phase *N. gonorrhoeae* F62 cells were fixed in fixative solution (4% paraformaldehyde, 00.1M cacodylic buffer and 0.05% glutraldehyde in PBS buffer) at 4°C for 1 hr. Fixed cell were washed thoroughly, dehydrated in increasing alcohol concentration (50, 70, 90, 100%) 10 mins each while reducing the temperature at each stage. Then the cell were infiltrated with 50% uncryl resin at -20°C for 2 hrs, 75% resin for another 2 hrs, and infiltrated with fresh resin at 20 ºC for 2 nights. Followed by irradiated with UV light at 20 ºC for 36 hrs.

Ultrathin sections were treated with 1% glycine and blocking agent 1% bovine serum albumin (BSA) in PBS for 30 mins each. Sections were then incubated in PBS buffer with 1/100 or 1/500 dilutions of anti-$FtsA_{Ng}$ antibody, 0.05% Tween-20, 1% BSA and 5% FSA at room temperature for 3 hr and washed in the same buffer. The washed sections were incubated with 1:20 fold dilution for anti-rabbit-gold (10 nm in diameters) at room temperature for 2 hrs and washed in the same buffer and distilled water, followed by staining in 2% uranyl acetate and 0.2% lead citrate. A Hitachi H-7000 electron microscope at 75 Kv was used to examine the sections (Surgical Medical Research Unit, University of Alberta). Affinity purified anti-$FtsA_{Ng}$ antisera, prepared previously in our laboratory (Salimnia *et al*, 2000), was used.

2.11.3. Fluorescence microscopy

For fluorescence microscopy, an o/n culture of *E. coli* PB103 containing either pUC18AE or pUC18EA (Table 3) was diluted 1:100 and incubated at 37°C with 400 µM IPTG for induction. When the OD_{600} reached 0.3, cells were directly immobilized on coverslips using 2% LB low-melting point agarose (Ramirez-Arcos *et al.*, 2002). Samples were subsequently examined using an Olympus BX61 microscope (Olympus Canada Inc. Markham, Ontario, Canada) with DIC and fluorescence microscopy capabilities, and equipped with a Photometrics CoolSmap ES camera, ImagePro Version 6 software (Media

Cybenetics, Bethesda, MD) and InVitro 3 (Media Cybenetics) software. When required, raw images were enhanced using standard options available in the ImagePro software (revision 6.0).

2.12. Complementation of *ftsA*-depletion *E. coli*

Plasmids pDSW209-A_{Ec} (encodes wild-type $FtsA_{Ec}$, positive control), pDSW209-A_{Ng} (encodes wild-type $FtsA_{Ng}$) and pSEB306-D242E (encodes $FtsA_{Ec}$D242E, negative control) were transformed into *E. coli ftsA*-depletion strain P163 at 30°C, individually (Hale and de Boer, 1999), in which chromosomal $ftsA_{Ec}$ gene had been inactivated and in which $ftsA_{Ec}$ was supplied *in trans* on plasmid pDB280. This plasmid is temperature sensitive for replication and only permits growth at 30°C (Hale and de Boer, 1999). Overnight cultures of *E. coli* P163 harboring the indicated plasmid were diluted 1:100 and either incubated at 30°C or induced at 42°C for 2 hrs. 20 μl of serial 10-fold dilutions, starting with 10^{-1} dilution, were then spotted on LB agar. Four sets of LB agar plates containing increasing IPTG concentrations (0, 15, 30, 60, 100, 200 μM) were prepared. Two sets of plates were used for spotting the diluted cultures from 30°C and incubated at 30°C and 42°C, respectively. Another two sets of plates were used for spotting the diluted cultures from 42°C and incubated at 30°C and 42°C, respectively. *E. coli* P163 carrying the indicated plasmid was examined for cell viability after o/n incubation (14-18 hrs) by counting the viable colonies.

2.13. Methods for protein-protein interaction

2.13.1. Bacterial two-hybrid assay

B2H assays were performed as described by Di Lallo *et al.*, (2001) also based on the method of Miller (1972). Single plasmids or plasmid pairs to be tested were transformed into *E. coli* R721. A 1:100 dilution of o/n cultures containing single plasmids and 1:50 dilution for

plasmid pairs was made in 5 ml LB broth with appropriate antibiotics (34 µg /ml Cm, 30 g/ml Kan and 50 g/ml Amp) and grown at 34°C to log-phase. 100 µM IPTG was added to induce protein expression after 1hr of incubation. Log-phase cultures of *E. coli* R721 containing the indicated plasmids were pelleted. The cell density was standardized to an OD_{600} of ~ 0.4 by resuspending in Z-buffer (0.06 M $Na_2HPO4.7H_2O$, 0.04 M $NaH_2PO_4.H_2O$, 0.01 M KCl, 0.001 M $MgSO_4$, 0.05 M β-mercaptoethanol, pH 7.0), followed by permeabilization with 100 µl of chloroform and 50 µl 0.1% SDS. The β-galactosidase reaction was initiated by the addition of 0.2 ml o-nitro-phenyl-D-galactopyranoside (ONPG, 4 mg/ml) and stopped after the development of a yellow color by the addition of 0.5 ml of 1 M $NaCO_3$. Samples were centrifuged for 5 mins at 13,000 g and the optical density of the supernatant was measured at 420 and 550 nm for calculation of the Miller units (1972).

The rationale of B2H assay is that if two chimeric proteins formed by the N-terminal portion of phage 434 cI repressor fused in-frame with the division protein X (cI434-X), and the N-terminal portion of phage P22 cI repressor fused in-frame with the division protein Y (cIP22-Y), form the heterodimer cI434-X/cIP22-Y by interaction of their C-terminal domains, a fully functional repressor will be formed. This repressor will be able to shut down the expression of the *lacZ* reporter gene under the control of the 434/P22 hybrid promoter/ operator region (D'Ulisse *et al.*, 2007). The loss of binding to the operator sequence is deduced by the activation of β-galactosidase synthesis. A ≥ 50% reduction of the β-galactosidase activities of the bacterial strain R721 carrying every pair as compared to that of *E. coli* R721 without plasmid is considered to be a significant protein interaction (Di Lallo *et al*., 2001; D'Ulisse *et al*., 2007). Each value was the mean of at least three independent experiments.

2.13.2. GST pull-down assay

Vectors constructed for GST pull-down assays (pETA, pETAT2, pETAT3, pETAT4, pETAT4, pETAT7, pETAT8, pGEX2T, pGEX-Z) (Table 3) were individually transformed into *E. coli* C41 (*DE3*). Protein expression was induced using 100 µM IPTG. The GST-$FtsZ_{Ng}$ fusion was extracted under denaturing conditions. Pelleted cells were resuspended into 1X GST Bind/Wash buffer (GBW) (Novagen) with 6 M urea and 2% Triton X-100, followed by 1 hr incubation on ice with agitation. The denatured GST-$FtsZ_{Ng}$ recovered in the supernatant was dialyzed in 1X GBW o/n at 4°C. A plasmid with GST only (pGEX-2T) was used as a negative control in the GST pull-down experiments (Novagen).

Bacterial protein extracts (400 µl) containing the GST-FtsZ fusion or GST alone were added to 200 µl GST resin (Novagen), which had been washed 3x with 1x GBW with 1% Trition X-100. The mixture was incubated for 1 hr at 4°C with agitation. GST-embedded beads were then rinsed with GBW buffer. *N. gonorrhoeae* cell extracts containing native FtsA protein (200 µl) were incubated with the GST-embedded beads at 4°C for 1 hr with agitation. The resin was then rinsed with 1x GBW and samples were run on 15% SDS-PAGE. Western blotting to detect $FtsA_{Ng}$ proteins was performed using anti-6xHis antibody.

2.14. Statistical analysis

Statistical analyses using the unpaired Student's *t* test were performed to determine whether differences in average diameter or length between normal and aberrant cells were significant ($P < 0.05$). Unpaired Student's *t* test was also used to determine the significance of the growth curves of *E. coli* with or without $FtsA_{Ng}$ overexpression at each time point ($P < 0.05$). In B2H assays, the values close to 50% were examined using the unpaired Student's *t* test to determine if they were significantly different from 50% cut-off criteria ($P < 0.05$). Standard deviation was used to calculate how much variation is from the average miller units

for each pair of protein interaction, which were shown as error bars in B2H images. Standard deviation also was used to show the variability at each time point in growth curve studies.

CHAPTER 3 RESULTS

3.1. Genetic background

3.1.1. Genetic relationship of FtsAs

The complete gonococcal *ftsA* gene was amplified from *N. gonorrhoeae* CH811. The DNA sequence of $ftsA_{Ng}$ was determined to be 1245 base pair (bp) encoding a putative protein of 415 aa with a predicted molecular mass of 44 kilodalton (kDa). A BLAST search of the draft genomic sequence of *N. gonorrhoeae* FA1090 (Roe *et al*., 2000) with the $ftsA_{Ng}$ sequence from *N. gonorrhoeae* CH811 showed 100% identity between the two *ftsA* sequences.

$FtsA_{Ng}$ was compared by multiple protein sequence alignments to 50 other FtsA homologues from various organisms; 29 of which shared ≥ 50% identity to $FtsA_{Ng}$ were aligned with $FtsA_{Ng}$ as shown in Fig. 3.1. The 30 sequence alignments of FtsA showed regions of extensive conservation, particularly in the 2A and 2B domains, as well as completely conserved glycine (e.g. FtsA G14, G35, G43, G47, G82, G92, G146, G203, G210-212, G223, G322,, G328, G329, G373) amino acid residues distributed throughout FtsA (Fig. 3.1, arrows). The carboxy ends of the FtsAs did not have significant similarity except for a domain of ~15 residues, the Membrane Targeting Sequence (MTS), located at the extreme C-terminus (Fig. 3.1, red bar), which targets FtsA and FtsZ to the membrane (Pichoff and Lutkenhaus, 2005; Yim *et al.*, 2000). $FtsA_{Ng}$ had 40% identity to $FtsA_{Ec}$. The overall percentage identity for domains between the two FtsAs was 36% (1A domain), 39% (1C domain), 50% (2A domain) and 38% (2B domain), respectively.

3.1.2. Structure homology modeling of *N. gonorrhoeae* FtsA and FtsA domains

To identify the functional domains in $FtsA_{Ng}$ that might be implicated in the interactions with divisome proteins, the solved crystal structure of FtsA from *T. maritima* (van den Ent and Lowe, 2000) was used to generate a homology model of $FtsA_{Ng}$. *T. maritima* FtsA was

Fig. 3.1. Sequence alignment of FtsA proteins from 30 bacterial species. Abbreviation: Ng, *Neisseria gonorrhea* (YP_208577); Nm, *Neisseria meningitides* (NP_273474); Eco, *Eikenella corrodens* (ZP_03712920); Ln, *Lutiella nitroferrum* (ZP_03699185); Cv, *Chromobacterium violaceum* (NP_904009); Of, *Oxalobacter formigenes* (ZP_04577492); Bm, *Burkholderia mallei* (YP_104090); Ha, *Herminiimonas arsenicoxydans* (YP_001101042); Mf, *Methylobacillus flagellates* (YP_546372); Rm, *Ralstonia metallidurans* (YP_585265); Ct, *Cupriavidus taiwanensis* (YP_002006716); Gf, *Gallionella ferruginea* (ZP_04831827); Cb, *Coxiella burnetii* (YP_002304270); Da, *Dechloromonas aromatica* (YP_286693); Ne, *Nitrosomonas eutropha* (YP_746490); Aa, *Aromatoleum aromaticum* (YP_157812); Td, *Thiobacillus denitrificans* (YP_313882); Kk, *Kangiella koreensis* (YP_003145881); Hc, *Hahella chejuensis* (YP_436953); Avi, *Allochromatium vinosum* (ZP_04774123); Ma, *Marinobacter aquaeolei* (YP_959710); Bp, *Bordetella petrii* (YP_001629304); Sd, *Saccharophagus degradans* (YP_526326); Pm, *Pseudomonas mendocina* (YP_001186426); Ae, *Alkalilimnicola ehrlichii* (YP_743020); Av, Azotobacter vinelandii (YP_002798530); Lp, *Legionella pneumophila* (YP_127862); Sl, *Sideroxydans lithotrophicus* (ZP_05340066); Tt, *Teredinibacter turnerae* (YP_003074422); Ec, *Escherichia coli* (NP_285790). The amino acids, percentage of identity and similarity of each FtsA sequence to $FtsA_{Ng}$ were shown at the end of each sequence. The bars show on the top of alignment indicating the FtsA domains. Arrows indicate the conserved glycine amino acids. Red bar showed MTS at the extreme C-terminus.

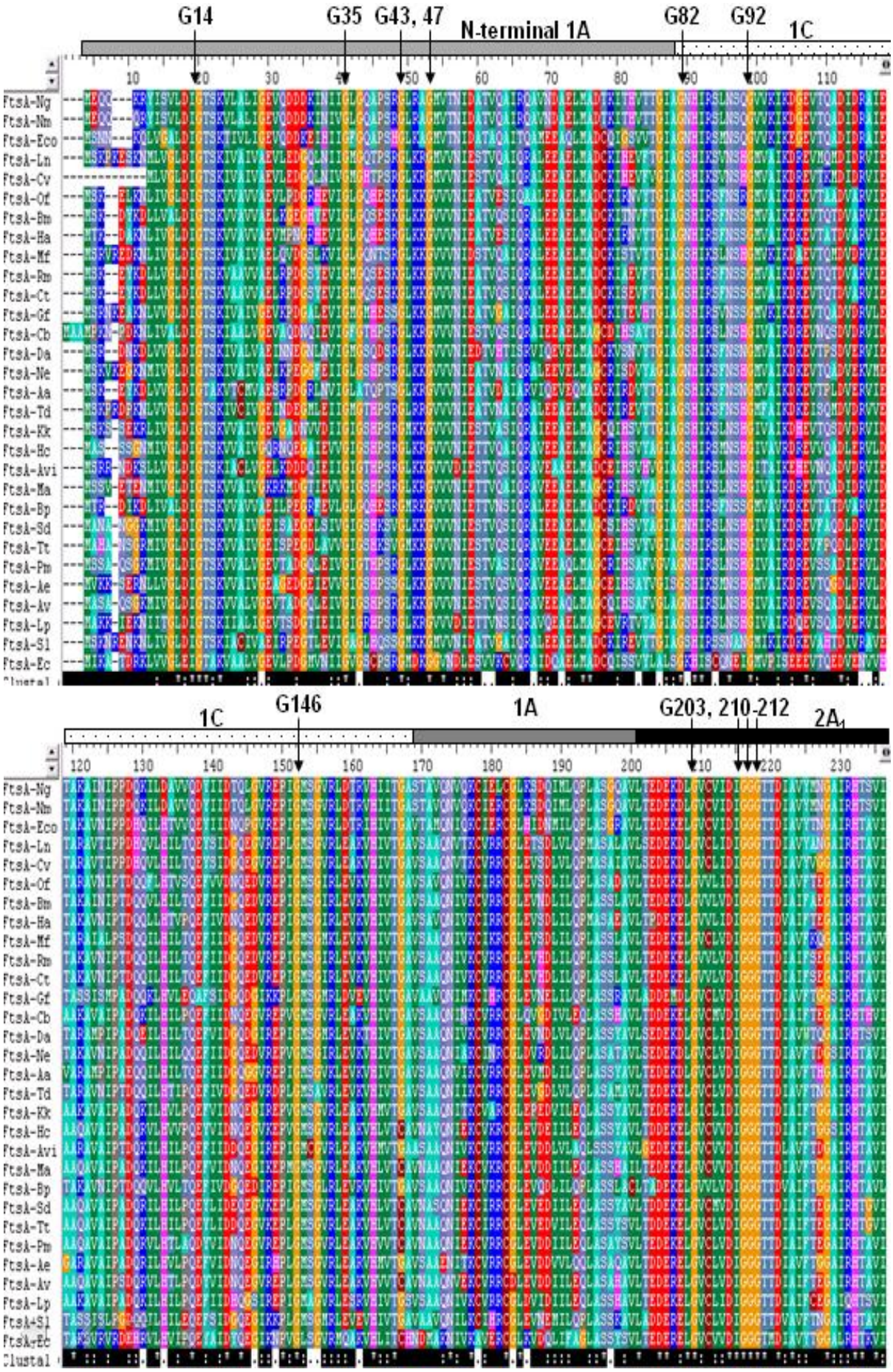
G14
G35
G43, 47
N-terminal 1A
G82
G92
1C
G146
1C
1A
G203, 210-212
2A

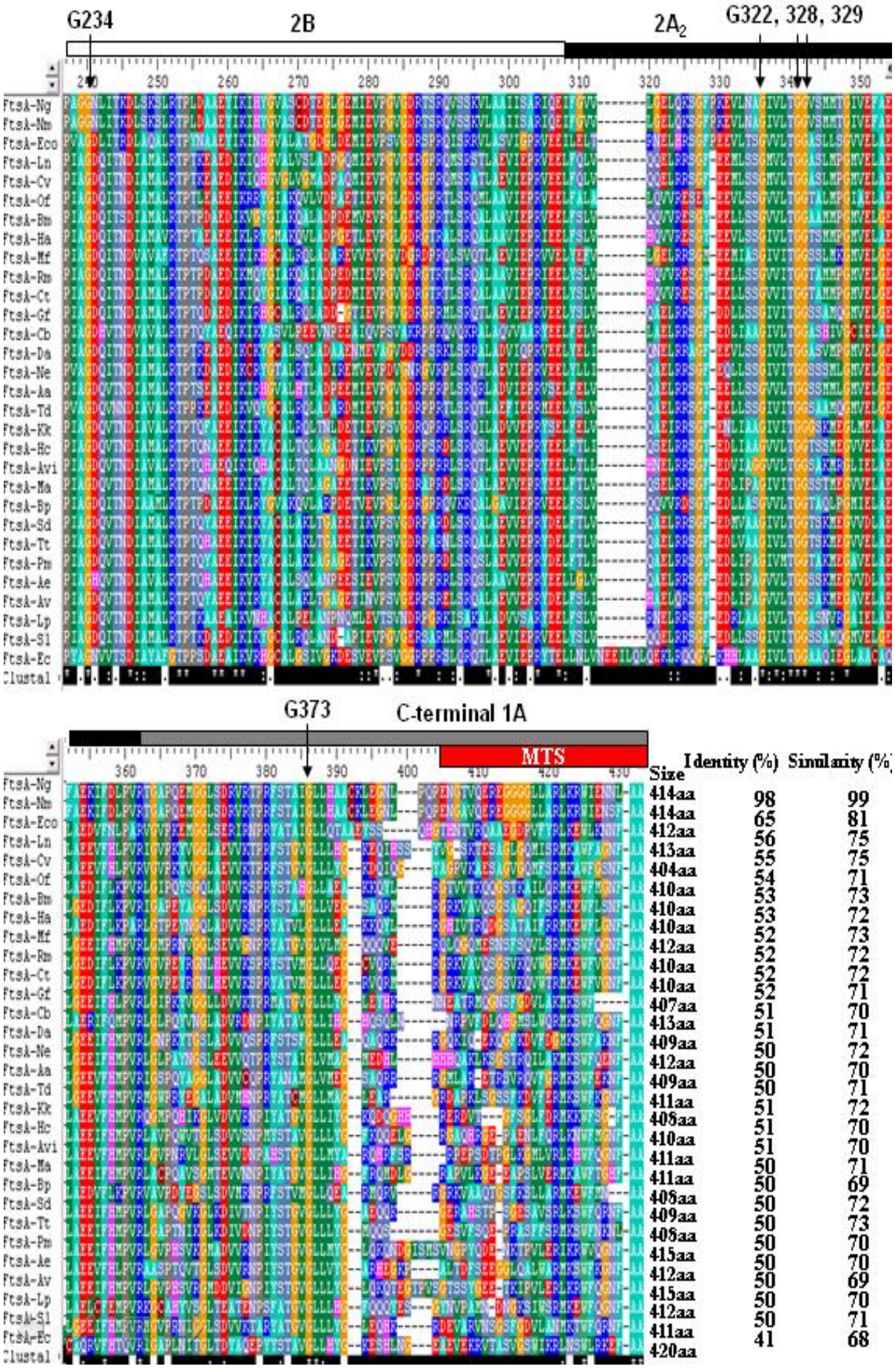
G234
2B
2A2
G322, 328, 329
G373
C-terminal 1A
MTS
Size
Identity (%)
Similarity (%)
414aa 98 99
414aa 65 81
412aa 56 75
413aa 55 75
404aa 54 71
410aa 53 73
410aa 53 72
410aa 52 73
412aa 52 72
410aa 52 72
410aa 52 71
407aa 51 70
413aa 51 71
409aa 50 72
412aa 50 70
409aa 50 71
411aa 51 72
408aa 51 70
410aa 51 70
411aa 50 71
411aa 50 69
408aa 50 72
409aa 50 73
408aa 50 70
415aa 50 70
412aa 50 69
415aa 50 70
412aa 50 71
411aa 41 68
420aa

19% and 17% identical to *N. gonorrhoeae* FtsA and *E. coli* FtsA, respectively. Homology modeling generated similar structures for $FtsA_{Ng}$ and $FtsA_{Ec}$ (Fig. 3.2). Four domains of $FtsA_{Ng}$ were identified, which corresponded to domains 1A, 1C, 2A and 2B of *T. maritima* FtsA (Fig. 3.3A). A schematic presentation of wild-type $FtsA_{Ng}$ domains is shown in Fig. 3.3B. Domain1A includes three subdomains: $1A_N$ (Gln3-Asn84), 1A (Ser163-Val194), and $1A_C$ (Ala352-Leu414). Domain 1C encompasses His85 to Ala162. Domain 2A includes two subdomains: $2A_1$ (Leu195-Ile230) and $2A_2$ (Ile302-Gly351). Domain 2B includes amino acid residues Pro231 to Glu301 (Fig. 3.3B, van den Ent and Löwe 2000).

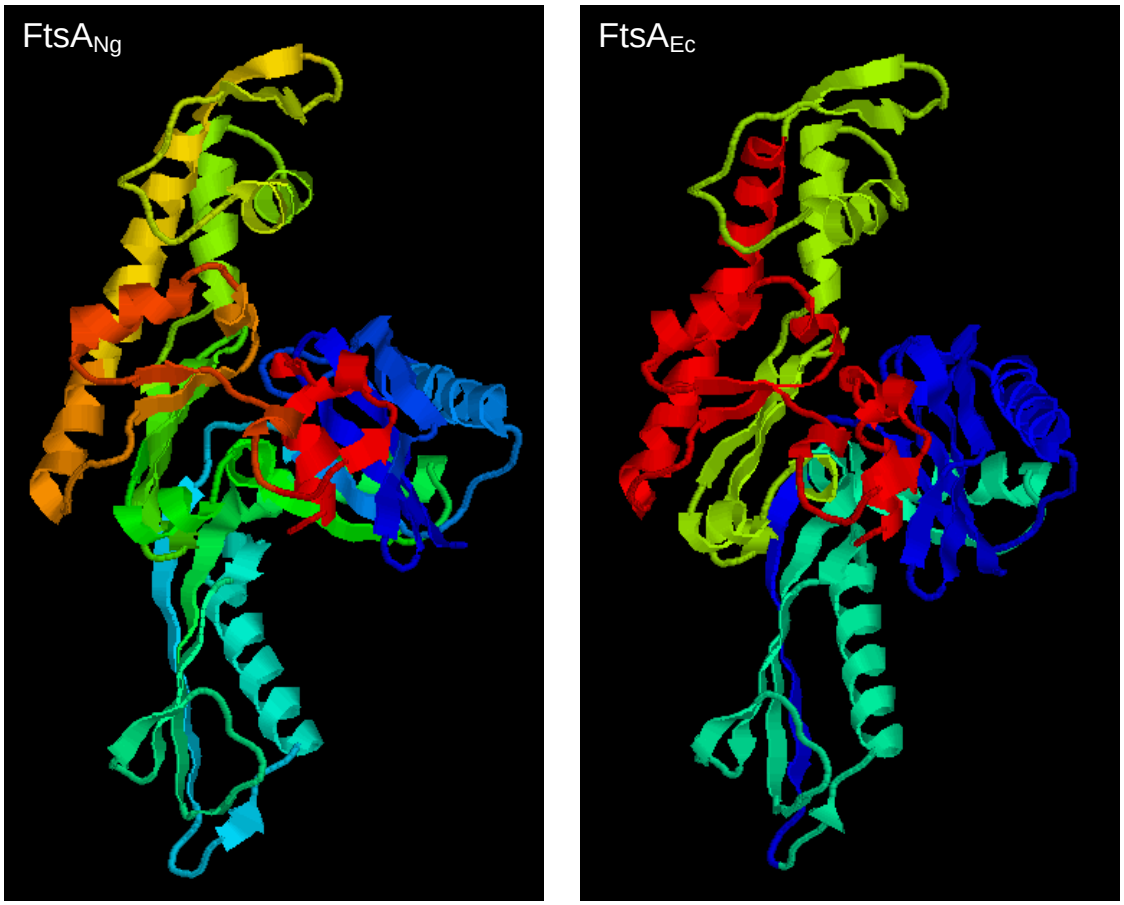

Fig. 3.2. Structural homology modeling of *N. gonorhoeae* FtsA and *E. coli* FtsA.

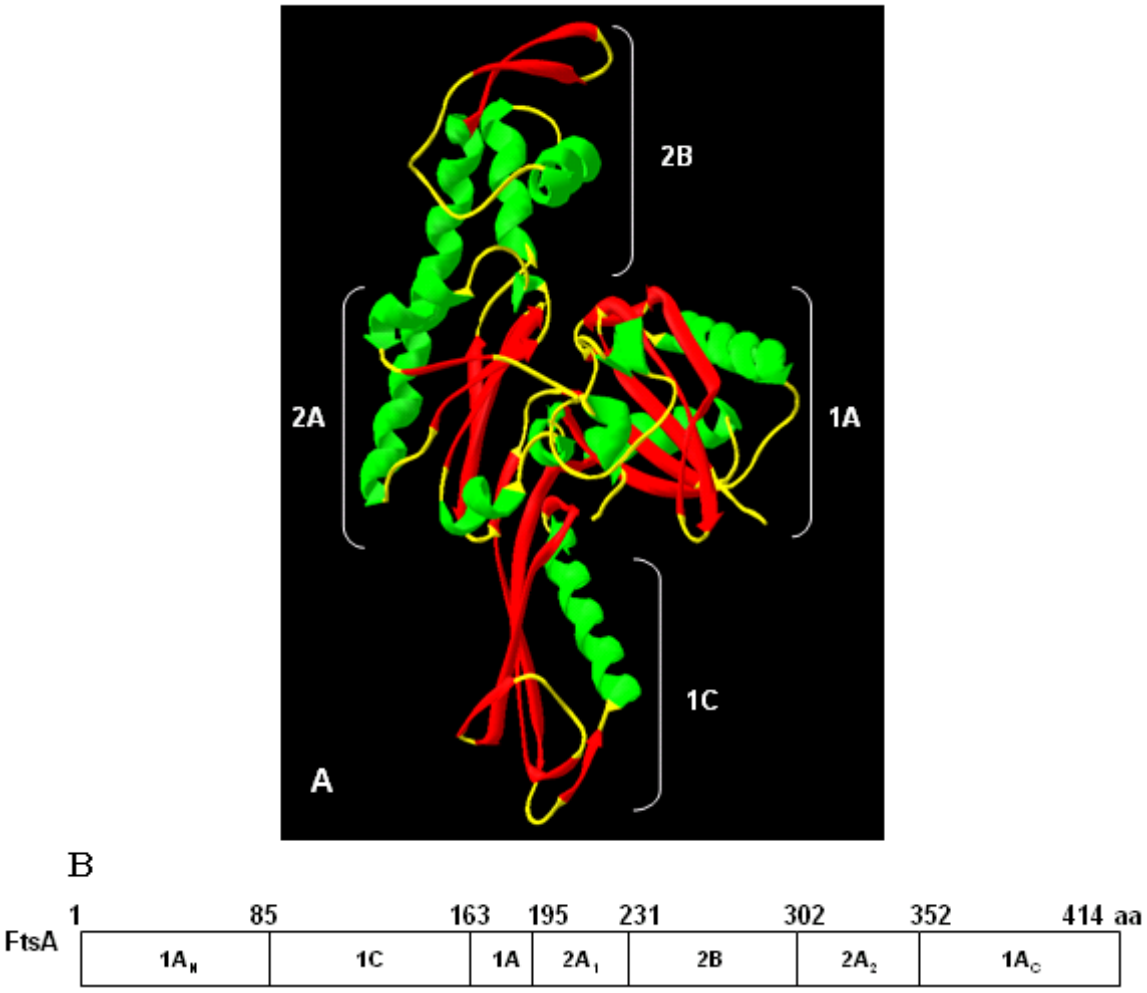

Fig. 3.3. (A) Structural homology modeling of *Neisseria gonorhoeae* FtsA. Secondary structure elements are labeled in different colors. Green indicates helices; red indicates sheets; yellow indicates coils. **(B) Schematic representation of $FtsA_{Ng}$ domains**, indicating the order of each domain in the primary sequence of FtsA.

3.2. Bacterial two-hybrid data for the interactions of divisome proteins

We examined the potential interactions among the divisome proteins identified in *N. gonorrhoeae*, including FtsZ, FtsA, ZipA, FtsK, FtsQ, FtsI, FtsW, FtsN, FtsE and FtsX (see Introduction for a review of these proteins). The first 8 proteins are essential for divisome formation (Errington *et al.*, 2003) and the last two proteins FtsE and FtsX are not essential for cell division but act to regulate the activity of divisome, at least in *E. coli* (Corbin *et al.*, 2007). The B2H assays were used to examine the potential interactions, a method which was successfully used to describe the interaction webs of divisome proteins in both *E. coli* and *S. pneumoniae* (Di Lallo *et al.*, 2003; Maggi *et al*., 2008).

As the negative controls, B2H plasmids carrying single genes or empty plasmids were transformed into *E. coli* R721. The residual β-galactosidase activities of the negative controls were similar to wild-type *E. coli* R721 in all experiments, indicating that no fusion was self-activated. B2H results are presented as the ratio between the β-galactosidase activities (Miller units) produced by the strain harbouring the two recombinant plasmids (Tables 3.1, 3.2). A 50% cut-off value was adopted as criterium differentating positive and negative interactions as described by Di Lallo *et al*. (2001). A β-galactosidase activity of each protein pair lower than 50% indicates a positive interaction whereas a β-galactosidase activity of each protein over 50% indicates a negative interaction. Values close to 50% (40% ~ 60%) were examined by *t* test to determine whether difference between these values and 50% value were significant ($P < 0.05$) (Table 3.3). Those values that did not show statistically significant difference from 50% were considered to represent weak or transient interactions.

3.2.1. Interaction between $FtsA_{Ng}$ and $FtsZ_{Ng}$

Previous work in *E. coli* has shown that FtsZ interaction with FtsA was critical for cell division (Pichoff and Lutkenhaus, 2002) and has been experimentally documented by several

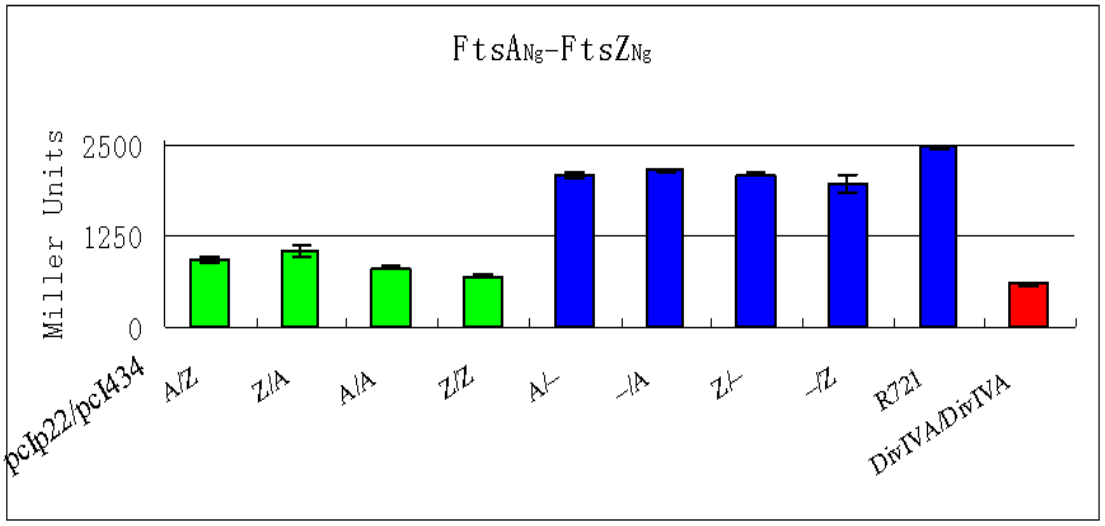

Fig 3.4. Interaction between $FtsA_{Ng}$ (A) and $FtsZ_{Ng}$ (Z) and self-interactions of $FtsA_{Ng}$ and $FtsZ_{Ng}$ determined by B2H assay. *$ftsA_{Ng}$* and *$ftsZ_{Ng}$* were cloned into pcIp22 and pcI434 and constructs were transformed into *E. coli* R721 either singly or in combination. *E. faecalis* DivIVA self-interaction was used as positive control (red bar). R721 without plasmids and single transformants were used as negative controls (blue bars). R721 without plasmids had a β-galactosidase activity of 2504±34 Miller Units. The β-galactosidase activity of each combination was compared to that of R721. Values of less than 50% (<1250 Miller Unites) indicate a positive interaction between two proteins (green bars). Error bars indicate the standard deviations, n=9.

independent approaches (e.g. Y2H and B2H systems) (Di Lallo *et al*., 2003; Karimova *et al*., 2005). In order to determine whether FtsA interacts with FtsZ in *N. gonorrhoeae*, B2H vectors with either $ftsA_{Ng}$ and/or $ftsZ_{Ng}$ were transformed into *E. coli* R721 (Di Lallo *et al*., 2001) and examined for protein-protein interactions. In this B2H system, repressed β-galactosidase activity only occurs if there is an interaction between the two proteins. *E. coli* R721 transformed singly with either one of the plasmids showed a high residual β-galactosidase activity (Fig. 3.4, blue bars), indicating that the fusion proteins themselves were incapable of blocking the *lacZ* gene expression. A 40% residual β-galactosidase activity was observed when the interaction between $FtsA_{Ng}$ and $FtsZ_{Ng}$ was assayed (Fig. 3.4, green bars). As examined by *t* test, the difference between values 40% and 50% was considered to be very significant (Table 3.3), indicating a positive interaction between $FtsA_{Ng}$ and $FtsZ_{Ng}$. The self-interactions of wild-type $FtsA_{Ng}$ and $FtsZ_{Ng}$ were also examined using B2H assays. A 33% and a 28% residual β-galactosidase activities was revealed for self-interactions of $FtsA_{Ng}$-$FtsA_{Ng}$ and $FtsZ_{Ng}$-$FtsZ_{Ng}$, respectively, (Fig. 3.4, green bars), indicative of positive interactions.

The interaction of $FtsA_{Ng}$-$FtsZ_{Ng}$ was also confirmed by GST pull-down assay (Fig. 3.5). In this system, GST-$FtsZ_{Ng}$ fusion was used as a bait to capture the potential interacting proteins from *N. gonorrhoeae* cell culture extract. GST alone was used a negative control, which was not expected to capture any protein from the cell culture extract. Native $FtsA_{Ng}$ was pulled down by GST-$FtsZ_{Ng}$ fusion and detected by Western blotting using anti-$FtsA_{Ng}$ antibody, indicating an interaction between $FtsA_{Ng}$ and $FtsZ_{Ng}$ (Fig. 3.5, lane 3). $FtsA_{Ng}$ was not pulled down by GST alone (Fig. 3.5, lane 2). Thus, my research clearly demonstrates the interaction between FtsZ and FtsA in *N. gonorrhoeae*.

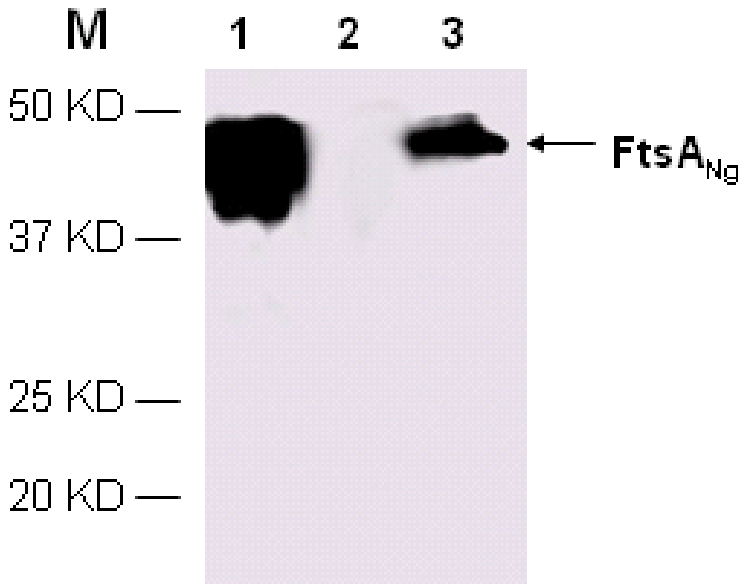

Fig 3.5. Interaction of FtsA$_{Ng}$ and FtsZ$_{Ng}$ determined by GST pull-down assay. Samples were separated on 12% SDS-PAGE gel and the pulled-down FtsA$_{Ng}$ was detected using anti-6xHis antibody. Lane 1: purified FtsA$_{Ng}$ was loaded as positive control. Lane 2: GST with FtsA$_{Ng}$ was loaded as negative control. Lane 3: GST-FtsZ$_{Ng}$ with FtsA$_{Ng}$. FtsA$_{Ng}$ was not pulled down by GST alone (lane 2), but was successfully pulled down by the GST-FtsZ$_{Ng}$ (lane 3), which showed same size as purified FtsA$_{Ng}$ (lane 1), indicating the positive interaction between FtsA$_{Ng}$ and FtsZ$_{Ng}$.

3.2.2. Interactions between $FtsA_{Ng}$ and other divisome proteins

In order to determine which divisome proteins from *N. gonorrhoeae* interacted with $FtsA_{Ng}$, B2H vectors with combinations of $FtsA_{Ng}$, $ZipA_{Ng}$ $FtsK_{Ng}$, $FtsQ_{Ng}$, $FtsW_{Ng}$, $FtsI_{Ng}$, $FtsN_{Ng}$, $FtsE_{Ng}$, or $FtsX_{Ng}$ were transformed into *E. coli* R721 and examined for potential interactions. $FtsA_{Ng}$ interacted with $FtsN_{Ng}$, displaying 24% residual β-galactosidase activity, (Fig. 3.6B), consistent with previous reports in *E. coli* (Di Lallo *et al*., 2003; Karimova *et al.*, 2005). One novel interaction of FtsA-FtsK was detected in *N. gonorrhoeae*, giving 30% residual β-galactosidase activity (Fig. 3.6C). An interaction between FtsA and FtsI was not observed in *N. gonorrhoeae*, giving an 83% residual β-galactosidase activity (Fig. 3.6E). $FtsA_{Ng}$ have weak interaction with $FtsQ_{Ng}$, and $FtsW_{Ng}$ displaying 48% and 45% residual β-galactosidase activities, respectively (Fig. 3.6A, D) and the *t* test also did not show a significant difference between these values and the 50% cut-off criterium (Table 3.3). In addition, the interactions of $FtsA_{Ng}$ with $FtsQ_{Ng}$, and $FtsW_{Ng}$ were further confirmed by identifying the $FtsA_{Ng}$ functional domains involved in interactions with those two proteins (see 3.2.4, table 3.1). $FtsA_{Ng}$-$FtsX_{Ng}$ interaction testing produced a 51% residual β-galactosidase activity (Fig. 3.6H), which did not show significant difference from 50% cut-off criterium, indicating transient or no interaction between these two proteins. Thus this is a questionable interaction and needs to be further confirmed using other methods. In addition, $FtsA_{Ng}$ did not interact with either $ZipA_{Ng}$ or $FtsE_{Ng}$, displaying 77% and 85% residual β-galactosidase activities, respectively (Fig. 3.6F-G). All the interactions were examined in two reciprocal ways, pcIp22-X_{Ng}/pcI434-Y_{Ng} and pcIp22-Y_{Ng}/pcI434-X_{Ng}. Only the interaction of $FtsA_{Ng}$-$FtsK_{Ng}$ was examined unidirectionally, i.e. pcIp22-$FtsA_{Ng}$/pcI434-$FtsK_{Ng}$, because all attempts to clone *ftsK*$_{Ng}$ into pcIp22 failed.

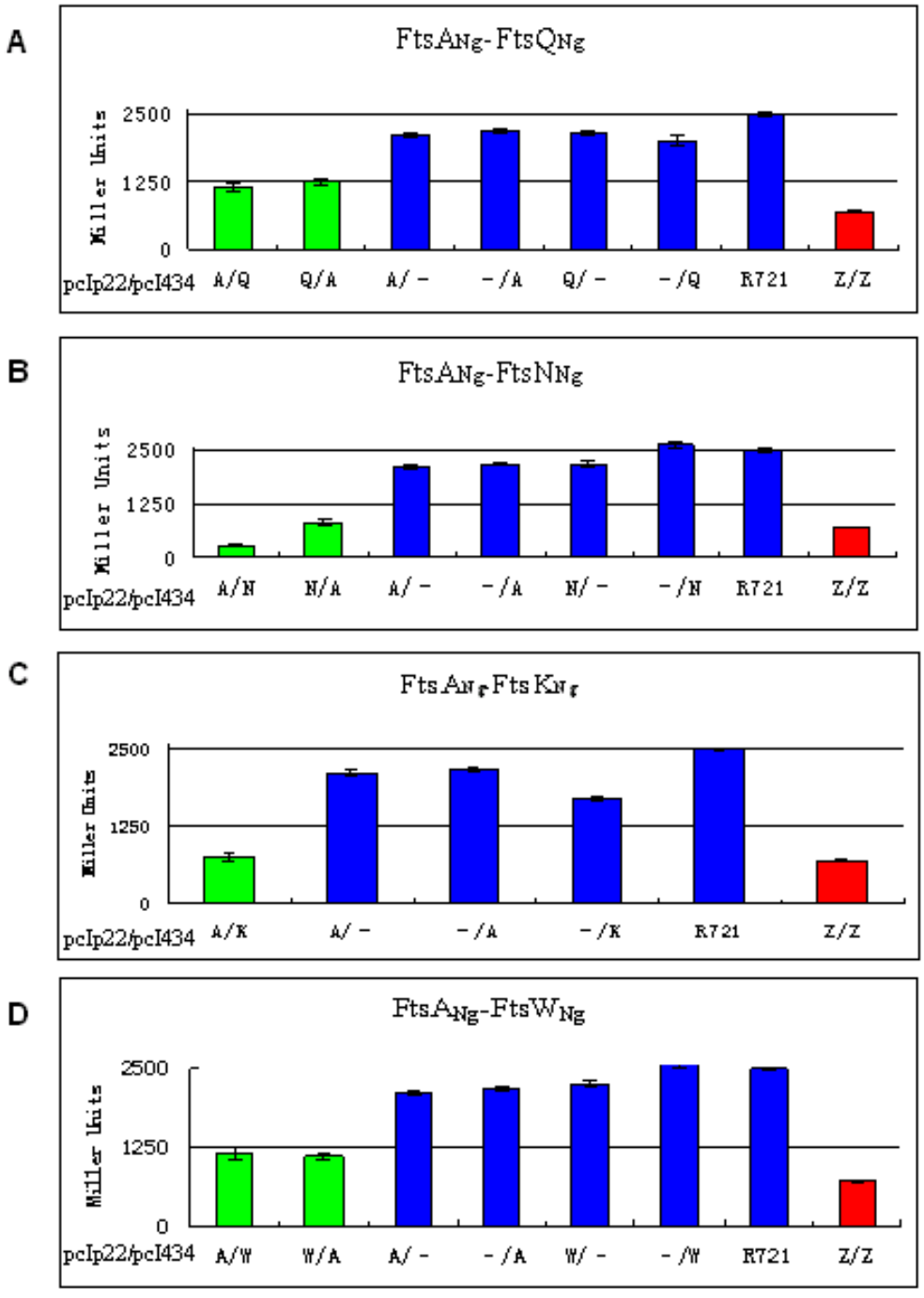
A
FtsANg-FtsQNg
Miller Units
2500
1250
0
pclp22/pcI434
A/Q
Q/A
A/ -
- /A
Q/ -
- /Q
R721
Z/Z
B
FtsANg-FtsNNg
Miller Units
2500
1250
0
pclp22/pcI434
A/N
N/A
A/ -
- /A
N/ -
- /N
R721
Z/Z
C
FtsANgFtsKNg
Miller Units
2500
1250
0
pclp22/pcI434
A/K
A/ -
- /A
- /K
R721
Z/Z
D
FtsANg-FtsWNg
Miller Units
2500
1250
0
pclp22/pcI434
A/W
W/A
A/ -
- /A
W/ -
- /W
R721
Z/Z

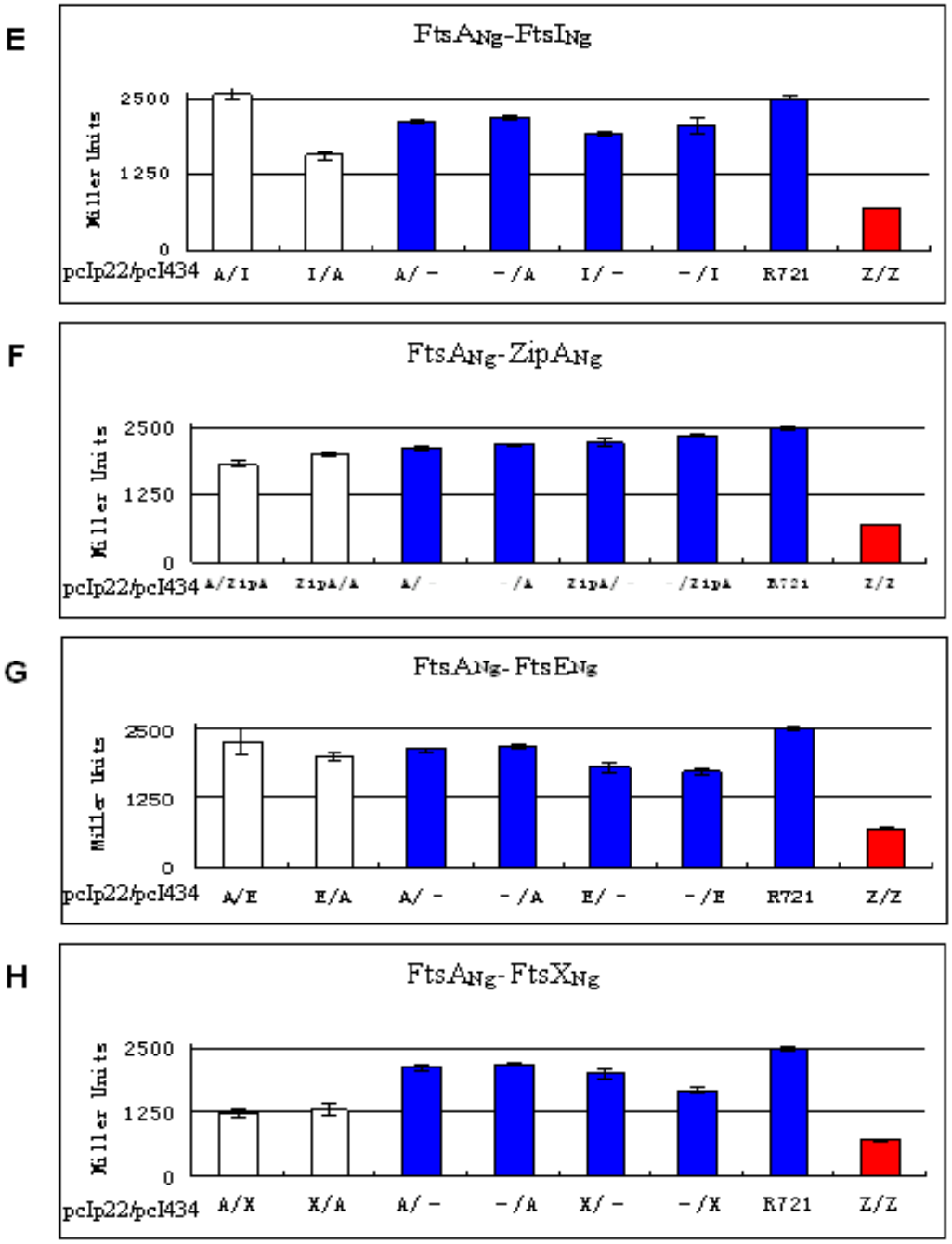

Fig. 3.6. Interaction of FtsA$_{Ng}$ (A) with other divisome proteins, ZipA$_{Ng}$, FtsK$_{Ng}$ (K), FtsI$_{Ng}$ (I), FtsQ$_{Ng}$ (Q), FtsW$_{Ng}$ (W), FtsN$_{Ng}$ (N), FtsE$_{Ng}$ (E) and FtsX$_{Ng}$ (X) determined by B2H assay. Each gene was cloned into pcIp22 and pcI434 and constructs were transformed into *E. coli* R721 either singly or in combination. *N. gonorrhoeae* FtsZ self-interaction was used as positive control (red bar). R721 without plasmids and single transformants were used as negative controls (blue bars). R721 without plasmids had a β-galactosidase activity of 2504±34 Miller units. The β-galactosidase activity of each combination was compared to that of R721. Values of less than 50% (<1250 Miller Unites) indicate a positive interaction between two proteins (green bars) while values of more than 50% (>1250 Miller Units) indicate a negative interaction between the two proteins (white bars). Error bars indicate the standard deviations, n=9.

3.2.3. Identification of $FtsA_{Ng}$ domains involved in the interactions with $FtsZ_{Ng}$

As we determined that $FtsA_{Ng}$ interacted with $FtsZ_{Ng}$, the B2H method was used to further identify the interaction region of $FtsA_{Ng}$ with $FtsZ_{Ng}$. To identify the functional domains of $FtsA_{Ng}$ involved in the interaction with $FtsZ_{Ng}$, 6 $FtsA_{Ng}$ truncations (T1-T6) (Fig. 2.1) were cloned into B2H vectors. *E. coli* R721 and transformants with single plasmids were used as negative controls. $FtsZ_{Ng}$ self-interaction was used as positive control. As determined by B2H assay, truncations T4, T5 and T6 retained interactions with $FtsZ_{Ng}$, displaying 38%, 40% and 35% residual β-galactosidase activities, respectively, while truncations T1, and T2 did not show interaction with $FtsZ_{Ng}$, displaying 92% and 100% residual β-galactosidase activities, respectively (Fig. 3.7). The residual β-galactosidase activity of $FtsA_{Ng}$T3-$FtsZ_{Ng}$, was 45% (Fig. 3.7), which was not significantly different from the 50% cut-off, indicating weak or transient interaction (Table 3.3). However, this interaction between $FtsA_{Ng}$T3 and $FtsZ_{Ng}$ was confirmed using GST pull-down assay (Fig. 3.8). Therefore, compared to T1 (i.e. $1A_N$-1C) and T2 (i.e. T1+1A), T3 (i.e. T2+$2A_1$) contained domain $2A_1$ and showed interaction with $FtsZ_{Ng}$,, indicating that domain $2A_1$ of $FtsA_{Ng}$ was responsible for the interaction with $FtsZ_{Ng}$ (Fig. 3.7). Truncations T4 (i.e. 2B), T5 (i.e. T4+$2A_2$) and T6 (i.e. T4+$2A_2$+$1A_C$), which interacted with $FtsZ_{Ng}$, and all contained a common domain 2B, indicating that domain 2B was responsible for the interaction of $FtsA_{Ng}$ with $FtsZ_{Ng}$ (Fig. 3.7).

Although truncations T5 and T6 interacted with $FtsZ_{Ng}$, it was impossible to tell whether subdomain $2A_2$ or $1A_C$ was involved in the interaction with $FtsZ_{Ng}$. To clarify this, T7 and T8 truncations were used for B2H assays; T7 contains domains $2A_2$ and $1A_C$, while T8 contains domain $1A_C$ only (Fig. 3.7). T7 (i.e. T8+$2A_2$) interacted with $FtsZ_{Ng}$, displaying 42% residual β-galactosidase activity (Fig. 3.7), which was significantly different from the 50% cut-off (Table 3.3), but T8 (i.e. $1A_C$) did not interact with $FtsZ_{Ng}$, indicating an interaction of domain

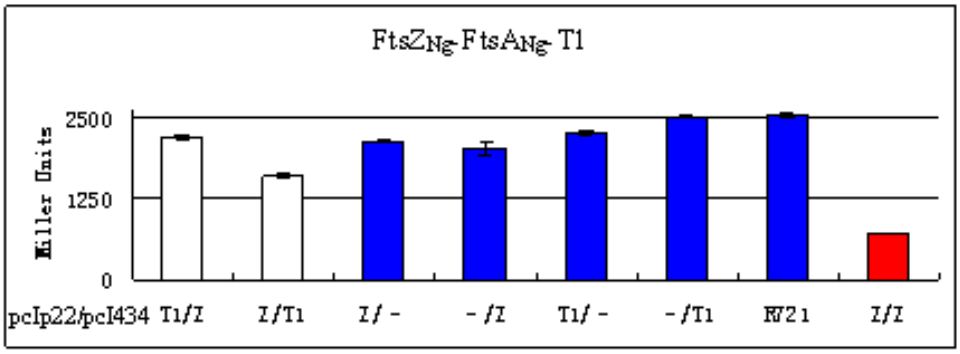
FtsZNg-FtsANg- T1
Miller Units
2500
1250
0
pcIp22/pcI434
T1/I
I/T1
I/ -
- /I
T1/ -
- /T1
RY21
I/I

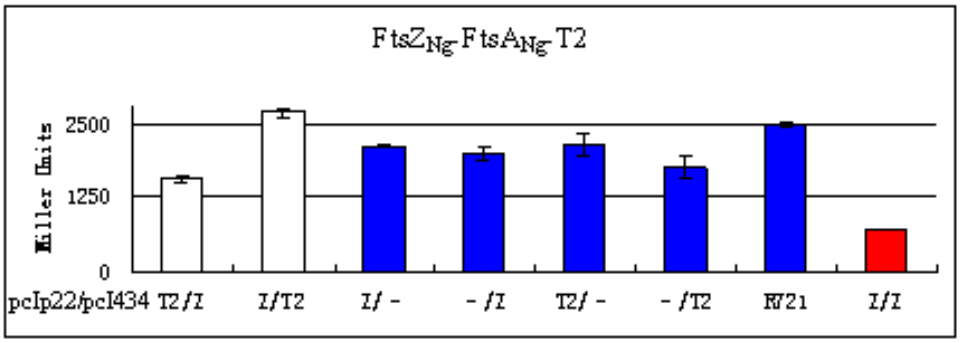
FtsZNg-FtsANg- T2
Miller Units
2500
1250
0
pcIp22/pcI434
T2/I
I/T2
I/ -
- /I
T2/ -
- /T2
RY21
I/I

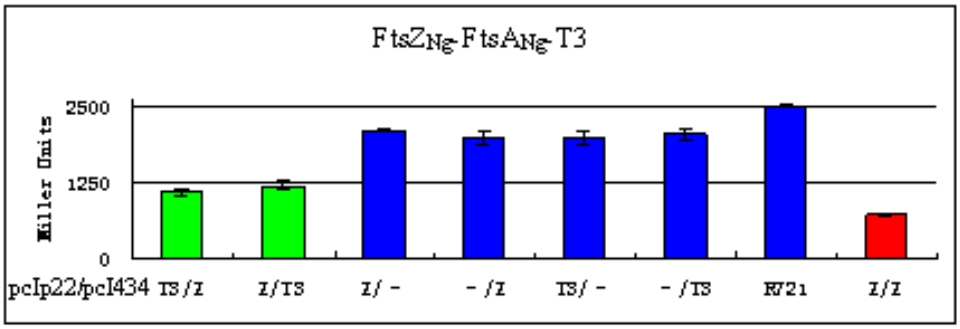
FtsZNg-FtsANg- T3
Miller Units
2500
1250
0
pcIp22/pcI434
T3/I
I/T3
I/ -
- /I
T3/ -
- /T3
RY21
I/I

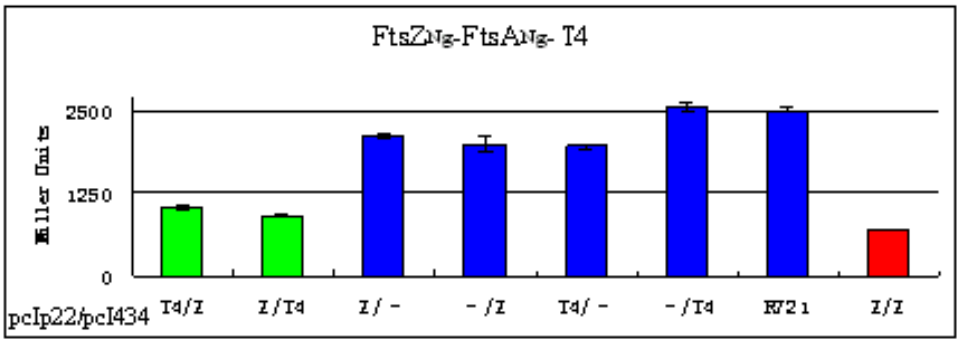
FtsZNg-FtsANg- T4
Miller Units
2500
1250
0
pcIp22/pcI434
T4/I
I/T4
I/ -
- /I
T4/ -
- /T4
RY21
I/I

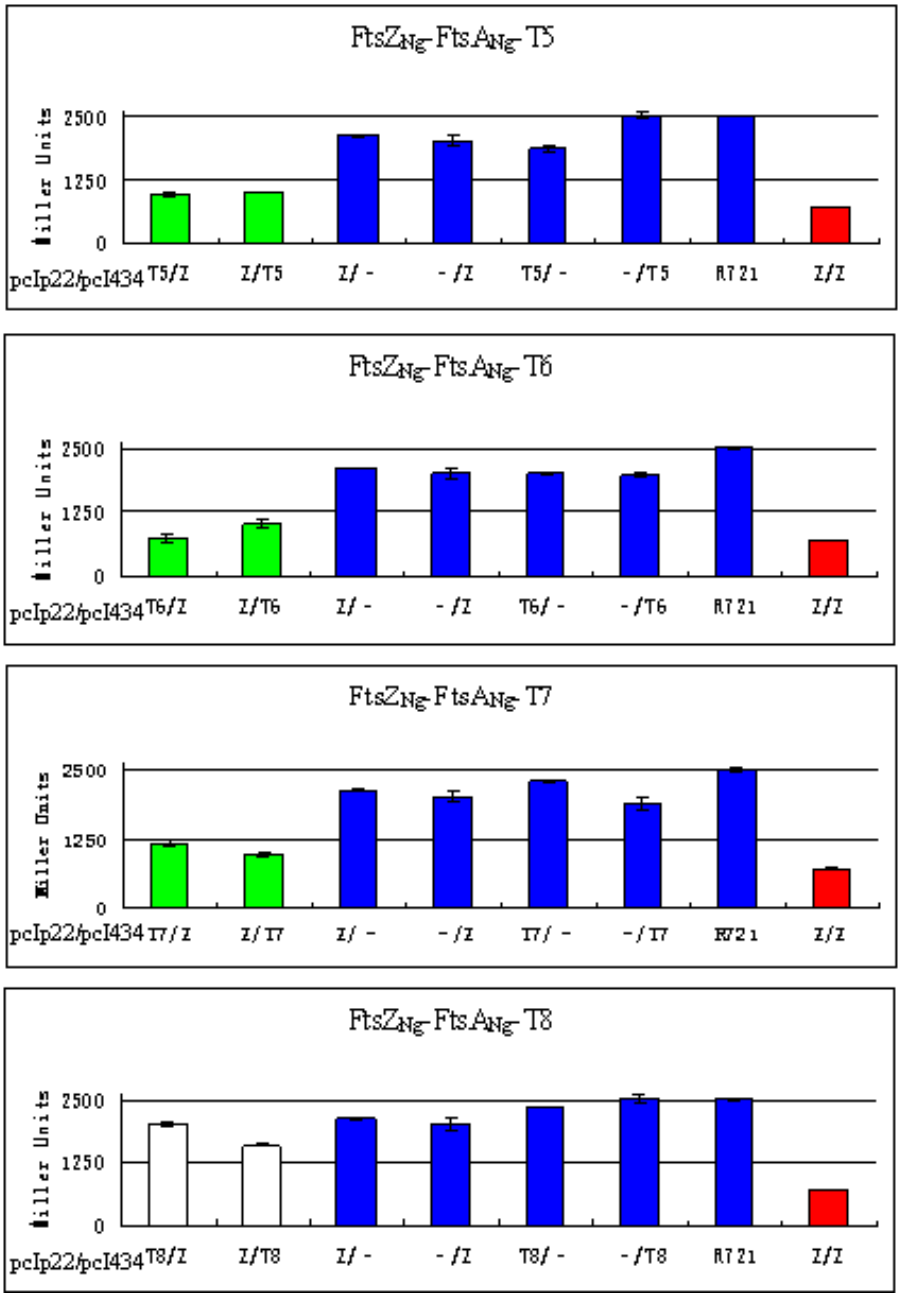

Fig. 3.7.Interactions between $FtsA_{Ng}$ domains (T1, T2, T3, T4, T5, T6, T7 and T8) and $FtsZ_{Ng}$ (Z) determined by B2H assay. Each gene was cloned into pcIp22 and pcI434 and constructs were transformed into *E. coli* R721 either singly or in combination. *N. gonorrhoeae* FtsZ self-interaction was used as positive control (red bar). R721 without plasmids and single transformants were used as negative controls (blue bars). R721 without plasmids had a β-galactosidase activity of 2504±34 Miller units. The β-galactosidase activity of each combination was compared to that of R721. Values of less than 50% (<1250 Miller Unites) indicate a positive interaction between two proteins (green bars) while values of more than 50% (>1250 Miller Units) indicate a negative interaction between the two proteins (white bars). T1 (i.e. $1A_N$+1C), T2 (i.e. T1+1A), T3 (i.e. T2+$2A_1$), T4 (i.e. 2B), T5 (i.e. T4+$2A_2$), T6 (i.e. T4+$2A_2$+$1A_C$), T7 (i.e. T8+$2A_2$), T8 (i.e. $1A_C$). Error bars indicate the standard deviations, n=9.

$2A_2$ with $FtsZ_{Ng}$ (Fig. 3.7). All results together showed that domains 2A (including $2A_1$ and $2A_2$) and 2B of $FtsA_{Ng}$ interacted with $FtsZ_{Ng}$.

The $FtsA_{Ng}$ domains interacting with $FtsZ_{Ng}$ identified by B2H assay were confirmed using GST pull-down assay and $FtsA_{Ng}$ truncations T2, T3, T4, T7 and T8 were examined (Fig. 3.8). The results showed that GST alone as negative control did not pull down any of $FtsA_{Ng}$ truncations (Fig. 3.8, Lane 2), suggesting that when any $FtsA_{Ng}$ truncation is pulled down by GST-$FtsZ_{Ng}$, $FtsZ_{Ng}$ contributes to the interaction. Truncations T3 (i.e. T2+$2A_1$), T4 (i.e. 2B) and T7 (i.e. T8+$2A_2$), which individually contain the $2A_1$, 2B and $2A_2$ domains, were pulled down by GST-$FtsZ_{Ng}$, while truncations T2 (i.e. $1A_N$+1C+1A) and T8 (i.e. $1A_C$), which does not contain either 2A or 2B, were not pulled down by GST-$FtsZ_{Ng}$ (Fig. 3.8). These results indicated that each of $2A_1$, $2A_2$ and 2B of $FtsA_{Ng}$ was sufficient for the interaction with $FtsZ_{Ng}$ as identified by B2H assays.

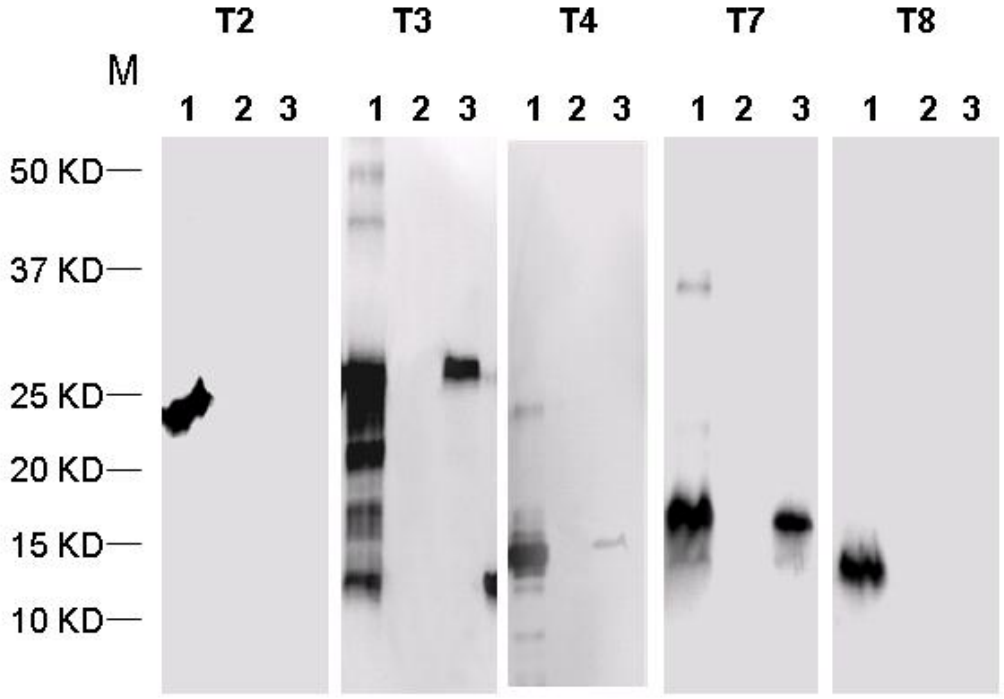

Fig. 3.8. GST pull-down assay to test the interaction between $FtsA_{Ng}$ truncations and $FtsZ_{Ng}$. Samples that contained GST or each $FtsA_{Ng}$ truncation were separated on 12% SDS-PAGE gel where the pull-down of $FtsA_{Ng}$ proteins were detected using anti-6xHis antibody. Lane 1: purified $FtsA_{Ng}$ truncations, T2, T3, T4, T7 and T8 were loaded as positive controls. Lane 2: GST with $FtsA_{Ng}$ T2, T3, T4, T7 and T8 were used as negative controls. Lane 3 : GST-$FtsZ_{Ng}$ with $FtsA_{Ng}$ T2, T3, T4, T7 and T8. None of $FtsA_{Ng}$ truncation was pulled down by GST alone (lane 2), while $FtsA_{Ng}$ truncations, T3, T4 and T7 were successfully pulled down by GST-$FtsZ_{Ng}$ (lane 3), which showed same size as purified T3, T4 and T7 (lane 1). T2 and T8 were not pulled down by GST-$FtsZ_{Ng}$ (lane 3). T2 (i.e. T1+1A), T3 (i.e. T2+$2A_1$), T4 (i.e. 2B), T7 (i.e. T8+$2A_2$), T8 (i.e. $1A_C$).

3.2.4. Novel domains of $FtsA_{Ng}$ involved in the interactions with other divisome proteins

$FtsA_{Ng}$ was determined to interact with several divisome proteins downstream of $FtsA_{Ng}$, including $FtsK_{Ng}$, $FtsQ_{Ng}$, $FtsW_{Ng}$, and $FtsN_{Ng}$, by B2H assay. In order to identify the functional domains that are required for these interactions, the $FtsA_{Ng}$ truncations (T2, T3, T4, T7 and T8) were used to test their ability to interact with these divisome proteins (Fig. 3.9-3.12). The most combinations were examined in two reciprocal ways and showed similar results, except $FtsK_{Ng}$. The interactions between $FtsA_{Ng}$ truncations and $FtsK_{Ng}$ were examined unidirectionally, i.e. pcIp22-$FtsA_{Ng}$ truncation/pcI434-$FtsK_{Ng}$, because the reciprocal vector pcIp22-$FtsK_{Ng}$ was not available.

As shown in Fig. 3.9, $FtsK_{Ng}$ interacted with truncations T3 (i.e. T2+$2A_1$), giving 36% residual β-galactosidase activities, and did not interacted with truncations T2 (i.e. $1A_N$-1C-1A) and T8 (i.e. $1A_C$), displaying 61% and 100% residual β-galactosidase activities, respectively. These results demonstrate that $FtsK_{Ng}$ interacted with domains $2A_1$. Based on B2H data, $FtsK_{Ng}$ may interact with truncation T4 (i.e. 2B), as it produced 45% residual β-galactosidase activity (Table 3.1). $FtsK_{Ng}$ may not interact with truncation T7 (i.e. T8+$2A_2$), as it produced 53% residual β-galactosidase activity (Table 3.1). The *t* test analysis showed that either 45% or 53% was not significantly different from the 50% cut-off criterium (Table 3.3), indicating transient or no interactions. Thus the interactions of $FtsK_{Ng}$ with $FtsA_{Ng}$ truncations T4 and T7 need to be further confirmed using other methods.

$FtsQ_{Ng}$ interacted with T4 (i.e. 2B) and T7 (i.e. T8+$2A_2$), giving 22% and 33% residual β-galactosidase activities, respectively, and did not interact with truncations T2 (i.e. $1A_N$-1C-1A), T3 (i.e. T2+$2A_1$) and T8 (i.e. $1A_C$), displaying 75%, 90%, and 63% residual β-galactosidase activities, respectively (Fig. 3.10). These results demonstrate that domains 2B and $2A_2$ of $FtsA_{Ng}$ interacted with $FtsQ_{Ng}$.

$FtsW_{Ng}$ did not interact any $FtsA_{Ng}$ truncation except T7 (i.e. T8+$2A_2$), giving a 20% residual β-galactosidase activity (Fig. 3.11), indicating the interaction between domain $2A_2$ of $FtsA_{Ng}$ and $FtsW_{Ng}$ (Table 3.1).

$FtsN_{Ng}$ interacted with truncations T4 (i.e. 2B) and T7 (i.e. T8+$2A_2$), giving 20%, and 32% residual β-galactosidase activities, respectively, and did not interacted with truncations T2 (i.e. $1A_N$-1C-1A) and T8 (i.e. $1A_C$), displaying 66% and 80% residual β-galactosidase activities, respectively, (Fig. 3.12). Protein pair T3-$FtsN_{Ng}$ displayed a 43% residual β-galactosidase activity (Fig. 3.12), which was significantly different from 50% as determined by *t* test (Table 3.3), indicating an interaction between $FtsA_{Ng}$ truncation T3 (i.e. T2+$2A_1$) and $FtsN_{Ng}$. These results demonstrate that domains $2A_1$, 2B and $2A_2$ of $FtsA_{Ng}$ interacted with $FtsN_{Ng}$ (Table 3.1).

As a summary shown in Table 3.1, truncation T2 (i.e. $1A_N$-1C-1A) did not interact with any divisome protein, while T3 (i.e. T2+$2A_1$) interacted with $FtsK_{Ng}$ and $FtsN_{Ng}$, indicating that domain $2A_1$ of $FtsA_{Ng}$ was responsible for the interaction with $FtsK_{Ng}$ and $FtsN_{Ng}$. Analogously, truncation T8 (i.e. $1A_C$) did not interaction with any divisome protein, while T7 (i.e. T8+$2A_2$) interacted with $FtsQ_{Ng}$, $FtsW_{Ng}$ and $FtsN_{Ng}$, indicating that domain $2A_2$ of FtsA was responsible for the interaction with $FtsQ_{Ng}$, $FtsW_{Ng}$ and $FtsN_{Ng}$. Truncation T4 (i.e. 2B) interacted with $FtsQ_{Ng}$ and $FtsN_{Ng}$ and possibly also interacted with $FtsK_{Ng}$, indicating that domain 2B of $FtsA_{Ng}$ was responsible for these interactions.

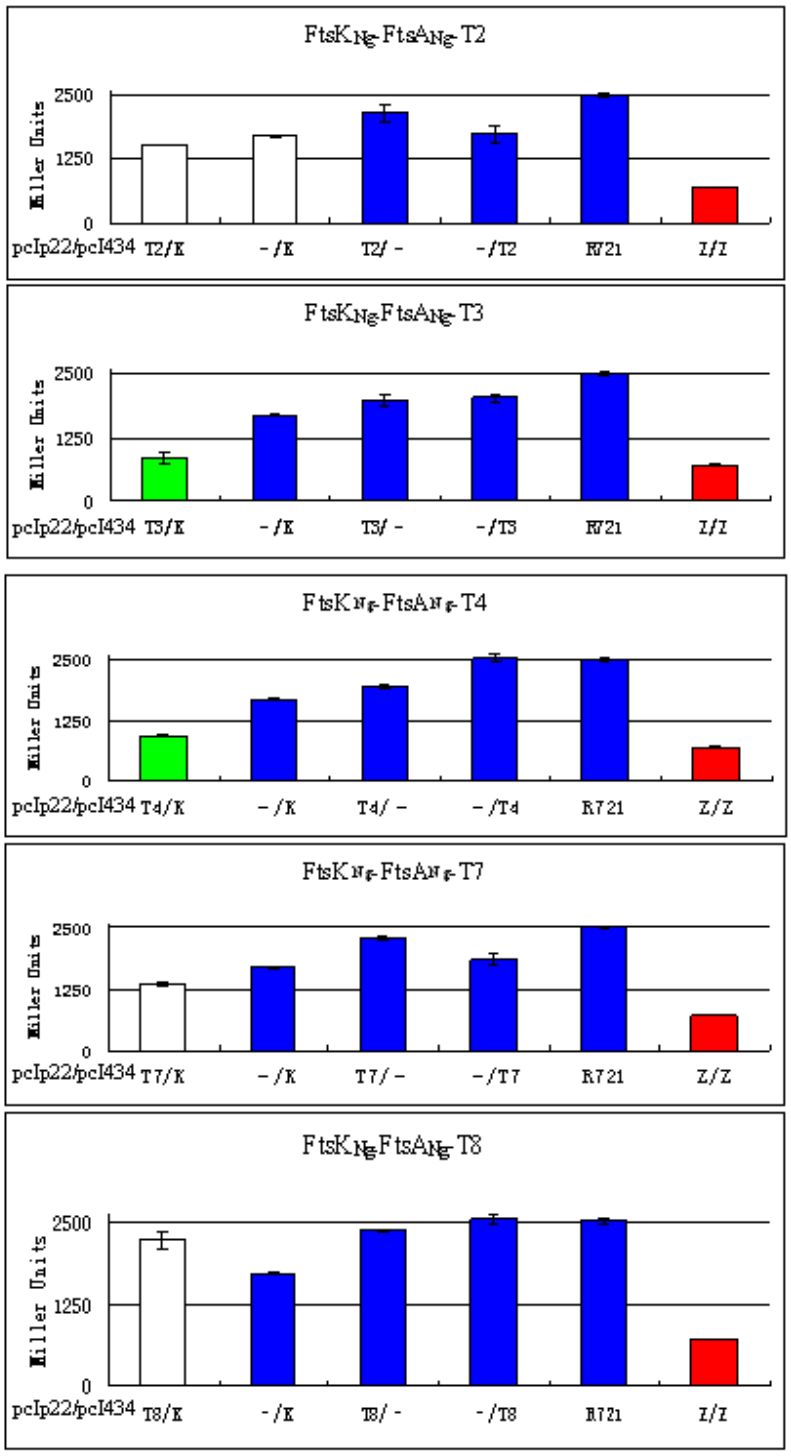

Fig. 3.9. Interactions between $FtsA_{Ng}$ domains (T2, T3, T4, T7 and T8) and $FtsK_{Ng}$ (K) determined byB2H assay. Each gene was cloned into pcIp22 and pcI434 and constructs were transformed into *E. coli* R721 either singly or in combination. *N. gonorrhoeae* FtsZ self-interaction was used as positive control (red bar). R721 without plasmids and single transformants were used as negative controls (blue bars). R721 had a β-galactosidase activity of 2504±34 Miller units. The β-galactosidase activity of each combination was compared to that of R721. Values of less than 50% (<1250 Miller Units) indicate a positive interaction between two proteins (green bars) while values of more than 50% indicate a negative interaction between the two proteins (white bars). T2 (i.e. T1+1A), T3 (i.e. $T2+2A_1$), T4 (i.e. 2B), T7 (i.e. $T8+2A_2$), T8 (i.e. $1A_C$). Error bars indicate standard deviations, n=9.

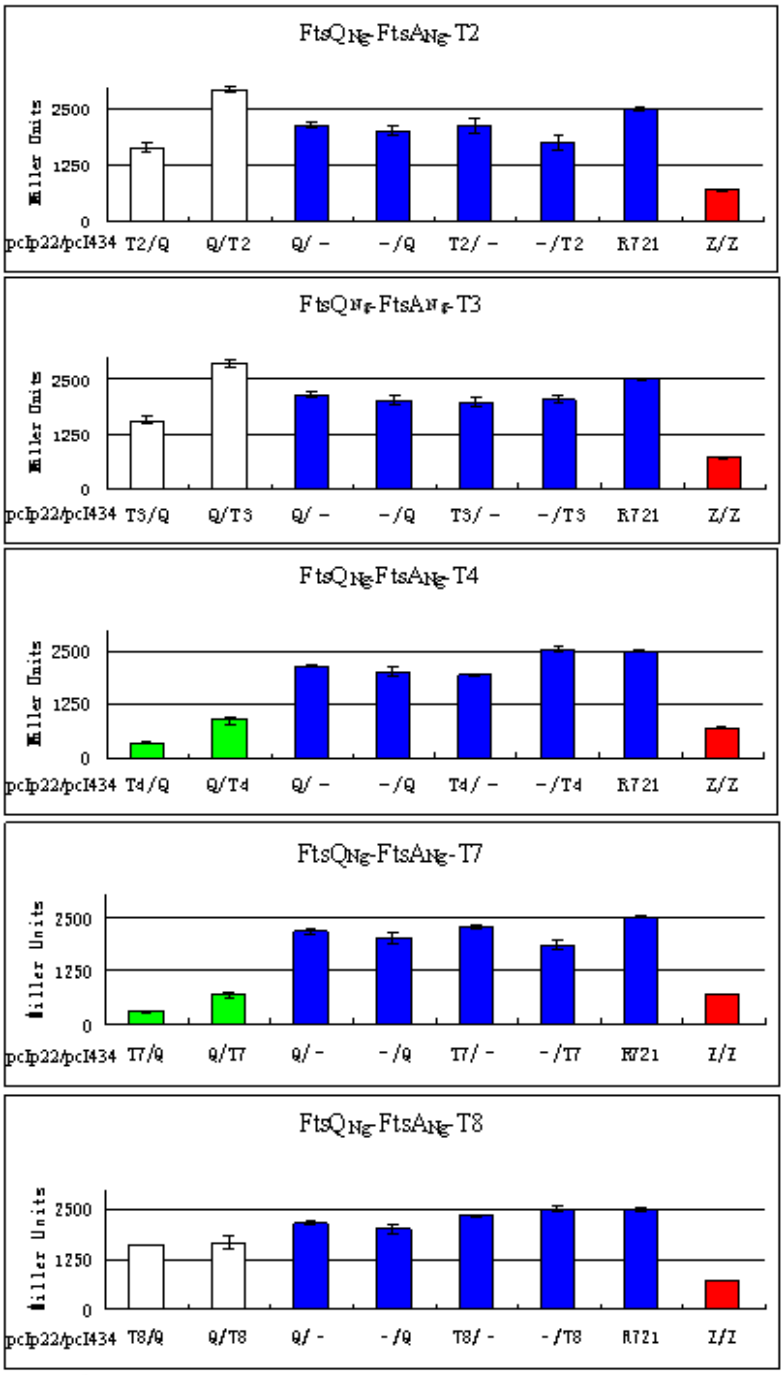

Fig. 3.10.Interactions between $FtsA_{Ng}$ domains (T2, T3, T4, T7 and T8) and $FtsQ_{Ng}$ (Q) determined by B2H assay. Each gene was cloned into pcIp22 and pcI434 and constructs were transformed into *E. coli* R721 either singly or in combination. *N. gonorrhoeae* FtsZ self-interaction was used as positive control (red bar). R721 without plasmids and single transformants were used as negative controls (blue bars). R721 had a β-galactosidase activity of 2504±34 Miller units. The β-galactosidase activity of each combination was compared to that of R721. Values of less than 50% (<1250 Miller Units) indicate a positive interaction between two proteins (green bars) while values of more than 50% indicate a negative interaction between the two proteins (white bars). T2 (i.e. T1+1A), T3 (i.e. $T2+2A_1$), T4 (i.e. 2B), T7 (i.e. $T8+2A_2$), T8 (i.e. $1A_C$). Error bars indicate standard deviations, n=9.

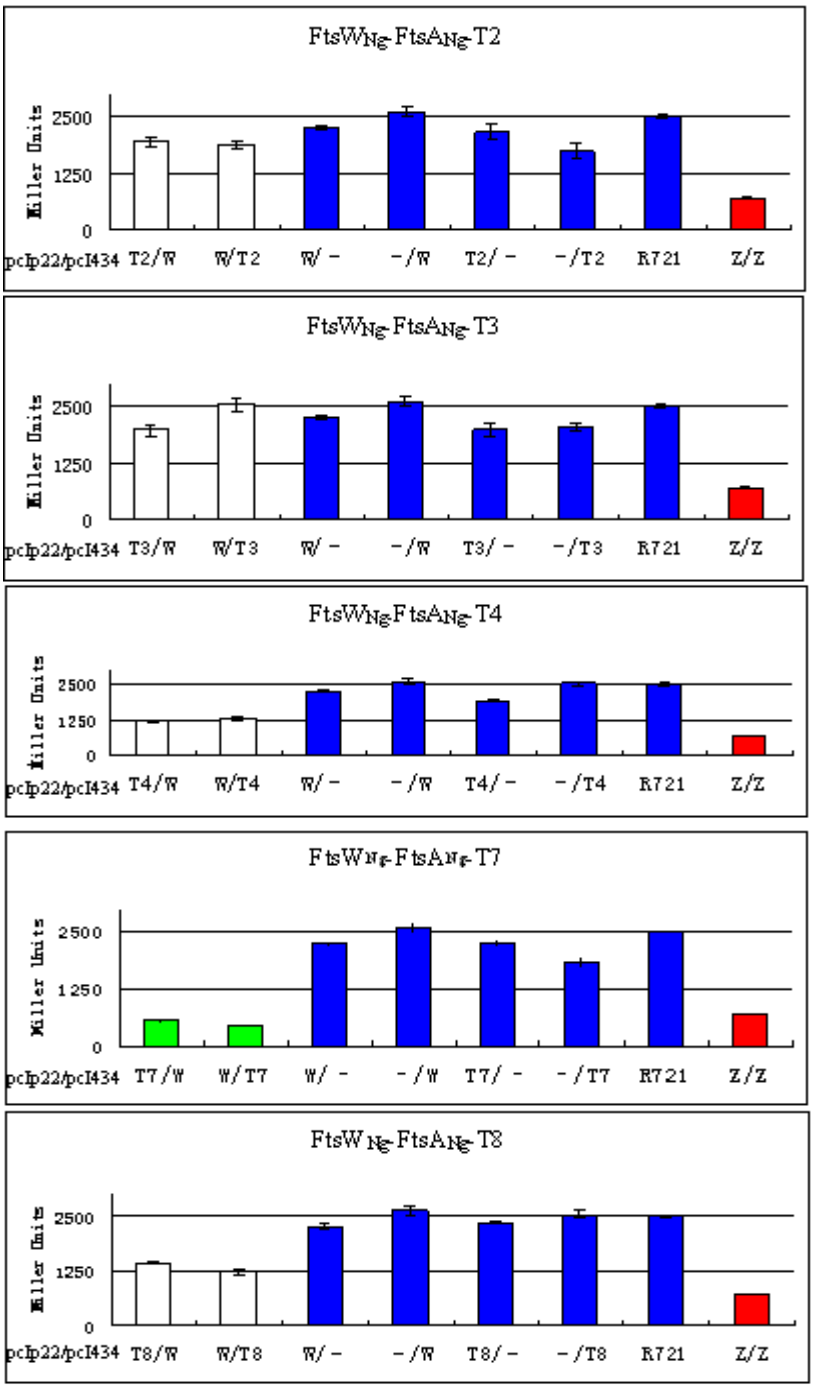

Fig. 3.11.Interactions between $FtsA_{Ng}$ domains (T2, T3, T4, T7 and T8) and $FtsW_{Ng}$ (W) determined by B2H assay. Each gene was cloned into pcIp22 and pcI434 and constructs were transformed into *E. coli* R721 either singly or in combination. *N. gonorrhoeae* FtsZ self-interaction was used as positive control (red bar). R721 without plasmids and single transformants were used as negative controls (blue bars). R721 had a β-galactosidase activity of 2504±34 Miller units. The β-galactosidase activity of each combination was compared to that of R721. Values of less than 50% (<1250 Miller Units) indicate a positive interaction between two proteins (green bars) while values of more than 50% indicate a negative interaction between the two proteins (white bars). T2 (i.e. T1+1A), T3 (i.e. $T2+2A_1$), T4 (i.e. 2B), T7 (i.e. $T8+2A_2$), T8 (i.e. $1A_C$). Error bars indicate standard deviations, n=9.

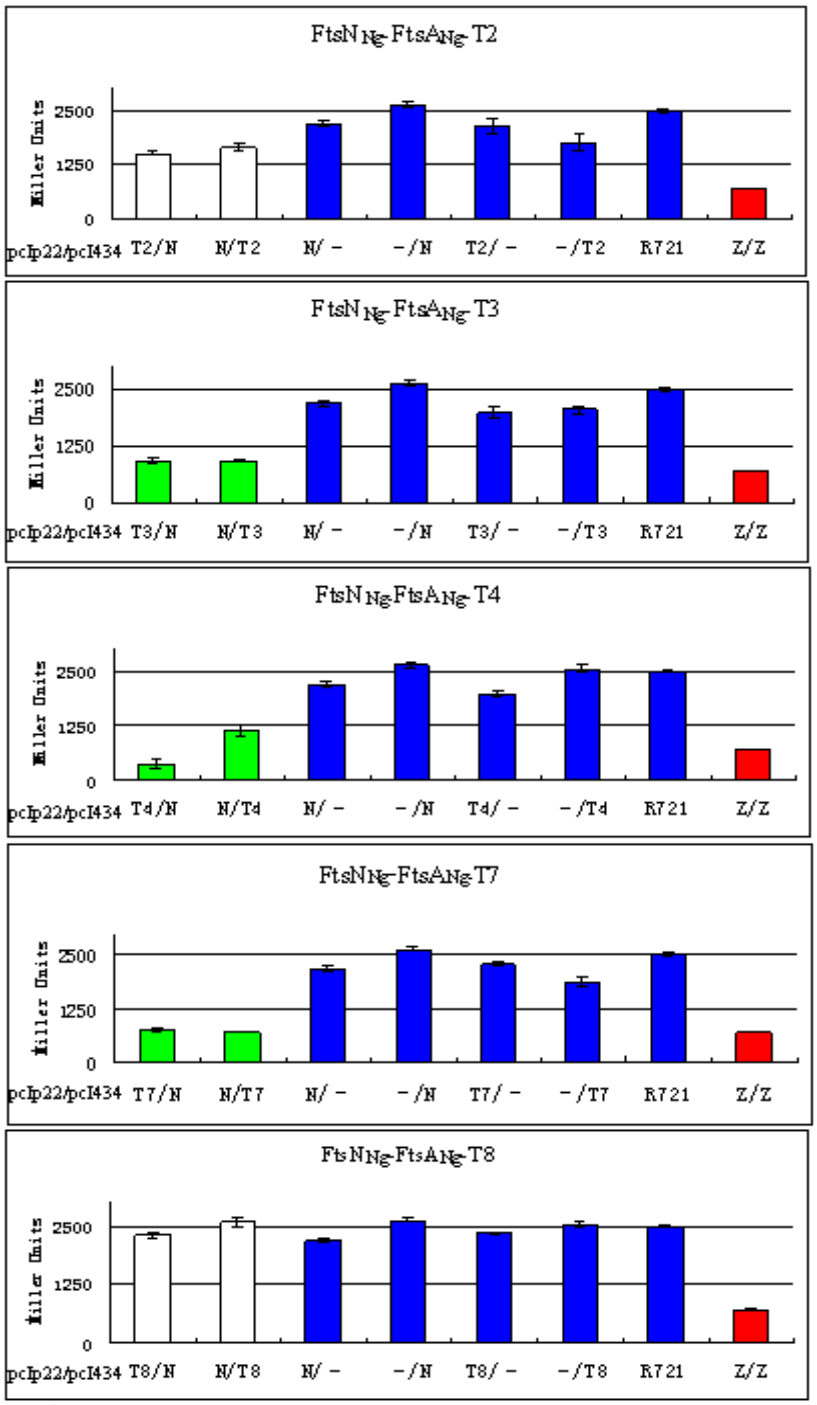

Fig. 3.12.Interactions between $FtsA_{Ng}$ domains (T2, T3, T4, T7 and T8) and $FtsN_{Ng}$ (N) determined by B2H assay. Each gene was cloned into pcIp22 and pcI434 and constructs were transformed into *E. coli* R721 either singly or in combination. *N. gonorrhoeae* FtsZ self-interaction was used as positive control (red bar). R721 without plasmids and single transformants were used as negative controls (blue bars). R721 had a β-galactosidase activity of 2504±34 Miller units. The β-galactosidase activity of each combination was compared to that of R721. Values of less than 50% (<1250 Miller Units) indicate a positive interaction between two proteins (green bars) while values of more than 50% indicate a negative interaction between the two proteins (white bars). T2 (i.e. T1+1A), T3 (i.e. $T2+2A_1$), T4 (i.e. 2B), T7 (i.e. $T8+2A_2$), T8 (i.e. $1A_C$). Error bars indicate standard deviations, n=9.

Table 3.1. Summary of interactions of $FtsA_{Ng}$ truncations with $FtsZ_{Ng}$, $FtsK_{Ng}$, $FtsQ_{Ng}$, $FtsW_{Ng}$ and $FtsN_{Ng}$ as determined by B2H assays. Residual ß-galactosidase activity of < 50% (in bold) indicates an interaction between the divisome protein and peptide coded by the particular $FtsA_{Ng}$ truncation. NT, not tested. "+" indicates that domain presents in $FtsA_{Ng}$ truncation.

$FtsA_{Ng}$	Domains							β-galactosidase activity				
Truncations	**$1A_N$**	**1C**	**1A**	**$2A_1$**	**2B**	**$2A_2$**	**$1A_C$**	**FtsZ**	**FtsK**	**FtsQ**	**FtsW**	**FtsN**
T1	+	+						92%	NT	NT	NT	NT
T2	+	+	+					100%	61%	75%	86%	66%
T3	+	+	+	+				**45%**	**36%**	90%	90%	**43%**
T4					+			**38%**	**45%**	**22%**	55%	**20%**
T5					+	+		**40%**	NT	NT	NT	NT
T6					+	+	+	**35%**	NT	NT	NT	NT
T7						+	+	**42%**	53%	**33%**	**20%**	**32%**
T8							+	72%	100%	63%	53%	80%

3.2.5. Interactions between $FtsZ_{Ng}$ and other divisome proteins

The potential interactions between $FtsZ_{Ng}$ and other 8 divisome proteins, $ZipA_{Ng}$, $FtsK_{Ng}$, $FtsI_{Ng}$, $FtsQ_{Ng}$, $FtsW_{Ng}$, $FtsN_{Ng}$, $FtsE_{Ng}$, and $FtsX_{Ng}$ were examined using B2H assays. $FtsZ_{Ng}$ was found to interact with $FtsK_{Ng}$, giving a 40% residual β-galactosidase activity (Fig. 3.13A), an extremely significant difference from 50% cut-off criterium as determined by *t* test (Table 3.3). $FtsZ_{Ng}$ interacted with $FtsE_{Ng}$, giving 39% residual β-galactosidase activity, (Fig. 3.13B). $FtsZ_{Ng}$ interaction with $FtsW_{Ng}$ was novel in *N. gonorrhoeae,* giving 39% residual β-galactosidase activity (Fig. 3.13C). $FtsZ_{Ng}$ interacted with $FtsX_{Ng}$, as it produced a 42% residual β-galactosidase activity (Fig. 3.13D). However, the value of 42% was not significantly different from the 50% cut-off criterium as determined by *t* test (Table 3.3), indicating weak or transient interaction between $FtsZ_{Ng}$ and $FtsX_{Ng}$. This interaction needs to be further confirmed by performing other methods. $FtsZ_{Ng}$ did not interact with $ZipA_{Ng}$, $FtsI_{Ng}$, $FtsQ_{Ng}$ and $FtsN_{Ng}$ in *N. gonorrhoeae*, giving 71%, 91%, 73%, and 76% residual β-galactosidase activities, respectively (Fig. 3.13E-H). All the interactions were examined with both the pcIp22-X_{Ng}/pcI434-Y_{Ng} and pcIp22-Y_{Ng}/pcI434-X_{Ng} pairs, except $FtsZ_{Ng}$–$FtsK_{Ng}$. Interaction of FtsZ-FtsK was examined with pcIp22-$FtsZ_{Ng}$/pcI434-$FtsK_{Ng}$ only, as the reciprocal one is not available.

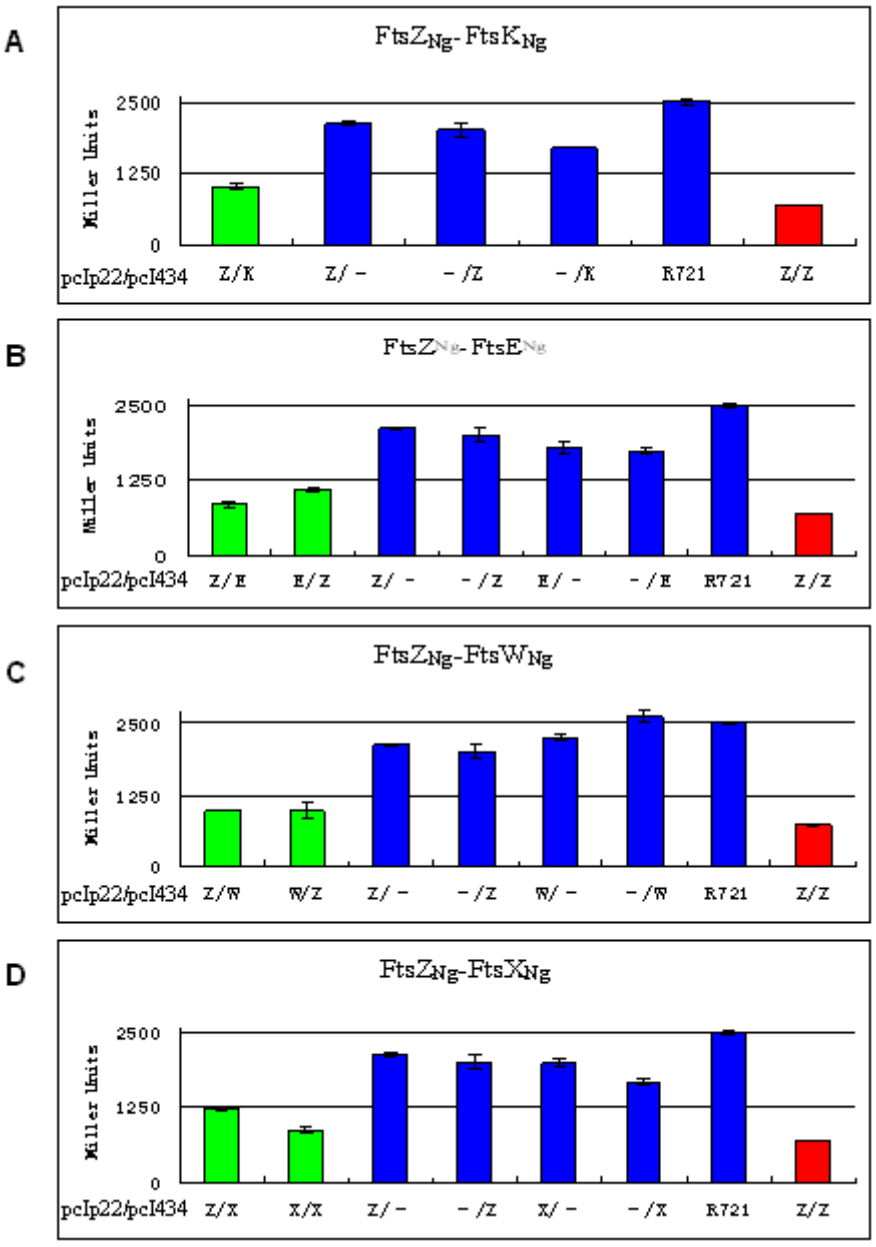
A
FtsZNg-FtsKNg
Miller Units
2500
1250
0
pcIp22/pcI434
Z/K
Z/ -
- /Z
- /K
R721
Z/Z
B
FtsZNg-FtsENg
Miller Units
2500
1250
0
pcIp22/pcI434
Z/E
E/Z
Z/ -
- /Z
E/ -
- /E
R721
Z/Z
C
FtsZNg-FtsWNg
Miller Units
2500
1250
0
pcIp22/pcI434
Z/W
W/Z
Z/ -
- /Z
W/ -
- /W
R721
Z/Z
D
FtsZNg-FtsXNg
Miller Units
2500
1250
0
pcIp22/pcI434
Z/X
X/X
Z/ -
- /Z
X/ -
- /X
R721
Z/Z

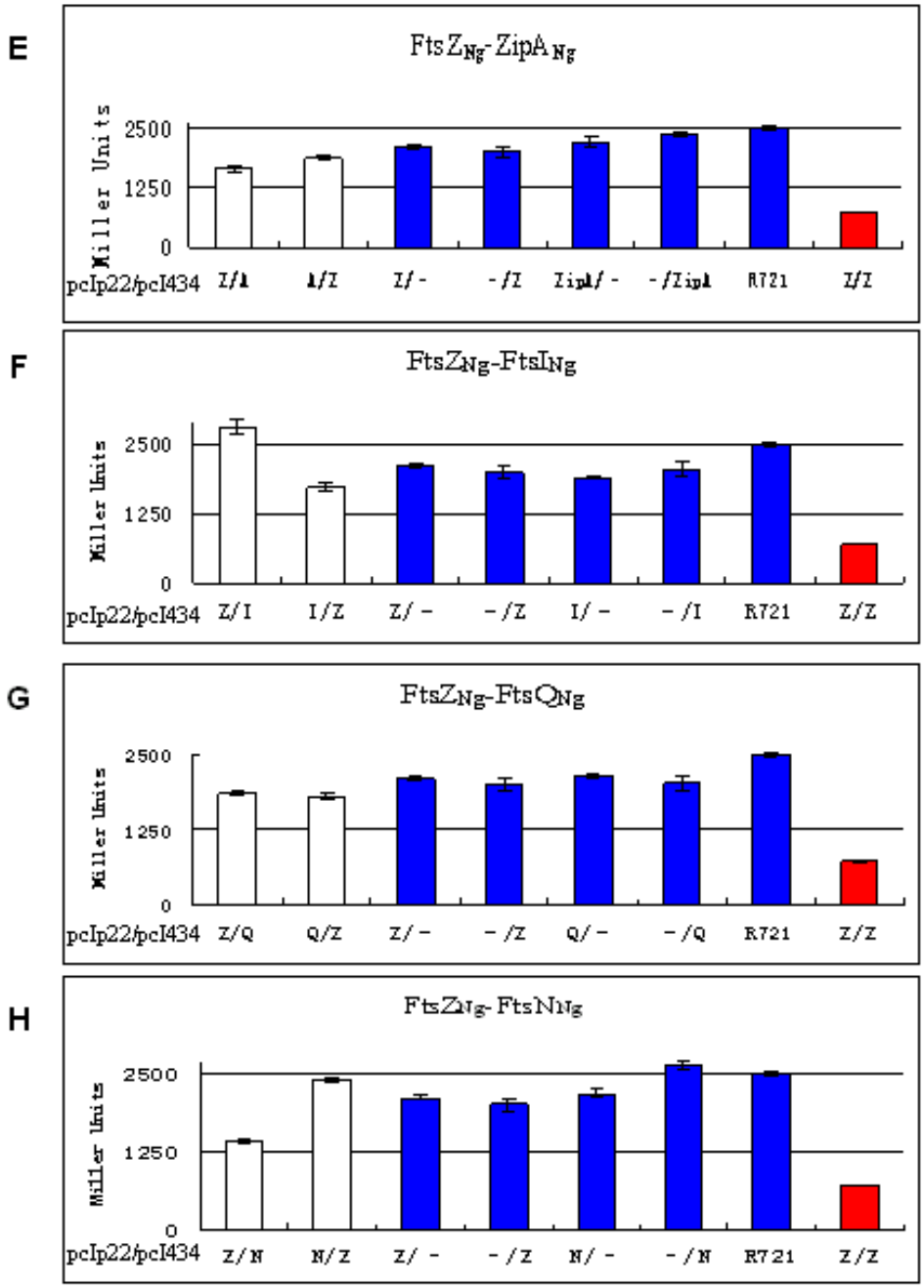

Fig. 3.13. Interaction of $FtsZ_{Ng}$ (Z) with other divisome proteins, $ZipA_{Ng}$, $FtsK_{Ng}$ (K), $FtsI_{Ng}$ (I), $FtsQ_{Ng}$ (Q), $FtsW_{Ng}$ (W), $FtsN_{Ng}$ (N), $FtsE_{Ng}$ (E) and $FtsX_{Ng}$ (X) determined by B2H assays. Each gene was cloned into pcIp22 and pcI434 and constructs were transformed into *E. coli* R721 either singly or in combination. *N. gonorrhoeae* FtsZ self-interaction was used as positive control (red bar). R721 without plasmids and single transformants were used as negative controls (blue bars). R721 without plasmids had a β-galactosidase activity of 2504±34 Miller units. The β-galactosidase activity of each combination was compared to that of R721. Values of less than 50% (<1250 Miller Units) indicate a positive interaction between two proteins (green bars) while values of more than 50% (>1250 Miller Unites) indicate a negative interaction between the two proteins (white bars). Error bars indicate standard deviations, n=9.

3.2.6. Interactions between divisome proteins downstream of $FtsA_{Ng}$

Hetero-interactions of 7 *N. gonorrhoeae* divisome proteins downstream of $FtsA_{Ng}$ (FtsK, FtsQ, FtsI, FtsW, FtsN, FtsE and FtsX) were examined using B2H assays. Twenty one possible combinations of any two proteins were tested; 6 showed interactions, 1 showed weak or transient interaction while 14 showed no interaction (Fig. 3.14, Table 3.2, 3.3). The interactions of $FtsK_{Ng}$ with other divisome proteins downstream of $FtsA_{Ng}$ were examined with pcIp22-$FtsK_{Ng}$/pcI434-Fts_{Ng} only. The rest of interactions all were examined with both pcIp22-X_{Ng}/pcI434-Y_{Ng} and pcIp22-Y_{Ng}/pcI434-X_{Ng} pairs.

$FtsK_{Ng}$ interacted with only one downstream divisome protein, $FtsN_{Ng}$, giving a 29% residual β-galactosidase activity. $FtsK_{Ng}$ did not interact with $FtsI_{Ng}$, $FtsQ_{Ng}$, $FtsW_{Ng}$, $FtsE_{Ng}$ and $FtsX_{Ng}$, displaying 76%, 88%, 100%, 100%, and 100% residual β-galactosidase activities, respectively (Fig. 3.14, Table 3.2).

Protein pairs of $FtsQ_{Ng}$-$FtsE_{Ng}$ and $FtsQ_{Ng}$-$FtsX_{Ng}$ interaction produced 44% and 46% residual β-galactosidase activities, respectively (Fig. 3.14). *t* test analysis showd that the difference between values 44% and 50% was considered to be significant (Table 3.3), indicating a positive interaction between $FtsQ_{Ng}$ and $FtsE_{Ng}$. However, *t* test analysis showd that the difference between values 46% and 50% was not considered to be significant (Table 3.3), indicating weak or transient or no interaction between $FtsQ_{Ng}$ and $FtsX_{Ng}$. $FtsQ_{Ng}$ did not interact with $FtsK_{Ng}$, $FtsI_{Ng}$, $FtsW_{Ng}$ and $FtsN_{Ng}$, displaying 88%, 90%, 100%, and 88% residual β-galactosidase activities, respectively (Fig. 3.14, Table 3.2).

As predicted by results from studies performed with *E. coli*, *N. gonorrhoeae* FtsI interacted with $FtsW_{Ng}$, giving a 35% residual β-galactosidase activity. $FtsI_{Ng}$ did not interact with other divisome proteins downstream of $FtsA_{Ng}$, $FtsK_{Ng}$, $FtsQ_{Ng}$, $FtsN_{Ng}$, $FtsE_{Ng}$ and $FtsX_{Ng}$, displaying 76%, 90%, 100%, 78%, and 97% residual β-galactosidase activities, respectively (Fig. 3.14, Table 3.2).

$FtsW_{Ng}$ interacted with two proteins $FtsI_{Ng}$ giving 35% residual β-galactosidase activity as observed in *E. coli* (Di Lallo *et al.*, 2003). $FtsW_{Ng}$ also interacted with $FtsX_{Ng}$, giving a 40% residual β-galactosidase activity, which showed significant difference from the 50% cut-off criterium as determined by the *t* test (Table 3.3). $FtsW_{Ng}$ did not interact with $FtsK_{Ng}$, $FtsQ_{Ng}$, $FtsN_{Ng}$ and $FtsE_{Ng}$, displaying 100%, 100%, 97%, and 80% residual β-galactosidase activities, respectively (Fig. 3.14, Table 3.2).

$FtsN_{Ng}$ interacted with $FtsK_{Ng}$ and $FtsX_{Ng}$, giving 31% and 18% residual β-galactosidase activities, respectively. FtsN did not interact with $FtsI_{Ng}$, $FtsQ_{Ng}$, $FtsW_{Ng}$ and $FtsE_{Ng}$, displaying 100%, 88%, 97%, and 89% residual β-galactosidase activities, respectively (Fig. 3.14, Table 3.2).

$FtsE_{Ng}$ interacted with $FtsQ_{Ng}$ and $FtsX_{Ng}$, giving 44% and 40% residual β-galactosidase activities, respectively (Fig. 3.14), a significant difference from the 50% cut-off criterium (Table 3.3). $FtsE_{Ng}$ did not interact with $FtsK_{Ng}$, $FtsI_{Ng}$, $FtsW_{Ng}$ and $FtsN_{Ng}$, displaying 100%, 78%, 80%, 89% residual β-galactosidase activities, respectively (Fig. 3.14, Table 3.2).

$FtsX_{Ng}$ interacted with $FtsW_{Ng}$ $FtsN_{Ng}$ and $FtsE_{Ng}$ in *N. gonorrhoeae* as I descriped above, giving 40%, 18%, and 40% residual β-galactosidase activities, respectively (Fig. 3.14, Tables 3.2, 3.3). $FtsX_{Ng}$ might interact weakly with $FtsQ_{Ng}$, giving a 46% residual β-galactosidase activity. $FtsX_{Ng}$ did not interact with $FtsK_{Ng}$ and $FtsI_{Ng}$, displaying 100% and 97% residual β-galactosidase activities, respectively (Fig. 3.14, Table 3.2).

Fig. 3.14. Interactions between $FtsK_{Ng}$ (K), $FtsI_{Ng}$ (I), $FtsQ_{Ng}$ (Q), $FtsW_{Ng}$ (W), $FtsN_{Ng}$ (N), $FtsE_{Ng}$ (E) and $FtsX_{Ng}$ (X) determined by B2H assays. Each gene was cloned into pcIp22 and pcI434 and constructs were transformed into *E. coli* R721 either singly or in combination. *N. gonorrhoeae* FtsZ self-interaction was used as positive control (red bar). R721 without plasmids and single transformants were used as negative controls (blue bars). R721 without plasmids had a β-galactosidase activity of 2504±34 Miller units. The β-galactosidase activity of each combination was compared to that of R721. Values of less than 50% (<1250 Miller Units) indicate a positive interaction between two proteins (green bars) while values of more than 50% (>1250 Miller Unites) indicate a negative interaction between the two proteins (white bars). Error bars indicate standard deviations, n=9.

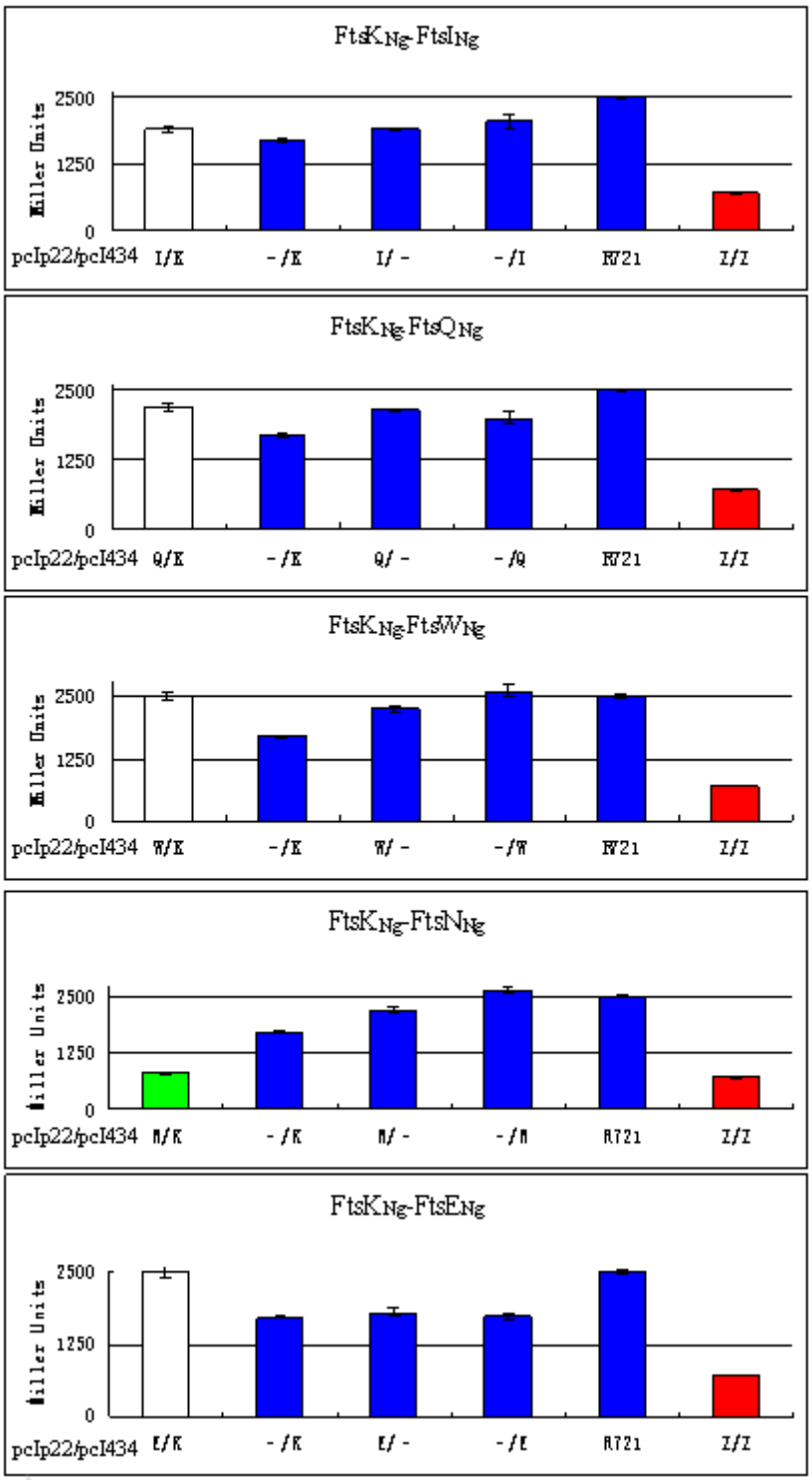
FtsK$_{Ng}$-FtsI$_{Ng}$
Miller Units
2500
1250
0
pcIp22/pcI434
I/K
-/K
I/-
-/I
RV21
I/I
FtsK$_{Ng}$-FtsQ$_{Ng}$
Miller Units
2500
1250
0
pcIp22/pcI434
Q/K
-/K
Q/-
-/Q
RV21
I/I
FtsK$_{Ng}$-FtsW$_{Ng}$
Miller Units
2500
1250
0
pcIp22/pcI434
W/K
-/K
W/-
-/W
RV21
I/I
FtsK$_{Ng}$-FtsN$_{Ng}$
Miller Units
2500
1250
0
pcIp22/pcI434
N/K
-/K
N/-
-/N
RV21
I/I
FtsK$_{Ng}$-FtsE$_{Ng}$
Miller Units
2500
1250
0
pcIp22/pcI434
E/K
-/K
E/-
-/E
RV21
I/I

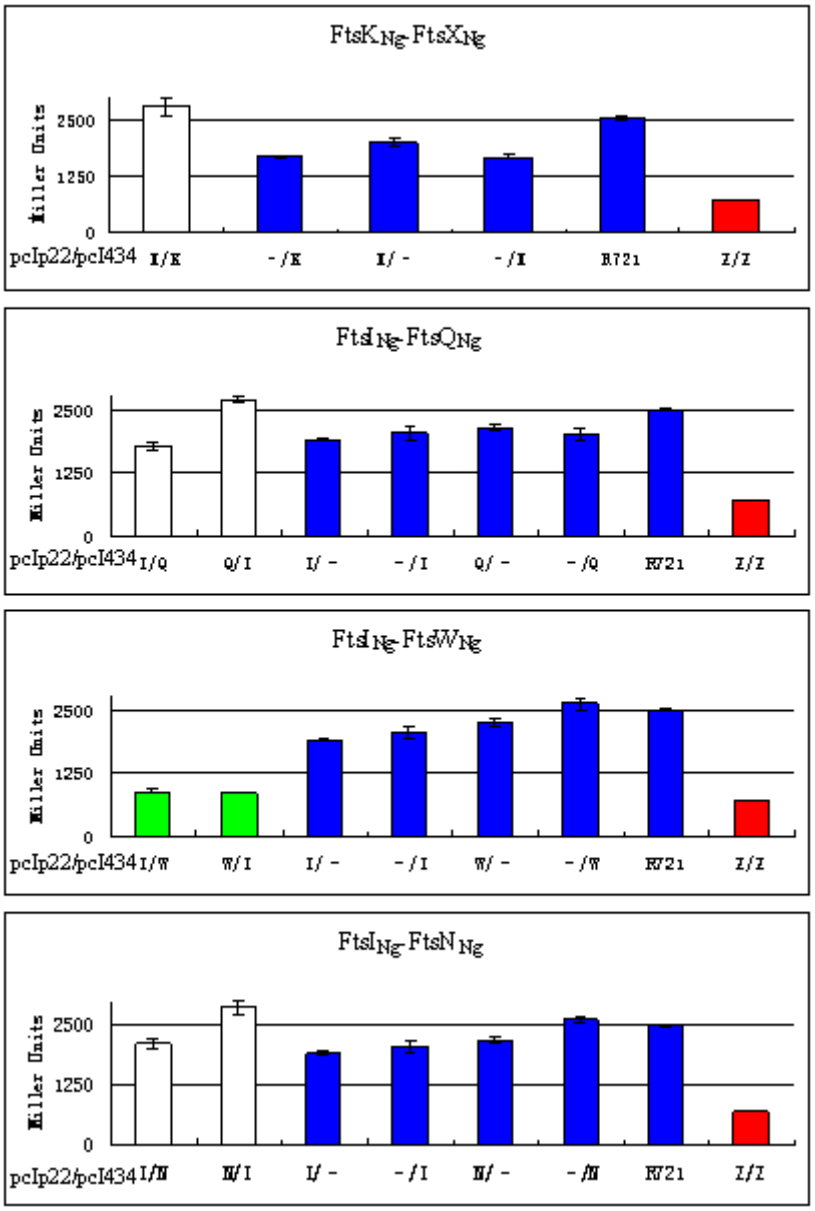
FtsK$_{Ng}$-FtsX$_{Ng}$
Miller Units
2500
1250
0
pcIp22/pcI434
I/K
-/K
I/-
-/I
R721
I/I
FtsI$_{Ng}$-FtsQ$_{Ng}$
Miller Units
2500
1250
0
pcIp22/pcI434
I/Q
Q/I
I/-
-/I
Q/-
-/Q
R721
I/I
FtsI$_{Ng}$-FtsW$_{Ng}$
Miller Units
2500
1250
0
pcIp22/pcI434
I/W
W/I
I/-
-/I
W/-
-/W
R721
I/I
FtsI$_{Ng}$-FtsN$_{Ng}$
Miller Units
2500
1250
0
pcIp22/pcI434
I/N
N/I
I/-
-/I
N/-
-/N
R721
I/I

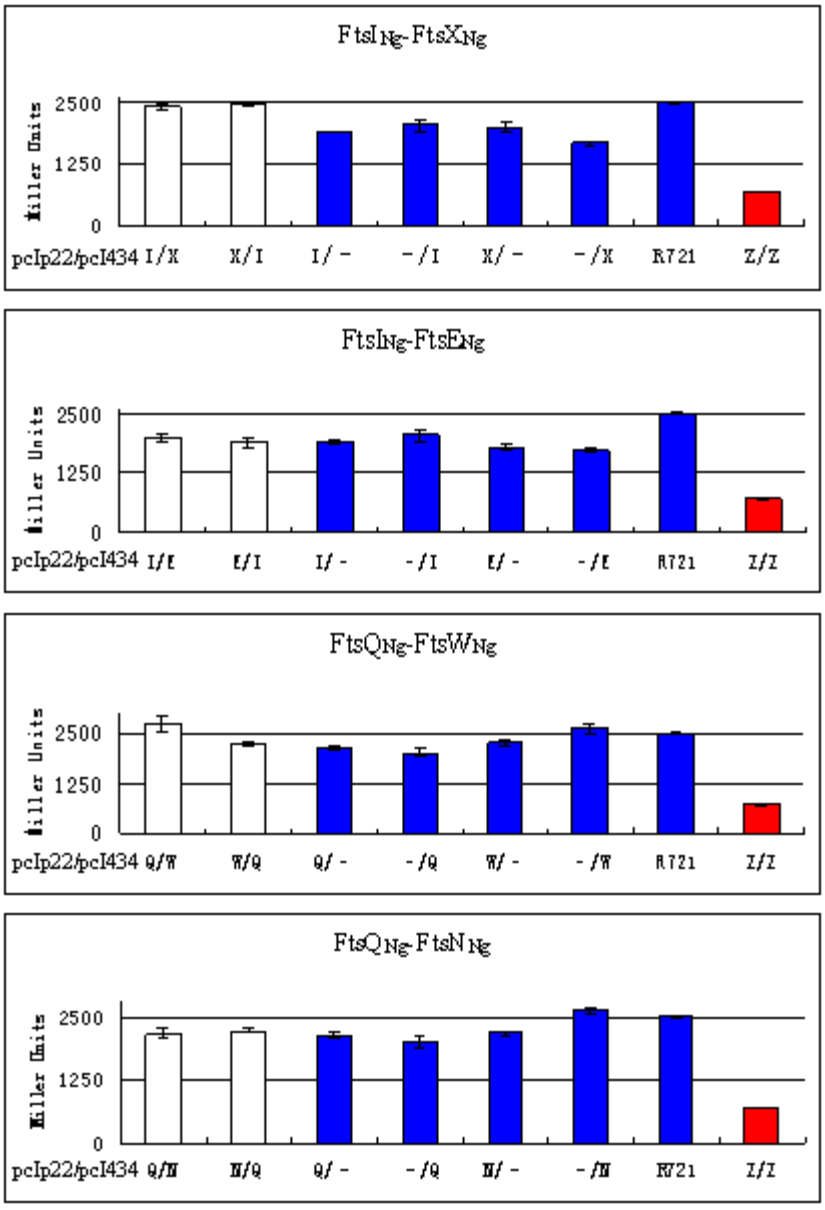
FtsI$_{Ng}$-FtsX$_{Ng}$
Miller Units
2500
1250
0
pclp22/pcI434 I/X X/I I/- -/I X/- -/X R721 Z/Z
FtsI$_{Ng}$-FtsE$_{Ng}$
Miller Units
2500
1250
0
pclp22/pcI434 I/E E/I I/- -/I E/- -/E R721 Z/Z
FtsQ$_{Ng}$-FtsW$_{Ng}$
Miller Units
2500
1250
0
pclp22/pcI434 Q/W W/Q Q/- -/Q W/- -/W R721 Z/Z
FtsQ$_{Ng}$-FtsN$_{Ng}$
Miller Units
2500
1250
0
pclp22/pcI434 Q/N N/Q Q/- -/Q N/- -/N R721 Z/Z

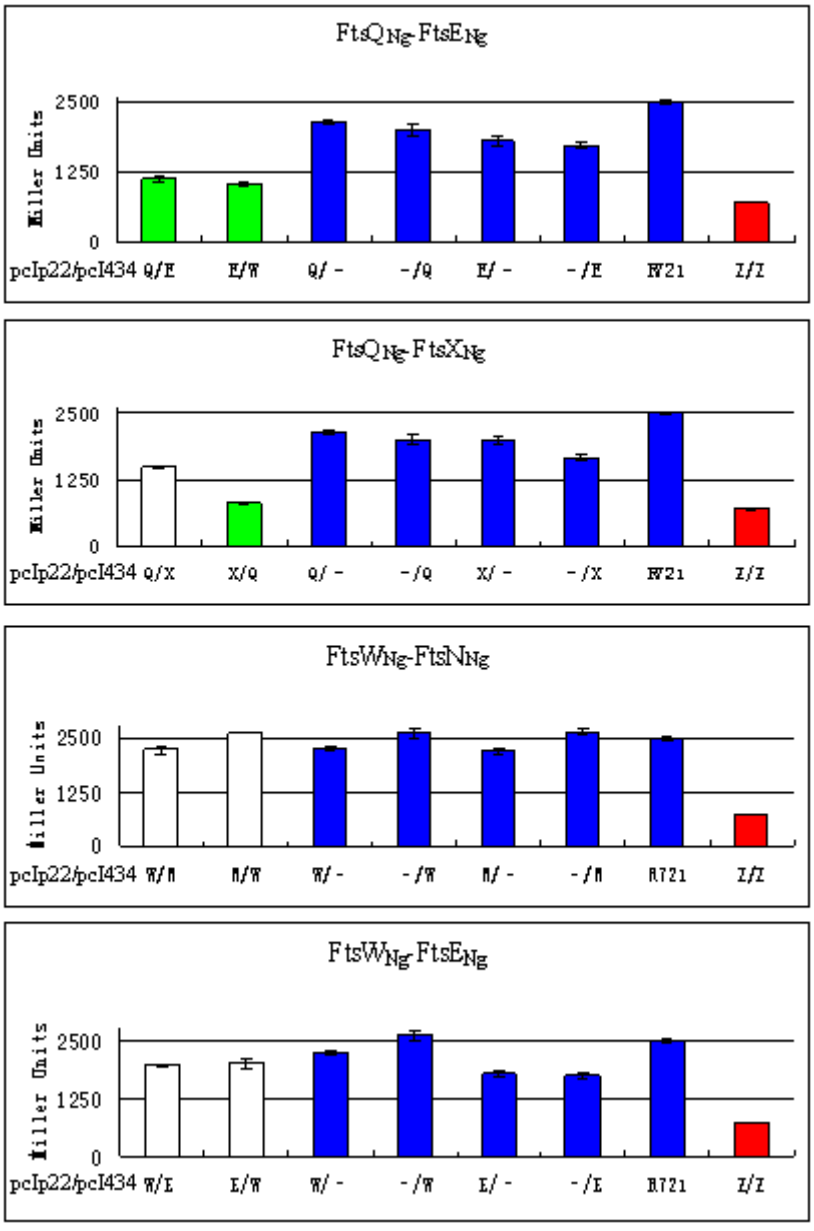
FtsQNg-FtsENg
Miller Units
2500
1250
0
pcIp22/pcI434 Q/E
E/W
Q/ -
-/Q
E/ -
-/E
W21
Z/Z
FtsQNg-FtsXNg
Miller Units
2500
1250
0
pcIp22/pcI434 Q/X
X/Q
Q/ -
-/Q
X/ -
-/X
W21
Z/Z
FtsWNg-FtsNNg
Miller Units
2500
1250
0
pcIp22/pcI434 W/N
N/W
W/ -
-/W
N/ -
-/N
R721
Z/Z
FtsWNg-FtsENg
Miller Units
2500
1250
0
pcIp22/pcI434 W/E
E/W
W/ -
-/W
E/ -
-/E
R721
Z/Z

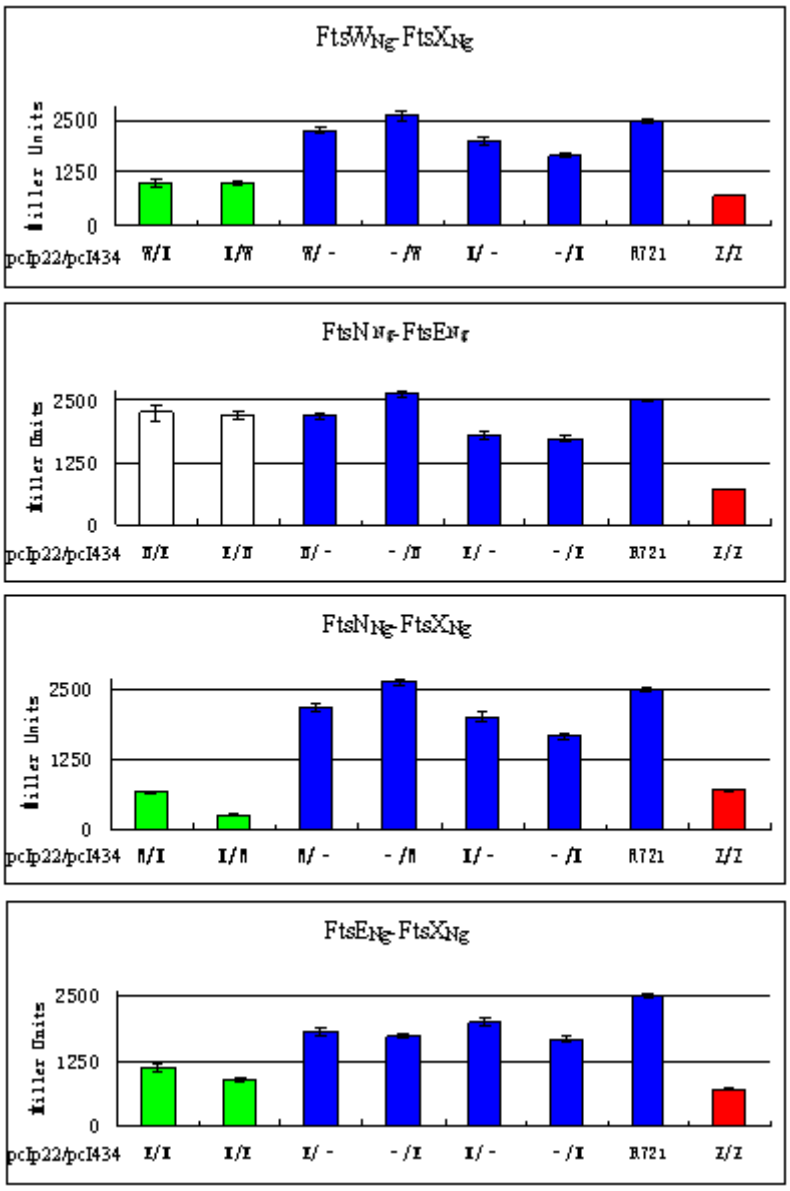
FtsW$_{Ng}$-FtsX$_{Ng}$
Miller Units
2500
1250
0
pcIp22/pcI434
W/I
I/W
W/ -
- /W
I/ -
- /I
R721
I/I
FtsN$_{Ng}$-FtsE$_{Ng}$
Miller Units
2500
1250
0
pcIp22/pcI434
N/I
I/N
N/ -
- /N
I/ -
- /I
R721
I/I
FtsN$_{Ng}$-FtsX$_{Ng}$
Miller Units
2500
1250
0
pcIp22/pcI434
N/I
I/N
N/ -
- /N
I/ -
- /I
R721
I/I
FtsE$_{Ng}$-FtsX$_{Ng}$
Miller Units
2500
1250
0
pcIp22/pcI434
E/I
I/E
E/ -
- /E
I/ -
- /I
R721
I/I

3.2.7. Interactions between $ZipA_{Ng}$ and divisome proteins downstream of $FtsA_{Ng}$

Since ZipA did not interact with FtsZ in *N. gonorrhoeae*, it may be involved in cell division by interacting with other divisome proteins. Thus the interactions between ZipA and the proteins downstream of $FtsA_{Ng}$ were examined using B2H assays. As shown in Fig. 3.15, all protein pairs composed of ZipA and another divisome proteins presented high β-galactosidase activities (> 1250 Miller Units), indicating the lack of protein interactions.

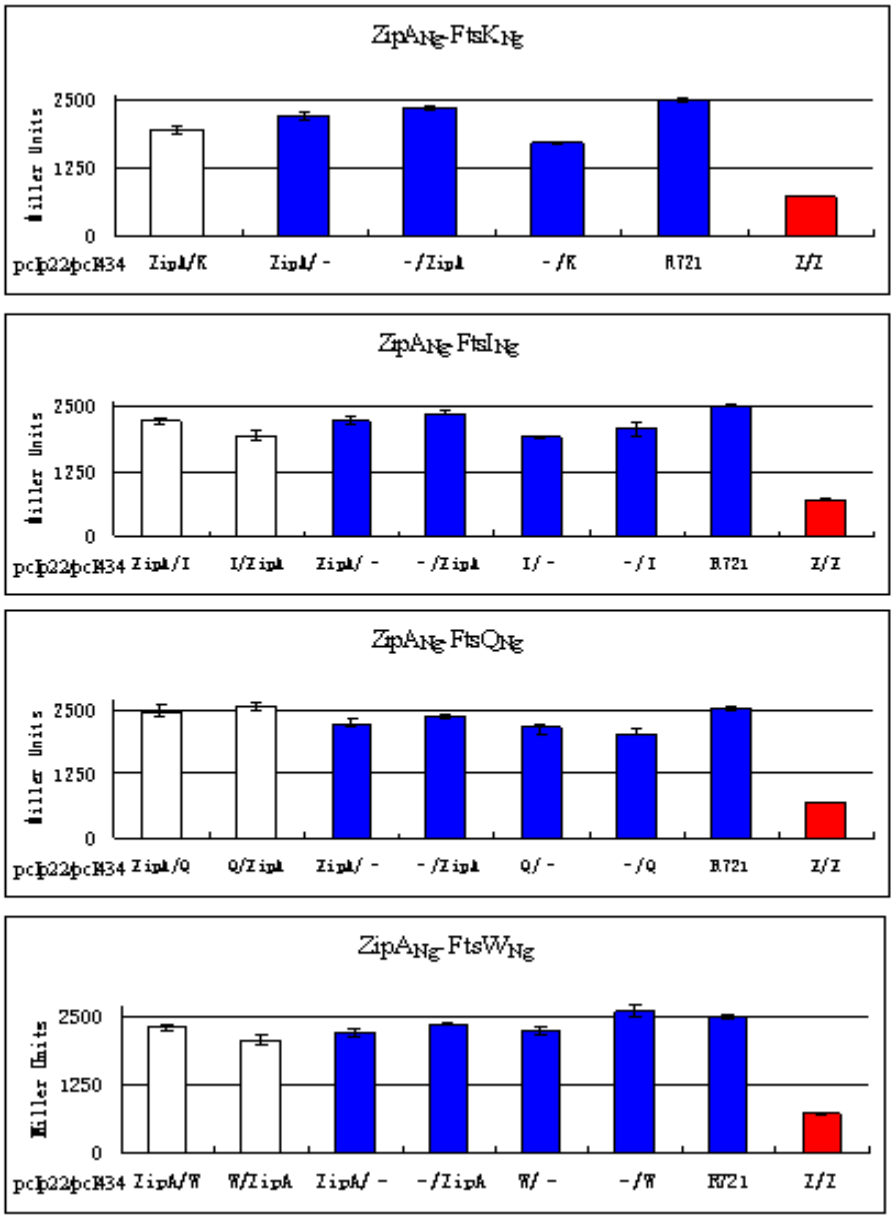
ZipANg-FtsKNg
Miller Units
2500
1250
0
pcb22pcM34 ZipA/K ZipA/- -/ZipA -/K R721 Z/Z
ZipANg-FtsINg
Miller Units
2500
1250
0
pcb22pcM34 ZipA/I I/ZipA ZipA/- -/ZipA I/- -/I R721 Z/Z
ZipANg-FtsQNg
Miller Units
2500
1250
0
pcb22pcM34 ZipA/Q Q/ZipA ZipA/- -/ZipA Q/- -/Q R721 Z/Z
ZipANg-FtsWNg
Miller Units
2500
1250
0
pcb22pcM34 ZipA/W W/ZipA ZipA/- -/ZipA W/- -/W R721 Z/Z

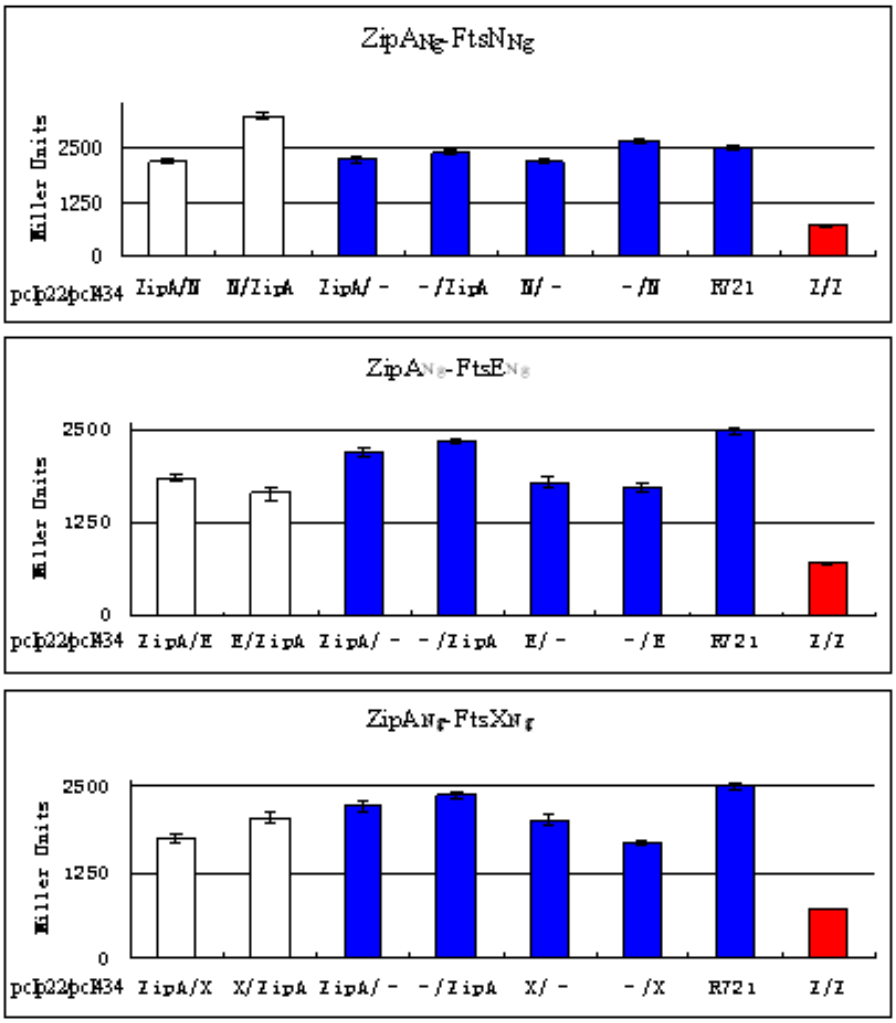

Fig. 3.15. Interaction of ZipA$_{Ng}$ with divisome proteins downstream of FtsA$_{Ng}$, FtsK$_{Ng}$ (K), FtsI$_{Ng}$ (I), FtsQ$_{Ng}$ (Q), FtsW$_{Ng}$ (W), FtsN$_{Ng}$ (N), FtsE$_{Ng}$ (E) and FtsX$_{Ng}$ (X) determined by B2H assay. Each gene was cloned into pcIp22 and pcI434 and constructs were transformed into *E. coli* R721 either singly or in combination. *N. gonorrhoeae* FtsZ self-interaction was used as positive control (red bar). R721 without plasmids and single transformants were used as negative controls (blue bars). R721 without plasmids had a β-galactosidase activity of 2504±34 Miller units. The β-galactosidase activity of each combination was compared to that of R721. Values of less than 50% (<1250 Miller Units) indicate a positive interaction between two proteins (green bars) while values of more than 50% (>1250 Miller Unites) indicate a negative interaction between the two proteins (white bars). Error bars indicate standard deviations, n=9.

As shown in Table 3.2, the results obtained from B2H assays highlighted that out of 45 combinations among the 10 divisome proteins in *N. gonorrhoeae*, 16 showed interactions while 29 did not interact. The interacting groups revealed by the assay were the following: FtsZ- (FtsA, FtsK, FtsW, FtsE, FtsX); FtsA- (FtsZ, FtsK, FtsQ, FtsW, FtsN); FtsK- (FtsZ, FtsA, FtsN); FtsQ- (FtsA, FtsE, FtsX); FtsW- (FtsZ, FtsA, FtsI, FtsX); FtsN- (FtsA, FtsK, FtsX); FtsE- (FtsZ, FtsQ, FtsX). FtsX- (FtsZ, FtsQ, FtsW, FtsN, FtsE). FtsI interacted with only protein FtsW. ZipA did not interact with any other divisome proteins tested in this study. These results suggest a large number of interactions existed amongst *N. gonorrhoeae* divisome proteins.

Table 3.2. Heterodimerization of 10 divisome proteins with B2H assay.

Values lower than 50% (in bold) indicate an interaction between two proteins under investigation. Standard deviations were determined for the cases in which the values were lower than 60%. The statistically significant values for the protein-protein interaction are underlined.

Proteins	ZipA	FtsZ	FtsA	FtsK	FtsI	FtsQ	FtsW	FtsN	FtsE
FtsZ	71%								
FtsA	77%	**40%** ±3.4%							
FtsK	78%	**40%** ±2.3%	**30%** ±2.2%						
FtsI	83%	91%	83%	76%					
FtsQ	100%	73%	**48%** ±3.6%	88%	90%				
FtsW	87%	**39%** ±3.2%	**45%** ±3.8%	100%	**35%** ±1.5%	100%			
FtsN	100%	76%	**24%** ±12%	**29%** ±1%	100%	88%	97%		
FtsE	70%	**39%** ±6.2	85%	100%	78%	**44%** ±3.6%	80%	89%	
FtsX	76%	**42%** ±8%	51% **±**6.9%	100%	97%	**46%** ±15%	**40%** ±2.2%	**18%** ±8.9%	**40% ±5.8%**

Table 3.3. *t* test was performed for *N. gonorrhoeae* divisome protein pairs which had mean values between 40% and 60% to determine whether these values are significantly different from 50% cut-off criteria ($P < 0.05$).

Protein pairs	**Residual β-galactosidase activity**	***P*-value**	***t* test result**
FtsA T3-FtsZ	45%	0.0667	**Not** statistically significant difference
FtsA T5-FtsZ	40%	**0.0003**	Very statistically significant difference
FtsA T7-FtsZ	42%	**0.002**	Very statistically significant difference
FtsA T4-FtsK	45%	0.093	**Not** statistically significant difference
FtsA T7-FtsK	53%	0.533	**Not** statistically significant difference
FtsA T4-FtsW	55%	**0.007**	Statistically significant difference
FtsA T8-FtsW	53%	0.0626	**Not** statistically significant difference
FtsA T3-FtsN	43%	**0.024**	Statistically significant difference
FtsZ-FtsA	40%	**0.0014**	Very statistically significant difference
FtsZ-FtsK	40%	**0.0002**	Extremely statistically significant difference
FtsZ-FtsX	42%	0.1316	**Not** statistically significant difference
FtsA-FtsQ	48%	0.393	**Not** statistically significant difference
FtsA-FtsW	45%	**0.084**	**Not** quite statistically significant difference
FtsA-FtsX	51%	0.8526	**Not** statistically significant difference
FtsQ-FtsE	44%	**0.0224**	Statistically significant difference
FtsQ-FtsX	46%	0.6713	**Not** statistically significant difference
FtsW-FtsX	40%	**0.0002**	Extremely statistically significant difference
FtsE-FtsX	40%	**0.0248**	Statistically significant difference

3.2.8. *N. gonorrhoeae* FtsA fails to interact with either *E. coli* FtsA or FtsZ

Since $FtsA_{Ec}$ interacts with $FtsZ_{Ec}$ and self-interacts, would $FtsA_{Ng}$ interact with these heterologous proteins to disrupt *E. coli* cell division? To test this, *ftsZ* and *ftsA* from *E. coli* and *ftsA* from *N. gonorrhoeae* were cloned into B2H vectors to study potential protein-protein interactions. *E. coli* R721 and transformants with single plasmids were used as negative controls and demonstrated high β-galactosidase activity (Fig. 3.16, blue bars). $FtsZ_{Ng}$ self-interaction was used as positive control (Fig. 3.16, red bar). B2H assay showed that the residual β-galactosidase activity for $FtsA_{Ng}$-$FtsZ_{Ec}$ and $FtsA_{Ng}$-$FtsA_{Ec}$ were 100% and 73%, respectively (Fig. 3.16 white bars), indicating that $FtsA_{Ng}$ did not interact with either $FtsZ_{Ec}$ or $FtsA_{Ec}$.

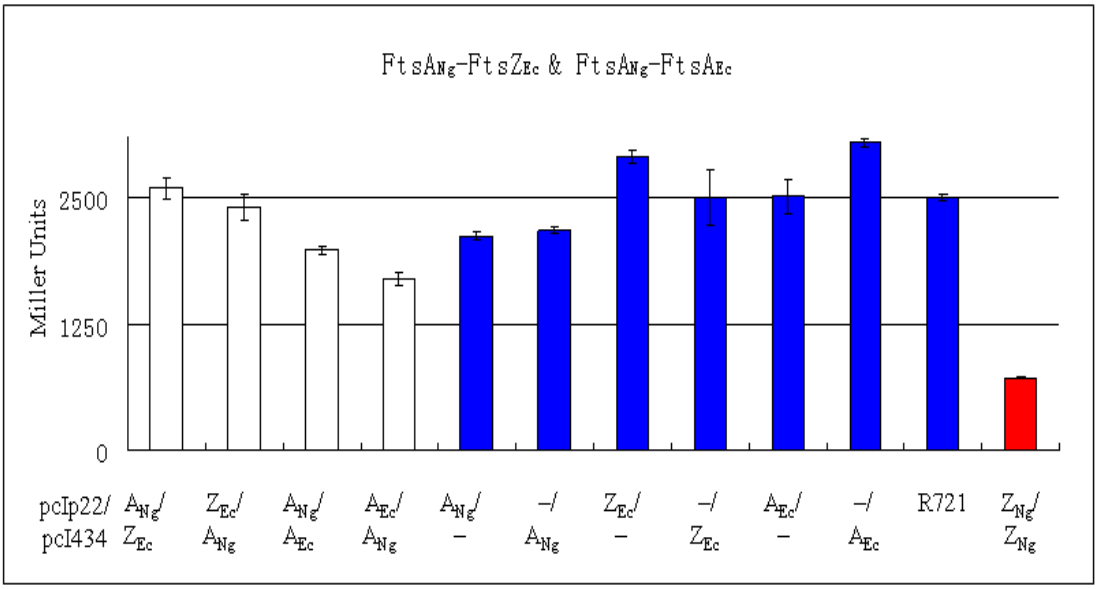

Fig 3.16. Interaction between *N. gonorrhoeae* FtsA (A_{Ng}) and *E. coli* FtsZ (Z_{Ec}) and FtsA (A_{Ec}) determined by B2H assay. *ftsA*$_{Ng}$, *ftsZ*$_{Ec}$, and *ftsA*$_{Ec}$ were cloned into pcIp22 and pcI434 and constructs were transformed into *E. coli* R721 either singly or in combination. *N. gonorrhoeae* FtsZ self-interaction was used as positive control (red bar). R721 without plasmids and single transformants were used as negative controls (blue bars). R721 without plasmids had a β-galactosidase activity of 2504±34 Miller units. The β-galactosidase activity of each combination was compared to that of R721, and values of more than 50% (>1250 Miller Units) indicate a negative interaction between two proteins (white bars). Error bars indicate standard deviations, n=9.

3.3. Biological studies of $FtsA_{Ng}$

3.3.1. Localization of FtsA in *N. gonorrhoeae*

Gonococci characteristically divide along two alternating, perpendicular planes (Fitz-James, 1964; Westling-Häggström *et al*., 1977). *E. coli* FtsA was shown to interact with FtsZ and co-localize with FtsZ at the division site in *E. coli* (Ma *et al*., 1996). Previous studies in our laboratory have shown that *N. gonorrhoeae* possesses both *ftsZ* ($ftsZ_{Ng}$) and *ftsA* ($ftsA_{Ng}$) within the *dcw* cluster of genes (Salimnia *et al.*, 2000). As part of the effort to generate a refined model of cell division in *N. gonorrhoeae,* localization of FtsA in dividing gonococcal cells was conducted using immunoelectron microscopy. Immunogold-labeling using anti-$FtsA_{Ng}$ antisera was performed on sections of fixed *N. gonorrhoeae* F62. 90% (40/50) of cells showed that $FtsA_{Ng}$ signals were found to accumulate at the two edges of the potential division sites (Fig. 3.17A, black dots). In single cocci, transmission electron micrographs revealed distinct accumulation of FtsA along one side of the cell, within a single invagination point that presumably indicated the initiation of a cell division event along one plane (Fig. 3.17B, arrow). The rest of the cells (10%) showed non-specific localization of $FtsA_{Ng}$ signals. These results suggest FtsA localizes to the division site in *N. gonorrhoeae* cells.

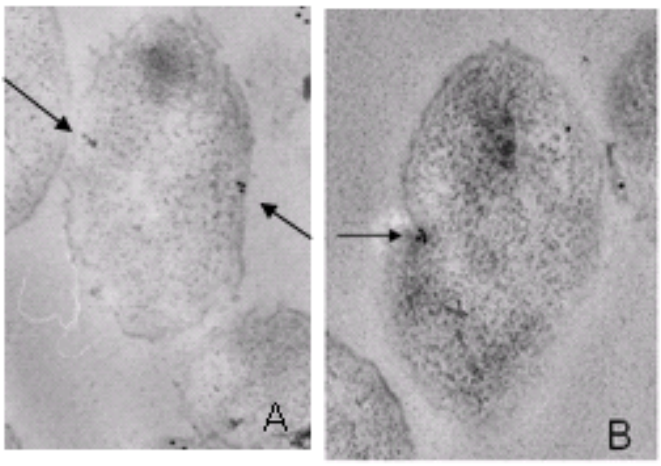

Fig 3.17. Immunogold localization of *N. gonorrhoeae* FtsA ($FtsA_{Ng}$) in cross sections of dividing gonococcal cells. (A) $FtsA_{Ng}$ accumulated at the potential division point (arrows, black dots). (B) In individual cocci, cell division is initiated at a single invagination point (arrow), where distinct accumulation of $FtsA_{Ng}$ is observed (black dots).

3.3.2. The ratio of FtsA:FtsZ in *N. gonorrhoeae* strains

In *E. coli*, overexpression of either FtsZ or FtsA inhibits the cell division process (Wang and Gayda, 1990). This suggests that the FtsA:FtsZ ratio is crucial for proper cell division (Dai and Lutkenhaus, 1992; Dewar *et al*., 1992). The amount of FtsA from *N. gonorrhoeae* CH811 cell extracts was determined using quantitative western blot analysis and compared with the relative abundance of FtsZ. The number of cells ml^{-1} was 1.4×10^{11} as determined by CFU, when the culture was took at an OD_{600} of 0.553. Different concentrations of cell extract were loaded on SDS-PAGE and the density of both FtsA and FtsZ bands were detected by Western blotting analysis and compared with the density observed over a 2-25 ng or 40-100 ng concentration range of purified FtsA and FtsZ proteins, respectively (Fig. 3.18). The quantities of both FtsA and FtsZ were calculated by taking into account the dilution of the sample and the number of cells. The amount of FtsA in *N. gonorrhoeae* CH811 was found to be much lower than that of FtsZ and the molecule number per cell of $FtsA_{Ng}$ and $FtsZ_{Ng}$ was estimated to be 15-25 and 528-783 respectively, giving an average ratio of 1:33.

The FtsA:FtsZ ratio and the amount of FtsA and FtsZ molecules in *N. gonorrhoeae* CH811 was repeatly examined again. This time, the number of cells ml^{-1} was 6.2×10^{9} as determined by CFU, when the culture was took at an OD_{600} of 0.78. By taking into account the dilution of the sample and the number of cells, the molecule number per cell of $FtsA_{Ng}$ and $FtsZ_{Ng}$ was estimated to be 1900-2200 and 62000-75000 respectively, giving an similar ratio of 1:34. However, these data showed a wide range of cell numbers from each repeat, which resulted in large variation of molecule numbers of $FtsA_{Ng}$ and $FtsZ_{Ng}$ in each cell. Thus amount of FtsA and FtsZ molecules in each *N. gonorrhoeae* cell can not be decided in this study, although they gave a similar ratio of FtsA and FtsZ. More experiments such as *N. gonorrhoeae* growth curve need to be performed to determine the cell number at each growth stage.

The ratios of FtsA to FtsZ in *N. gonorrhoeae* F62 and FA1090 were tested as with stain CH811, giving ratios of 1:27 and 1:24, respectively.

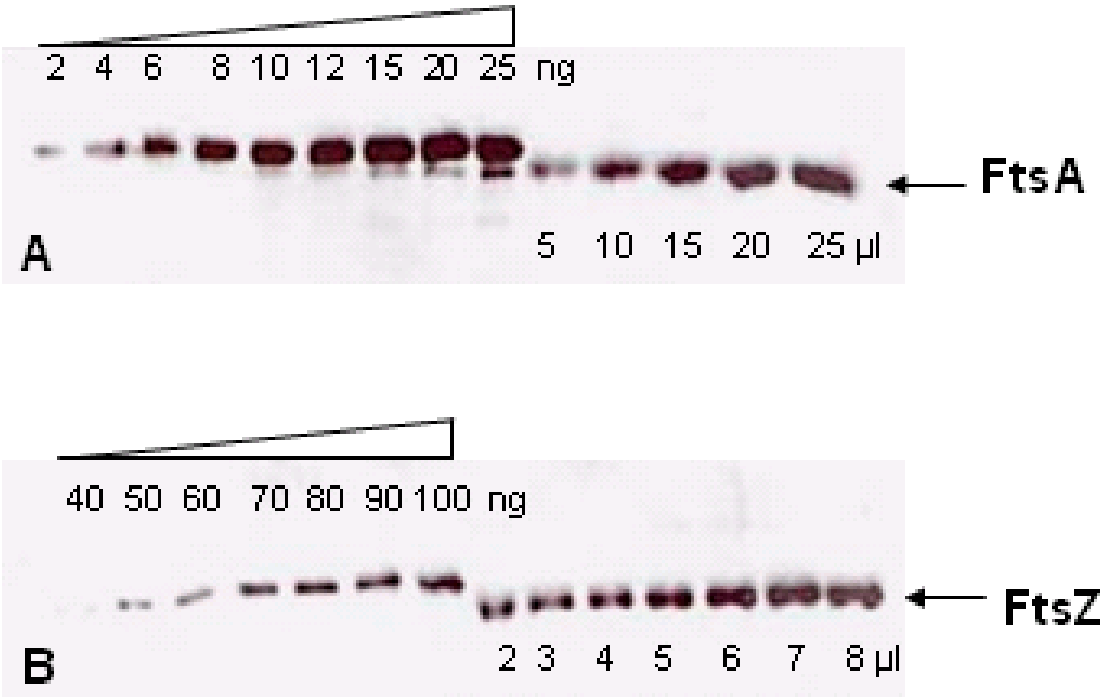

Fig. 3.18. Quantitative determination of FtsA and FtsZ proteins in *N. gonorrhoeae*. (A) Different amounts of cell extract (5, 10, 15, 20 and 25 µl) were loaded on SDS-PAGE and the density of $FtsA_{Ng}$ bands were detected by Western blotting analysis (right) and compared with the density observed over a 2-25 ng concentration range of purified $FtsA_{Ng}$ (left). (B) Different amounts of the same cell extract (2, 3, 4, 5, 6, 7 and 8 µl) were loaded on SDS-PAGE and the density of $FtsZ_{Ng}$ bands were detected by Western blotting analysis (right) and compared with the density observed over a 40-100 ng concentration range of purified $FtsZ_{Ng}$ (left).

3.3.3. Overexpression of FtsA disrupts cell division in *E. coli*

Overexpression of $FtsA_{Ng}$ in wild-type *E. coli* PB103

$FtsA_{Ng}$ was expressed in *E. coi* background to determine whether it could affect *E. coli* cell division. Wild-type *E. coli* PB103 cells (Table 2.1) were transformed with plasmid pUC18A, encoding $ftsA_{Ng}$ (Table 2.3). The effects of $FtsA_{Ng}$ overexpression in *E. coli* were examined by observing the cell morphologies of each transformant using DIC light microscopy. *E. coli* cells transformed with the negative control pUC18 vector exhibited typically short rod morphology as expected (Fig. 3.19A), indicating that this plasmid (devoid of *ftsA*) did not alter the morphology of *E. coli*. While the same strain transformed with pUC18A exhibited a mixed phenotype of long filaments and rods of various lengths (Fig. 3.19B) in the presence of IPTG induction, indicating the disruption of cell division. When 300 cells were randomly counted, measured and analyzed statistically after 4 hr, 6 hr and 8 hr of incubation, 36%, 23% and 19% of the cells with pUC18A were filamentous at the given time points, respectively (Fig. 3.20). The surface of the elongated cells was usually smooth, with no signs of constriction along the length of the cells, although some filaments displayed characteristic bulges in the middle. Overexpression of $FtsA_{Ng}$ in *E. coli* PB103 was confirmed by Western blot analysis using anti-$FtsA_{Ng}$ antibody (Fig. 3.19C). Western blot analysis confirmed $FtsA_{Ng}$ was overexpressed in *E. coli* transformed with pUC18A (Fig. 3.19C, lane 2) compared to the background level of native *E. coli* FtsA transformed with pUC18 (Fig. 3.19C, lane 1).

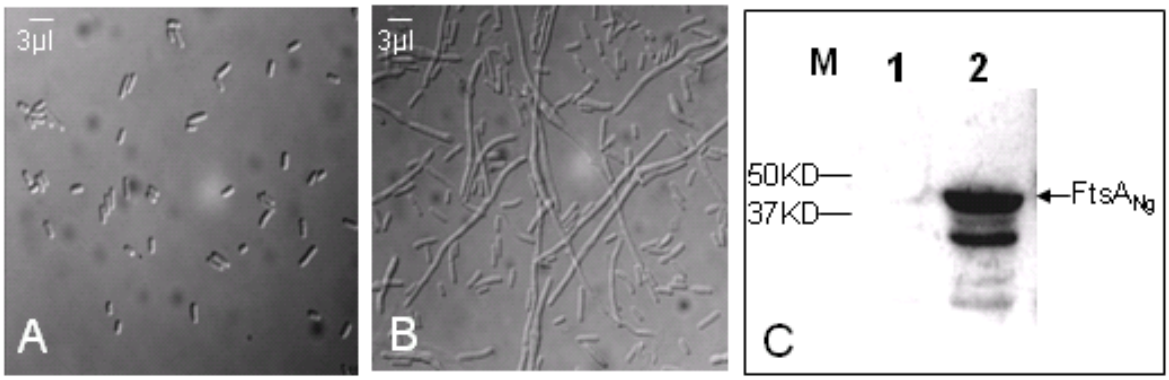

Fig. 3.19. Effect of overexpression of FtsA$_{Ng}$ in *E. coli* PB103 on cell morphology. (A) *E. coli* PB103 transformed with pUC18. (B) *E. coli* PB103 transformed with pUC18A (encoding *ftsA*$_{Ng}$). (C) Western blot using anti-FtsA$_{Ng}$ antibody for *E. coli* PB103-pUC18 (lane 1) and *E. coli* PB103-pUC18A (lane 2). Scale bars represent 3 µm.

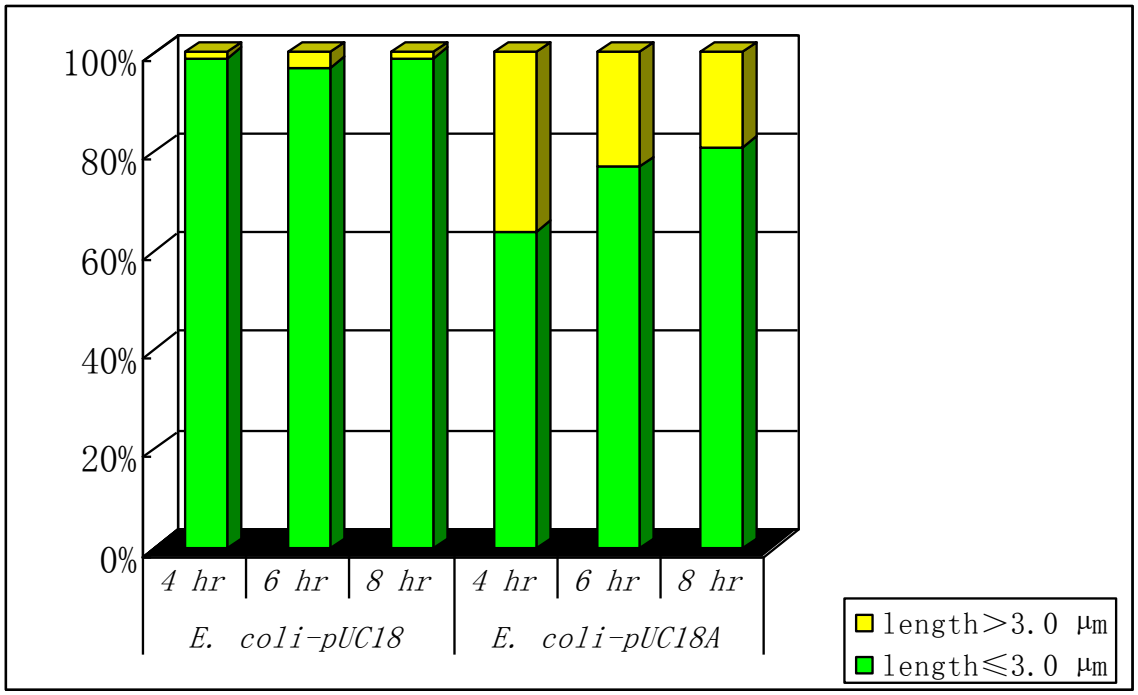

Fig. 3.20. Effect of overexpression of $FtsA_{Ng}$ in *E. coli* PB103 on cell morphology. *E. coli* PB103 with pUC18 derivatives were incubated in LB broth and cell cultures were taken for morphological observation and cell counting at time point of 4 hr, 6 hr and 8 hr, respectively. Length > 3.0 μm indicates *E. coli* rods of various length induced by $FtsA_{Ng}$ overexpression. Length ≤3.0 μm indicates normal-sized *E. coli* rod cells.

Overexpression of $FtsA_{Ng}$ in round *E. coli* KJB24 (*rodA*)

Round *E. coli* KJB24 (*rodA*) cells (Table 1) were also transformed with pUC18 and pUC18A to determine the effects of $FtsA_{Ng}$ overexpression in a coccal cell background. These cells lack the shape-determinant gene *rodA* and have a round cell morphology (Begg and Donachie, 1998). In addition, these cells divide along two perpendicular planes, as *N. gonorrhoeae* does, to produce a tetrad of daughter cells (Begg and Donachie, 1998); hence, they may present a suitable model to study cell division in coccal Gram-negative organisms. Cells transformed with pUC18 appeared uniform in size and shape (typical round morphology) (Fig. 3.21A), indicating that this plasmid (devoid of *ftsA*) did not alter the morphology of *E. coli*. The same strain transformed with pUC18A exhibited gross enlargement, aggregation and irregular phenotype (Fig. 3.21B), with cell diameters up to 3-4 times that of control cells, indicating the disruption of cell division. 300 cells were randomly selected, measured and statistically analyzed. It was determined that 31%, 13% and 11% of cells exhibited enlarged and irregular shapes at the time points of 4hrs, 6hrs and 8hrs, respectively, as compared to controls in the presence of IPTG (100 µM) (Fig. 3.22). Western blot analysis confirmed the overexpression of $FtsA_{Ng}$ in the enlarged round cells (Fig. 3.21C, lane 2) compared to the background level of native *E. coli* FtsA in negative control cells (Fig. 3.21C, lane 1).

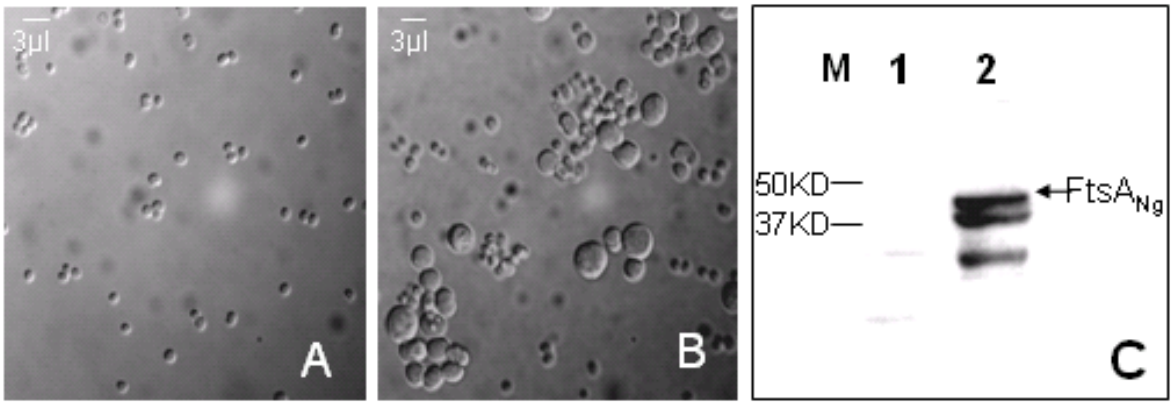

Fig. 3.21. Effect of overexpression of FtsA$_{Ng}$ in *E. coli* KJB24 on cell morphology. (A) *E. coli* PB103 transformed with pUC18. (B) *E. coli* PB103 transformed with pUC18A (encoding *ftsA*$_{Ng)}$. (C) Western blot using anti-FtsA$_{Ng}$ antibody for *E. coli* PB103-pUC18 (lane 1) and *E. coli* PB103-pUC18A (lane 2). Scale bars represent 3 µm.

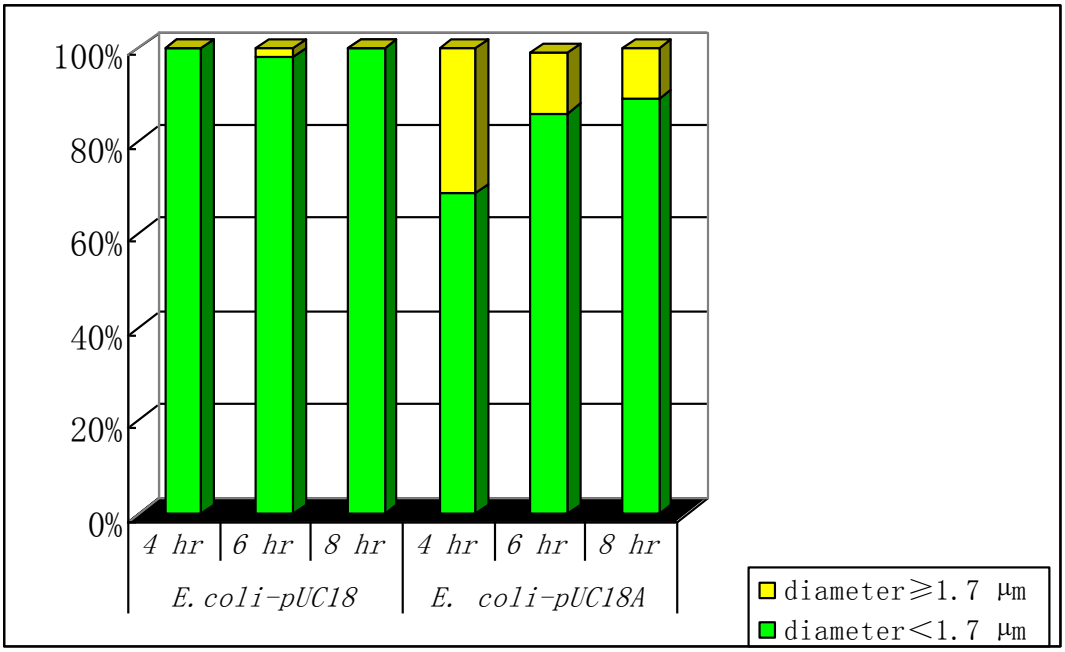

Fig. 3.22. Effect of overexpression of $FtsA_{Ng}$ in *E. coli* KJB24 on cell morphology. *E. coli* KJB24 with pUC18 derivatives were incubated in LB broth and cell cultures were took for morphological observation and cell counting at time-point of 4hr, 6hr and 8hr, respectively. Diameter > 1.7 μm indicates various enlarged *E. coli* cells induced by $FtsA_{Ng}$ overexpression. Diameter ≤ 3.0 μm indicates normal-sized round *E. coli* cells.

3.3.4. Overexpression of FtsA affects growth rate of *E. coli* at the early growth stage

It was postulated that $FtsA_{Ng}$ overexpression might affect cell growth as it has been shown to inhibit cell division in *E. coli*. Therefore, the growth rates of *E. coli* PB103 with pUC18A was determined and compared to the same strain transformed with negative control pUC18. The number of CFU of *E. coli* PB103 with pUC18A and PB103 with pUC18 showed differences in lag, exponential and post-stationary phases during a 20-hr incubation (Fig. 3.23). In the lag phase, the number of CFU of *E. coli* PB103 with pUC18A was lower than that of *E. coli* pB103 with pUC18 for approximately the first 3 hrs (1-3 hrs) but subsequently became more than that of wild-type in the following 3 hrs (3-6 hrs). From late exponential phase to early stationary phase (6-12 hrs), *E. coli* PB103 with pUC18A showed a similar growth pattern to *E. coli* PB103 with pUC18. A difference again appeared by 12 hrs, when *E. coli* PB103 with pUC18A showed a lower number of viable cells than wild type *E. coli* PB103 until 20 hrs. Statistically significant differences were noted at 2-hr, 6-hr, 16-hr and 20-hr ($p < 0.05$).

The growth rates of *E. coli* KJB24 with pUC18A were also determined and compared to the same strain transformated with pUC18. Significant differences between *E. coli* KJB24 with pUC18A and *E. coli* KJB24 with pUC18 were also noted in early exponential, stationary and post-stationary phase (Fig. 3.24). In the lag phase, these two strains displayed a similar initial CFU and showed similar growth in the first 2 hrs. In exponential phase, *E. coli* KJB24 with pUC18A had a lower number of viable cells than *E. coli* KJB24 with pUC18 from 4 to 6 hrs, and a similar growth pattern up to 10 hrs. From 10 to 12 hrs, the number of viable cells for *E. coli* KJB24 with pUC18 continued to rise after *E. coli* KJB24 with pUC18A had reached the onset of the stationary phase. By contrast, the post-stationary phase of *E. coli* KJB24 with pUC18A was 2 hrs earlier than *E. coli* KJB24 with pUC18. By 12 hrs, there was a log factor difference in viable cells between two strains. By 16 hrs the number of viable

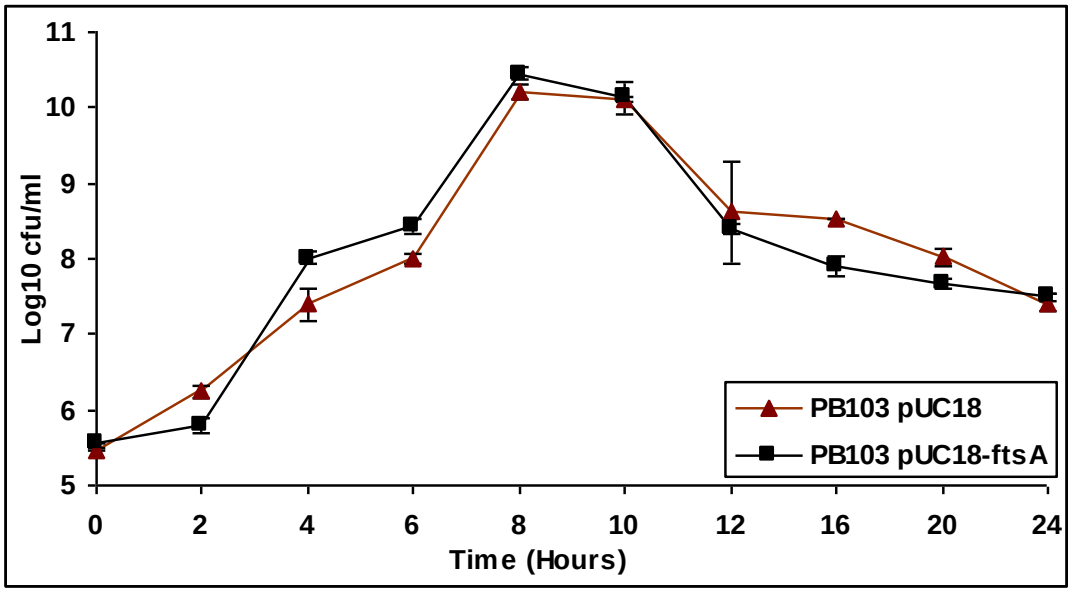

Fig. 3.23. Growth curve of *E. coli* PB103 cells. *E. coli* PB103 transformed with pUC18 or pUC18A. Averages are from 3 independent experiments done in triplicate. Error bars indicate ±1 standard deviation.

cells between two strains was nearly identical and decreased at the similar rate until the 20 hrs. Statistically significant differences were noted at 12-hr ($p < 0.05$).

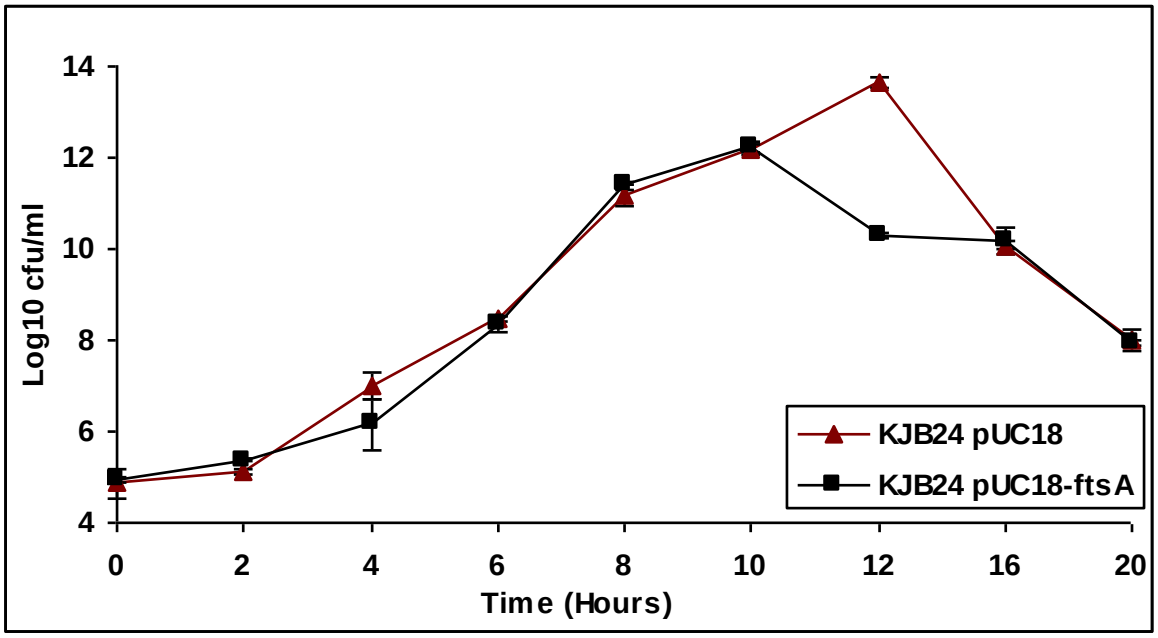

Fig. 3.24. Growth curve of *E. coli* KJB24 cells. *E. coli* KJB24 transformed with pUC18 or pUC18A. Averages are from 3 independent experiments done in triplicate. Error bars indicate ±1 standard deviation.

3.3.5. *N. gonorrhoeae* FtsA localizes at midcell in normal-sized *E. coli* cells

FtsA from *E. coli* localized with the Z-ring to the division site of *E. coli* cells (Ma *et al*., 1996). Since gonococcal FtsA could affect *E. coli* cell division, *egfp* fused at either the N- or C-terminus of $ftsA_{Ng}$ was constructed to determine whether the protein would also localize at the Z-ring in *E. coli* cells. EGFP was overexpressed in *E. coli* cells as negative control. Cells expressing EGFP were normal in size and EGFP exhibited an even fluorescence distribution throughout the cell (Fig. 3.25A), indicating no specific localization of EGFP in cells.

E. coli PB103 cells transformed with pUC18AE, encoding $ftsA_{Ng}$ at the N-terminal of *egfp*, were mostly normal short rod shape without or with low concentration of IPTG induction (100 μM). Fluorescence microscopy revealed that $FtsA_{Ng}$-EGFP mostly localized at both poles and/or the division site in these normal-sized cells (Fig. 3.25B-C). A total of 211 normal-sized cells (length ~ 3.0 μm) were examined; 41% (94/211) of the cells showed $FtsA_{Ng}$-EGFP localized at both the cell poles and midcell (Fig. 3.25C), 46% (87/211) showed $FtsA_{Ng}$-EGFP localized at the cell poles only (Fig. 3.25B), and 14% (30/211) of cells showed $FtsA_{Ng}$-EGFP non-specifically localized in the cytoplasm (Fig. 3.25D).

When overexpression of $FtsA_{Ng}$ was induced by a higher concentration of IPTG induction (300 μM), cell division was inhibited and cells became filamentous (Fig. 3.26A'-C'). Three classes of fluorescence patterns were observed in various lengths of filaments. In the filamentous cells with smooth surface, FtsA-EGFP exhibited as a single tubule with aggregated small dots extending from pole to pole (Fig. 3.26A'). These $FtsA_{Ng}$-EGFP tubule or small dots were detectable only with fluorescence but not with DIC microscopy (Fig. 3.26A), indicating these dots were not inclusion bodies (Ma *et al*., 1996). In other filamentous cells, $FtsA_{Ng}$-EGFP exhibited a possible spiral structure (Fig. 3.26B') or a series of irregularly spaced dots (Fig. 3.26C'), which could be observed with both fluorescence and DIC microscopy (Fig. 3.26B-C), indicating the formation of inclusion bodies (Ma *et al.*,

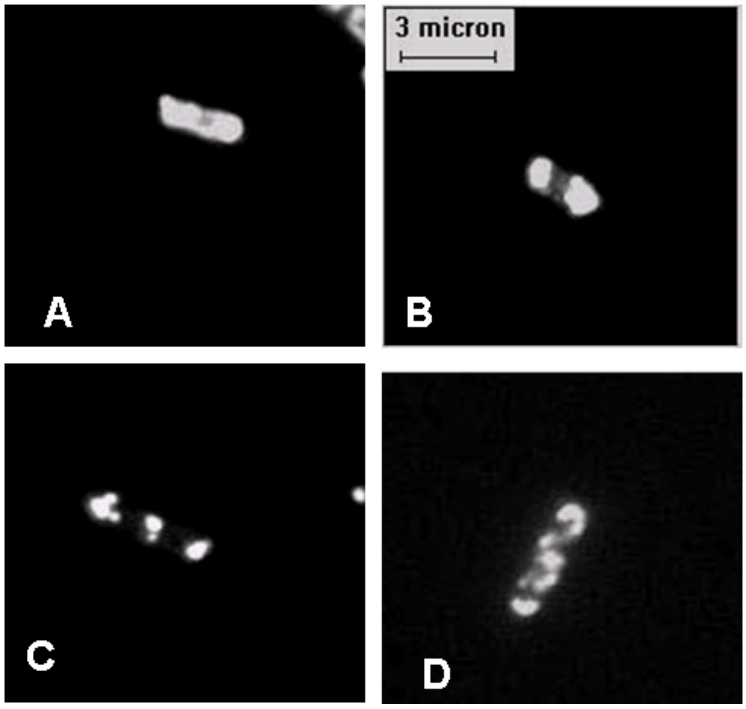

Fig. 3.25. $FtsA_{Ng}$-EGFP localization in normal-sized *E. coli* PB103 cells. (A) showed that EGFP exhibited an even fluorescence throughout the cell. (B) showed that $FtsA_{Ng}$-EGFP localized to the cell poles in normal-sized *E. coli* cells. (B-C) showed showed that $FtsA_{Ng}$-EGFP localized to both the cell poles and the division site in normal-sized *E. coli* cells. (D) showed non-specific localization of $FtsA_{Ng}$-EGFP in the cytoplasm of cells. 300 µM IPTG was used to induce protein overexpression. Scale bar represents 3 µm.

1996). The spacing between dots varies in individual cells. These results indicate $FtsA_{Ng}$ mostly formed as inclusion bodies and displayed nonspecific distribution of clumps all over the filaments.

E. coli KJB24 cells were too small to observe the localization of $FtsA_{Ng}$-EGFP in normal-sized cells. After induction with IPTG (300 μM), $FtsA_{Ng}$-EGFP was observed at the aberrant division sites in some enlarged *E. coli* KJB24 cells (6/30) (Fig. 3.27A, A'). $FtsA_{Ng}$-EGFP was also observed as irregularly spaced dots and displayed an irregular cytoplasmic distribution (23/30) (Fig. 3.27B, B') in most of enlarged *E. coli* KJB24 cells.

EGFP-$FtsA_{Ng}$ exhibited similar localization patterns in both *E. coli* PB103 and KJB24 derivatives (data not shown).

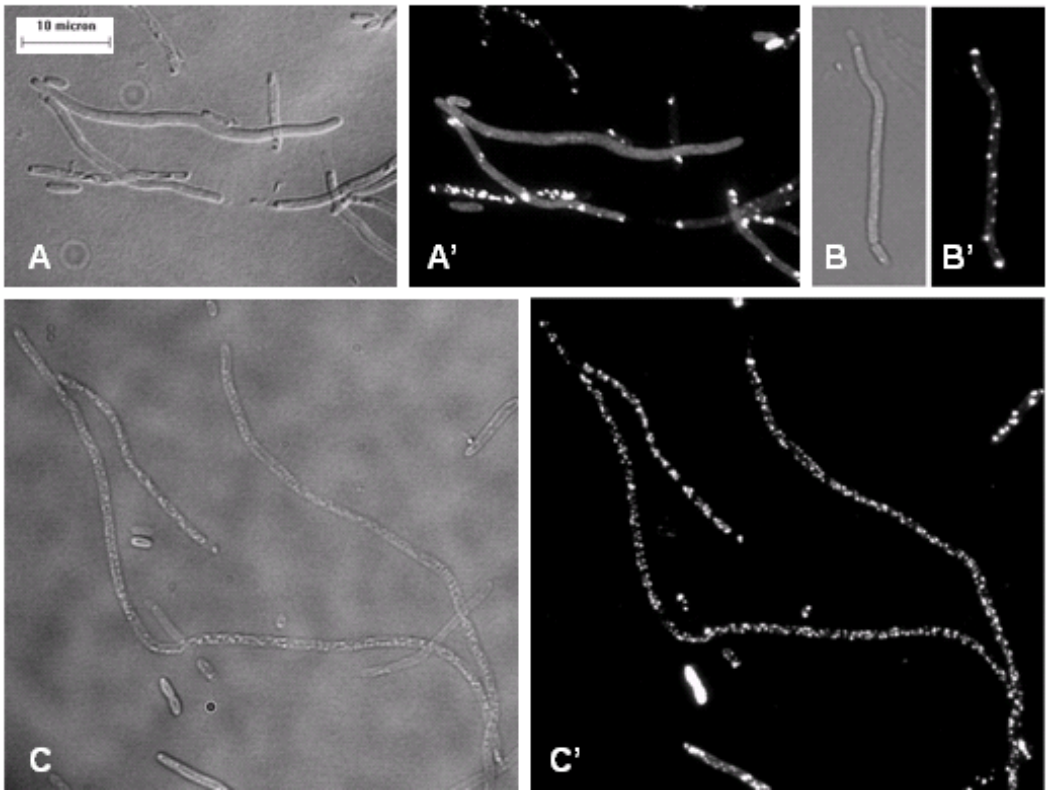

Fig. 3.26. $FtsA_{Ng}$-EGFP localization in *E. coli* PB103 filaments. (A-C) represented the DIC micrograph. (A'-C') represented the fluorescent images taken under the same screen. (A-C, A'-C') showed three types of $FtsA_{Ng}$-EGFP localization patterns observed in filaments, i.e. $FtsA_{Ng}$-EGFP tubule with small dots in (A'), a possible spiral structure in (B') and irregularly spaced dots in (C'). 300 µM IPTG was used to induce protein overexpression. Scale bar represents 10 µm.

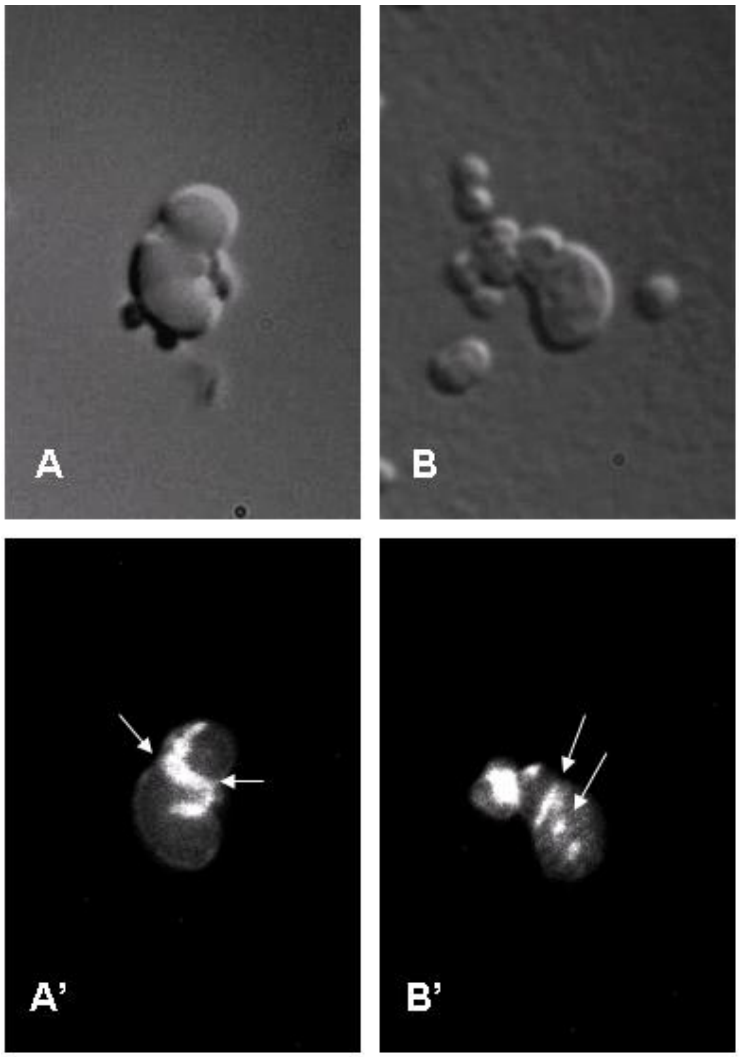

Fig. 3.27. $FtsA_{Ng}$-EGFP localization in *E. coli* KJB24. *E. coli* KJB24 transformed with pUC18-AE. (A-B) represented the DIC micrograph. (A'-B') represented the fluorescent images took under the same screen. (A, A') showed that $FtsA_{Ng}$-EGFP localized at the aberrant division sites in some enlarged *E. coli* cells. (B, B') showed $FtsA_{Ng}$-EGFP irregularly distributed in cytoplasmic as fluorescence dots. 300 µM IPTG was used to induce protein overexpression.

3.3.6. *N. gonorrhoeae* FtsA does not complement an *E. coli ftsA*-depletion strain

E. coli P163 is an $ftsA_{Ec}$-depletion strain. This strain grows at a permissive temperature (30°C) and can be complemented by wild-type $ftsA_{Ec}$ at a nonpermissive temperature (42°C), which normally would not support growth (Hale and de Boer, 1999). Plasmid pDSW209-A_{Ng} was introduced into the $ftsA_{Ec}$-delpetion strain *E. coli* P163 to determine whether $ftsA_{Ng}$ could complement this $ftsA_{Ec}$-depletion mutant. At 30°C, all three *E. coli* P163 strains containing $FtsA_{Ng}$, $FtsA_{Ec}$ (positive control), or $FtsA_{Ec}$D242E (negative control) grew well at various culture dilutions under the induction of various IPTG concentrations as expected (Fig. 3.28A). When the same strains were incubated at 42 °C with various concentrations of IPTG induction (Fig. 3.28B), *E. coli* P163 containing pDSW209-A_{Ec} (encoding $ftsA_{Ec}$) grew well when induced with 60 µM and higher IPTG (Fig. 3.28B4-B6, lane 2), demonstrating that $FtsA_{Ec}$ can complement *ftsA*-depletion strain *E. coli* P163 as expected (Hale and de Boer, 1999). The negative control, *E. coli* P163 with pSEB306-D242E (a mutated $FtsA_{Ec}$) did not grow (Fig. 3.28B1-B6, lane 3), demonstrating that the $FtsA_{Ec}$D242E did not complement *E. coli* P163, as shown previously (Pichoff and Lutkenhaus, 2007). *E. coli* P163 containing pDSW209-A_{Ng} did not grow even under the induction of high concentrations of IPTG (e.g. 200 µM) (Fig. 3.28B1-B6, lane 1), indicating *N. gonorrhoeae* FtsA can not complement the $ftsA_{Ec}$-depletion strain *E. coli* P163.

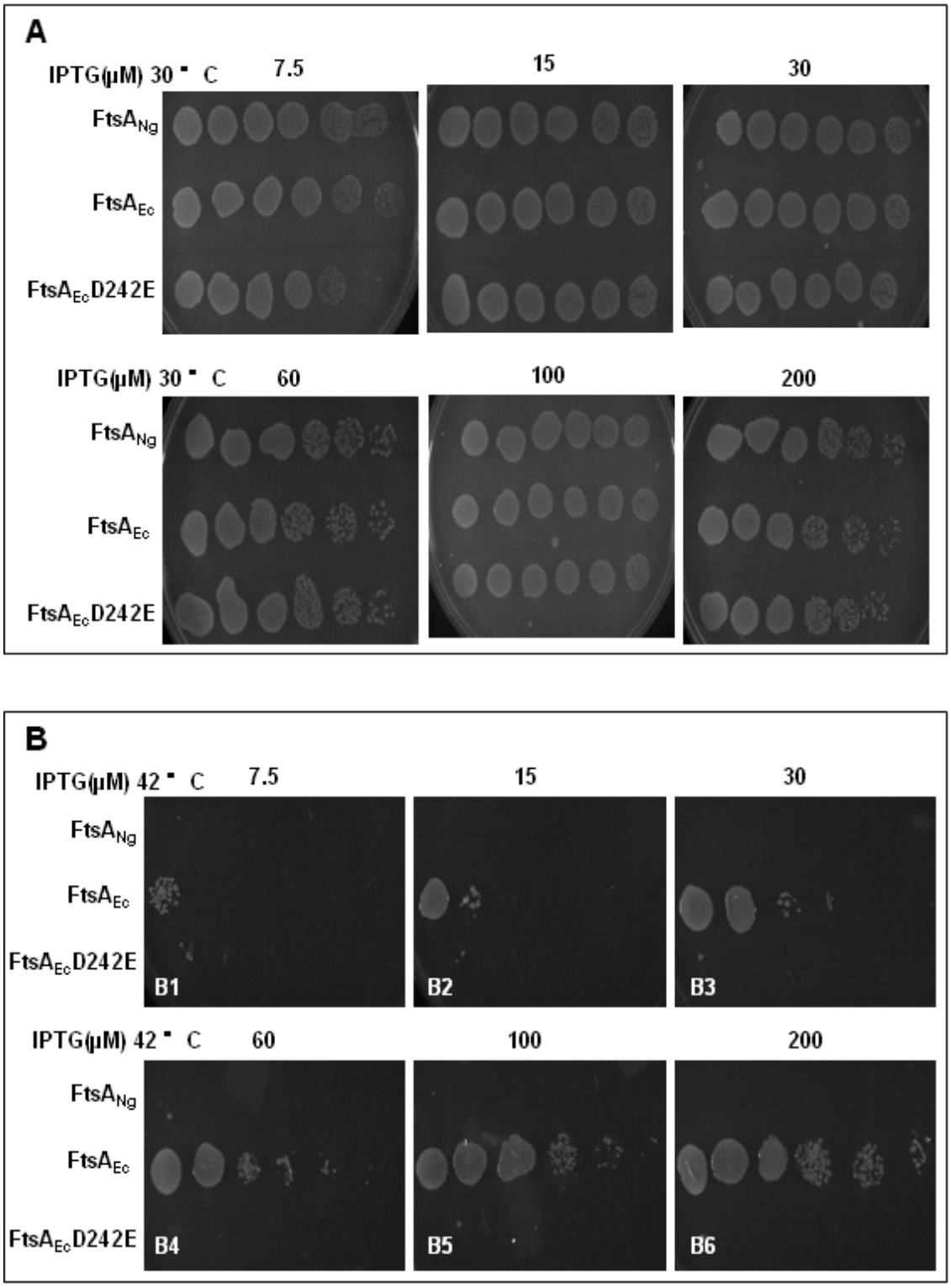

Fig. 3.28. Lack of complementation of the *ftsA*$_{Ec}$-depletion strain *E. coli* P163 [(*recA*::Tn*10 ftsA0*)/pDB280 (*repAts ftsA*+)] by FtsA$_{Ng}$. P163 cells containing the indicated plasmids shown at left were tested for colony viability after incubation at 30°C (permissive) or 42°C (to deplete FtsA$_{Ec}$). IPTG was present in the plates at 0, 7.5, 15, 30, 60, 100 or 200 μM, as shown at the top of each image.

CHAPTER 4 DISCUSSION AND CONCLUSIONS

Present knowledge of bacterial cell division has largely arisen from extensive studies of cell division in rod-shaped bacteria, particularly *E. coli* and *B. subtilis* (Errington *et al*., 2003). Cell division is initiated by the formation of the Z-ring at the division site, which acts as a scaffold to recruit at least 12 proteins to form the divisome in *E. coli* (Errington *et al*., 2003; Vicente *et al.*, 2006). Our laboratory has studied the central division protein FtsZ in *N. gonorrhoeae* and its localization to the midcell (Salimnia *et al.*, 2000). The specific interaction of FtsZ with MinC also has been explored, which regulates the ability of FtsZ to form rings at the midcell and thus to recruit other proteins of the divisome (Greco-Stewart *et al*., 2007). Thus the objective of present research is to understand the divisome formation in *N. gonorrhoeae* by initiating studies on FtsA, the first divisome protein recruited to midcell once the Z-rings established.

4.1. $FtsA_{Ng}$ is crucial for interacting with $FtsZ_{Ng}$ and other divisome proteins in *N. gonorhoeae*

FtsA homologues are conserved in a variety of organisms, both in Gram-negative and Gram-positive bacteria. Thus one might expect conserved functionality. Multiple sequence alignments of FtsA proteins showed that they were highly conserved, particularly in the 2A and 2B domains and the extreme C-terminus (Fig. 3.1). Studies from *E. coli* indicate that the residues directly involved in interacting with FtsZ were mostly distributed throughout the 2B domain (Pichoff and Lutkenhaus, 2007). In addition, the MTS targets FtsA and subsequently the Z-ring to the membrane, is located at the extreme C-terminus (Pichoff and Lutkenhaus, 2005; Yim *et al.*, 2000). These studies from *E. coli* are in support of the overall conserved nature of these regions. Their wide distribution and conservation across genera and species suggests that FtsA proteins have important roles for cellular functionalities.

It is noted that FtsA is thought to be more important than ZipA in cell division in *E. coli*, although ZipA with FtsA stabilizes the Z-ring and participates in the recruitment of other divisome proteins in *E. coli* (Hale and de Boer, 2002). A ZipA-like protein, SLO7ORF3, was identified in *N. gonorrhoeae*, which can complement the growth defect caused by $ZipA_{Ec}$ depletion in *E. coli*, but it only partially alleviates the defect in cell division (Du and Arvidson, 2003). However, $ZipA_{Ng}$ displayed low sequence identity to ZipA from *E. coli* (14% identity). In *E. coli*, although ZipA did not interact with the late divisome proteins as determined by B2H assays (Di Lallo *et al.*, 2003), it interacted with FtsZ and was required to recruit FtsK, FtsQ, FtsL and FtsN to midcell by localization studies (Di Lallo *et al*., 2003; Hale and de Boer, 2002). *N. gonorrhoeae* ZipA did not interact with either FtsZ or any other downstream divisome proteins (Table 3.2). Thus *N. gonorrhoeae* FtsA may play much more important roles in the Z-ring stability and the recruitment of downstream divisome proteins than in *E. coli*.

In *E. coli*, FtsZ polymerizes to form the Z-ring and recruites FtsA for stabilization (Lutkenhaus and Addinall, 1997). The dimerization of FtsA enhanced the integrity of the Z-ring (Shiomi and Margolin, 2007b). Thus the correct establishment of FtsA-FtsZ interaction and self-interaction of FtsA are required for proper cell septation (Yim *et al.*, 2000). In *N. gonorrhoeae*, I determined that $FtsA_{Ng}$ interacted with $FtsZ_{Ng}$ (Fig. 3.4). $FtsA_{Ng}$ self-interaction and $FtsZ_{Ng}$ self-interaction were also detected using B2H assays (Fig. 3.4). These results are consistent with previous observations made in *E. coli* and other bacteria (Ma and Margolin, 1999; Di Lallo, *et al*., 2003), verifying that FtsA-FtsZ interaction and self-interactions are conserved in bacteria.

$FtsA_{Ng}$ was shown to interact with downstream divisome proteins in *N. gonorrhoeae*. However, the proteins that interacted with FtsA in *N. gonorrhoeae* differ from *E. coli*, which also differ from other bacteria, indicating a possibly different divisome protein interactome in

N. gonorrhoeae. My results showed that $FtsK_{Ng}$, $FtsQ_{Ng}$, $FtsW_{Ng}$ and $FtsN_{Ng}$ interacted with $FtsA_{Ng}$ in *N. gonorrhoeae* (Fig. 3.6). In contrast $FtsI_{Ec}$, $FtsQ_{Ec}$ and $FtsN_{Ec}$ were reported to interact with $FtsA_{Ec}$ in *E. coli* (Corbin *et al*., 2004; Di Lallo *et al.*, 2003; Karimova *et al.*, 2005) while $FtsI_{Sp}$, $FtsK_{Sp}$, and $FtsL_{Sp}$ interacted with $FtsA_{Sp}$ in *S. pneumoniae* (Maggi *et al.*, 2008). FtsA is cytoplasmic protein and contains a MTS at the extreme C-terminus, which targets FtsA and FtsZ to the membrane (Pichoff and Lutkenhaus, 2005; Yim *et al.*, 2000). FtsW, FtsK, FtsQ and FtsN are membrane proteins, which are characterized by single or multiple transmembrane segments and a cytoplasmic domain (Dorazi and Dewar, 2000; Guzman *et al*., 1992, 1997; Dai *et al.*, 1996; Bowler and Spartt, 1989). Thus, I hypothesize that those membrane proteins interact with the cytoplasmic protein, FtsA probably via their transmembrane segments or cytoplasmic domains at the inner cell membrane. To prove this hypothesis, further investigation needs to be performed in the future.

Since more divisome proteins were found to interact with FtsA in *N. gonorrhoeae* as compared to *E. coli* and *S. pneumoniae,* it is possible that either more FtsA molecules or additional interacting FtsA domains involve in these interactions. The former hypothesis can be eliminated because the ratios of FtsA to FtsZ showed that the relative cellular concentration of FtsA in *N. gonorrhoeae* is lower than in *E. coli* and other bacteria. I have determined an FtsA:FtsZ ratio of 1:33 in *N. gonorrhoeae* CH811. While a FtsA:FtsZ ratio of 1: 5 was demonstrated in *E. coli* and *B. subtilis* (Rueda *et al.*, 2003; Feucht *et al*., 2001), and 1:1.5 in *S. pneumoniae* (Lara *et al.*, 2005).

On the other hand, I determined that domains $2A_1$, $2A_2$ and 2B of $FtsA_{Ng}$ were involved in interactions with $FtsZ_{Ng}$ using both B2H and GST pull-down assays (Figs. 3.7-3.8). Any one of the 3 domains in $FtsA_{Ng}$ was sufficient for interaction with $FtsZ_{Ng}$. In *E. coli*, domain 2B of FtsA is required for interaction with FtsZ and domains 1A and 2A may be involved; this is suggested by the observations that among 15 FtsA mutations affecting interaction with

FtsZ, 13 of them were mapped to domain 2B and the other two were mapped to domains 1A and 2A (Pichoff and Lutkenhaus, 2007). Therefore, my results confirmed that not only 2B domain but also its adjacent $2A_1$ and $2A_2$ domains were involved in the interaction with FtsZ in *N. gonorrhoeae*. This supports my second hypothesis that compared to FtsA in *E. coli*, more functional domains of $FtsA_{Ng}$ are involved in interaction with $FtsZ_{Ng}$ in *N. gonorrhoeae*. It is likely that the multiple domain involvement in the interactions enhances the stabilization of the Z-ring complex, but this remains to be proved. Multiple interaction domains of FtsL have also been observed with FtsB from *E. coli*, thus the FtsL-FtsB complex can act as a scaffold for divisome assembly (Gonzalez *et al*., 2010). Analogous evidence would be found from *E. coli* FtsQ and FtsK functional domain studies using B2H assays (D'Ulisse *et al*., 2007; Grenda *et al*., 2008). Two periplasmic subdomains of $FtsQ_{Ec}$ were implicated for interactions with both $FtsI_{Ec}$ and $FtsN_{Ec}$, which might enhance the ability of FtsQ-FtsL-FtsB complex to recruit the downstream proteins in *E. coli* (D'Ulisse *et al*., 2007). Both the $FtsK_{Ec}$ linker and the C-terminal domain were determined to interact with $FtsI_{Ec}$, which may play a role in divisome stabilization (Bigot *et al.*, 2004; Grenga *et al.*, 2008). It is also possible that in *N. gonorrhoeae,* one molecule of FtsA may bind to 3 or even more FtsZ molecules, indicating a high affinity of FtsA interacting with FtsZ. To verity this possibility, the FtsA-FtsZ interaction strength needs to be studied and compared from different organisms.

Interestingly, besides interaction with FtsZ, the highly conserved 2A and 2B domains of FtsA also exhibit multifunctional regions and play roles in other aspects of cell division. $FtsA_{Ec}$* (R286W) located in the 2B domain was able to bypass the requirement for FtsN and ZipA in divisome formation (Geissler *et al*., 2003, 2007). The S12-S13 strands in the 2B domain have been shown to affect localization to the Z-ring (Rico *et al.*, 2004). A couple of *E. coli* FtsA mutations, located in either the 2A or 2B domain, were found to either reduce FtsA ATP binding ability (T215 and G336) (Sanchez *et al*., 1994) or to inactivate FtsA

irreversibly at 42°C (G205, D217), causing extensive damage to the division machinery (Robinson *et al.*, 1988).

After the determination of $FtsA_{Ng}$ interaction with $FtsK_{Ng}$, $FtsW_{Ng}$, $FtsQ_{Ng}$ and $FtsN_{Ng}$, the functional domains of $FtsA_{Ng}$ that were responsible for these interactions were further identified using the B2H assays. My results showed that unlike *E. coli*, domain 1C of $FtsA_{Ng}$ was not involved in the interaction of $FtsA_{Ng}$ with those downstream divisome proteins; instead domains $2A_1$, $2A_2$ and 2B mediated the interaction of $FtsA_{Ng}$ with $FtsK_{Ng}$, $FtsW_{Ng}$, $FtsQ_{Ng}$ and $FtsN_{Ng}$ in *N. gonorrhoeae* (Figs. 3.9-3.12). Specifically, domain $2A_1$ interacted with $FtsK_{Ng}$ and $FtsN_{Ng}$. Domain 2B of $FtsA_{Ng}$ interacted with $FtsQ_{Ng}$, and $FtsN_{Ng}$ and possbly with $FtsK_{Ng}$,. Domain $2A_2$ of $FtsA_{Ng}$ interacted with $FtsQ_{Ng}$, $FtsW_{Ng}$, and $FtsN_{Ng}$. The functional domains of $FtsA_{Ec}$ interaction with the late divisome proteins have not been ascertained in *E. coli*, although domain 1C of $FtsA_{Ec}$ was required for the recruitment of late divisome proteins $FtsI_{Ec}$, $FtsQ_{Ec}$ and $FtsN_{Ec}$ as determined by localization studies (Corbin *et al.*, 2004; Rico *et al.*, 2004).

It is not known if, or how, the protein interaction might be related to the protein recruitment. The role of the FtsA 1C domain in the recruitment of late divisome proteins was only tested in *E. coli* but has not been studied in other bacteria. No evidence indicates that FtsA 1C domain is the unique competent domain to interact with downstream divisome proteins, although domain 1C of FtsA from *T. maritima* has different spatial position within the molecule compared to other members of the ATPase superfamily (van den Ent and Löwe, 2001).

Sequence alignment for the 4 domains between $FtsA_{Ng}$ and $FtsA_{Ec}$ showed that domain 2A (50% identity) was more highly conserved than other domains, but domain 1C (39% identity) was as conserved as domain 2B (38% identity). Based on the structure homology modeling studies, each domain of *N. gonorrhoeae* FtsA did not show significant difference

from FtsA from *E. coli* on their predicted secondary protein structure. This indicates that there are other reasons that may account for the different functions of FtsA domains in interaction with divisome proteins rather than primary sequence divergence or the dimensional structural differences.

The variation of FtsA interaction partners in different organisms would be a possible reason that caused different FtsA domains interacting with divisome proteins downstream of FtsA. In *E. coli*, FtsI, FtsQ and FtsN are bitopic membrane proteins and interact with FtsA, but FtsI plays a key role for the recruitment of the other two proteins FtsQ and FtsN. In *E. coli*, the FtsA 1C domain was proposed to specifically contact either FtsI or the proteins that interacted with FtsI (Corbin *et al*., 2004). Interactions of FtsI-FtsQ and FtsI-FtsN were also determined by B2H assays in *E. coli* (Di Lallo *et al*., 2003) and the localization of FtsN was dependent on FtsI in *E. coli* (Addinall *et al*., 1997). However, in *N. gonorrhoeae*, FtsI did not interact with either of FtsA, FtsQ or FtsN as determined using B2H assay (Table 3.2). This would be explained by the different penicillin binding proteins in *E. coli* and *N. gonorrheae*; FtsI is PBP3 in *E. coli* while FtsI is PBP2 in *N. gonorrhoeae* (Spratt, 1988). Therefore, all these differences may account for domains 2A and 2B of $FtsA_{Ng}$ rather than domain 1C as in *E. coli* implicated in interactions with divisome proteins downstream of FtsA in *N. gonorrhoeae*.

4.2. *N. gonorrhoeae* may have a different divisome assembly from *E. coli*

The division process in different bacteria undoubtedly varies since the complement of cell division proteins and the relationships of these proteins differ. For example, based on sequence homology of individual genes on *dcw* cluster, *N. gonorrhoeae* possesses 9 of the 12 divisome proteins identified in *E. coli*, but lacks FtsB and probably ZipA and FtsL; the putative ZipA protein in *N. gonorrhoeae* has very low identity to its *E. coli* counterpart (Du and Arvidson, 2003). The $FtsL_{Ng}$-like protein (264aa) differs in sequence similarity (7% identity) and amino acid length from $FtsL_{Ec}$ (366aa) (Li *et al*., unpublished).

In order to understand divisome assembly in *N. gonorrhoeae*, the potential interactions between divisome proteins in *N. gonorrhoeae* were examined (Figs. 3.13-3.15, Table 3.2) and the interactome in *N. gonorrhoeae* was compared with those reported from *E. coli* and *S. pneumoniae* (Di Lallo *et al*., 2003; Maggi *et al.*, 2008) (Fig. 4.1). Many of these interactions represented newly identified molecular interactions and were different from either *E. coli* or *S. pneumoniae*. *N. gonorrhoeae* shares 8 common divisome proteins with *E. coli*, FtsZ, FtsA, FtsK, FtsQ, FtsI, FtsW, FtsN and ZipA (Fig. 4.1a-b). A total of 9 interactions detected among *N. gonorrhoeae* proteins and of these 4, FtsZ-FtsW, FtsA-FtsK, FtsA-FtsW, and FtsK-FtsN, have not been reported in *E. coli* (Di Lallo *et al*., 2003; Karimova *et al*., 2005). *N. gonorrhoeae* has 6 divisome proteins in common with *S. pneumoniae* - FtsZ, FtsA, FtsK, FtsW, DivIB (homologue FtsQ), and PBP2X (homologue of FtsI) (Fig. 4.1 a, c). A total of 7 interactions were detected among these common *N. gonorrhoeae gonorrhoeae* proteins and of these 2, FtsA-FtsW and FtsI-FtsW, have not been reported in *S. pneumoniae* (Maggi *et al*., 2008). Only two interactions of FtsZ-FtsA and FtsZ-FtsK were conserved amongst the 3 organisms (Fig. 4.1). Although these data should be confirmed by other methodologies, they provide a protein-protein interaction profile in *N. gonorrhoeae*, which may help us to understand the recruitment of divisome proteins. I have also performed Y2H assay and GST

Fig. 4.1. Species-specific interaction profile amongst divisome proteins in *N. gonorrhoeae*, *E. coli* and *S. pneumoniae*, including the common divisome proteins in 3 organisms as well as FtsB and FtsL in *E. coli* and *S. pneumoniae*. (a) Interaction web among 8 *N. gonorrhoeae* divisome proteins - FtsZ, FtsA, ZipA, FtsK, FtsQ, FtsW, FtsI and FtsN as described in Table 3.2. (b) Interaction web among 10 *E. coli* divisome proteins, FtsZ, FtsA, ZipA, FtsK, FtsQ, FtsL, FtsB, FtsW, FtsI and FtsN as described previously (Di Lallo *et al.*, 2003; Karinova *et al*., 2005). (c) Interaction web among 8 *S. pneumoniae* divisome proteins, FtsZ, FtsA, FtsK, DivIB, FtsL, DivIC, FtsW, and FtsI as described by Maggi *et al*. (2008). The red lines indicate the interactions between upstream and downstream divisome proteins, while the blue lines indicate the interaction among downstream divisome proteins. The dashed blue lines indicate the interaction related to the protein complex FtsQ-FtsB-FtsL.

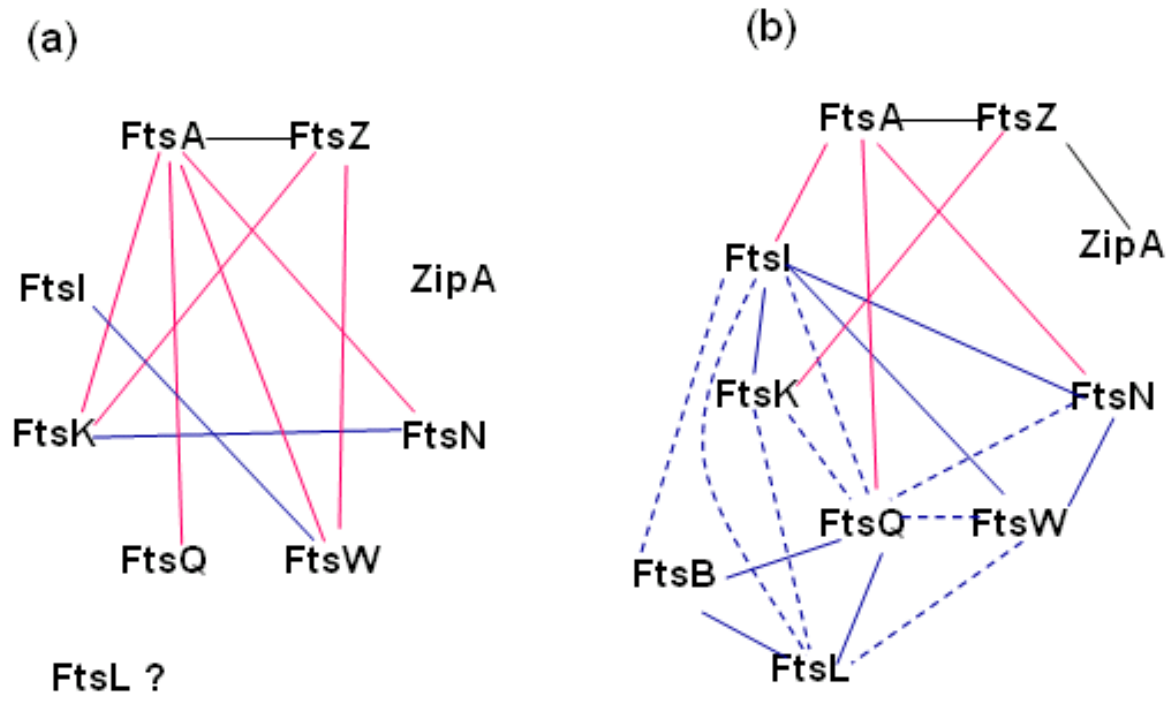
(a)
FtsA
FtsZ
FtsI
ZipA
FtsK
FtsN
FtsQ
FtsW
FtsL ?
Neisseria gonorrhoeae
(b)
FtsA
FtsZ
ZipA
FtsI
FtsK
FtsN
FtsQ
FtsW
FtsB
FtsL
Escherichia coli

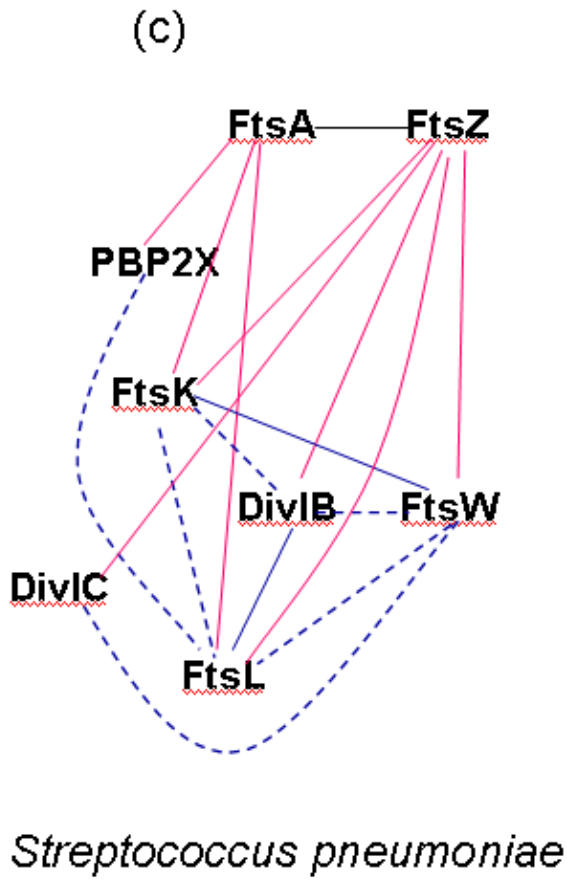
(c)
FtsA
FtsZ
PBP2X
FtsK
DivIB
FtsW
DivIC
FtsL
Streptococcus pneumoniae

pull-down assay to examine the interactions identified by B2H assays (Appendix B and Appendix C). Attempts to determine divisome protein interactions using Y2H assays failed (Appendix B). With the use of GST pull-down assays, $FtsA_{Ng}$ and its functional domains interaction with $FtsZ_{Ng}$ has been confirmed. I have done a part of other divisome protein purification and antibody productions, which can be used for future GST pull-down assays.

Compared to *E. coli*, more interactions were observed in total between divisome proteins downstream of FtsA and divisome proteins upstream of FtsA (including FtsA) in *N. gonorrhoeae* and *S. pneumoniae* (Table 4.1 and Fig. 4.1a-c, red lines). In *N. gonorrhoeae*, 6 interactions were observed between upstream and downstream proteins; FtsK, FtsQ, FtsW, and FtsN were involved in these interactions (Fig. 4.1a, red lines) and 8 interactions were observed in *S. pneumoniae*, which involved in all the downstream divisome proteins (Fig. 4.1c, red lines). While 4 interactions were observed in *E. coli* (FtsI, FtsK, FtsQ and FtsN were involved in these interactions) (Fig. 4.1b, red lines). Interaction of FtsA-FtsW is unique to *N. gonorrhoeae*. Interactions of FtsA-FtsK and FtsZ-FtsW were conserved in *N. gonorrhoeae* and *S. pneumoniae* but absent in *E. coli*. These data indicate that the interactomes of *N. gonorrhoeae* FtsA and FtsZ are more similar to *S. pneumoniae*, but differ from that in *E. coli*. This may be ascribed to the inability of ZipA in *N. gonorrhoeae* to interact with the divisome proteins and the absence of ZipA in *S. pneumoniae*. In *E. coli*, ZipA was required to recruit the late divisome proteins to Z-ring probably via its interaction with FtsZ since ZipA interacted with FtsZ only rather than any other divisome proteins (Fig. 4.1b, black line, Di Lallo *et al*., 2003; Karimova *et al*., 2005). $ZipA_{Ec}$ interacting with $FtsZ_{Ec}$ might induce a specific conformation of the Z-ring or the $FtsZ_{Ec}$-$FtsA_{Ec}$ complex that is required for recruitment of late divisome components. However, a ZipA homologue was absent in *S. pneumoniae* (Maggi *et al*., 2008). *N. gonorrhoeae* ZipA showed no significant similarities in the primary sequences to ZipA from *E. coli*. $ZipA_{Ng}$ is so named based on its similarity to *E.*

Table 4.1. Protein-protein interactions of FtsA and FtsZ with divisome proteins downstream of FtsA in *N. gonorrhoeae*, *E. coli* and *S. pneumoniae*.

Downstream divisome proteins	*E. coli*[a)]		*S. pneumoniae*		*N. gonorrhoeae*	
	FtsA	**FtsZ**	**FtsA**	**FtsZ**	**FtsA**	**FtsZ**
FtsK	-	+	+	+	+	+
FtsQ/DivIB	+	-	-	+	+	-
FtsB/DivIC	-	-	-	+	**n/a**	**n/a**
FtsL	-	-	+	+	**n/a**	**n/a**
FtsI/PBP2X	+	-	+	-	-	-
FtsW	-	-	-	+	+	+
FtsN	+	-	**n/a**	**n/a**	+	-

"+" indicates the interaction between two proteins; "-" indicates the lack of interaction between two proteins; n/a indicates data not available.

[a)] Protein-protein interactions in *E. coli* and *S. Pneumoniae* were examined by the same B2H assays as used in my research (Di Lallo *et al.*, 2003; Maggi *et al*., 2008).

coli ZipA at its C-terminal region (15% identity) and its ability to complement the growth defect caused by $ZipA_{Ec}$ depletion in *E. coli*. However, the expression of $ZipA_{Ng}$ in *E. coli* z*ipA*-depletion strain just partially alleviated the defect in cell division (Du and Arvidson, 2003). This indicates that the role of $ZipA_{Ng}$ in cell division is not as important as it is in cell growth. As determined by B2H assays, *N. gonorrhoeae* ZipA did not interact with either FtsZ or any other divisome proteins, indicating that $ZipA_{Ng}$ may not be involved in cell division (Fig. 4.1a). Thus *N. gonorrhoeae* FtsA might substitute for role of ZipA and is responsible to recruit more downstream divisome proteins to the division ring. These data indicates that the recruitment of the downstream divisome proteins in *N. gonorrhoeae* probably depends on FtsA.

Interactions between divisome proteins downstream of FtsA observed in *N. gonorrhoeae* (2 interactions) were fewer than in *E. coli* (15 interactions) and in *S. pneumoniae* (8 interactions) (Table 4.2 and Fig. 4.1a-c, blue lines). As a connection between divisome proteins upstream and downstream of FtsA, FtsK interacted with FtsL, FtsQ and FtsI in *E. coli* (Di Lallo *et al.*, 2003) and with DivIB, FtsW and FtsL in *S. pneumoniae* (Maggi *et al*., 2008). FtsK only interacted with FtsN in *N. gonorrhoeae*. FtsQ from *E. coli* is the protein that establishes the highest number of interactions with other protein components of the Z-ring. It was found to interact with almost all divisome proteins downstream of FtsA in *E. coli*, including FtsL, FtsB, FtsK, FtsW, FtsI, and FtsN as determined by B2H assays and other methods (such as Co-IP and another bacterial two-hybrid assay called BACTH) (Di Lallo *et al.*, 2003; Karimova *et al.*, 2005; D'Ulisse *et al*., 2007; Buddelmeijer and Beckwith, 2004). In *S. pneumoniae*, the FtsQ homologue DivIB interacted with a couple of divisome proteins downstream of FtsA, i.e. FtsK, FtsL and FtsW (Maggi *et al.*, 2008). However, *N. gonorrhoeae* FtsQ did not interact with any divisome proteins downstream of FtsA; this is significantly different from FtsA interactions with downstream proteins in *E. coli* and *S.*

Table 4.2. Protein-protein interactions between divisome proteins downstream of FtsA in *N. gonorrhoeae*, *E. coli* and *S. pneumoniae*.

Protein interacitons	*E. coli* [a)]	*S. pneumoniae*	*N. gonorrhoeae*
FtsQ-FtsB	+	-	n/a
FtsQ-FtsL	+	+	n/a
FtsB-FtsL	+	-	n/a
FtsQ-FtsW	+	+	-
FtsQ-FtsN	+	n/a	-
FtsQ-FtsI	+	-	-
FtsQ-FtsK	+	+	-
FtsB-FtsK	-	-	n/a
FtsB-FtsW	-	+	n/a
FtsB-FtsI	+	-	n/a
FtsB-FtsN	-	n/a	
FtsL-FtsI	+	+	n/a
FtsL-FtsK	+	+	n/a
FtsL-FtsW	+	+	n/a
FtsL-FtsN	-	n/a	n/a
FtsI-FtsK	+	-	-
FtsI-FtsW	+	-	+
FtsI-FtsN	+	n/a	-
FtsW-FtsN	+	n/a	-
FtsK-FtsN	-	n/a	+
FtsK-FtsW	-	+	-

"+" indicates the interaction between two proteins; "-" indicates the lack of interaction between two proteins. Red "+" indicates that the interactions related to protein complex FtsQ-FtsB-FtsL. n/a indicates data not available.

[a)] Protein-protein interactions in *E. coli* and *S. pneumoniae* were examined by the same B2H assays as used in my research (Di Lallo *et al.*, 2003; Maggi *et al.*, 2008).

pneumoniae. *E. coli* FtsI acts like a central linker protein for the interactions with FtsA and all the divisome proteins downstream of FtsA (Di Lallo *et al.*, 2003). While FtsI interacted with FtsL only in *S. pneumoniae* (Maggi *et al.*, 2008) and FtsI did not interact with any downstream proteins except FtsW in *N. gonorrhoeae* (Fig. 4.1a).

N. gonorrhoeae lacks FtsB and FtsL and hence lacks the FtsQ-FtsB-FtsL complex, which might in turn suppress its interactions with other proteins. FtsQ, FtsL and FtsB assembled into a stable complex in several bacteria, such as *E. coli*, *S. pneumoniae* and *B. subtilis* (Daniel *et al.*, 2006; Noirclerc-Savoye *et al.*, 2005; Robichon *et al.*, 2008) independent of other known division proteins and of the division status of the cell. This complex appeared to be the bridge between the predominantly cytoplasmic cell divisome proteins (i.e. FtsK) and the predominantly periplasmic cell divisome proteins (i.e. FtsW and FtsI) (Buddelmeijer and Beckwith, 2004).

The integrality and stability of a protein complex is important for its functionality and enhances its interactions with other divisome proteins. For example, FtsB when complexed with FtsL, is sufficient for recruitment of FtsW and FtsI in *E. coli* (Gonzalez and Beckwith, 2009; Gonzalez *et al.*, 2010). Fifteen interactions were observed among *E. coli* downstream proteins of FtsA (including FtsB and FtsL) and of those 8 were associated with FtsQ-FtsB-FtsL (Table 4.2, red; Fig. 4.1b, dashed blue line). The homologue FtsQ-FtsB-FtsL complex in *S. pneumoniae* is DivIB-DivIC-FtsL (Noirclerc-Savye *et al.*, 2005). The ability of this complex (i.e. DivIB-DivIC-FtsL) to enhance the interactions of divisome proteins downstream of FtsA was also observed in *S. pneumoniae* (Maggi *et al.*, 2008); eight interactions were observed among *S. pneumoniae* downstream proteins (including FtsB and FtsL) and of those 6 were associated with DivIB-DivIC-FtsL (Table 4.2, red; Fig. 4.1c, dashed blue line). However, in *N. gonorrhoeae*, only 2 interactions (FtsI-FtsW, FtsK-FtsN) were observed between divisome proteins downstream of FtsA and FtsQ did not interact with

any of those downstream divisome proteins (Table 4.2; Fig. 4.1a). Taken together, the reduced interactions between divisome proteins downstream of FtsA in *N. gonorrhoeae* might be ascribed to the failure to form an FtsQ-FtsL-FtsB complex, which in turn would force the divisome proteins downstream of FtsA to be recruited by another route, such as interaction with the divisome proteins upstream of FtsA. This may explain why not only FtsA but also FtsZ were observed to interact with more downstream divisome proteins in *N. gonorrhoeae*.

No divisome protein downstream of FtsA interacted with both FtsA and FtsZ in *E. coli* (Fig. 4.1b) (Di Lallo *et al*., 2003), while FtsK and FtsL in *S. pneumoniae* (Maggi *et al*., 2008) (Fig. 4.1c) and FtsK and FtsW in *N. gonorrhoeae* interacted with both FtsA and FtsZ (Fig. 4.1a). Given the inability of $ZipA_{Ng}$ to interact with other divisome proteins and the reduced interactions between divisome proteins downstream of FtsA in *N. gonorrhoeae*, the direct interactions of divisome proteins downstream FtsA with both FtsA and FtsZ would serve to ensure that those downstream divisome proteins would be recruited to the Z-ring.

As an additional comment, since the putative FtsL protein in *N. gonorrhoeae* showed extremely low identity (7%) and similarity (22%) to FtsL from *E. coli* at the amino acid level (Li *et al.*, unpublished), the FtsL homologue was thought to be absent in *N. gonorrhoeae* (Francis *et al*., 2000). However, FtsL was later identified as being part of *N. gonorrhoeae dcw* cluster by a sequence search to *N. gonorrhoeae* FA1090 genome sequence database (Snyder *et al*., 2001, 2003). The low homology of $FtsL_{Ng}$ to $FtsL_{Ec}$ might result in the divergent functionality of $FtsL_{Ng}$ in cell division, thus I adopted the former proposal that FtsL lacks in *N. gonorrhoeae* and did not test the interactions of $FtsL_{Ng}$ with other divisome proteins in this study. However, to clarify the role of protein complex in enhancing downstream division interactions, some work further needs to be completed in this regard and to investigate the formation of protein complex $FtsQ_{Ng}$-$FtsL_{Ng}$ in *N. gonorrhoeae*.

Finally, the comparison of divisome protein interactomes from different organisms indicates that the divisome protein interactome of *N. gonorrhoeae* is more similar to that of *S. pneumoniae* but differs from that of *E. coli*. In *E. coli*, late divisome proteins formed protein complexes independently of FtsA, which were subsequently recruited to the midcell once the Z-ring complex (composed of FtsZ, FtsA and ZipA) was established (Goehring *et al*., 2006). Divisome assembly in *S. pneumoniae* is not clear. In *N. gonorrhoeae*, FtsZ interacting with FtsA might form a complex FtsZ-FtsA, which might subsequently act as a scaffold for the recruitment of divisome proteins downstream of FtsA to the Z-ring. These downstream divisome proteins might be recruited sequentially depending on FtsA. Further studies are needed to ascertain the temporal order of divisome assembly in *N. gonorrhoeae*.

4.3. FtsA exhibits species-specific functionality

N. gonorrhoeae is a fastidious organism, with only a few genetic tools available for studying its molecular biology (Pagotto *et al*., 2000). In contrast, *E. coli* is much easier to culture and to genetically manipulate. Furthermore, there are many expression vectors that are suitable for protein studies in *E. coli*. Because *N. gonorrhoeae* cells are too small (~ 0.3-1 μm) for some morphological observations (e.g. protein cellular localization or protein overexpressions effect on cell division other than enlargement), *E. coli* is often used as a host organism to test the functionality of cell division proteins from bacteria such as *N. gonorrhoeae* (Szeto *et al*., 2001, 2004; Ramirez-Arcos *et al.*, 2002, 2005). Morphological changes indicative of cell division disruption have been observed when heterologous cell division genes (e.g. $ftsZ_{Ng}$ or min_{Ng}) were expressed in either rod or round *E. coli* backgrounds (Ramirez-Arcos *et al.*, 2002, 2005). Thus $FtsA_{Ng}$ was expressed in *E. coli* backgrounds to determine whether *E. coli* could be used as heterologous model for studying $FtsA_{Ng}$ function. Overexpression of $FtsA_{Ec}$ in *E. coli* has been previously shown to cause filamentous cell phenotype (Dai and Lutkenhaus, 1992; Dewar *et al.*, 1992; Geissler *et al.*, 2007). The overexpression of $FtsA_{Ng}$ in wild-type *E. coli* led to the similar negative effect on cell division, indicative of cell division disruption at potential division sites along the length of the rod. This ability to disrupt *E. coli* cell division indicates that $FtsA_{Ng}$ is functional in *E. coli*.

While $FtsA_{Ng}$ was unable to be overexpressed in its native *N. gonorrhoeae* background from a shuttle vector (data not shown), $FtsA_{Ng}$ was overexpressed in *E. coli* KJB24, which divides in alternating perpendicular planes as *N. gonorrhoeae* does, to determine its effects in a coccal background. These cells have been previously used to study Min_{Ng} protein expression (Szeto *et al.*, 2001). In the present study, high expression of $FtsA_{Ng}$ inhibited cell

division in coccal background and led to gross cell enlargement, which verified the ability of $FtsA_{Ng}$ to disrupt cell division in a coccal background.

It was reported that *E. coli* cells overexpressing $FtsA_{Ec}$ appeared primarily as long and smooth filaments, although some cells of normal length and short filaments were also present (Wang and Gayda, 1990). In my experiments, although $FtsA_{Ng}$ overexpression in *E. coli* PB103 led to the similar morphological changes as filaments, normal-sized cells were the predominant morphological phenotype, mixed with cells of various lengths (Fig. 3.19). Extremely long filaments observed were less than 36% and the number of normal-sized cells rose with increased incubation time from 4 hrs to 8 hrs, indicating that normal cell division resumed with incubation. The proportion of irregular enlarged round *E. coli* cells gradually decreased from 4 hrs (31%) to 8 hrs (11%) (Fig. 3.20), indicating that normal cell division got resumed.. There are two possible reasons to explain this phenomenon. This first reason is that FtsA from *N. gonorrhoeae* is not a strong division inhibitor, which disrupts cell division only in some *E. coli* cells and its effect becomes weaker with cell growth. It is also possibly due to the decreased protein level over time because of the depleted IPTG, since $FtsA_{Ng}$ overexpression in *E. coli* cells depends on IPTG induction. To further clarify the reason, the protein levels of $FtsA_{Ng}$ expressed in *E. coli* have to be analyzed at different time points.

To understand how $FtsA_{Ng}$ affects cell division in *E. coli*, the viability of *E. coli* cells overexpressing $FtsA_{Ng}$ was examined. The CFUs of *E. coli* with $FtsA_{Ng}$ were lower than those of *E. coli* without $FtsA_{Ng}$ in the first 3 hrs and rose from 3 hrs to 6 hrs (Fig. 3.23, 24). This is consistent with the increasing proportion of normal-sized *E. coli* cells observed by DIC microscopy from 4 hrs to 8 hrs (Fig. 3. 20, 22). Thus the growth curves also indicate that $FtsA_{Ng}$ probably disrupted *E. coli* cell division mainly at the early growth phase.

$FtsA_{Ng}$ localized at the mid-cell and the cell poles in normal-sized *E. coli* cells (Fig. 3.25), which may reflect the true $FtsA_{Ng}$ localization in *E. coli* cells, as no inclusion bodies

were observed judged by DIC microscopy (Ma *et al*., 1996). Overexpression of $FtsA_{Ng}$ caused filamentous cells with inclusion bodies as judged by DIC microscopy (Fig. 3.26, Ma *et al.*, 2006). These filaments usually exhibited various extents of damage or even lysis, indicating the formation of inclusion bodies probably account for cell morphology changes. The formation of inclusion bodies physically occupies space in the cytoplasm, which might result in the loss of cell mass, as observed, or even cell death (Fig. 3.26). This might account for the fewer viable cells observed in the post-stationary phase of the growth curve in *E. coli* with $FtsA_{Ng}$ overexpression rather than in *E. coli* without $FtsA_{Ng}$ (Fig. 3.23). The space between $FtsA_{Ng}$-EGFP dots was irregular and too small to be the position of nucleoid, indicating non-specific localization of $FtsA_{Ng}$ in filamentous cells. $FtsA_{Ng}$-EGFP showed similar non-specific localization in enlarged round *E. coli* cells.

The normal cell division process is thought to require a proper FtsA:FtsZ ratio; disruption of this ratio was reported to cause defects in cell division in *E. coli* (Dai and Lutkenhaus, 1992; Dewar *et al.*, 1992). Since overexpression of $FtsA_{Ng}$ in *E. coli* inhibited cell division in some cells, it is possible that $FtsA_{Ng}$ might disrupt the FtsA: FtsZ ratio in *E. coli* by interacting with $FtsZ_{Ec}$ or $FtsA_{Ec}$. To test this possibility, the interspecies $FtsA_{Ng}$-$FtsZ_{Ec}$ and $FtsA_{Ng}$-$FtsA_{Ec}$ interactions were examined. I found that *N. gonorrhoeae* FtsA was unable to interact with either FtsZ or FtsA from *E. coli* (Fig. 3.16). Interestingly, FtsA from both *Agrobacterium tumefaciens* and *Rhizobium melitoli* also failed to demonstrate an interaction with $FtsZ_{Ec}$. Overexpression of FtsA from either *A. tumefaciens* or *R. melitoli* in *E. coli* caused no morphological changes, in contrast to $FtsA_{Ng}$, although these proteins also localized at the *E. coli* midcell (Ma *et al*., 1997). Even though $FtsA_{Ng}$ failed to interact with both $FtsZ_{Ec}$ and $FtsA_{Ec}$, it disrupted cell division in some *E. coli* cells. One possibility to explain this is that $FtsA_{Ng}$ interfered with the cell division process by interacting with late

divisome proteins as opposed to $FtsA_{Ec}$ and $FtsZ_{Ec}$; further studies should be performed to test this hypothesis.

I also determined that $FtsA_{Ng}$ was not able to complement *E. coli* P163, an *ftsA*-depletion strain (Fig. 3.28). This result is consistent with other observations; FtsA from *B. subtilis* did not complement an *E. coli* temperature-sensitive *ftsA* mutant, although the expression of $FtsA_{Bc}$ resulted in filamentation in *E. coli* as $FtsA_{Ng}$ did (Beall *et al*., 1988). FtsAs from *N. gonorrhoeae*, *A. tumefaciens* and *R. melitoli* were 40%, 29% and 30% identical to *E. coli* FtsA, respectively. The observed sequence divergence between FtsA homologues might explain the failure of heterologous FtsAs to complement *E. coli* mutants together with the failure of cross-species protein-protein interactions. The failure of $FtsA_{Ng}$ to complement the *E. coli ftsA*-depletion strain might be either because $FtsA_{Ng}$ did not interact with the proteins of the *E. coli* cell division machinery (such as $FtsZ_{Ec}$ or $FtsA_{Ec}$) or because $FtsA_{Ng}$ did not recognize $FtsA_{Ec}$-specific target sites.

4.4. Consideration of two-hybrid methods to detect protein-protein interactions

Two-hybrid systems are now classical methods to test protein-protein interactions. I first used Y2H system to examine the potential interactions amongst divisome proteins in *N. gonorrhoeae* (Appendix B). However, no protein pairs showed interaction, which is consistent with previous reports by Greco-Stewart *et al.* (2007) and Hu *et al*. (1999). An interaction between MinC and FtsZ could not be detected in *N. gonorrhoeae* using Y2H system, but it was demonstrated by using a B2H system (Greco-Stewart *et al.*, 2007). Y2H assays also did not detect any association between *E. coli* MinC and FtsZ, although purified *E. coli* MinC has been demonstrated to interact with FtsZ (Hu *et al*., 1999). This suggests that Y2H system may not be optimal for studying bacterial cell division protein interactions.

The B2H system is a widely used method to detect protein-protein interactions, and is particularly pertinent to the *in vivo* study of bacterial cell division proteins. It was initially explored to test the divisome protein interactions in *E. coli* (Di Lallo *et al*., 2001, 2003) and subsequently was used to identify the interaction domains of *E. coli* divisome proteins, such as FtsK and FtsQ (Grenda *et al.*, 2007; D'Ulisse *et al.*, 2007). The B2H system was also successfully used to detect divisome protein interactions in *S. pneumoniae* (Maggi *et al*., 2008). The interactions between MinC, FtsZ, and MinD in *N. gonoeehoeae* were successfully demonstrated by this system (Greco-Stewart *et al.*, 2007). Thus the B2H system was the best assay, given the failure of the Y2H system, to test the interactions between divisome proteins in *N. gonorrhoeae*.

Since the proteins are expressed in a heterologous system to test their interactions, it is important to ascertain whether various *N. gonorrhoeae* fusion constructs are functional when expressed in *E. coli* system. In this study, the negative and positive controls were measured in each interaction and all of them worked well; the β-galactosidase activities of all the negative controls were close to or even higher than that of R721 while the β-galactosidase activity of

positive control ($FtsZ_{Ng}$ self-interaction) was consistent in all measurements and showed an averaged 28% residual β-galactosidase activity compared to that of R721 (see the results in Chapter 3), indicating the B2H system was functional. As seen in Table 3.2, each protein, except for ZipA, interacted with one or more other proteins, indicating that they were functional in the B2H system. ZipA did not interact with any partner in present study, which probably reflects the real lack of interaction between ZipA and other divisome proteins in *N. gonorrhoeae*. The ZipA fusions were created using the similar cloning strategies as with other proteins, thus ZipA was expected to be functional in the B2H system as other proteins.

The results obtained from B2H system are all based on the activity of a protein expressed, steric considerations, and protein stability in another host. Thus the two-hybrid assays are frequently prone to false positive or negative interactions. False positives could be due to the overexpression of the reporter protein fusions, which could result in magnifying potentially weak interactions. The false negatives could be due to low expression levels and/or instability of the molecules tested. Presently, I have no data that would allow evaluation of the limit of B2H in my study. However, in order to eliminate the false positives that are possible due to the overexpression of proteins magnifying potentially weak interactions, the cut-off criteria of 50% residual β-galactosidase activity was introduced to judge the positive or negative interaction, as used in other divisome protein studies (Di Lallo *et al*., 2003; Maggi *et al*., 2008). The rationale for this cut-off criteria was reported in previous work, which was supported in accordance with cluster analysis using the statistical program SPSS and results of other authors (Di Lallo *et al.*, 2003; D'Ulisse *et al.*, 2007; Fadda *et al*., 2007). The averaged β-galactosidase activities were obtained by performing each interaction, in triplicate, independently. These manipulations ensured that the positive results obtained from B2H assays were reliable and reflect a real interaction between two proteins. A β-galactosidase activity of each protein pair lower than 50% indicates a positive interaction

whereas a β-galactosidase activity of each protein over 50% indicates a negative interaction. However, those protein pairs in which the values close to the 50% cut-off criterium can not be arbitrarily considered to have positive or negative interactions, such as $FtsA_{Ng}$-$FtsQ_{Ng}$ (48%), $FtsA_{Ng}$-$FtsW_{Ng}$ (45%), $FtsA_{Ng}$-$FtsX_{Ng}$ (51%) and $FtsQ_{Ng}$-$FtsX_{Ng}$ (46%) (Table 3.2). Thus, in this study, the *t* test was used to determine if these cut-off values which had a mean between 40% and 60% were significantly different from the 50% cut-off criterium. As shown in Table 3.3, the values between 45% and 53% were not statistically significantly different from the 50% stated cut-off, while the values lower than 45% or over 53% were statistically significantly different. The only exception was the interaction of $FtsZ_{Ng}$ with $FtsX_{Ng}$, as it produced 42% $\pm$ 8% residual β-galactosidase activity but did not show a significant difference from the 50% cut-off criterium (Table 3.2, 3.3). This may have been produced by the high standard deviation for this particular assay. Thus, based on my statistical analysis, I interpreted that protein pairs with β-galactosidase values lower than 45% represented a real protein-protein interaction while protein pairs with β-galactosidase values over than 53% represented no interaction between proteins. I interpreted the protein pairs which had a mean β-galactosidase values between 45% and 53% as having weak, transient or no interactions. The interactions for some those protein pairs (i.e. $FtsA_{Ng}$-$FtsQ_{Ng}$ (48%), $FtsA_{Ng}$-$FtsW_{Ng}$ (45%), $FtsA_{Ng}$-$FtsX_{Ng}$ (51%), $FtsQ_{Ng}$-$FtsX_{Ng}$ (46%) and $FtsZ_{Ng}$-$FtsX_{Ng}$ (42%)) are still questionable and need to be confirmed using other methods. Presently, the interactions of $FtsA_{Ng}$ with $FtsQ_{Ng}$ and $FtsW_{Ng}$ were further confirmed by identifying the specific $FtsA_{Ng}$ domains that were responsible for the interaction with $FtsQ_{Ng}$ and $FtsW_{Ng}$. I determined that the $FtsA_{Ng}$ 2B and $2A_2$ domains interacted with $FtsQ_{Ng}$, giving a 22% residual β-galactosidase activity and a 33% residual β-galactosidase activity, respectively (Table 3.1). The $FtsA_{Ng}$ $2A_2$ domain was also the interaction domain with $FtsW_{Ng}$, giving a 20% residual

β-galactosidase activity (Table 3.1). However, the interactions of $FtsZ_{Ng}$-$FtsX_{Ng}$, $FtsA_{Ng}$-$FtsX_{Ng}$, and $FtsQ_{Ng}$-$FtsX_{Ng}$ need to be further confirmed using other methods.

Some data also suggest that the B2H system excludes other kinds of the false (or indirect) interactions that are induced by the third part of a "bridge" protein. As analyzed by Maggi *et al.* (2008), if a protein X interacts with both A and B, false positives could be due to indirect interaction between A and B mediated by X in a complex such as A–X–B. i.e. potential FtsK and FtsQ interaction could be mediated by FtsA, since they both interacted with FtsA. Actually, the B2H assay did not reveal interactions between *N. gonorrhoeae* proteins FtsK-FtsQ, FtsK-FtsW, FtsQ-FtsW, FtsQ-FtsN, although all of them interacted with FtsA in common. Analogous evidence can be found from *E. coli* and *S. pneumoniae* divisome protein interactions tested by the same B2H system; the assays did not reveal interactions of FtsZ-FtsW and FtsZ-FtsQ/DivIB in both *E. coli* and *S. pneumoniae*, although all of them interacted with ZapA (Fig. 1.9) (Di Lallo *et al*., 2003; Maggi *et al.*, 2008). In addition, the interactions described in this study were observed in a heterologous system. The formation of false positives should need an *E. coli* 'bridge' protein able to interact with both the *N. gonorrhoeae* partners. However, it appears that certain divisome proteins from *N. gonorrhoeae* do not exhibit cross-species functionality, since *N. gonorrhoeae* FtsA was unable to interact with *E. coli* FtsZ or FtsA. More evidence can be found from the heterologous interactions between *E. coli* and *S. pneumoniae* divisome proteins as determined by the same B2H system, i. e. *E. coli* FtsK interacted with both *S. pneumoniae* FtsZ and FtsL, which may induce a potential interaction of $FtsZ_{Sp}$-$FtsL_{Sp}$, but $FtsZ_{Sp}$ did not interact with $FtsL_{Sp}$ (Maggi *et al*., 2008).

In issue of false negative interactions that result from the low expression levels or protein stability, can be easily solved by observing whether there are two molecules, X and Y, that do not interact with each other, but each of which is able to interact with other

partners; thus the lack of interaction between them is real. This condition was verified for 21 proteins pairs that did not shown any interactions between them, as all divisome proteins tested were functional and able to interact with at least one partner, except ZipA.

Confirmation of the interactions between divisome proteins from *N. gonorrhoeae* using Y2H method were not possible (Appendix B). I also tried to purify the divisome proteins to produce antibodies for other confirmatory assays. A part of divisome protein purification and antibody production have been completed as described in Appendix C; however some membrane proteins were difficult to purify. Thus, in the future, other methods such as GST pull-down or Co-IP assays can be used to confirm the data obtained from B2H assays.

4.5. Further considerations and concluding statements

Knowledge about bacterial divisome assembly has mostly advanced from studies with *E. coli*. Our laboratory has pioneered investigations of the *dcw* cluster of genes in *N. gonorrhoeae* (Francis *et al.*, 2000), particularly the central division protein FtsZ (Salimnia *et al*., 2000). In my research, the interaction network between divisome proteins in *N. gonorrhoeae* was examined and the comparison of the *N. gonorrhoeae* divisome protein interactome with those of *E. coli* and *S. pneumoniae* was performed. The comparisons demonstrated a significantly different interactome in *N. gonorrhoeae* as compared to *E. coli*, indicating a possible different divisome assembly model in *N. gonorrhoeae*. In *E. coli*, divisome assembly follows a concerted model rather than a strictly linear hierarchy. One outstanding characteristic of the concerted model is the preformed protein complexes, which are the Z-ring complex composed of FtsZ, FtsA and ZipA, the periplasmic connector protein complex of FtsQ-FtsB-FtsL and the murein synthesis complex of FtsW-FtsI (Goehring *et al.*, 2006). Protein complexes in bacteria take part in majority of cellular processes involving cell division, membrane transport, energetic metabolism, biosysthesis of essential compounds and maintaining homeostasis (Dresler *et al*., 2011). Thus, in order to understand the recruitment of divisome proteins and how the divisome assembles in *N. gonorrhoeae*, it is necessary to investigate whether divisome proteins preform complexes before recruited to the division ring and what they are.

For particular investigation of divisome protein complexes, a premature targeting approach would be good choice. The premature targeting approach permits a direct assessment of a protein's ability to recruit other cell division components in the absence of upstream components normally required for its own localization (Goehring *et al*., 2005). This approach was successfully used to explore the divisome protein complexes in *E. coli* and demonstrated a model for divisome organization in *E. coli* (Goehring *et al.*, 2006). In this

approach, a protein fused to the FtsZ binding protein ZapA is directly localized to the Z-ring. It then can be assessed how the localization of other divisome proteins is affected as these upstream proteins are removed (Goehring *et al*., 2006). Since ZapA is absent in *N. gonorrhoeae,* the premature targeting approach may not be feasible in *N. gonorrhoeae* if no other FtsZ binding protein is available. Blue native polyacrylamide gel electrophoresis (BN-PAGE) can be an alternative method. BN-PAGE is a relatively simple and sensitive method for the study of membrane bacterial complexes. BN-PAGE is a special electrophoretic approach developed by Schagger and von Jagow (1991) that was originally used for analyses of mitochondrial protein complexes. This method can be applied to protein complexes ranging in molecular weights from 10 to 10,000 kDa (Schagger *et al.*, 1994) and has been widely used for the analysis of membrane protein complexes (Dresler *et al*., 2011). In this approach, the native complexes are separated by BN-PAGE from the native cell extracts in the first dimension. These complexes can be denatured and separated according to their size in the second dimension using regular SDS-PAGE. The proteins belonging to the same complex are aligned vertically in the second SDS dimension (Krause, 2006).

Bacterial cell division is an attractive antibacterial target because they comprise a group of proteins that are all conserved and essential throughout the bacteria but absent from humans. Among those proteins, FtsZ is a specific target to develop agents. Selective small-molecule inhibitors of FtsZ polymerization or GTPase activity have been screened and identified, which do not affect tubulin, human FtsZ homologue, and could be new potential candidates for novel antibacterial agents (Paradis-Bleau *et al.,* 2007; Margalit *et al.,* 2004; Wang *et al.,* 2003; Lappchen *et al.,* 2005). Similar to FtsZ, FtsA is such a protein that meets all conditions to be a potential antimicrobial target: essential in prokaryotic cell division, widespread in the bacteria, absent in the mitochondria of higher eukaryotes and evolutionary distant from actin, the human FtsA homologue. The $FtsA_{Ng}$ 2A and 2B domains might be

good candidates to target, because they are highly conserved and important in interactions with $FtsZ_{Ng}$ and other divisome proteins. Studies from *E. coli* also showed that these domains exhibited multiple functionalities in other aspects of cell division (Geissler *et al*., 2003; Sanchez *et al.*, 1994; Robinson *et al.*, 1988). Thus, with further studies of biochemical activities and atomic structure of $FtsA_{Ng}$, a long-term attractive project would be tend to detect unique $FtsA_{Ng}$ target sites for the development of novel antimicrobials.

Conclusion statements

1. This study determined the association of $FtsA_{Ng}$ with $FtsZ_{Ng}$ and other divisome proteins in *N. gonorrhoeae* and identified the functional domains of $FtsA_{Ng}$ involved in these interactions. $FtsA_{Ng}$ interacted with $FtsZ_{Ng}$, $FtsK_{Ng}$, $FtsW_{Ng}$, $FtsQ_{Ng}$, and $FtsN_{Ng}$. Each of the domains $2A_1$, $2A_2$ and 2B of $FtsA_{Ng}$ was sufficient to interact with $FtsZ_{Ng}$. Domain $2A_1$ interacted with $FtsK_{Ng}$ and $FtsN_{Ng}$. Domain 2B of $FtsA_{Ng}$ interacted with $FtsQ_{Ng}$, and $FtsN_{Ng}$. Domain $2A_2$ of $FtsA_{Ng}$ interacted with $FtsQ_{Ng}$, $FtsW_{Ng}$, and $FtsN_{Ng}$. These data suggest that FtsA in *N. gonorrhoeae* plays a key role in the interactions with FtsZ and other divisome proteins.
2. The potential interactions between divisome proteins in *N. gonorrhoeae* were examined using B2H assays. The comparisons between the *N. gonorrhoeae* divisome protein interaction network and those of *E. coli* and *S. pneumoniae* were also performed. The comparisons revealed more interactions between divisome proteins upstream of FtsA (including FtsA) and divisome proteins downstream of FtsA while fewer interactions between divisome proteins downstream of FtsA in *N. gonorrhoeae*. The possible reasons could be the inability of $ZipA_{Ng}$ to interact with other divisome proteins and the lack of FtsL and FtsB, and hence the "lack" of an FtsQ-FtsB-FtsL complex in *N. gonorrhoeae*.

These results indicate a possibly different divisome assembly in *N. gonorrhoeae* from proposed models for *E. coli*.

3. $FtsA_{Ng}$ was located at the division site in *N. gonorrhoeae* cells and the ratio of FtsA to FtsZ ratio ranged from 1:24 to 1:33 in three *N. gonorrhoeae* strains, which gave a lower cellular concentration of FtsA compared to other organisms.
4. I also determined that $FtsA_{Ng}$ failed to complement an $ftsA_{Ec}$-deletion *E. coli* strain although the overexperssion of $FtsA_{Ng}$ disrupted *E. coli* cell division. In addition, overexpression of $FtsA_{Ng}$ only affected cell division in some cells and its localization in *E. coli* was independent of interaction with *E. coli* FtsA or FtsZ. These results indicate both that $FtsA_{Ng}$ exhibits a species-specific functionality and that *E. coli* is not a suitable model for studying $FtsA_{Ng}$ functionality.

REFERENCES:

Aaron, M., Charbon, G., Lam, H., Schwarz, H., Vollmer, W. and Jacobs-Wagner, C. (2007) The tubulin homologue FtsZ contributes to cell elongation by guiding cell wall precursor synthesis in *Caulobacter crescentus*. Mol Microbiol **64**: 938-952.

Aarsman, M. E. G., Piette, A., Fraipont, C., Vinkenvleugel, T. M. F., Nguyen-Disteche, M. and Den Blaauwen, T. (2005) Maturation of the *Escherichia coli* divisome occurs in two steps. Mol Microbiol **55**: 1631-1645.

Addinall, S. G. and Holland, B. (2002) The tubulin ancestor, FtsZ, draughtsman, designer and driving force for bacterial cytokinesis. J Mol Biol **318**: 219-236.

Addinall, S., Bi, E. and Lutkenhaus, J. (1996) FtsZ ring formation in *fts* mutants. J Bacteriol **178**: 3877-3884.

Addinall, S., Cao, C. and Lutkenhaus, J. (1997) FtsN, a late recruit to the septum in *Escherichia coli*. Mol Microbiol **25**: 303-309.

Alexeeva, S., Gadella, T. W. Jr, Verheul, J., Verhoeven, G. S. and den Blaauwen, T. (2010) Direct interactions of early and late assembling division proteins in *Escherichia coli* cells resolved by FRET. Mol Microbiol **77**: 384-98.

Anderson, D. E., Gueiros-Filho, F. J. and Erickson, H. P. (2004) Assembly dynamics of FtsZ rings in *Bacillus subtilis* and *Escherichia coli* and effects of FtsZ-regulating proteins. J Bacteriol **186**: 5775-5781.

Anderson, J. E., Hobbs, M. M., Biswas, G. D. and Sparling, P. F. (2003) Opposing selective forces for expression of the gonococcal lactoferrin receptor. Mol Microbiol **48**:1325-1337.

Arends, S. J., Williams, K., Scott, R. J., Rolong, S., Popham, D. L. and Weiss, D. S. (2010) Discovery and characterization of three new *Escherichia coli* septal ring proteins that contain a SPOR domain: DamX, DedD, and RlpA. J Bacteriol **192**: 242-55.

Ayala, J. A., Garrido, T., de Pedro, M. A. and Vicente, M. (1994) Molecular biology of bacterial septation. In *Bacterial cell wall*. Ghuysen, J. M. and Hakenbeck, R. (ed.) Amsterdam: Elsevier, pp. 73-102.

Bath, J., Wu, L. J., Errington, J. and Wang. J. C. (2000) Role of *Bacillus subtilis* SpoIIIE in DNA transport across the mother cell-prespore division septum. Science **290**: 995-997.

Beall, B., Lowe, M. and Lutkenhaus, J. (1988) Cloning and characterization of *Bacillus subtilis* homologs of *Escherichia coli* cell division genes *ftsZ* and *ftsA*. *J Bacteriol* **170**: 4855-4864.

Begg, K. and Donachie, W. (1998) Division planes alternate in spherical cells of *Escherichia coli*. J Bacteriol **180:** 2564-2567.

Bernard, C.S., Sadasivam, M., Shiomi, D. and Margolin, W. (2007) An altered FtsA can compensate for the loss of essential cell division protein FtsN in *Escherichia coli*. Mol Microbiol **64**: 1289-1305.

Bernatchez, S., Francis, F., Salimnia, H., Beveridge, T., Li, H. and Dillon, J. R. (2000) Genomic, transcriptional and phenotypic analysis of *ftsE* and *ftsX* of *Neisseria gonorrhoeae*. DNA Research **7**: 75-81.

Bernhardt, T. G. and de Boer, P. A. J. (2005) SlmA, a nucleoid-associated, FtsZ binding protein required for blocking septal ring assembly over chromosomes in *Escherichia coli*. Mol Cell **18**: 555-564.

Bi, E. and Lutkenhaus, J. (1991) FtsZ ring structure associated with division in *Escherichia coli*. Nature **354**: 161-164.

Bigot, S., Corre, J., Louarn, J. M., Cornet, F. and Barre, F. X. (2004) FtsK activities in Xer recombination, DNA mobilization and cell division involve overlapping and separate domains of the protein. Mol Microbiol **54**: 876-886.

Bigot, S., Sivanthan, V., Possoz, C., Barre, F. X. and Cornet, F. (2007) FtsK, a literate chromosome segregation machine. Mol Microbiol **64**: 1434-1441.

Bork, P., Sander, C. and Valencia, A. (1992) An ATPase domain common to prokaryotic cell cycle proteins, sugar kinases, actin and hsp70 heat shock proteins. Proc Natl Acad Sci USA **89**: 7290-7294.

Botta, G. A. and Park, J. T. (1981) Evidence for involvement of penicillin binding protein 3 in murein synthesis during septation but not during cell elongation. J Bacteriol **145**: 333-340.

Bowler, L. D. and Spratt, B. G. (1989) Membrane topology of penicillin binding protein 3 of *Escherichia coli.* Mol Microbiol **3**: 1277-1286.

Boyle, D. S., Khattar, M. M., Addinall, S. G., Lutkenhaus, J. and Donachie, W. D. (1997) *ftsW* is an essential cell-division gene in *Escherichia coli.* Mol Microbiol **24**: 1263-1273.

Bramkamp, M., Emmins, R., Weston, L., Donovan, C., Daniel, R. A. and Errington, J. (2008) A novel component of the division-site selection system of *Bacillus subtilis* and a new mode of action for the division inhibitor MinCD. Mol Microbiol **70**: 1556-1569.

Brun, Y. V., Marczynski, G. and Shapiro, L. (1994) The expression of asymmetry during *Caulobacter* cell differentiation. Annu Rev Biochem **63**: 419-450.

Buddelmeijer, N. and Beckwith, J. (2002) Assembly of cell division proteins at the *Escherichia coli* cell center. Curr Opin Microbiol **5**: 553-557.

Buddelmeijer, N. and Beckwith, J. (2004) A complex of the *Escherichia coli* cell division proteins FtsL, FtsB and FtsQ forms independently of its localization to the septal region. Mol Microbiol **52**: 1315-1327.

Carettoni, D., Gomez-Puertas, P., Yim, L., Mingorance, J., Massidda, O. and Vicente, M. (2003) Phage-display and correlated mutations identify an essential region of subdomain 1C involved in homodimerization of *Escherichia coli* FtsA. Proteins **50**: 192-206.

CDC (2007, 2008) Sexually transmitted disease surveillance, Atlanta, GA.

CDC (2006) Update to CDC's sexually transmitted diseases treatment guidelines, 2006: fluoroquinolones no longer recommended for treatment of gonococcal infections. MMWR **56**: 332-336.

CDC (2006) Workowski, K.A. and Berman, S. M. Sexually transmitted diseases treatment guidelines, 2006. MMWR Recomm Rep **55**(RR-11): 1-94.

Cha, J. and Stewart, G. (1997) The *divIVA* minicell locus of *Bacillus subtilis*. J Bacteriol **179**: 1671-1683.

Chen, A., Boulton, I. C., Pongoski, J., Cochrane, A. and Gray-Owen, S. D. (2003) Induction of HIV-1 long terminal repeat-mediated transcription by *Neisseria gonorrhoeae*. Aids **17**: 625-628.

Chen, J. C. and Beckwith, J. (2001) FtsQ, FtsL and FtsI require FtsK, but not FtsN, for co-localization with FtsZ during *Escherichia coli* cell division. Mol Microbiol **42**: 395-413.

Chen, J. C., Weiss, D. S., Ghigo, J. and Beckwith, J. (1999) Septal localization of FtsQ, an essential cell division protein in *Escherichia coli*. J Bacteriol **181**: 521-530.

Chen,Y. and Erickson, H. P. (2005) Rapid *in vitro* assembly dynamics and subunit turnover of FtsZ demonstrated by fluorescence resonance energy transfer. J Biol Chem **280**: 22549-22554.

Cohen, M. S. (1998) Sexually transmitted diseases enhance HIV transmission: no longer a hypothesis. Lancet **351**(Suppl): S5-7.

Corbin, B. D., Geissler, B., Sadasivam, M. and Margolin, W. (2004) Z-ring-independent interaction between a subdomain of FtsA and late septation proteins as revealed by a polar recruitment assay. J Bacteriol **186**: 7736-7744.

Corbin, B. D., Wang, Y., Beuria, T. K. and Margolin, W. (2007) Interaction between cell division proteins FtsE and FtsZ. J Bacterial **189**: 3026-3035.

Cordell, S. C. and Lowe, J. (2001) Crystal structure of the bacterial cell division regulator MinD. FEBS Lett **492**: 160-165.

Costa, T., Priyadarshini1, R. and Jacobs-Wagner, C. (2008) Localization of PBP3 in *Caulobacter crescentus* is highly dynamic and largely relies on its functional transpeptidase domain. Mol Microbiol **70**: 634-651.

D'Ulisse, V., Fagioli, M., Ghelardini, P. and Paolozzi, L. (2007) Three functional subdomains of the *Escherichia coli* FtsQ protein are involved in its interaction with the other division proteins. Microbiology **153**: 124-138.

Dai, K. and Lutkenhaus, J. (1992) The proper ratio of FtsZ to FtsA is required for cell division to occur in *Escherichia coli*. J Bacteriol **174**: 6145-6151.

Dai, K., Xu, Y. and Lutkenhaus, J. (1996) Topological characterization of the essential *Escherichia coli* cell division protein FtsN. J Bacteriol **178**: 1328-1334.

Dai, K., Y. Xu and Lutkenhaus, J. (1993) Cloning and characterization of *ftsN*, an essential cell division gene in *Escherichia coli* isolated as a multicopy suppressor of *ftsA12*(Ts). J Bacteriol **175**: 3790-3797.

Dajkovic, A., Lan, G., Sun, S. X., Wirtz, D. and Lutkenhaus, J. (2008) MinC spatially controls bacterial cytokinesis by antagonizing the scaffolding function of FtsZ. Curr Biol **18**: 235-244.

Dajkovic, A., Pichoff,S., Lutkenhaus, J. and Denis Wirtz, D. (2010) Cross-linking FtsZ polymers into coherent Z rings. Mol Microbiol **78**: 651-668.

Daniel, R. A., Harry, E. J. and Errington, J. (2000) Role of penicillin-binding protein PBP 2B in assembly and functioning of the division machinery of *Bacillus subtilis.* Mol Microbiol **35**: 299-311.

Daniel, R. A., Harry, E. J., Katis, V. L., Wake, R. G. and Errington, J. (1998) Characterization of the essential cell division gene *ftsL* (*yIID*) of *Bacillus subtilis* and its role in the assembly of the division apparatus. Mol Microbiol **29**: 593-604.

Daniel, R. A., Noirot-Gros, M. F., Noirot, P. and Errington, J. (2006) Multiple interactions between the transmembrane division proteins of *Bacillus subtilis* and the role of FtsL instability in divisome assembly. J Bacteriol **188**: 7396-404.

Datta, P., Dasgupta, A., Singh, A. K., Mukherjee, P., Kundu, M. and Basu, J. (2006) Interaction between FtsW and penicillin-binding protein 3 (PBP3) directs PBP3 to mid-cell, controls cell septation, and mediates the formation of a trimeric complex involving FtsZ, FtsW, and PBP3 in mycobacteria. Mol Microbiol **62**: 1655-1673.

Davie, E., Sydnor, K. and Rothfield, L. I. (1984) Genetic basis of minicell formation in *Escherichia coli* K-12. J Bacteriol **158**: 1202-1203.

de Boer, P. A. and Crossley, R. (1989) A division inhibitor and a topological specificity factor coded for by the minicell locus determine proper placement of the division septum in *Escherichia coli*. Cell **56**: 641-649.

de Boer, P. A., Crossley, R. and Rothfield, L. (1988) Isolation and properties of *minB*, a complex genetic locus involved in correct placement of the division site in *Escherichia coli*. J Bacteriol **170**: 2106-2112.

de Boer, P. A., Crossley, R. and Rothfield, L. (1992) Roles of MinC and MinD in the site-specific septation block mediated by the MinCDE system of *Escherichia coli*. J Bacteriol **174**: 63-70.

Dehio, C., Gray-Owen, S. D. and Meyer, T. F. (2000) Host cell invasion by pathogenic *Neisseriae*. Subcell Biochem **33**: 61-96.

Descoteaux, A. and Drapeau, G. R. (1987) Regulation of cell division in *Escherichia coli* K-12: probable interactions among proteins FtsQ, FtsA, and FtsZ. J Bacteriol **169**: 1938-1942.

Dewar, S. J., Begg, K. J. and Donachie, W. D. (1992) Inhibition of cell division initiation by an imbalance in the ratio of FtsA to FtsZ. J Bacteriol **174**: 6314-6316.

Di Lallo, G., Castagnoli, L., Ghelardini, P. and Paolozzi, L. (2001) A two-hybrid system based on chimeric operator recognition for studying protein homo/heterodimerization in *Escherichia coli*. Microbiology **147**: 1651-1656.

Di Lallo, G., Fagioli, M., Barionovi, D., Ghelardini, P. and Paolozzi, L. (2003) Use of a two-hybrid assay to study the assembly of a complex multicomponent protein machinery: bacterial septosome differentiation. Microbiology **149**: 3353-3359.

Dillard, J. P. and Seifert, H. S. (2001) A variable genetic island specific for *Neisseria gonorrhoeae* is involved in providing DNA for natural transformation and is found more often in disseminated infection isolates. Mol Microbiol **41**: 263-277.

Dillon, J. R. and Pauze M. (1981) Relationship between plasmid content and auxotype in *Neisseria gonorrhoeae* isolates. Infection and Immunity 33: 625-628.

Dillon, J. R. and Pagotto, F. (1999) Importance of drug resistance in gonococci: from mechanisms to monitoring. Curr Opin Infect Dis **12**:35-40.

Din, N., Quardokus, E.M., Sackett, M.J. and Brun, Y.V. (1998) Dominant C-terminal deletions of FtsZ that affect its ability to localize in *Caulobacter* and its interaction with FtsA. Mol Microbiol **27**: 1051-1064.

Donachie, W. (1993) The cell cycle of *Escherichia coli*. Annu Rev Microbiol **47**： 199-230.

Dorazi, R. and Dewar, S. J. (2000) Membrane topology of the N-terminus of the *Escherichia coli* FtsK division protein. FEBS Lett **478**: 13-18.

Draper, G. C. and Gober, J. W. (2002) Bacterial chromosome segregation. Annu Rev Microbiology **56**: 567-597.

Draper, G. C., McLennan, N., Begg, K., Masters, M. and Donachie, W. D. (1998) Only the N-terminal domain of FtsK functions in cell division. J Bacteriol **180**: 4621-4627.

Dresler, J., Klimentova, J. and Stulik, J. (2011) Bacterial protein complexes investigation using blue native PAGE. Microbiological Research **166**: 47-62.

Du, Y. and Arvidson, C. G. (2003) Identification of ZipA, a signal recognition particle-dependent protein from *Neisseria gonorrhoeae*. J Bacteriol **185**: 2122-2130.

Edwards, D. and Errington, J. (1997) The *Bacillus subtilis* DivIVA protein targets to the division septum and controls the site specificity of cell division. Mol Microbiol **25**: 905-915.

Elkins, C., Carbonetti, N. H., Coímbre, A. J., Thomas, C. E. and Sparling, P. F. (1994) Cloning and constitutive expression of structural genes encoding gonococcal porin protein in *Escherichia coli* and attenuated *Salmonella typhimurium* vaccine strains. Gene **138**: 43-50.

Eng, N. F., Szeto, J., Acharya, S., Tessier, D. and Dillon, J. R. (2006) The C-terminus of MinE from *Neisseria gonorrhoeae* acts as a topological specificity factor by modulating MinD activity in bacterial cell division. Res Microbiol **157**: 333-344.

Erickson, H. P. (2001) The FtsZ protofilament and attachment of ZipA-structural constraints on the FtsZ power stroke. Curr Opin Cell Biol **13**: 55-60.

Errington, J., Bath, J. and Wu, L. J. (2001) DNA transport in bacteria. Nat Rev Mol Cell Biol **2**: 538-545.

Errington, J., Daniel, R. A. and Scheffers, D. J. (2003) Cytokinesis in bacteria. Microbiol Mol Biol Rev **67**: 52-65.

Feucht, A., Lucet, I., Yudkin, M. D. and Errington, J. (2001) Cytological and biochemical characterization of the FtsA cell division protein of *Bacillus subtilis*. Mol Microbiol **40**: 115-125.

Figge, R. M., Easter, J. and Gober, J. W. (2003) Productive interaction between the chromosome partitioning proteins, ParA and ParB, is required for the progression of the cell cycle in *Caulobacter crescentus*. Mol Microbiol **47**: 1225-1237.

Fitz-James, P. (1964) Thin sections of dividing *Neisseria gonorrhoeae*. J Bacteriol **87:** 1477-1482.

Fleischmann, R. D., Adams, M. D., White, O., Clayton, R. A., Kirkness, E. F. and Kerlavage, A. R. (1995) Whole-Genome random sequencing and assembly of Haemophilus influenzae Rd. Science **269**: 496-512.

Francis, F., Ramirez-Arcos, S., Salimnia, H., Victor, C. and Dillon, J. R. (2000) Organization and transcription of the division cell wall (*dcw*) cluster in *Neisseria gonorrhoeae*. Gene **251**: 141-151.

Fussenegger, M., Kahrs, A. F., Facius, D. and Meyer, T. F. (1996) Tetrapac (*tpc*), a novel genotype of *Neisseria gonorrhoeae* affecting epithelial cell invasion, matural transformation competence and cell separation. Mol Microbiol **19**: 1357-1372.

Gamba, P., Veening, J., Saunders, N. J., Hamoen, L. W. and Daniel, R. A. (2009) Two-step assembly dynamics of the *Bacillus subtilis* divisome. J Bacteriol **191**: 4186-4194.

Geissler, B., Elraheb, D. and Margolin, W. (2003) A gain-of-function mutation in *ftsA* bypasses the requirement for the essential cell division gene *zipA* in *Escherichia coli*. Proc Natl Acad Sci USA **100**: 4197-4202.

Geissler, B., Shiomi, D. and Margolin, W. (2007) The *ftsA** gain-of-function allele of *Escherichia coli* and its effects on the stability and dynamics of the Z ring. Microbiology **153**: 814-825.

Gerding, M. A., Liu, B., Bendezu, F. O., Hale, C. A., Bernhardt, T. G. and de Boer. P. A. (2009) Self-enhanced accumulation of FtsN at division sites, and roles for other proteins with a SPOR domain (DamX, DedD, and RlpA) in *Escherichia coli* cell constriction. J Bacteriol **191**: 7383-7401.

Goehring, N. W., Gonzalez, M. D. and Beckwith, J. (2006) Premature targeting of cell division proteins to midcell reveals hierarchies of protein interactions involved in divisome assembly. Mol Microbiol **61**: 33-45.

Goehring, N. W., Petrovska, I., Boyd, D. and Beckwith, J. (2007) Mutants, suppressors, and wrinkled colonies: mutant alleles of the cell division gene *ftsQ* point to functional domains in FtsQ and a role for domain 1C of FtsA in divisome assembly. J Bacteriol **189**: 633-645.

Goehring, N.W., Gueiros-Filho, F. and Beckwith, J. (2005) Premature targeting of a cell division protein to midcell allows dissection of divisome assembly in *Escherichia coli*. Genes Dev **19**: 127-137.

Gonzalez, M. D., Akbay, E. A., Boyd, D. and Beckwith, J. (2010) Multiple interaction domains in FtsL, a protein component of the widely conserved bacterial FtsLBQ cell division complex. J Bacteriol **192**: 2757-2768.

Gonzalez, M. D. and Beckwith, J. (2009) Divisome under construction: distinct domains of the small membrane protein FtsB are necessary for interaction with multiple cell division proteins. J Bacteriol **191**: 2815-25.

Goodman, S. D. and Scocca, J. J. (1988) Identification and arrangement of the DNA sequences recognized in specific transformation of *Neisseria gonorrhoeae*. Proc Natl Acad Sci USA **85**: 6982-6986.

Greco-Stewart, V., Ramirez-Arcos, S., Liao, M. and Dillon, J. R. (2007) N terminus determinants of MinC from *Neisseria gonorrhoeae* mediate interaction with FtsZ but do not affect interaction with MinD or homodimerization. Arch Microbiol **187**: 451-458.

Gregory, J. A., Becker, E. C. and Pogliano, K. (2008) *Bacillus subtilis* MinC destabilizes FtsZ-rings at new cell poles and contributes to the timing of cell division. Genes and Develop **22**: 3475-3488.

Grenga, L., Luzi, G., Paolozzi, L. and Ghelardini, P. (2008) The *Escherichia coli* FtsK functional domains involved in its interaction with its divisome protein partners. FEMS Microbiol Lett **287**: 163-167.

Gueiros-Filho. J. and Losick, R. (2002) A widely conserved bacterial cell division protein that promotes assembly of the tubulin-like protein FtsZ. Genes Dev **16**: 2544-2556.

Guzman, L. M., Barondess, J. J. and Beckwith, J. (1992) FtsL, an essential cytoplasmic membrane protein involved in cell division in *Escherichia coli*. J Bacteriol **174**: 7716-28.

Guzman, L. M., Weiss, D. S. and Beckwith, J. (1997) Domain-swapping analysis of FtsI, FtsL, and FtsQ, bitopic membrane proteins essential for cell division in *Escherichia coli.* J Bacteriol **179**: 5094-5103.

Haeusser, D. P., Schwartz, R. L., Smith, A. M., Oates, M. E. and Levin, P. A. (2004) EzrA prevents aberrant cell division by modulating assembly of the cytoskeletal protein FtsZ. Mol Microbiol **52**: 801-814.

Hale, C. A. and de Boer, P. A. (1997) Direct binding of FtsZ to ZipA, an essential component of the septal ring structure that mediates cell division in *Escherichia coli*. Cell **88**: 175-185.

Hale, C. and de Boer, P. (1999) Recruitment of ZipA to the septal ring of *Escherichia coli* is dependent on FtsZ and independent of FtsA. J Bacteriol **181:** 167-176.

Hale, C. A. and de Boer, P. A. (2002) ZipA is required for recruitment of FtsK, FtsQ, FtsL, and FtsN to the septal ring in *Escherichia coli*. J Bacteriol **184**: 2552-2556.

Hale, C. A., Rhee, A. C. and de Boer, P. A. (2000) ZipA-induced bundling of FtsZ polymers mediated by an interaction between C-terminal domains. J Bacteriol **182**: 5153-5166.

Haney, S. A., Glasfeld, E., Hale, C. A., Keeney, D., He, Z. and de Boer, P. A. (2001) Genetic analysis of the *Escherichia coli* FtsZ-ZipA interaction in the yeast two-hybrid system: Characterization of FtsZ residues essential for the interactions with ZipA and with FtsA. J Biol Chem **276**:11980-11987.

Hebeler, B. H. and Young, F. E. (1976) Chemical composition and turnover of peptidoglycan in *Neisseria gonorrhoeae*. J Bacterial **126**: 1180-1185.

Henriques, A. O., Glaser, P. and Piggot, P. J. M. C. P. Jr. (1998) Control of cell shape and elongation by the *rodA* gene in *Bacillus subtilis*. Mol Microbiol **28**: 235-247.

Howard, B. J. (1994) *Neisseria*. In *Clinical and Pathogenic Microbiology*. Howard B.J., Klass, J., Rubin, S.J., Weissfeld, A.S. and Tilton, R.C. (ed.). The C.V. Mosby Company.

Hu, Z. and Lutkenhaus, J. (2001) Topological regulation of cell division in *E. coli*: spatiotemporal oscillation of MinD requires stimulation of its ATPase by MinE and phospholipid. Mol Cell **7**: 1337-1343.

Hu, Z. and Lutkenhaus, J. (2003) A conserved sequence at the C-terminus of MinD is required for binding to the membrane and targeting MinC to the septum. Mol Microbiol **47**: 345-355.

Hu, Z., Mukherjee, A., Pichoff, S. and Lutkenhaus, J. (1999) The MinC component of the division site selection system in *Escherichia coli* interacts with FtsZ to prevent polymerization. Proc Natl Acad Sci USA **96**: 14819-14824.

Hu, Z., Saez, C. and Lutkenhaus, J. (2003) Recruitment of MinC, an inhibitor of Z-ring formation, to the membrane in *Escherichia coli*: Role of MinD and MinE. J Bacteriol **185**: 196-203.

Ikeda, M., Sato, T., Wachi, M., Jung, H. K., Ishino, F. and Kobayashi, Y. (1989) Structural similarity among *Escherichia coli* FtsW and RodA proteins and *Bacillus*

subtilis SpoVE protein, which function in cell division, cell elongation, and spore formation, respectively. J Bacteriol **171**: 6375-6378.

Jensen, R. B. (2006) Coordination between chromosome replication, segregation, and cell division in *Caulobacter crescentus*. J Bacteriol **188**: 2244-2253.

Jensen, R. B., Wang, S. C. and Shapiro, L. (2002) Dynamic localization of proteins and DNA during a bacterial cell cycle. Nat Rev Mol Cell Biol **3**: 167-176.

Jensen, S. O., Thompson, L. S. and Harry, E. J. (2005) Cell division in *Bacillus subtilis:* FtsZ and FtsA association is Z-ring independent, and FtsA is required for efficient midcell Z-ring assembly. J Bacteriol **187**: 6536-6544.

Johnson, J. E., Lackner, L. L. and de Boer, P. A. (2002) Targeting of (D)MinC/MinD and (D)MinC/DicB complexes to septal rings in *Escherichia coli* suggests a multistep mechanism for MinC-mediated destruction of nascent FtsZ rings. J Bacteriol **184**: 2951-2962.

Johnson, J. E., Lackner, L. L., Hale, C. A. and de Boer, P. A. (2004) ZipA is required for targeting of (D)MinC/DicB, but not (D)MinC/MinD, complexes to septal ring assemblies in *Escherichia coli*. J Bacteriol **186**: 2418-2429.

Jordan, P. W., Snyder, L. A. S. and Saunders, N. J. (2005) Strain-specific difference in *Nersseriia gonorrhoeae* associated with the phase variable gene repertoire. BMC Microbiology **5**: 21-32.

Karimova, G., Dautin, N. and Ladant, D. (2005) Interaction network among *Escherichia coli* membrane proteins involved in cell division as revealed by bacterial two-hybrid analysis. J Bacteriol **187**: 2233-2243.

Katis, V. L., Wake, R. G. and Harry, E. J. (2000) Septal localization of the membrane-bound division proteins of *Bacillus subtilis* DivIB and DivIC is codependent only at high temperatures and requires FtsZ. J Bacteriol **182**: 3607-3611.

Kellogg, Jr. D. S., Peacock, Jr., Deacon, W. F., Brown, L. and Pirkle, C. I. (1963) *Neisseria gonorrhoeae* I. Virulence genetically linked to clonal variation. J Bacteriol **85:** 1274-1279.

Kelly, A. J., Sackett, M. J., Din, N., Quardokus, E. M. and Brun, Y. V. (1998) Cell cycle-dependent transcriptional and proteolytic regulation of FtsZ in *Caulobacter*. Genes Dev **12**: 880-893.

Kerle, K. K., Mascola, J. R. and Miller, T. A. (1992) Disseminated gonococcal infection. Am Fam Physician **45**: 209-214.

Knapp, J. S. and Holmes, K. K. (1975) Disseminated gonococcal infections caused by *Neisseria gonorrhoeae* with unique nutritional requirements. J Infect Dis **132**: 204-208.

Krause, F. (2006) Detection and analysis of protein–protein interactions in organellar and prokaryotic proteomes by native gel electrophoresis: (membrane) protein complexes and supercomplexes. Electrophoresis **27**: 2759-2781.

Lackner, L. L., Raskin, D. M. and de Boer, P. A. (2003) ATP-dependent interactions between *Escherichia coli* Min proteins and the phospholipid membrane *in vitro*. J Bacteriol **185**: 735-749.

Lan, G., Dajkovic, A., Wirtz, D. and Sun, S. X. (2008) Polymerization and bundling kinetics of FtsZ filaments. Biophys J **95**: 4045-56.

Lan, G., Daniels, B. R., Dobrowsky, T. M., Wirtz, D. and Sun, S. X. (2009) Condensation of FtsZ filaments can drive bacterial cell division. Proc Natl Acad Sci USA **106**: 121-126.

Lappchen, T., Harton, A. F., Pinas, V. A., Koomen, G. and den Balluwen, T. (2005) GTP analogue inhibits polymerization and GTPase activity of the bacterial protein FtsZ without affecting its eukaryotic Homologue Tubulin. Bichemistry **44**: 7879-7884.

Lara, B., Rico, A. I., Petruzzelli, S., Santona, A., Dumas, J. and Biton, J. (2005) Cell division in cocci: localization and properties of the *Streptococcus pneumoniae* FtsA protein. Mol Microbiol **55**: 699-711.

Levin, P. A., Kurtser, I. G. and Grossman, A. D. (1999) Identification and characterization of a negative regulator of FtsZ ring formation in *Bacillus subtilis*. Proc Natl Acad Sci USA **96**: 9642-9647.

Li, Z., Trimble, M. J., Brun, Y. V. and Jensen, G. J. (2007) The structure of FtsZ filaments *in vivo* suggests a force-generating role in cell division. EMBO J **26**: 4694-708.

Liu, G., Draper, G. C. and Donachie, W. D. (1998) FtsK is a bifunctional protein involved in cell division and chromosome localization in *Escherichia coli*. Mol Microbiol **29**: 893-903.

Low, H.H., Moncrieffe, M.C. and Lowe, J. (2004) The crystal structure of ZapA and its modulation of FtsZ polymerisation. J Mol Biol **341**: 839-852.

Löwe, J. and Amos, L. (1998) Crystal structure of the bacterial cell-division protein FtsZ. Nature **391**: 203-206.

Löwe, J. and Amos, L. A. (1999) Tubulin-like protofilaments in Ca^{2+}-induced FtsZ sheets. EMBO J **18**: 2364-71.

Lu, C., Reedy, M. and Erickson, H. P. (2000) Straight and curved conformations of FtsZ are regulated by GTP hydrolysis. J Bacteriol **182**: 164-70.

Lutkenhaus, J. and Addinall, S. G. (1997) Bacterial cell division and the Z ring. Annu Rev Biochem **66**: 93-116.

Ma, L. Y., King, G. F. and Rothfield, L. (2004) Positioning of the MinE binding site on the MinD surface suggests a plausible mechanism for activation of the *Escherichia coli* MinD ATPase during division site selection. Mol Microbiol **54**: 99-108.

Ma, X. and Margolin, W. (1999) Genetic and functional analyses of the conserved C-terminal core domain of *Escherichia coli* FtsZ. J Bacteriol **181**: 7531-7544.

Ma, X., Ehrhardt, D. and Margolin, W. (1996) Colocalization of cell division proteins FtsZ and FtsA to cytoskeletal structures in living *Escherichia coli* cells by using green fluorescent protein. Proc Natl Acad Sci USA **93**: 12998-13003.

Ma, X., Sun, Q., Wang, R., Singh, G., Jonietz, E. L. and Margolin, W. (1997) Interactions between heterologous FtsA and FtsZ proteins at the FtsZ ring. J Bacteriol **179:** 6788-6797.

Maggi, S., Massidda, O., Luzi, G., Fadda, D., Paolozzi, L. and Ghelardini, P. (2008) Division protein interaction web: identification of a phylogenetically conserved common interactome between *Streptococcus pneumoniae* and *Escherichia coli*. Microbiology **154**: 3042-3052.

Marczynski, G.T. (1999) Chromosome methylation and measurement of faithful, once and only once per cell cycle chromosome replication in *Caulobacter crescentus*. J Bacteriol **181**: 1984-1993.

Margalit, D. N., Romberg, L., Mets, R. B., Hebert, A. M., Mitchison, T. J., Kirschner, M. W. and RayChaudhuri, D. (2004) Targeting cell division: Small-molecule inhibitors of FtsZ GTPase perturb cytokinetic ring assembly and induce bacterial lethality, Proc Natl Acad Sci USA **101**: 11821-11826.

Margolin, W. (2005) FtsZ and the division of prokaryotic cells and organelles. Nat Rev Mol Cell Biol **6**: 862-871.

Martin, M. E., Trimble, M. J. and Brun, Y. V. (2004) Cell cycle-dependent abundance, stability and localization of FtsA and FtsQ in *Caulobacter crescentus*. Mol Microbiol **54**: 60-74.

Massidda, O., Anderluzzi, D., Friedli, L. and Feger, G. (1998) Unconventional organization of the division and cell wall gene cluster of *Stretococcus pneumoniae*. Microbiology **144**: 3069-3078.

Matsuhashi, M., Wachi, M. and Ishino, F. (1990) Machinery for cell growth and division: penicillin-binding proteins and other proteins. Res Microbiol **141**: 89-103.

Meitzner, T. A. and Cohen, M. S. (1997) Vaccines against gonococcal infection. In New Generation Vaccines Marcel Dekker, Inc., New York; 817-842.

Mengin-Lecreulx, D., Ayala, J., Bouhss, A., van Heijenoort, J., Parquet, C. and Hara, H. (1998) Contribution of the P_{mra} promoter to expression of genes in the *Escherichia coli mra* cluster of cell envelope biosynthesis and cell division genes. J Bacteriol **180**: 4406-4412.

Mercer, K. L. and Weiss, D. S. (2002) The *Escherichia coli* cell division protein FtsW is required to recruit its cognate transpeptidase, FtsI (PBP3), to the division site. J Bacteriol **184**: 904-912.

Merz, A. J. and So, M. (2000) Interactions of pathogenic *Neisseriae* with epithelial cell membranes. Annu Rev Cell Dev Biol **16**: 423-457.

Miller, J. H. (1972) Assay of β-galactosidase. In *Experiments in Molecular Genetics*. Miller, J. H. (ed.) New York: Cold Spring Harbor Laboratory, Cold Spring Harbor, pp. 352-355.

Mingorance, J., Rivas, G., Velez, M., Gomez-Puertas, P. and Vicente, M. (2010) Strong FtsZ is with the force: mechanisms to constrict bacteria. Trends in Microbiology **18**: 348-356.

Mingorance, J., Tamames, J. and Vicente, M. (2004) Genomic channeling in bacterial cell division. J Mol Recognit **17**: 481-487.

Miroux, B. and Walker, J. E. (1996) Over-production of proteins in *Escherichia coli*: mutant hosts that allow synthesis of some membrane proteins and globular proteins at high levels. J Mol Biol **260:** 289-298.

Mosyak, L., Zhang, Y., Glasfeld, E., Haney, S., Stahl, M., Seehra, J. and Somers, W. S. (2000) The bacterial cell-division protein ZipA and its interaction with an FtsZ fragment revealed by X-ray crystallography. EMBO J **19**: 3179-3191.

Moy, F. J., Glasfeld, E., Mosyak, L. and Powers, R. (2000) Solution structure of ZipA, a crucial component of *Escherichia coli* cell division. Biochemistry **39**: 9146-9156.

Mukherjee, A. and Lutkenhaus, J. (1994) Guanine nucleotide-dependent assembly of FtsZ into filaments. J Bacteriol **176**: 2754-8.

Mukherjee, A. and Lutkenhaus, J. (1998) Dynamic assembly of FtsZ regulated by GTP hydrolysis. EMBO J **17**: 462-469.

Mukherjee, A. and Lutkenhaus, J. (1998) Purification, assembly, and localization of FtsZ. Methods Enzymol **298**: 296-305.

Mukherjee, A., Saez, C. and Lutkenhaus, J. (2001) Assembly of an FtsZ mutant deficient in GTPase activity has implications for FtsZ assembly and the role of the Z ring in cell division. J Bacteriol **183**: 7190-7197.

Nanninga, N. (1998) Morphogenesis of *Escherichia coli*. Microbiol Mol Biol Rev **62:** 110-129.

Nguyen-Disteche, M., Fraipont, C., Buddelmeijer, N. and Nanninga, N. (1998) The structure and function of *Escherichia coli* penicillin-binding protein 3. Cell Mol Life Sci **54**: 309-316.

Noble, R. C., Reyes, R. R., Parekh, M. C. and Haley, J. V. (1984) Incidence of disseminated gonococcal infection correlated with the presence of AHU auxotype of *Neisseria gonorrhoeae* in a community. Sex Transm Dis **11**: 68-71.

Noirclerc-Savoye, M., Le Gouëllec, A., Morlot, C., Dideberg, O., Vernet, T. and Zapun, A. (2005) *In vitro* reconstitution of a trimeric complex of DivIB, DivIC and FtsL, and their transient co-localization at the division site in *Streptococcus pneumoniae*. Mol Microbiol **55**: 413-424.

Ohashi, T., Hale, C. A., de Boer, P. A. and Erickson, H. P. (2002) Structural evidence that the P/Q domain of ZipA is an unstructured, flexible tether between the membrane and the C-terminal FtsZ-binding domain. J Bacteriol **184**: 4313-4315.

Ohta, N., Ninfa, A., Allaire, N., Kulick, L. and Newton, A. (1997) Identification, characterization, and chromosomal organization of cell division cycle genes in *Caulobacter crescentus*. J Bacteriol **179**: 2169-2180.

Osawa, M., Anderson, D. E. and Erickson, H. P. (2008) Reconstitution of contractile FtsZ rings in liposomes. Science **320**: 792-794.

Pagotto, F., Salimnia, H., Totten, P. A. and Dillon, J. R. (2000) Development of a stable shuttle vector for *Neisseria gonorrhoeae, Haemophilus sp.* and other bacteria. Gene **244:** 13-19.

Paradis-Bleau, C., Beaumont, M., Sanschagrin, F., Voyer, N. and Levesque, R. C. (2007) Parallel solid synthesis of inhibitors of the essential cell division FtsZ enzyme as a new potential class of antibacterials. Bioorganic and Medicinal Chemistry. **15**: 1330-1340.

Patrick, J. E. and Kearns, D. B. (2008) MinJ (YvjD) is a topological determinant of cell division in *Bacillus subtilis*. Mol Microbiol **70**: 1166-1179.

Pease, P. J., Levy, O., Cost, G. J., Gore, J., Ptacin, J. L. and Sherratt, D. (2005) Sequence-directed DNA translocation by purified FtsK. Science **307**: 586-590.

Picard, F. J. and Dillon, J. R. (1989) Biochemical and genetic studies with arginine and proline auxotypes of *Neisseria gonorrhoeae*. Can J Microbiol **35:** 1069-1075.

Pichoff, S. and Lutkenhaus, J. (2002) Unique and overlapping roles for ZipA and FtsA in septal ring assembly in *Escherichia coli*. EMBO J **21**: 685-693.

Pichoff, S. and Lutkenhaus, J. (2005) Tethering the Z ring to the membrane through a conserved membrane targeting sequence in FtsA. Mol Microbiol **55**: 1722-1734.

Pichoff, S. and Lutkenhaus, J. (2007) Identification of a region of FtsA required for interaction with FtsZ. Mol Microbiol **64**: 1129-1138.

Piette, A., Fraipont, C., Den Blaauwen, T., Aarsman, M. E., Pastoret, S. and Nguyen-Distèche, M. (2004) Structural determinants required to target penicillin-binding protein 3 to the septum of *Escherichia coli*. J Bacteriol **186**: 6110-6117.

Pogliano, J., Pogliano, K., Weiss, D. S., Losick, R. and Beckwith, J. (1997) Inactivation of FtsI inhibits constriction of the FtsZ cytokinetic ring and delays the assembly of FtsZ rings at potential division sites. Proc Natl Acad Sci USA **94**: 559-564.

Public Health Agency of Canada (PHAC). (2009) Gonorrhoea resurgence in Canada. http://www.phac-aspc.gc.ca/std-mts/gono-eng.php

Quardokus, E. M., Din, N. and Brun, Y. V. (2001) Cell cycle and positional constraints on FtsZ localization and the initiation of cell division in *Caulobacter crescentus*. Mol Microbiol **39**: 949-959.

Quardokus, E., Din, N. and Brun, Y. V. (1996) Cell cycle regulation and cell type-specific localization of the FtsZ division initiation protein in *Caulobacter*. Proc Natl Acad Sci USA **93**: 6314-6319.

Ramirez-Arcos, S., Liao, M., Marthaler, S., Rigden, M. and Dillon, J. R. (2005) *Enterococcus faecalis divIVA*: an essential gene involved in cell division, cell growth and chromosome segregation. Microbiology **151**: 1381-1393.

Ramirez-Arcos, S., Salimnia, H., Bergevin, I., Paradisa, M. and Dillon, J. R. (2001a) Expression of *Neisseria gonorrhoeae* cell division genes *ftsZ*, *ftsE* and *minD* is influenced by environmental conditions. Res Microbiol **152**: 781-791.

Ramirez-Arcos, S., Szeto, J., Beveridge, T. J., Victor, C., Francis, F. and Dillon, J. R. (2001b) Deletion of the cell division inhibitor MinC results in lysis of *Neisseria gonorrhoeae*. Microbiology **147**: 225-237.

Ramirez-Arcos, S., Szeto, J., Dillon, J. R. and Margolin, W. (2002) Conservation of dynamic localization among MinD and MinE orthologs: oscillation of *Neisseria gonorrhoeae* proteins in *Esherichia coli*. Mol Microbiol **46**: 493-504.

Raskin, D. M. and de Boer, P. A. (1999) MinDE-dependent pole-to-pole oscillation of division inhibitor MinC in *Escherichia coli*. J Bacteriol **181**: 6419-6424.

RayChaudhuri, D. (1999) ZipA is a MAP-Tau homolog and is essential for structural integrity of the cytokinetic FtsZ ring during bacterial cell division. EMBO J **18**: 2372-2383.

Real, G. and Henriques, A. O. (2006) Localization of the *Bacillus subtilis murB* gene within the *dcw* cluster is important for growth and sporulation. J Bacteriol **188**: 1721-1732.

Rico, A. I., García-Ovalle, M., Palacios, P., Casanova, M. and Vicente, M. (2010) Role of *Escherichia coli* FtsN protein in the assembly and stability of the cell division ring. Mol Microbiol **76**: 760-771.

Rico, A. I., Marta, G., Mingorance, J. and Vicente, M. (2004) Role of two essential domains of *Escherichia coli* FtsA in localization and progression of the division ring. Mol Microbiol **53**: 1359-1371.

Robichon, C., King, G. F., Goehring, N. W. and Beckwith, J. (2008) Artificial septal targeting of *Bacillus subtilis* cell division proteins in *Escherichia coli*: an interspecies approach to the study of protein-protein interactions in multiprotein complexes. J Bacteriol **190**: 6048-6059.

Robinson, A. C., Begg, K. J. and Donachie, W. D. (1988) Mapping and characterization of mutants of the *Escherichia coli* cell division gene, *ftsA*. Mol Microbiol **2**: 581-588.

Roe, B. A., Lin, S. P., Song, L., Yuan, X., Clifton, S., Ducey, T. *et al.* (2000) Gonococcal Genome Sequencing Project (Funded by USPHS/ NIH grant # AI 38399). University of Oklahoma.

Rowland, S. L., Fu, X., Sayed, M. A., Zhang, Y., Cook, W. R. and Rothfield, L. I. (2000) Membrane redistribution of the *Escherichia coli* MinD protein induced by MinE. J Bacteriol **182**: 613-619.

Rueda, S., Vicente, M. and Mingorance, J. (2003) Concentration and assembly of the division ring proteins FtsZ, FtsA, and ZipA during the *Escherichia coli* cell cycle. J Bacteriol **185**: 3344-3351.

Ryan, K. R. and Shapiro, L. (2003) Temporal and spatial regulation in prokaryotic cell cycle progression and development. Annu Rev Biochem **72**: 367-394.

Sackett, M. J., Kelly, A. J. and Brun, Y. V. (1998) Ordered expression of *ftsQA* and *ftsZ* during the *Caulobacter crescentus* cell cycle. Mol Microbiol **28**: 421-434.

Salimnia, H., Radia, A., Bernatchez, S. and Dillon, J. R. (2000) Characterization of the *ftsZ* cell division gene of *Neisseria gonorrhoeae*: expression and localization in *Esherichia coli* and *N. gonorrhoeae*. Arch Microbiol **173**: 10-20.

Sambrook, J., Fritsch, E. F. and Maniatis, T. (1989) *Molecular Cloning, 2nd edition. A Laboratory Manual.* Cold Spring Harbour, New York: Cold Spring Harbour Press.

Sambrook, J. and Russell D.W. (2001) *Molecular cloning: a laboratory manual*. Cold Spring Harbour, New York: Cold Spring Harbour Laboratory Press.

Sanchez, M., Valencia, A., Ferrandiz, M., Sander, C. and Vicente, M. (1994) Correlation between the structure and biochemical activities of FtsA, an essential cell division protein of the actin family. EMBO J **13**: 4919-4925.

Schagger, H., Cramer, W. A. and von Jajow, G. (1994) Analysis of molecular masses and oligomeric states of protein complexes by blue native electrophoresis and isolation of membrane protein complexes by two-dimensional native electrophoresis. Anal Biochem **217**: 220-230.

Schagger, H. and von Jagow, G. (1991) Blue native electrophoresis for isolation of membrane protein complexes in enzymatically active form. Anal Biochem **199**: 223-231.

Scheffers, D. J. (2008) The effect of MinC on FtsZ polymerization is pH dependent and can be counteracted by ZapA. FEBS Lett **582**: 2601-2608.

Scheffers, D. J., Robichon, C., Haan, G. J., den Blaauwen, T., Koningstein, G., van Bloois, E., Beckwith, J. and Luirink, J. (2007) Contribution of the FtsQ transmembrane segment to localization to the cell division site. J Bacteriol **189**: 7273-7280.

Selinger, D. W., Saxena, R. M., Cheung, K. J., Church, G. M. and Rosenow, C. (2003) Global RNA half-life analysis in *Escherichia coli* reveals positional patterns of transcript degradation. Genome Res **13**: 216-223.

Shen, B. and Lutkenhaus, J. (2009) The conserved C-terminal tail of FtsZ is required for the septal localization and division inhibitory activity of MinC(C)/MinD. Mol Microbiol **72**: 410-424.

Shih, Y. L., Le, T. and Rothfield, L. (2003) Division site selection in *Escherichia coli* involves dynamic redistribution of Min proteins within coiled structures that extend between the two cell poles. Proc Natl Acad Sci USA **100**: 7865-7870.

Shiomi, D. and Margolin, W. (2007a) The C-terminal domain of MinC inhibits assembly of the Z ring in *Escherichia coli*. J Bacteriol **189**: 236-243.

Shiomi, D. and Margolin, W. (2007b) Dimerization or oligomerization of the actin-like FtsA protein enhances the integrity of the cytokinetic Z ring. Mol Microbiol **66**: 1396-1415.

Skerker, J. M. and Laub, M. T. (2004) Cell-cycle progression and the generation of asymmetry in *Caulobacter crescentus*. Nat Rev Microbiol **2**: 325-337.

Small, E., Marrington, R., Rodger, A., Scott, D.J., Sloan, K., Roper, D., *et al.* (2007) FtsZ polymer-bundling by the *Escherichia coli* ZapA orthologue, YgfE, involves a conformational change in bound GTP. J Mol Biol **369**: 210-221.

Snapper, C. M., Rosas, F. R., Kehry, M. R., Mond, J. J. and Wetzler, L. M. (1997) Neisserial porins may provide critical second signals to polysaccharide-activated murine B cells for induction of immunoglobulin secretion. Infect Immun **65**: 3203-3208.

Snyder, L. A. S., Saunders, N. J. and Shafer, W. M. (2001) A putatively phase variable gene (*dca*) required for natural competence in *Neisseria gonorrhoeae* but not *Neisseria meningitidis* is located within the division cell wall (*dcw*) gene cluster. J Bacteriol **183**: 1233-1241.

Snyder, L. A. S., Shafer, M. W. and Saunders, N. J. (2003) Divergence and transcriptional analysis of the division cell wall (*dcw*) gene cluster in *Neisseria* spp. Mol Microbiol **47**: 431-441.

Snyder, L. A., Davies, J. K. and Saunders, N. J. (2004) Microarray genomotyping of key experimental strains of *Neisseria gonorrhoeae* reveals gene complement diversity and five new neisserial genes associated with Minimal Mobile Elements. BMC Genomics **5**: 23.

Sparling, P. F. (1999) Biology of *Neisseria gonorrhoeae*. In *Sexually transmitted diseases*. Holmes, K. K., Mardh, P. A., Sparling, P. F., Lemon, S. M., Stamm, W. E., and Piot, P. (ed.) New York: McGraw-Hill, pp. 433-449.

Stricker, J., Maddox, P., Salmon, E. D. and Erickson, H. P. (2002) Rapid assembly dynamics of the *Escherichia coli* FtsZ-ring demonstrated by fluorescence recovery after photobleaching. Proc Natl Acad Sci USA **99**: 3171-3175.

Sun, Q. and Margolin, W. (2001) Influence of the nucleoid on placement of FtsZ and MinE rings in *Escherichia coli*. J Bacteriol **183**: 1413-1422.

Szeto, J. (2004) Splitting heirs: A study of the cell division site determinant MinD from the coccus *Neisseria gonorrhoeae*. Ottawa, Ontario: University of Ottawa, Ph.D. thesis.

Szeto, J., Acharya, S., Eng, N. F. and Dillon, J. R. (2004) The N terminus of MinD contains determinants which affect its dynamic localization and enzymatic activity. J Bacteriol **186**: 7175-7185.

Szeto, J., Eng, N. F., Acharya, S., Rigden, M. D. and Dillon, J. R. (2005) A conserved polar region in the cell division site determinant MinD is required for responding to MinE-induced oscillation but not for localization within coiled arrays. Res Microbiol **156**: 17-29.

Szeto, J., Ramirez-Arcos, S., Raymond, C., Hicks, L. D., Kay, C. M. and Dillon, J. R. (2001) Gonococcal MinD affects cell division in *Neisseria gonorrhoeae* and *Escherichia coli* and exhibits a novel self-interaction. J Bacteriol **183**: 6253-6264.

Tamames, J., Gonzalez-Moreno, M., Mingorance, J., Valencia, A. and Vicente, M. (2001) Bringing gene order into bacterial shape. Trends Genet **17**: 124-126.

Tapsall, J. W. (2009) *Neisseria gonorrhoeae* and emerging resistance to extended spectrum cephalosporins. Curr Opin Infect Dis **22**:87-91.

Tapsall, J. W., Phillips, E. A., Shultz, T. R., Way, B. and Withnall, K. (1992) Strain characteristics and antibiotic susceptibility of isolates of *Neisseria gonorrhoeae* causing disseminated gonococcal infection in Australia. Members of the Australian Gonococcal Surveillance Programme. Int J STD AIDS 1992, **3**: 273-277.

Thanbichler, M. and Shapiro, L. (2006) MipZ, a spatial regulator coordinating chromosome segregation with cell division in *Caulobacter*. Cell **126**: 147-162.

Ursinus, A., van den Ent, F., Brechtel, S., de Pedro, M., Holtje, J. V., Löwe, J. and Vollmer, W. (2004) Murein (peptidoglycan) binding property of the essential cell division protein FtsN from *Escherichia coli*. J Bacteriol **186**: 6728-6737.

van Baarle, S. and Bramkamp, M. (2010) The MinCDJ system in *Bacillus subtilis* prevents minicell formation by promoting divisome disassembly. Plos One **5**: 9850-9862.

van den Ent, F. and Löwe, J. (2000) Crystal structure of the cell division protein FtsA from *Thermotoga maritima*. EMBO J **19**: 5300-5307.

van den Ent, F., Vinkenvleugel, T. M., Ind, A., West, P., Veprintsev, D., Nanninga, N., den Blaauwen, T. and Löwe, J. (2008) Structural and mutational analysis of the cell division protein FtsQ. Mol Microbiol **68**: 110-123.

Vaughan, S., Wickstead, B., Gull, K. and Addinall, S. G. (2004) Molecular evolution of FtsZ protein sequences encoded within the genomes of archaea, bacteria, and eukaryota. J Mol Evol **58**: 19-29.

Vicente, M. and Errington, J. (1996) Structure, function and controls in microbial division. Mol Microbiol **20**: 1-7.

Vicente, M., Gomez, M. and Ayala, J. (1998) Regulation of transcription of cell division genes in the *Escherichia coli dcw* cluster. Cell Mol Life Sci **54**: 317-324.

Vicente, M., Rico, A. I., Martinez-Arteaga, R. and Mingorance, J. (2006) Septum enlightenment: Assembly of bacterial division proteins. J Bacteriol **188**: 19-27.

Wang, H. C. and Gayda, R. C. (1990) High-level expression of the FtsA protein inhibits cell septation in *Escherichia coli* K-12. J Bacteriol **172**: 4736-4740.

Wang, H., and Gayda, R. C. (1992) Quantitative determination of FtsA at different growth rates in *Escherichia coli* using monoclonal antibodies. Mol Microbiol **6**: 2517-2524.

Wang, J., Galgoci, A., Kodali, S., Herath, K. B., Jayasuriya, H., Dorso, K., Vicente, F., Gonza´lez, A., Cully, D., Bramhill, D. and Singh, S. (2003) Discovery of a small molecule that inhibits cell division by blocking FtsZ, a novel therapeutic target of antibiotics, J Biol Chem **278**: 44424-44428.

Wang, L. and Lutkenhaus, J. (1998) FtsK is an essential cell division protein that is localized to the septum and induced as part of the SOS response. Mol Microbiol **29**: 731-40.

Wang, L., Khattar, M. K., Donachie, W. D. and Lutkenhaus, J. (1998) FtsI and FtsW are localized to the septum in *Escherichia coli*. J Bacteriol **180**: 2810-2816.

Wang, S. C. E., West. L. and Shapiro, L. (2006) The bifunctional Ftsk protein mediates chromosome partitioning and cell division in *Caulobacter*. J Bacterial **188**: 1497-1508.

Wang, X. D., Huang, J. A., Mukherjee, A., Cao, C. and Lutkenhaus, J. (1997) Analysis of the interaction of FtsZ with itself, GTP, and FtsA. J Bacteriol **179**: 5551-5559.

Wang, X. and Lutkenhaus, J. (1993) The FtsZ protein of *Bacillus subtilis* is localized at the division site and has GTPase activity that is dependent upon FtsZ concentration. EMBO J **10**: 3363-3372.

Weiss, D. S. (2004) Bacterial cell division and the septal ring. Mol Microbiol **54**: 588-597.

Weiss, D. S., Chen, J. C., Ghigo, J. M., Boyd, D. and Beckwith, J. (1999) Localization of FtsI (PBP3) to the septal ring requires its membrane anchor, the Z ring, FtsA, FtsQ, and FtsL. J Bacteriol **181**: 508-520.

Weiss, D., Pogliano, K., Carson, M., Guzman, L., Fraipont, C., Nguyen-Disteche, M. *et al.* (1997) Localization of the *Escherichia coli* cell division protein FtsI (PBP3) to the division site and cell pole. Mol Microbiol **25**: 671-681.

West, S. E. and Clark, V. L. (1989) Genetic loci and linkage associations in *Neisseria gonorrhoeae* and *Neisseria meningitidis*. Clin Microbiol Rev **2:** S92-S103.

Westling-Haggstrom, B., Elmros, T., Normark, S. and Winblad, B. (1977) Growth pattern and cell division in *Neisseria gonorrhoeae*. J Bacteriol **29**: 333-342.

Wissel, M. C. and Weiss, D. S. (2004) Genetic analysis of the cell division protein FtsI (PBP3): amino acid substitutions that impair septal localization of FtsI and recruitment of FtsN. J Bacterial **186**: 490-502.

Wissel, M. C., Wendt, J. L., Mitchell, C. J. and Weiss, D. S. (2005) The transmembrane helix of the *Escherichia coli* division protein FtsI localizes to the septal ring. J Bacteriol **187**: 320-328.

Woldringh, C. L., Mulder, E., Valkenburg, J. A., Wientjes, F. B., Zaritsky, A. and Nanninga, N. (1990) Role of the nucleoid in the toporegulation of division. Res Microbiol **141**: 39-49.

World Health Organization (WHO). (2009) Sexually transmitted diseases. http://www.who.int/vaccine_research/diseases/soa_std/en/print.html.

World Health Organization (WHO). The WHO Western Pacific gonococcal antimicrobial surveillance programme. Surveillance of antibiotic resistance in *Neisseria gonorrhoeae* in the WHO Western Pacific region, 2002 Commun Dis Intell 2003; 27:487-490.

Wu, L. J. and Errington, J. (2004) Coordination of cell division and chromosome segregation by a nucleoid occlusion protein in *Bacillus subtillis*. Cell **117**: 915-925.

Wu, L.J., Ishikawa, S., Kawai, Y., Oshima, T., Ogasawara, N. and Errington, J. (2009) Noc protein binds to specific DNA sequences to coordinate cell division with chromosome segregation. EMBO J **28**: 1940-1952.

Yan, K., Pearce, K. H. and Payne, D. J. (2000) A conserved residue at the extreme C-terminus of FtsZ is critical for the FtsA-FtsZ interaction in *Staphylococcus aureus*. Biochem Biophys Res Commun **270**: 387-392.

Yang, J. C., van Den Ent, F., Neuhaus, D., Brevier, J. and Löwe, J. (2004) Solution structure and domain architecture of the divisome protein FtsN. Mol Microbiol **52**: 651-660.

Yang, Y., Liao, M., Gu, W. et al. (2006) Antimicrobial susceptibility and molecular determinants of quinolone resistance in *Neisseria gonorrhoeae* isolates from Shanghai. J Antimicrob Chemother **58**:868-867.

Yanouri, A., Daniel, R. A., Errington, J. and Buchanan, C. E. (1993) Cloning and sequencing of the cell division gene *pbpB*, which encodes penicillin binding protein 2B in *Bacillus subtilis*. J Bacteriol **175**: 7604-7616.

Yim, L., Vandenbussche, G., Mingorance, J., Rueda, S., Casanova, M., Ruysschaert, J. and Vicente, M. (2000) Role of the carboxy terminus of *Escherichia coli* FtsA in self-interaction and cell division. J Bacteriol **182**: 6366-6373.

Yu, X. and Margolin, W. (1999) FtsZ ring clusters in *min* and partition mutants: role of both the Min system and the nucleoid in regulating FtsZ ring localization. Mol Microbiol **32**: 315-326.

Yu, X.C., Tran, A.H., Sun, Q. and Margolin, W. (1998) Localization of cell division protein FtsK to the *Escherichia coli* septum and identification of a potential N-terminal targeting domain. J Bacteriol **180**: 1296-1304.

APPENDIX

The following appendix describes some other experiments that were performed in addition to my main research project. Each study contains a brief description on its purpose and why experiments were not investigated further in this project or included in the body of the thesis.

Appendix A. Morphological observation of dividing *N. gonorrhoeae*

N. gonorrhoeae is the causative agent of the sexually transmitted disease gonorrhoea. In male, this is typically associated with a purulent discharge from the urethra. In women, infection of the cervix is often asymptomatic while gonococcal spread up the urinary tract or invasion across the epithelial layers can cause additional complications such as disseminated gonococcal infection (DGI). Depending on geographical location, between 0.1%–3% of cases of uncomplicated gonorrhoea (UG) disseminate and cause DGI (Tapsall *et al.*, 1992; Kerle *et al*., 1992; Meitzner and Cohen, 1997). *N. gonorrhoeae* strains, now commonly used internationally for various studies were isolated from patients either with DGI or/and UG. For example, strain FA1090 was isolated from the cervix of a patient with DGI while strain F62 was isolated from patients with UG (Knapp and Holmes, 1975). Many attempts have been made to correlate disease phenotype with the genetic characteristics of the isolates. Certain phenotypes have been associated with DGI, including the arginine, hypoxanthine, and uracil auxotype (Knapp and Holmes, 1975; Noble *et al*., 1984).

N. gonorrhoeae was also reported to show strain-specific differences associated with the phase variable gene repertoire during *in vitro* growth (Jordan *et al.*, 2005), although microarray studies have revealed that there is little difference in the gene complements of these strains and that *N. gonorrhoeae* F62 contains all of the genes encoded by the *N. gonorrhoeae* FA1090 genome, which also used in the first *N. gonorrhoeae* genome project (Snyder *et al*., 2004). However, several differences have also been noted between these

strains, including the ability to acquire iron from lactoferrin due to expression of lactoferrin binding protein (Lbp) (Anderson *et al*., 2003) and the presence or absence of the Gonococcal Genetic Island in these strains (Dillard and Seifert, 2001; Snyder *et al*., 2004).

Differences can also be found between *N. gonorrhoeae* strains in genotype and relevant genetic manipulation. Most *N. gonorrhoeae* clinical isolates carry the cryptic plasmids, except for isolates with the praline-, citrulline-, and uracil-requiring auxotype (Dillon and Pauze, 1981). Strains F62 and FA1090 carry the cryptic plasmids, which could be successfully transformed with shuttle vector pFP20 and its derivatives (Szeto *et al*., 2001; Szeto, 2004). While the plasmid-free *N. gonorrhoeae* CH811, which was used for most cell division studies in *N. gonorrhoeae*, could not be transformed with the shuttle vector (Szeto, 2004).

N. gonorrhoeae cells divide in alternating perpendicular planes, resulting in the formation of tetrads. The position of nucleoid in dividing cells is unknown, particularly in tetrads. Further, *N. gonorrhoeae* strains CH811, F62 and FA1090, which were frequently used for various *N. gonorrhoeae* studies, were different in genotypes, genetic characteristics and disease phenotype. It is unknown whether *N. gonorrhoeae* strains divide different from each other. To achieve this, the nucleoid position modes and dividing patterns amongst *N. gonorrhoae* strains FA1090, F62 and CH811 were investigated using fluorescence microscopy with 4',6-diamidino-2-phenylindole (DAPI) staining.

Materials and methods

N. gonorrhoeae CH811, F62 and FA1090 were grown in GCMBD broth and aliquots were taken at different time points (4-hr, 8-hr and 12-hr) and fixed as described in the Material and Methods session.

DAPI (4',6-diamidino-2-phenylindole) fluoresces blue upon excitation with ultraviolet light only when complexed with double stranded DNA. To observe the distribution of

Table A.1. Strains and primers used in this study

Strains	Relevant characteristics	Source/reference
E. coli DH5α□	*supE44 ΔlacU169 (80lacZΔM15) hsdR17 endA1 gyrA96 thi-1 relA1*	Gibco
E. coli XL1-Blue	*recA1 endA1 gyrA96 thi-1 hsdR17 supE44 relA1 lac* [*F' proAB lacI*^{q} *ZΔM15]* Tn10	Stratagene
E. coli C41 (*DE3*)	F^{-} *ompT hsdS*$_{B}$ (r$^{-}_{B}$ m$^{-}_{B}$) *gal dcm Δ* (*srl-recA*) 306::Tn*10* (Tet^{r}) (*DE3*)	Miroux and Walker, 1996
E. coli BL21 (*DE3*)	*F*$^{-}$ *dcm ompT hsdS*$_{B}$ (r$^{-}_{B}$ m$^{-}_{B}$) *gal* □ (DE3)	Stratagene
E. coli C43 (*DE3*)	*F*$^{-}$ *ompT hsdSB* (r$^{-}_{B}$ m$^{-}_{B}$) *gal dcmD(srl-recA)* 306::Tn10 (Tet^{r}) (DE3)	Miroux and Walker (1996)
N. gonorrhoeae CH811	Auxotype (A)/serotype (S)/plasmid content (P) class: nonrequiring/IB-2/plasmid-free, Str^{r}	Picard and Dillon, 1989
N.gonorrhoeae F62	A/ S/ P: proline/IB-7/2.6	West *et al.*, 1989
N. gonorrhoeae FA1090	A/ S/ P: proline/IB-2/2.6	West *et al*., 1989
S. cerevisiae SFY526	*trp 1-901 leu2-3 112 can*^{r} *gal4-542 gal80-538 URA3::GAL1*$_{UAS}$*-GAL1*$_{TATA}$*-lacZ*	Clontech

nucleoid in *N. gonorrhoeae* cells, DAPI staining was used. Cells were fixed on pre-coated coverslips as described above. Five microliters of DAPI (0.2 μg/ml stock, Sigma) was placed on a small sheet of Parafilm® M and coverslips containing attached *N. gonorrhoeae* cells were gently pressed onto the DNA stain and left to incubate at room temperature for 2 mins. Coverslips were removed and gently washed with 10 ml PBS (pH 7.4) dispensed dropwise from a pipette. Coverslips were then placed over a 5 μl drop of 50% glycerol on a microscope slide and sealed (Ramires-Arcos *et al.,* 2001b). Slides were examined using an Olympus BX61 microscope with DIC and fluorescence microscopy capabilities.

Results and Discussion

N. gonorrhoeae cells were too small to see tetrads clearly using DIC microscopy (Fig. A.1 A-F). The single cells were round in shape and diplococci appear to be oval. Tetrads usually with obvious constrictions were somewhat larger than diplococci (Fig. A.1). When the same samples strained with DAPI were examined using fluorescence microscopy, it was much easy to differentiate the tetrads from diplococci based on the position and numbers of nucleoids. One centrally located nucleoid was observed in newly generated single cells (Fig. A.1 A-A'). As cell division progressed, two nucleoids were observed in diplococci, distributed along the long axis of cells. A black band was observed between two nucleoids (Fig. A.1 B-C, B'-C', white arrows), indicating that chromosome segregation and division were completed but that the daughter cells had yet not separated. Four coffee bean-shaped nucleoids were observed in tetrads (Fig. A.1C-E, C'-E'). A completed septum from the first round of division observed, which divides the nucleoid into two separated parts (Fig. A.1 C'-E', red arrows). An initial invagination was observed at each diplococcal cell junction and at a right angle to the first septum (Fig. A.1 C'-D', green arrows), as shown by transmission electron microcsopy (Westling-Häggström *et al*., 1977), resulting in a two-by-two (tetrad) arrangement of 4 nucleoids (Fig. A.1E'). This observation confirmed that the earliest visible

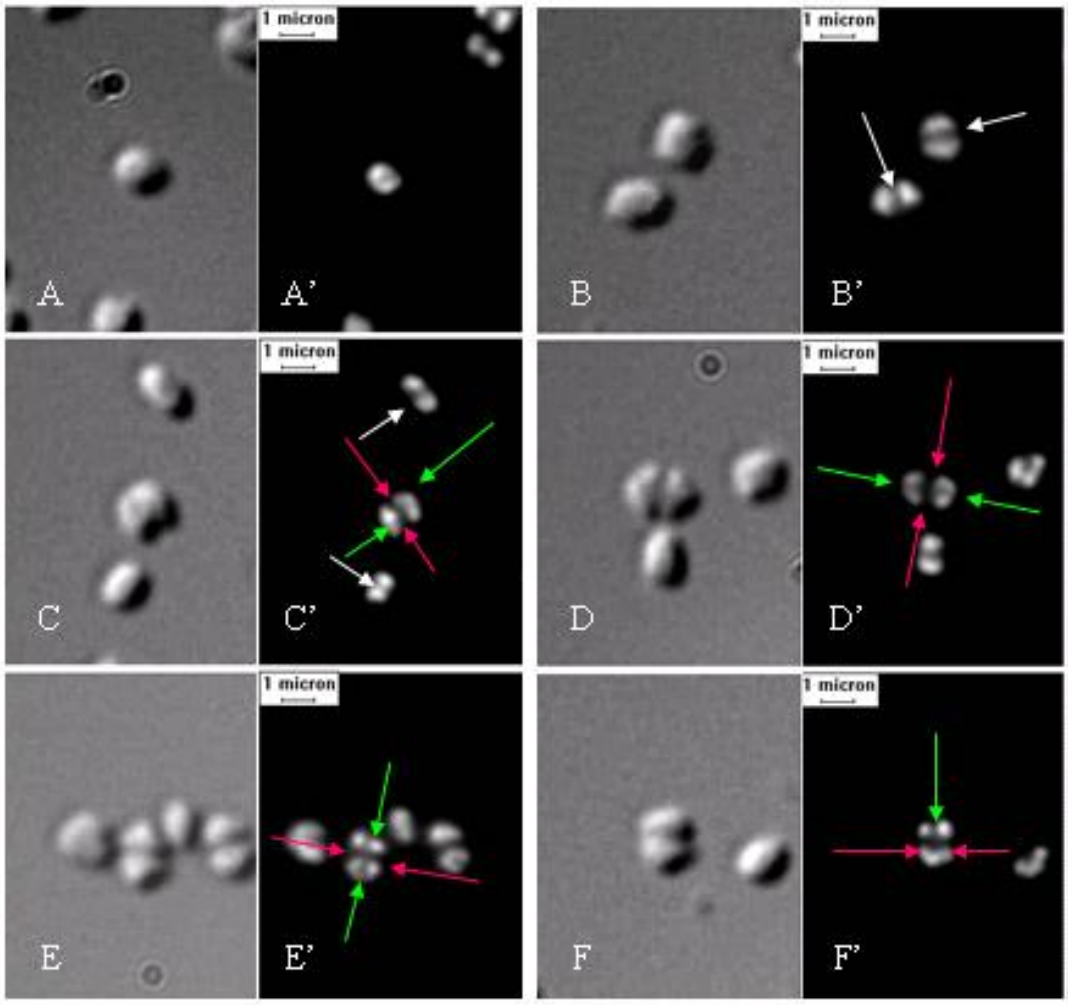

Fig. A.1. Nucleoids are positioned to facilitate cell division in alternating perpendicular planes in *N. gonorrhoeae* cells. *N. gonorrhoeae* FA1090 cells were observed using DIC microscopy (A-F) and DAPI fluoresces microscopy (A'-F'). Single cell is in round shape with a centrally located nucleoid (A, A'). Diplococci appear to be round to oval shape with two nucleoids (B-C, B'-C'). Tetrads are usually larger than diplococci in size and appear to be coffee-bean shape under DIC microscopy (D-E). 4 nucleoids in 2x2 arrangement are observed in most tetrads (D'-E') and 3 nucleoids are also observed in some tetrads (F, F'). White arrows indicate the cell division plane in diplococci. Red arrows indicate the first round of cell division plane in tetrads. Green arrows indicate the second round of perpendicular division plane in tetrads.

event of gonococcal cell division appeared to be a constriction that is more pronounced on one side of the coccus than the other (Fitz-James, 1964). Cells with 3 nucleoids were also observed occasionally, indicating that the second round of division initialed in diplococcal cells was not always started simultaneously (Fig. A.1F', green arrow).

300 cells were randomly counted for each strain at each time point and analyzed statistically. The distribution of monococci, diplococci, and tetrads of *N. gonorrhoeae* FA1090, CH811 and F62 at each time point of 4-hr, 8-hr and 12-hr are presented in Figure A.2. At 4-hr, monococci and diplococci were observed in all 3 strains with monococci predominanting and being 97%, 98% and 83% of cells for FA1090, F62, and CH811, respectively. At 8-hr, the numbers of monococci significantly decreased and diplococci were dominant in the culture, comprising 74%, 61%, and 64% of cells for FA 1090, F62, and CH811, respectively. Tetrads were observed at this time point and comprised 5%, 5% and 6% of cells for FA1090, F62, and CH811, respectively. At 12-hr, all 3 types of cells were observed. While the percentage of diplococci decreased, the percentage of monococci increased, probably because tetrads started to separate into single cells. The number of tetrads stayed constant, comprising 7%, 4%, and 5% for FA1090, F62, and CH811, respectively. A few differences of the morphology distribution were observed amongst 3 strains, for example, CH811 presented a higher number of diplococci than the other two strains at 4-hr and 12-hr, while FA1090 presented lower number of diplococci than the other strains at time point 12-hr (Fig. A.2).

Previous studies using transmission electron microscopy demonstrated how inner membrane constrictions occurred and extended to form diplococcal compartments and how cytoplasmic membrane invaginated to form a tetrad arrangement of 4 cells in gonococcal cells, indicating that *N. gonorrhoeae* divides in alternating perpendicular planes (Westling-Haggstrom *et al*., 1977). However, since transmission electron microscopy can not identify

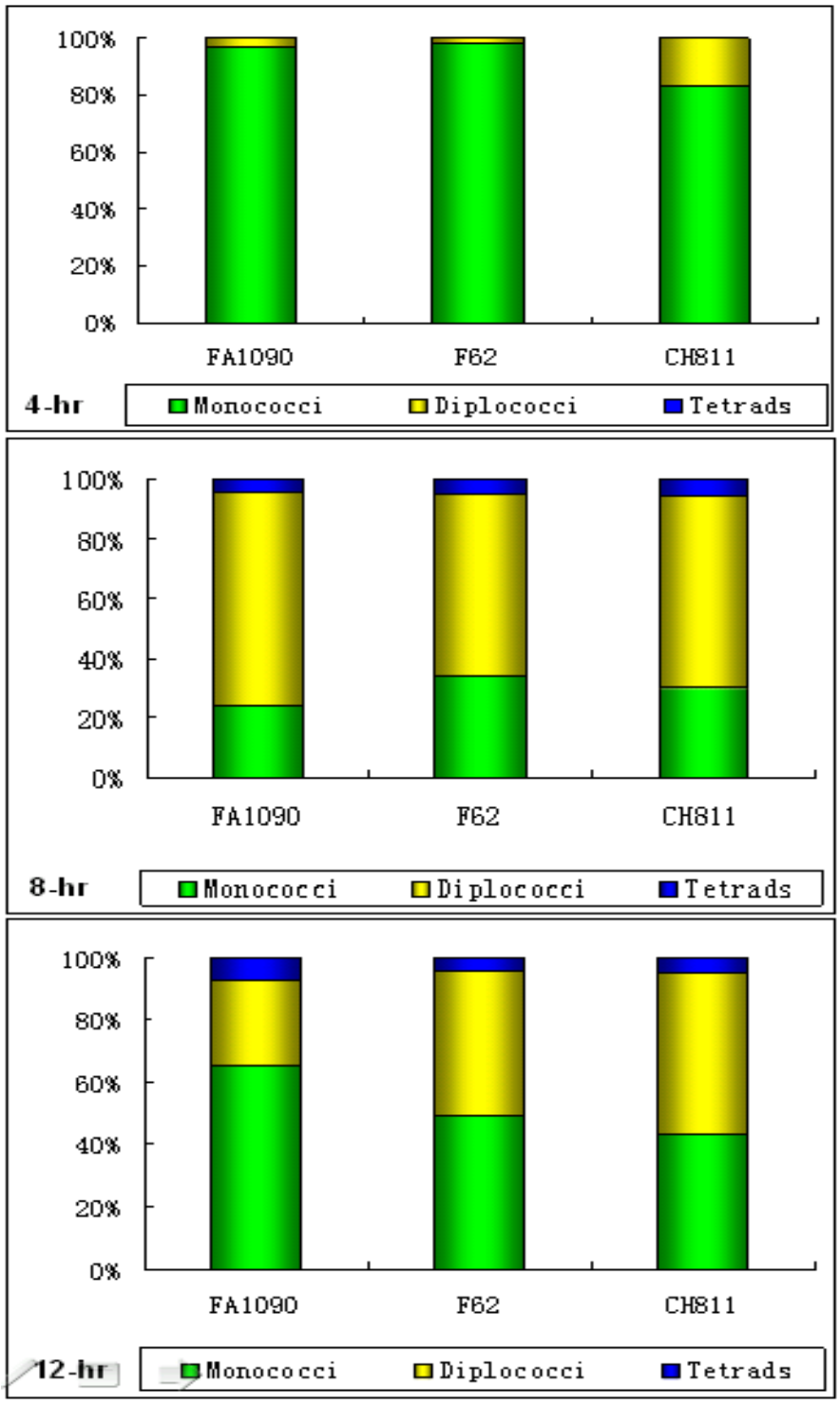

A.2. Distribution of *N. gonorrhoeae* monococci; diplococci; tetrads at time points of 4-hr, 8-hr and 12-hr. 300 cells were observed by DAPI fluorescence microscopy observation were counted for each strain at each time point and analyzed statistically.

the position of the nuceloid in the tetrads, it was difficult to establish that the tetrad truly contained 4 viable daughter cells with equal nucleoids. This was demonstrated by the observation of *N. gonorrhoeae* cells after DAPI staining. Monococci, diplococci and tetrads were observed in strained cells from all 3 gonococcal strains by DAPI micrographs. Four equal nucleoids were observed in most tetrads, thus providing further evidence to support the alternating perpendicular division mode in *N. gonorrhoeae*. This is the first study of nucleoid position in dividing *N. gonorrhoeae* cells. Tetrads were demonstrated by the observation of 4 nucleoids in 2x2 arrangements, offering further evidence to support the division pattern of alternating perpendicular planes in *N. gonorrhoeae*.

The morphological distribution of 3 cell types (monococcus, diplococci and tetrads) were studied amongst the *N. gonorrhoeae* strains based on growth phase. The proportions of monococci, diplococci and tetrads varied at different growth phases. However, no significance difference was observed for the morphological distributions of cell types amongst 3 strains. Monococci were consistently predominant at 4-hr and diplococci at 8-hr, in the gonococcal strains studied in my experiments. In addition, tetrads, indicating of cell division in alternating perpendicular planes, were observed in all 3 strains at 8 hrs as well as 12 hrs, but not at 4 hrs. This suggests that *N. gonohorreae* cells mainly divide in parallel planes at the early growth phase, as *E. coli* cells do. As growth proceeds, these cells start to divide in alternating perpendicular planes and form tetrads as observed at 8 hrs and 12 hrs. The number of tetrads at 12 hrs did not increase in all 3 strains, which might be explained either because the tetrads further completely separated into monococci, apparently increasing the amount of monococci at 12 hrs, or because of the tendency of *N. gonorrhoeae* to autolyze in a part of the population (Hebeler and Young, 1976). It appears that *N. gonorrhoeae* cells divide in alternating perpendicular planes dependent of growth phase. This might be explained by the reduction of murein hydrolase activity with cell growth (Fussenegger *et al.*,

1996). *N. gonorrhoeae tpc* (tetrapac) exhibited a 30% reduction in the overall murein hydrolase activity mutant and showed a distinctive bacterial growth of tetrapacs instead of diplococci, indicating a defect in cell division (Fussenegger *et al.*, 1996).

Appendix B. Interactions of divisome proteins in *N. gonorrhoeae* detected by yeast two-hybrid assays.

To confirm the protein interactions identified using B2H assays, another commonly used method to study protein-protein interactions, the yeast two-hybrid system (Y2H), was employed to examine the potential interaction of *N. gonorrhoeae* divisome proteins.

Materials and Methods

Saccharomyces cerevisiae SFY526 (Clontech, Palo Alto, CA) was used for yeast two-hybrid assays (Table A.1). *S. cerevisiae* cells were grown at 30 °C on yeast extract-peptone-adenine-dextrose (YPAD) media (Clontech) or on suitable synthetic dropout (SD) media, as described in the Clontech Yeast Two-Hybrid Protocols Manual (Clontech).

Construction of plasmids for yeast two-hybrid assays

Divisome genes *ftsA*, *ftsK*, *ftsI*, *ftsW*, *ftsQ*, *ftsN*, *ftsE* and *ftsX* were PCR amplified from *N. gonorrhoeae* CH811 using the following primers: $FtsA_{Ng}$- AP33/AP34; $FtsK_{Ng}$- AP35/AP36; $FtsI_{Ng}$- AP37/AP38; $FtsW_{Ng}$- AP39/AP40; $FtsQ_{Ng}$- AP41/AP42; $FtsN_{Ng}$- AP43/AP44; $FtsE_{Ng}$- AP45/AP46; $FtsX_{Ng}$- AP47/AP48 (Table A.2). PCR products were digested with EcoRI and BamHI and ligated into pre-digested Y2H vectors pGAD424 (carrying activating domain, AD) and PGBT9 (carrying binding domain, BD), yielding plasmids pGAD-A, pGAD-K, pGAD-I, pGAD-Q, pGAD-N, pGAD-E, pGAD-X; pGBT-A, pGBT-K, pGBT-I, pGBT-Q, pGBT-N, pGBT-E, pGBT-X. The PCR product of FtsI was digested with BamHI and PstI and ligated into BamHI/PstI digested Y2H vectors, yielding plasmid pGAD-W and pGBT-W (Table A.3). pGAD-Z and pGBT-Z were generated previously by Ramirez-Arcos *et al*. (2002).

Gene integrity and reading frame for all constructs were vertified by DNA sequence analysis (Plant Biotechnology Institute, National Research Council of Canada, Saskatoon, Saskatchewan).

Table A.2. Primers used in this study

Primers		Sequences (5'-3')
Cloned into pET30a with an N-terminal His-tag		
AP1	FwftsA-NcoI-pFP20	CGCGCCATGGTCTGCCGAAATGCTCCGCCGTTAT
AP2	ReftsA-PstI-pFP20	CGCGCTGCAGTCAGAGGTTGTTTTCAATCCACCGC
AP3	fwBglII-FtsK- pET30a	AGCCCAGATCTGATGTTTTGGATAGTTTTGATCGTTAT
AP4	reEcoRI-ftsK- pET30a	ATATCGAATTCTCAAGCATTGTCCAAGGGGACGAG
AP5	reBglII-ftsI-pET30a	AGCCCAGATCTGATGTTGATTAAAAGCGAATATAAGCC
AP6	reEcoRI-ftsI- pET30a	ATATCGAATTCTTAAGACGGTGTTTTGACGGCTGC
AP7	fwBglII-FtsQ- pET30a	AGCCCAGATCTGATGTGGGATAATGCCGAAGCGATG
AP8	reEcoRI-ftsQ- pET30a	ATATCGAATTCCTATTCTTCGGATTCTTTTTCGGG
AP9	fwBamHI-ftsW-pET30a	CGCGGGATCCATGAAGATTTCGGAAGTATTGGTAAA
AP10	reSalI-ftsW-pET30a	GCGCGTCGACTTACTCCACCCGGTAACCGCGCAT
AP11	fwBglII-FtsN- pET30a	AGCCCAGATCTGATGTTTATGAACAAATTTTCCCAATC
AP12	reEcoRI-ftsN- pET30a	ATATCGAATTCTTATTTGCCTTCAATCGCACGGAT
AP13	fwBglII-ftsE- pET30a	AGCCCAGATCTGATGATCCGTTTCGAACAAGTTTCC
AP14	reEcoRI-ftsE- pET30a	ATATCGAATTCTCATGCGAGTCGTCCTTTCGAGAG
AP15	fwBglII-ftsX-pET30a	AGCCCAGATCTGATGAGCATCATCCACTACTTCTCG
AP16	reEcoRI-ftsX- pET30a	ATATCGAATTCTTATTTTTTGGCTTTGAAGCAGAG
AP17	BglII-ZipAfor	CACAGATCTCATGATTTACATCGTACTGTTCC
AP18	ZipA-XhoIrev	GTGCTCGAGTTATGAAAACAGGCGCAGG
Cloned into pET30a with an C-terminal His-tag		
AP19	NdeI-FtsKfor	GCCCATATGATGTTTTGGATAG
AP20	FtsK-XhoIrev	CCACTCGAGTGAAGCATTGTCC
AP21	NdeI-FtsIfor	CGGCATATGATGTTGATTAAAAGC
AP22	FtsI-XhoIrev	CCCTCGAGTTGAGACGGTGTTTTG
AP23	NdeI-FtsW-for	CGACATATGAAGATTTCGGAAGTATTGG
AP24	FtsW-XhoI-rev	GTGCTCGAGTTGCTCCACCCGGTAACC
Cloned into pBADa with an N-terminal His-tag		
AP25	XhoI-FtsKfor	CCCCCTCGAGATGTTTTGGATAGTTTTGATCG
AP26	FtsK-HindIIIrev	GGGGAAGCTTTCAAGCATTGTCCAAGGGGACG
AP27	XhoI-FtsI (for)	CCCCTCGAGATGTTGATTAAAAGC
AP28	FtsI-HindIII (rev)	CCCAAGCTTTTAAGACGGTGTTTTG
AP29	XhoI-FtsWfor	CCCCCTCGAGATGAAGATTTCGGAAGTATTGG
AP30	FtsW-KpnIrev	CCCCGGTACCTTACTCCACCCGGTAACC
AP31	XhoI-FtsNfor	CCCCCTCGAGATGTTTATGAACAAATTTTCC
AP32	FtsN-EcoRIrev	GGGGGAATTCTTATTTGCCTTCAATCGCACG

Cloned into Y2H vectors		
AP33	ftsA-fwEcoRI-Y2H	CGCCGGAATTCATGGAACAGCAGAAAAGATACATC
AP34	ftsA-reBamHI-Y2H	CCCGGGGATCCTCAGAGGTTGTTTTCAATCCACC
AP35	fwEcoRI-ftsK-Y2H	CGCCGGAATTCATGTTTTGGATAGTTTTGATCGT
AP36	reBamHI-ftsK	CGCGGGATCCTCAAGCATTGTCCAAGGGGACGAG
AP37	fwEcoRI-ftsI-Y2H	CGCCGGAATTCATGTTGATTAAAAGCGAATATAAGCC
AP38	reBamHI-ftsI	CGCGGGATCCTTAAGACGGTGTTTTGACGGCTGC
AP39	fwEcoRI-ftsW-Y2H	CGCCGGGATCCGTATGAAGATTTCGGAAGTATTGG
AP40	rePstI-ftsW-Y2H	CGCGCTGCAGTTACTCCACCCGGTAACCGCGCAT
AP41	fwEcoRI-ftsQ-Y2H	CGCCGGAATTCATGTGGGATAATGCCGAAGCGATG
AP42	reBamHI-ftsQ	CGCGGGATCCCTATTCTTCGGATTCTTTTTCGGG
AP43	fwEcoRI-ftsN-Y2H	CGCCGGAATTCATGTTTATGAACAAATTTTCCCA
AP44	reBamHI-ftsN	CGCGGGATCCTTATTTGCCTTCAATCGCACGGAT
AP45	fwEcoRI-ftsE-Y2H	CGCCGGAATTCATGATCCGTTTCGAACAAGTTTCC
AP46	reBamHI-ftsE	CGCGGGATCCTCATGCGAGTCGTCCTTTCGAGAG
AP47	fwEcoRI-ftsX-Y2H	CGCCGGAATTCATGAGCATCATCCACTACTTCTCG
AP48	reBamHI-ftsX	CGCGGGATCCTTATTTTTTGGCTTTGAAGCAGAG

Table A.3. Plasmids created

Plasmid	Relevant genotype	Source/Reference
pET30a	Kan^R P_{T7}::6Xhis	Novagen
pET-K-N-term	Kan^R P_{T7}::*ftsK*$_{Ng}$-N-terminal tag of 6XHis	This study
pET-I-N-term	Kan^R P_{T7}::*ftsI*$_{Ng}$- N-terminal tag of 6XHis	This study
pET-Q-N-term	Kan^R P_{T7}::*ftsQ*$_{Ng}$- N-terminal tag of 6XHis	This study
pET-W-N-term	Kan^R P_{T7}::*ftsW*$_{Ng}$- N-terminal tag of 6XHis	This study
pET-N-N-term	Kan^R P_{T7}::*ftsN*$_{Ng}$- N-terminal tag of 6XHis	This study
pET-E-N-term	Kan^R P_{T7}::*ftsE*$_{Ng}$- N-terminal tag of 6XHis	This study
pET-X-N-term	Kan^R P_{T7}::*ftsX*$_{Ng}$- N-terminal tag of 6XHis	This study
pET-ZipA-N-term	Kan^R P_{T7}::*zipA*$_{Ng}$- N-terminal tag of 6XHis	This study
pET-K-C-term	Kan^R P_{T7}::*ftsK*$_{Ng}$- N-terminal tag of 6XHis	This study
pET-I-C-term	Kan^R P_{T7}::*ftsI*$_{Ng}$- N-terminal tag of 6XHis	This study
pET-W-C-term	Kan^R P_{T7}::*ftsW*$_{Ng}$- N-terminal tag of 6XHis	This study
pBAD/His A	Amp^R P_{BAD}::6XHis	Invitrogen
pBAD-K-N-term	Amp^R P_{BAD}:: *ftsK*$_{Ng}$-N-terminal tag of 6XHis	This study
pBAD-I-N-term	Amp^R P_{BAD}:: *ftsI*$_{Ng}$-N-terminal tag of 6XHis	This study
pBAD-W-N-term	Amp^R P_{BAD}:: *ftsW*$_{Ng}$-N-terminal tag of 6XHis	This study
pBAD-N-N-term	Amp^R P_{BAD}:: *ftsN*$_{Ng}$-N-terminal tag of 6XHis	This study
pGAD424	P_{ADH1}[a]::*gal4*(AD)[1] (Amp^R)	Clontech
pGBT9	P_{ADH1}::*gal4*(BD)[2] (Amp^R)	Clontech
pGAD-A	pGAD424; P_{ADH1}::*gal4*(AD)-*ftsA*$_{Ng}$ (Amp^R)	This study
pGAD-Z	pGAD424; P_{ADH1}::*gal4*(AD)-*ftsZ*$_{Ng}$ (Amp^R)	Ramirez-Arcos *et al.*, 2002
pGAD-K	pGAD424; P_{ADH1}::*gal4*(AD)-*ftsK*$_{Ng}$ (Amp^R)	This study
pGAD-I	pGAD424; P_{ADH1}::*gal4*(AD)-*ftsI*$_{Ng}$ (Amp^R)	This study
pGAD-W	pGAD424; P_{ADH1}::*gal4*(AD)-*ftsW*$_{Ng}$ (Amp^R)	This study
pGAD-Q	pGAD424; P_{ADH1}::*gal4*(AD)-*ftsQ*$_{Ng}$ (Amp^R)	This study

pGAD-N	pGAD424; P_{ADH1}::*gal4*(AD)-*ftsN*$_{Ng}$ (Amp^R)	This study
pGAD-E	pGAD424; P_{ADH1}::*gal4*(AD)-*ftsE*$_{Ng}$ (Amp^R)	This study
pGAD-X	pGAD424; P_{ADH1}::*gal4*(AD)-*ftsX*$_{Ng}$ (Amp^R)	This study
pGBT-A	pGBT9; P_{ADH1}::*gal4*(BD)-*ftsA*$_{Ng}$ (Amp^R)	This study
pGBT-Z	pGBT9; P_{ADH1}::*gal4*(BD)-*ftsZ*$_{Ng}$ (Amp^R)	Ramirez-Arcos *et al*., 2002
pGBT-K	pGBT9; P_{ADH1}::*gal4*(BD)-*ftsK*$_{Ng}$ (Amp^R)	This study
pGBT-I	pGBT9; P_{ADH1}::*gal4*(BD)-*ftsIC*$_{Ng}$ (Amp^R)	This study
pGBT-W	pGBT9; P_{ADH1}::*gal4*(BD)-*ftsW*$_{Ng}$ (Amp^R)	This study
pGBT-Q	pGBT9; P_{ADH1}::*gal4*(BD)-*ftsQ*$_{Ng}$ (Amp^R)	This study
pGBT-N	pGBT9; P_{ADH1}::*gal4*(BD)-*ftsN*$_{Ng}$ (Amp^R)	This study
pGBT-E	pGBT9; P_{ADH1}::*gal4*(BD)-*ftsE*$_{Ng}$ (Amp^R)	This study
pGBT-X	pGBT9; P_{ADH1}::*gal4*(BD)-*ftsX*$_{Ng}$ (Amp^R)	This study

Yeast Two-hybrid Assay

The Yeast Two-Hybrid (Y2H) system from Clontech was used to assess protein-protein interactions. Initially, each plasmid created for an Y2H assay was individually transformed into the reporter strain *S. cerevisiae* SFY526 by the lithium acetate method (Clontech Yeast Two-Hybrid Manual) to ensure that the GAL4 fusions did not activate the β-galactosidase reporter gene. SD-Leu media (Clontech) was used to plate yeast transformants that carried only pGAD424-derived vectors. SD-Trp media (Clontech) was used to plate yeast cells that only possessed pGBT9-derived vectors. Yeast, co-transformed with both pGAD424 and pGBT9 derivatives, was plated on SD-Leu/-Trp media (Clontech). Using sterile filters, colony lift assays were performed. These filters were immediately frozen with liquid nitrogen and then thawed to lyse the yeast cells. By adding completed Z-buffer (60 mM Na_2HPO_4, 40 mM $NaH_2PO_4{\cdot}H_2O$, 2 mM KCl, 1 mM $MgSO_4 7{\cdot}H_2O$, 0.28% β-mercaptoethanol) and 5-bromo-4-chloro-3-indolyl-β-D-galactopyranoside (X-gal) substrate o/n, colonies turned blue, indicating a protein-protein interaction. Interaction was quantified using liquid β-galactosidase assays with ONPG as substrate (Clontech Yeast Two-Hybrid Manual). Using a formula to calculate the β-galactosidase units (Miller, 1972), the relative average strength of each interaction was determined ± 1 standard deviation. All assays were performed in triplicate in 3 independent experiments.

Results and Discussion

In order to analyze the ability of the fusion proteins to activate reporter gene expression (so-called self-activation), the entire coding regions for $FtsA_{Ng}$ and other divisome proteins were cloned into the Y2H shuttle vector plasmids pGAD424 and pGBT9. The resulting hybrid plasmids carrying either AD or BD in-frame fusions with *ftsA* and other *fts* genes (Table A.3) were cotransformed with the relevant "empty" vector plasmid pGBT9 or pAD424 into yeast reporter strain *S. cerevisiae* SFY526 carries a *lacZ* reporter gene. From all fusions

tested in this study, only BD-FtsZ mediated significant background transcriptional activity (self-activation) (Fig. A.3A), similar to a report of *E. coli* FtsZ (Hu *et al.*, 1999), and therefore, with the exception of hybrid plasmid pGBT-FtsZ, all the other plasmids should be suitable for Y2H system.

The resultant hybrid plasmids carrying either AD or DBD in-frame fusions with *ftsA* and other *fts* genes (Table A.3) were cotransformed with the relevant plasmids carrying either BD or AD in-frame fusions with *ftsA* and other *fts* genes into yeast reporter strain *S. cerevisiae* SFY526 and performed Y2H assay. Colony lift assays using X-gal as substrate and β-galactosidase activity using ONPG as a substrate were tested.

The interaction between $FtsA_{Ng}$ and $FtsZ_{Ng}$ was tested first using colony lift assay. Blue colonies were observed with protein pair BD-$FtsA_{Ng}$-AD-$FtsA_{Ng}$, indicating $FtsA_{Ng}$ self-interaction (Fig. A.3B). Blue colonies were also observed from protein pairs BD-$FtsZ_{Ng}$-AD-$FtsZ_{Ng}$ and BD-$FtsZ_{Ng}$-AD-$FtsA_{Ng}$ (Fig. A.3 C-D), indicative of interactions. Since these two protein pairs contain BD-$FtsZ_{Ng}$, the protein interactions might be induced by the self-activation of BD-$FtsZ_{Ng}$. The protein pair AD-$FtsZ_{Ng}$-BD-$FtsA_{Ng}$ did not reveal any blue colony. The same results were obtained by testing the β-galactosidase activity using ONPG as a substrate (Fig. A.4). These results indicate Y2H system cannot detect the interaction of FtsA and FtsZ in *N. gonorrhoeae*.

Y2H assays were performed to test the potential interactions amongst other divisome proteins. Unfortunately, no interaction between any two of the divisome proteins was detected (data not shown), indicating that Y2H system did not allow the detection of interactions between divisome proteins in *N. gonorrhoeae*. This result is consistent with the previous reports that Y2H system was not suitable to study the cell division protein interaction from *N. gonorrhoeae* (Greco-Stewart *et al.*, 2007; Szeto, PhD thesis, 2004; Eng, PhD thesis, 2007).

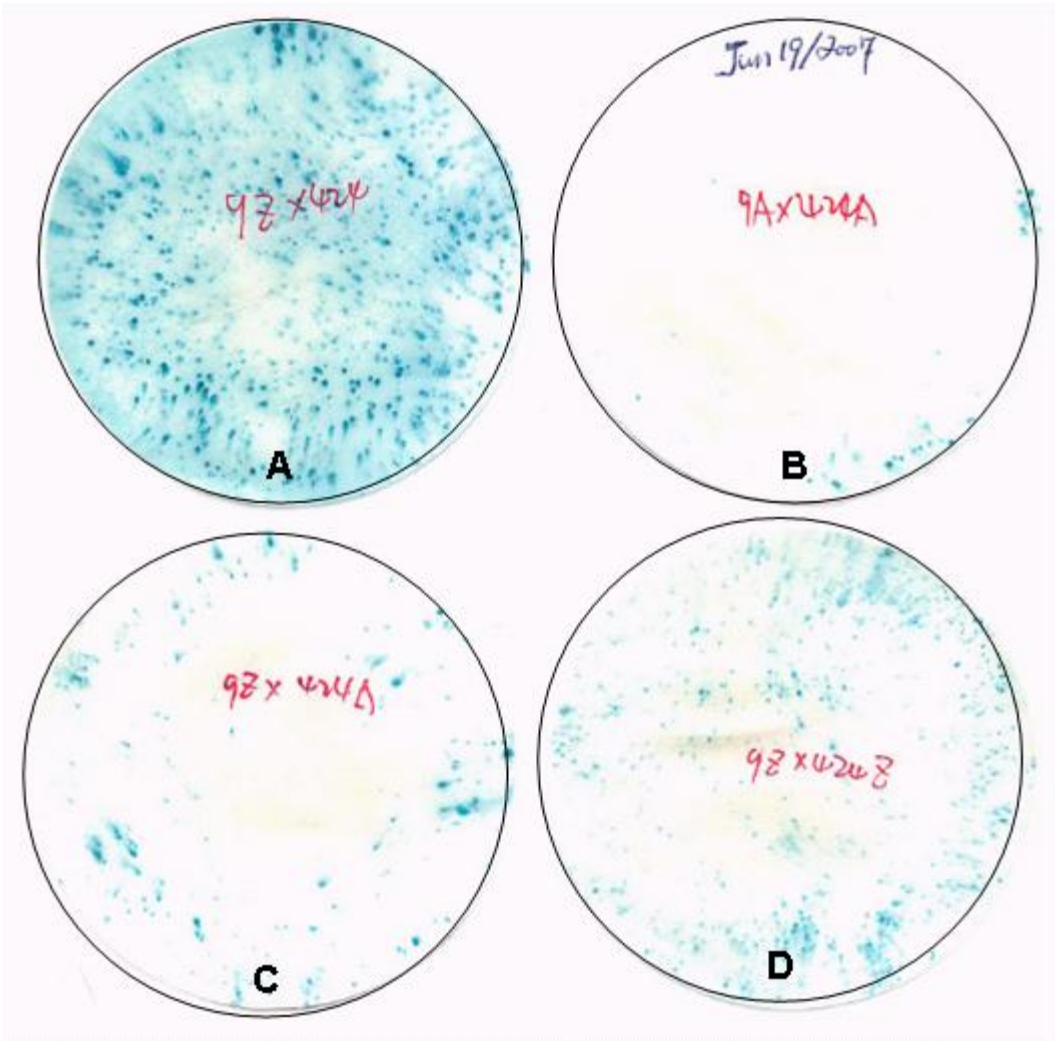

A.3. Colony lift assays to determine the interaction between $FtsA_{Ng}$ and $FtsZ_{Ng}$. If two proteins interact, blue colonies appear, indicating that *lacZ* is able to process the X-gal substrate. (A) A large number of blue colonies were observed with BD-$FtsZ_{Ng}$ fused empty AD vector, indicating strong self-inactivation of $FtsZ_{Ng}$. (B) Blue colonies were also observed with BD-$FtsA_{Ng}$ fused AD-$FtsA_{Ng}$, indicating the self-interaction of $FtsA_{Ng}$. (C and D) The protein pairs BD-$FtsZ_{Ng}$-AD-$FtsZ_{Ng}$ and BD-$FtsZ_{Ng}$-AD-$FtsA_{Ng}$ also revealed blue colonies, which might be induced by self-activation of BD-$FtsZ_{Ng}$. The replicated protein pair composed of DBD-$FtsA_{Ng}$ and AD-$FtsZ_{Ng}$ did not reveal any blue colonies.

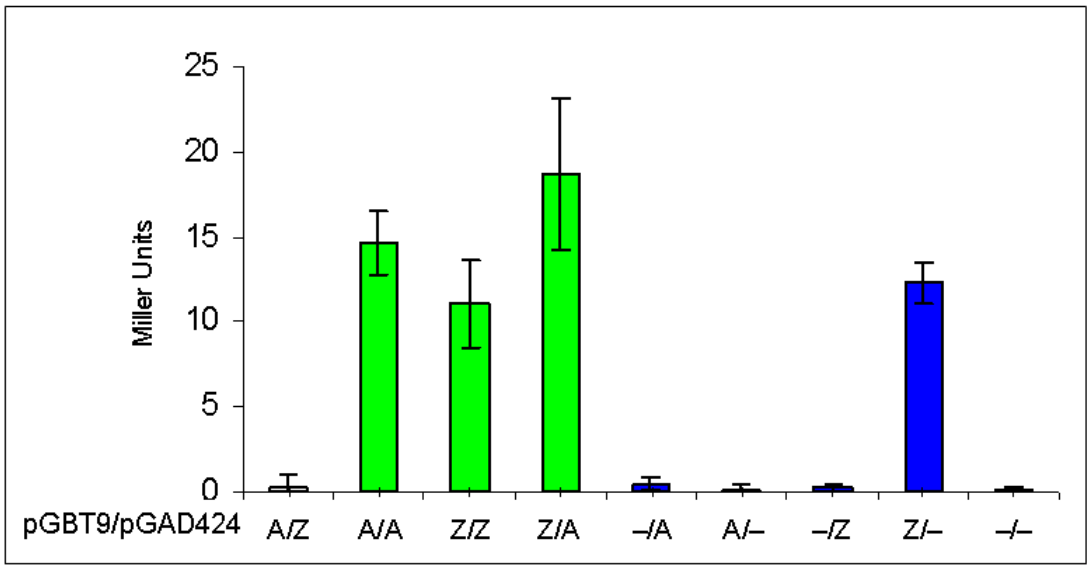

Fig. A.4. Interaction between FtsA (A) and FtsZ (Z) and self-interactions of $FtsA_{Ng}$ and $FtsZ_{Ng}$ determined by Y2H assay. $FtsA_{Ng}$ and $FtsZ_{Ng}$ were cloned into pGBT9 and pGAD424 and constructs were transformed into *S. cerevisiae* SFY526 either singly or in combination. *S. cerevisiae* The β-galactosidase activity was tested using ONPG as a substrate. SFY526 without plasmids and single transformants were used as negative controls (blue bars 5-9). BD-FtsZ showed self-activation (bar 8). Positive interactions indicated in green (bars 2-4); negative interaction indicates in white (bar 1).

Appendix C. Purification of *N. gonorrhoeae* divisome proteins and creation of their antibodies

I have examined the interactions between divisome proteins in *N. gonorrheae* using B2H assays. These interactions should to be confirmed by other methods, such as Co-IP or GST pull-down assays. Thus the antibodies that respond to each divisome protein need to be produced first. These antibodies will also be able to use for future investigation, such as localization or recruitment studies.

Material and methods

The divisome proteins were transformed into *E. coli* XL1 using pET30a and pBAD cloning systems, respectively. Wild-type *ftsK*$_{Ng}$, *ftsI*$_{Ng}$, *ftsQ*$_{Ng}$, *ftsW*$_{Ng}$, *ftsN*$_{Ng,}$ *ftsE*$_{Ng}$, *ftsX*$_{Ng}$, and *zipA*$_{Ng}$ were amplified from *N. gonorrhoeae* CH811 chromosomal DNA using the following primers: *ftsK*$_{Ng}$–AP3/AP4, *ftsI*$_{Ng}$–AP5/AP6, *ftsQ*$_{Ng}$–AP7/AP8, *ftsW*$_{Ng}$–AP9/AP10, *ftsN*$_{Ng}$–AP11/AP12, *ftsE*$_{Ng}$–AP13/AP14, *ftsX*$_{Ng}$–AP15/AP16, and *zipA*$_{Ng}$–AP17/AP18 (Table A.2). These amplicons were digested with indicated restriction enzymes and cloned into pET30a with an N-terminal His-tag to create a series of pET30a derivatives (Table A.3).

Wild-type *ftsK*$_{Ng}$, *ftsI*$_{Ng}$, and *ftsW*$_{Ng}$ were also amplified from *N. gonorrhoeae* CH811 chromosomal DNA using the following primers: *ftsK*$_{Ng}$–AP19/AP20, *ftsI*$_{Ng}$–AP21/AP22, and *ftsW*$_{Ng}$–AP23/AP24 (Table A.2). These amplicons were digested with indicated restriction enzymes and cloned into pET30a with a C-terminal His-tag to create a series of pET30a derivatives (Table A.3).

Wild-tyep *ftsK*$_{Ng}$, *ftsI*$_{Ng}$, *ftsW*$_{Ng}$, and *ftsN*$_{Ng,}$ were PCR amplified from *N. gonorrhoeae* CH811 chromosomal DNA using the following primers: *ftsK*$_{Ng}$–PA25/PA26, *ftsI*$_{Ng}$–PA27/PA28, *ftsW*$_{Ng}$–PA29/PA30, and *ftsN*$_{Ng}$–PA31/PA32 (Table A.2). These amplicons were digested with indicated restriction enzymes and cloned into pBADa with an N-terminal His-tag to create a series of pBADa derivatives (Table A.3).

The constructs from pET30a cloning system were transformed in *E. coli* XL1 or DH5α and expressed in *E. coli* C41, C43, or BL21, which were incubated in LB broth. The constructs from pBADa cloning system were transformed in *E. coli* DH5α and expressed *E. coli* LMG94 in RM medium (10g Casamino Acids, 50ml 10X M9 salts, 500ul $MgCl_2$, 5ml 20% Glucose and 445ml ddH_20). 10X M9 salts (1L) contains: 60g Na_2HPO_4, 30g KH_2PO_4, 5g NaCl, 10g NH_4Cl, 900 ml H_2O, pH7.4. Purification of His-tagged proteins and the production of antibodies in rabbits were performed as described in Materials and Methods (Chapter 2, section 7).

Antibody production in mice

Antiserum against $FtsA_{Ng}$ was produced as follows. 20 µl of adjuvant (Emulsigen-D, MVP Lab, Omaha, USA) was added to 80 µl of purified 6x His-$FtsA_{Ng}$ for mice injection. The resultant mixtures were injected into mice (100 µl for each mouse) (Animal Care Unit, Vaccine and Infectious Disease Organization, University of Saskatchewan). The first booster was administered three weeks after the initial injection (100 µl for each mouse). Blood was tested for the level of antibody 10 days after the first booster and a second booster was administered. Serum was collected from mouse blood 10 days after the last booster using established procedures (Sambrook and Russell, 2001). Antiserum was tested by Western blot assay as described in the body of this thesis (Chapter 2).

Results

ZipA:

zipA$_{Ng}$ was cloned into pET30a with an N-terminal His-tag. The resultant construct was transformed into *E. coli* expression strains BL21, C41 and C43, respectively. ZipA was expressed best in *E. coli* BL21 with IPTG (600µm) induction at 37ºC. ZipA protein was purified (aliquots in -20 ºC) and used for antibody production. Rabbit antibodies were of good quality (Fig. A.5).

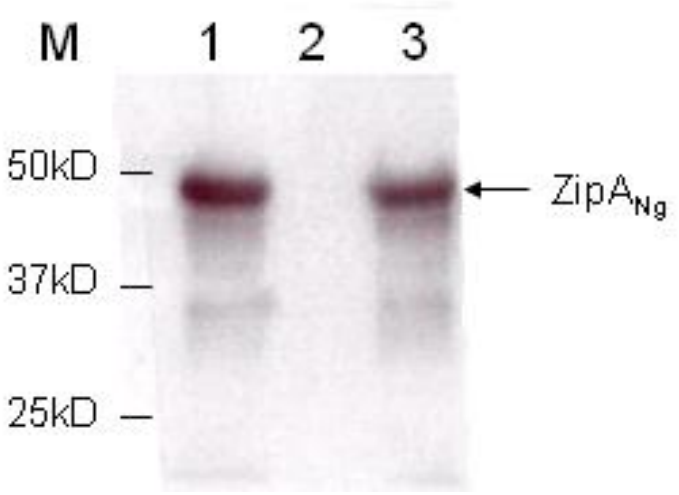

Fig. A.5 Polyclonal anti-ZipA$_{Ng}$ antibody tested by Western blot assay. Lane 1, *N. gonorrhoeae* CH811 cell extract pellet. Lane 2, *N. gonorrhoeae* CH811 cell extract supernate. Lane 3, pure 6xHis-ZipA$_{Ng}$.

.

FtsQ:

ftsQ$_{Ng}$ was cloned into pET30a with an N-terminal His-tag. The construct was transformed into *E. coli* BL21 for expression. FtsQ was expressed very well in *E. coli* BL21 with IPTG (400μm) induction at 37ºC. FtsQ protein was purified (aliquots in -20 ºC) and used for antibody production. Rabbit antibodies have been purified but the signal is very weak (Fig. A.6).

FtsK:

ftsK$_{Ng}$ was cloned into pET30 with an N-terminal His-tag. The resultant construct was transformed into *E. coli* expression strains BL21, C41 and C43, respectively. However, expression did not work. Subsequently I attempted to clone it into pET30a with a C-terminal His-tag. The construct was transformed into *E. coli* expression strains. Expression of the full-length protein FtsK did not work in *E. coli* BL21, C41, or C43. *ftsK*$_{Ng}$ was also cloned into pBADa with an N-terminal His-tag. It is transformed in *E. coli* DH5α and LMG194. Expression works in *E. coli* LMG94, with a 2 hrs growth at 37°C, followed an addition growth for 4 hrs at 30°C with D-arabinose (0.002-0.2%) induction. The protein needs to be purified for antibody production in future.

FtsW:

ftsW$_{Ng}$ was cloned into pET30 with an N-terminal His-tag first and the resultant construct was transformed into *E. coli* C41 and BL21 for protein expression. However, there was no expression from either strain. *ftsW*$_{Ng}$ was re-cloned into pET30a with a C-terminal His-tag. The construct was transformed into *E. coli* strains for expression. However, all attempts at expression failed in *E. coli* BL21, C41, and C43. Sequencing and digestion suggest a correct clone. *ftsW*$_{Ng}$ was subsequently cloned into pBADa with an N-terminal His-tag. The construct was transformed into *E. ocli* LMG94 for expression. All attempts at expression in pBAD also failed however sequencing indicates the plasmid is correct. Other cloning system need to be explored for FtsW expression in future.

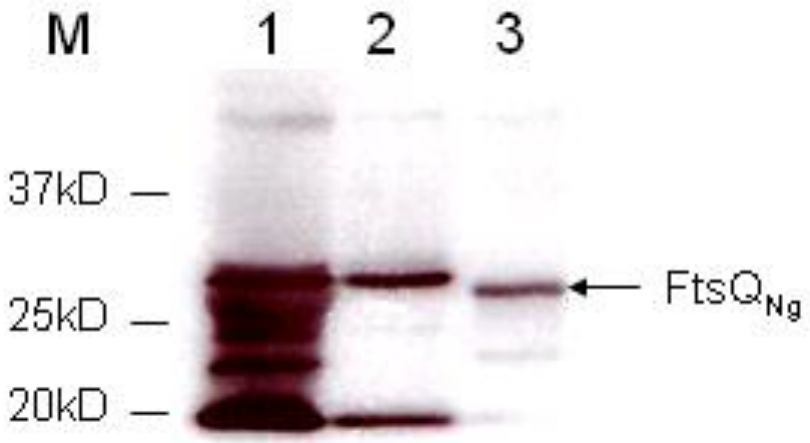

Fig. A.6 Polyclonal anti-$FtsQ_{Ng}$ antibody tested by Western blot assay. Lane 1, *N. gonorrhoeae* CH811 cell extract pellet. Lane 2, *N. gonorrhoeae* CH811 cell extract supernate. Lane 3, pure 6xHis-$FtsQ_{Ng}$.

FtsI:

ftsI$_{Ng}$ was cloned into pET30 with an N-terminal His-tag first and the resultant construct was transformed into *E. coli* C41 and BL21 for protein expression. However, there was no expression from either strain. Thus *ftsI*$_{Ng}$ was re-cloned into pET30a with a C-terminal His-tag. The resultant construct (C-term His) was transformed into *E. coli* BL21 but no expression was noted. The construct was transformed into C41 and C43 with the same results. The construct has been sequenced and digested. The sequence appears correct. I do not know why it is unable to be expressed. Finally, *ftsI*$_{Ng}$ was cloned into pBADa with an N-terminal His-tag. Future, the construct is stored in *E. coli* DH5α(- 20°C) and would have to be transformed into LMG194 for expression.

FtsN:

ftsN$_{Ng}$ was cloned into pET30a with an N-terminal His-tag. The construct was transformed into BL21, C41 and C43 for expression, respectively. Expression is best in *E.coli* BL21 although it is weak but present. I had the most abundant expression growing it for 2 hrs at 37°C, then inducing with varies IPTG concentration (a range of 0.4-0.8 mM made no difference) and growing for 3-4.5 hrs at 30°C. *ftsN*$_{Ng}$ was cloned into pBADa with a N-terminal His-tag. The construct is stored in *E. coli* DH5α(- 20°C) and needs to be transformed into LMG194 to test for expression.

FtsE and FtsX

ftsE$_{Ng}$ and *ftsX* $_{Ng}$ were successfully cloned into pET30a with an N-terminal His-tag. Sequencing indicates the resulted plasmids were correct. The constructs are stored into *E. coli* XL1 (- 20°C) and have to be transformed into *E. coli* strains C41, C41 or BL21 to test expression.

Appendix D. Improving B2H vectors for protein interactions

The B2H vectors pcIp22 and pcI434 constructed by Di Lallo *et al*. (2001) have only two restriction sites SalI and BamHI, which largely limit the gene cloning work. Thus modification of B2H vectors is necessary to allow more genes being cloned.

Material and Methods

The modified vectors pcIp22-linker and pcI434-linker were synthesized by inserting a linker containing more restriction endonuclease sites into pcIp22 and pcI434 for cloning purpose, respectively (GENEART, BioPark, Germany).

Results and Discussion

pcIp22-linker is generated from pcIp22 by inserting a linker containing multiple restriction endonuclease sites through SalI and BamHI. Based on sequence analyses, the available restriction endonuclease sites in pcIp22-linker included SalI, BglII, XhoI, PstI, SmalI and BamHI (Fig. A.7).

pcI434-linker is generated from pcI434 by inserting a linker containing multiple restriction endonuclease sites through SalI and BamHI. Based on sequence analyses, the available restriction endonuclease sites in pcIp22-linker included SalI, BglII, and BamHI (Fig. A.8).

pcIp22-linker and pcI434-linker were transformed into *E. coli* R721. They showed similar residual β-galactosidase activities to *E. coli* R721, indicating that these empty vectors did not self-activate. They were used to clone the $zipA_{Ng}$ for B2H assays in this study. There were also successfully used to study the divisome protein interactions in *Enterococcus faecalis* in our laboratory (unpublished data).

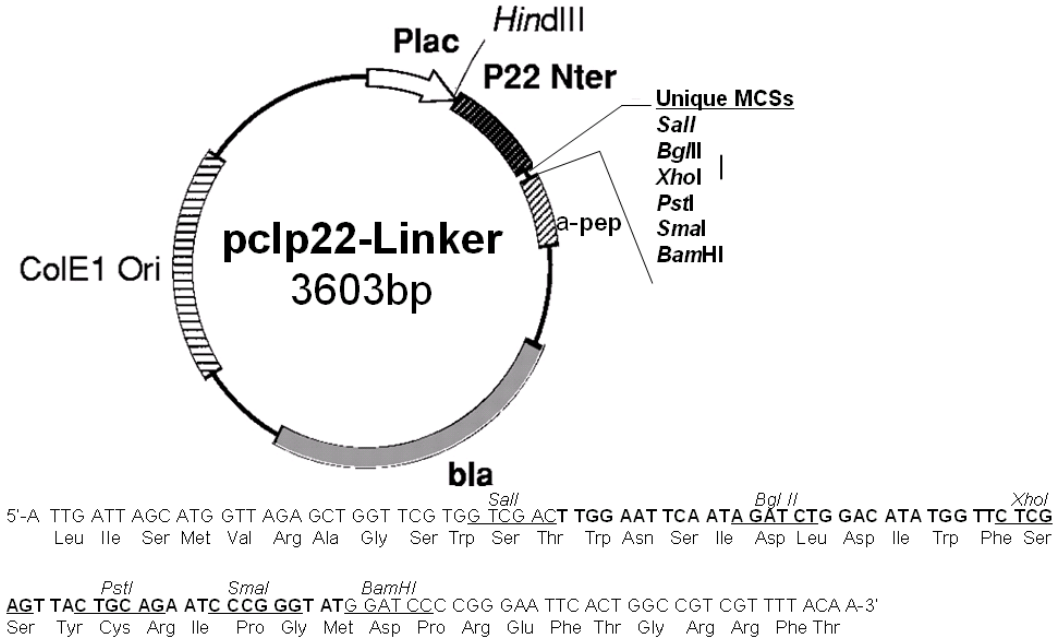

Fig. A.7. Schematic diagram of the modified B2H vector pcIp22-linker and the sequence of restriction sites. pcIp22 carries *ColE1* replication origin and the phage 22 N-terminal domain. The P*lac* promoter drives the transcription of the phase 22 N-terminal domain (Di Lallo *et al*., 2001). This vector carries the *bla* gene conferring ampicillin resistance. pcIp22-linker is generated from pcIp22 by inserting a linker containing multiple restriction endonuclease sites through *Sal*I and *Bam*HI.

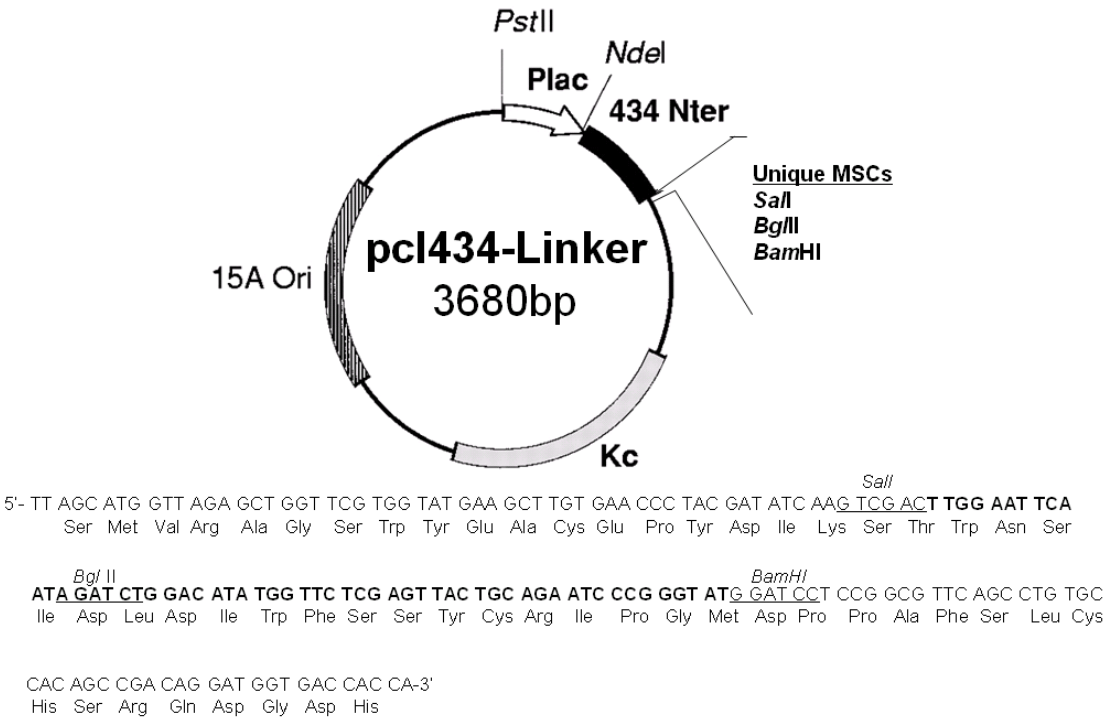

Fig. A.8. Schematic diagram of the modified B2H vector pcIp434-linker and the sequence of the restriction sites. pcI434 is a low-copy-number pACY177 derivative carrying the cI434 N-terminal (Nter) domain, and the P*lac* promoter drives the transcription of the phase 434 N-terminal domain (Di Lallo *et al*., 2001). This vector carries the *p15A* origin of replication (Ori) and a kanamycin resistance cassette (*Kc*). pcI434-linker is generated from pcI434 by inserting a linker containing multiple restriction endonuclease sites through *Sal*I and *Bam*HI.